

**THE METABOLIC AND FUNCTIONAL
CONSEQUENCES OF
HYPERAMMONAEMIA**

Daniel James Wilkinson

A thesis submitted in partial fulfilment of
the requirements of the University of
Brighton for the degree of Doctor of
Philosophy

June 2012

Abstract

Ammonia is an essential intermediate of a number of metabolic pathways in the body, from the maintenance of normal brain function, efficient immune response, to the production of energy within muscle cells to maintain contraction during exercise. However, ammonia levels must be carefully maintained within a low concentration range (no greater than 50-100 μ mol/L), or toxicity may develop. Excess ammonia, also known as hyperammonaemia, has been linked to the development of neurological dysfunction in liver disease states and certain in-born genetic metabolic defects (e.g. urea cycle enzyme deficiencies), whilst it is also believed to impair the regulation of protein metabolism in a number of tissues. This has led some to speculate that similar impairment could occur in healthy individuals where hyperammonaemia is common, such as extremes of exercise, and that hyperammonaemia may be implicit to the altered protein metabolism and fatigue development during such exercise. Both disease and exercise are complicated by a multitude of other metabolic disturbances, and although many functional disturbances in these states are related to the onset of hyperammonaemia, it is difficult to identify cause and effect due solely to ammonia itself in the presence of so many other variables. The aim of this thesis is therefore to investigate the metabolic and functional consequences of hyperammonaemia from a whole body to a cellular level using novel and innovative techniques. Experiment one of this thesis describes the design and implementation of a method for inducing a tolerable and pathologically/physiologically relevant state of hyperammonaemia in resting healthy adult males. This method isolates hyperammonaemia from other variables present in disease or exercise, thereby allowing the effects of ammonia on metabolism and function to be directly assessed. Experiment two uses this method and provides evidence for some subtle changes in response to hyperammonaemia. Using a double-blind placebo controlled cross-over design, it was found that there was a significantly higher level of sensations of fatigue reported during the hyperammonaemia trial compared to the placebo trial, with an absence of impairment in

psychological task performance. The mechanisms behind this increase in fatigue, due to ammonia, were investigated in experiment three using quantitative brain MRI techniques. Minimal structural or metabolic changes were identified in brain as a result of the hyperammonaemia, which reflects the lack of impairment in psychological task performance. It may therefore mean that ammonia alone has little influence on brain function, and the common psychological impairment associated with hyperammonaemia in disease is related to other co-morbidities and/or its interaction with these co-morbidities. Despite these findings, sensations of fatigue were still present following induction of hyperammonaemia, supporting the findings of the previous experiment. It was difficult to interpret what may be causing these changes in fatigue sensation, particularly with the lack of effect to MR imaging. A significant decrease in brain fractional anisotropy (FA) was observed, which could represent subtle microstructural changes in the brain related to water regulation due to ammonia, in turn influencing perceived sensations of fatigue. However, these brain FA changes were not supported by other MR measures of brain water regulation (MTR and ^1H -MRS), so this explanation remains speculative. Experiment four used a cell culture model to determine the effects of excess ammonia on skeletal muscle function, in the form of protein metabolism. Although brain is often the most investigated organ with regards to ammonia's effects, large concentrations are present in skeletal muscle in both exercise and disease, and therefore warrant further investigation. Findings from this study show a potent inhibition to protein synthesis, via control of mRNA translation at both initiation and elongation phases. These results will have wider impact if confirmed *in vivo*, as they provide new avenues for investigation with regards to the control of MPS, and may provide potential for development of new therapeutic/nutritional targets. Taken together, the findings of this thesis will have a wide ranging application in conditions where hyperammonaemia is prevalent, potentially identifying therapeutic targets for the reversal or delay in ammonia induced impairment, whilst also highlighting the need to investigate the interactive effects between ammonia and the other metabolic

changes present in liver disease and exercise, in addition to its array of related functional and metabolic disturbances.

Contents

ACKNOWLEDGEMENTS	14
AUTHOR DECLARATION	15
ABBREVIATIONS LIST	16
CHAPTER 1: INTRODUCTION	22
1.1 AMMONIA.....	22
1.1.1 AMMONIA PRODUCTION IN THE BODY.....	22
1.2 HYPERAMMONAEMIA; AN ACCUMULATION OF SYSTEMIC AMMONIA ABOVE THE PHYSIOLOGICAL NORM.....	27
1.2.1 PATHOLOGICAL HYPERAMMONAEMIA	27
1.2.2 PHYSIOLOGICAL HYPERAMMONAEMIA.....	29
1.3 PATHOGENIC MECHANISMS OF HYPERAMMONAEMIA	34
1.3.1 GLUTAMINE	39
1.3.2 GLUTAMATERGIC NEUROTRANSMISSION	41
1.4 EVIDENCE OF PSYCHOLOGICAL IMPAIRMENT DUE TO HYPERAMMONAEMIA	55
1.5 MRI CHANGES DUE TO LIVER DISEASE/HYPERAMMONAEMIA	59
1.5.1 MAGNETIZATION TRANSFER RATIO (MTR).....	59
1.5.2 DIFFUSION WEIGHTED IMAGING.....	63
1.5.3 ¹ H-MAGNETIC RESONANCE SPECTROSCOPY (¹ H-MRS).....	67
1.6 EFFECTS OF HYPERAMMONAEMIA ON PERIPHERAL TISSUES	70
1.7 QUESTIONS SURROUNDING THE ‘TOXIC’ EFFECTS OF AMMONIA	74
1.9 SUMMARY	78
CHAPTER 2: GENERAL METHODS AND MATERIALS	80
2.1 HEALTH AND SAFETY.....	80
2.2 PARTICIPANTS.....	81
2.3 STANDARDISATION.....	82
2.4 EXPERIMENTAL PROCEDURES FOR CHAPTERS 3, 4 AND 5.....	82
2.4.1 PSYCHOLOGICAL TASKS.....	86
2.5 MAGNETIC RESONANCE IMAGING (MRI)	88
2.5.1 SCAN TASKS.....	89
2.5.2 SCANNING ACQUISITION AND PARAMETERS	90
2.5.3 ANALYSIS.....	92
2.6 PREPARATION OF AMMONIUM CHLORIDE INFUSION FOR ADMINISTRATION	96
2.7 PLASMA AMMONIA CONCENTRATION ANALYSIS.....	96
2.7.1 PROCEDURE	99
2.7.2 STANDARDISATION OF ANALYTICAL TECHNIQUE	102
2.8 STATISTICAL ANALYSIS	105
CHAPTER 3: DEVELOPING A SIMPLE HUMAN MODEL OF ACUTE EXPERIMENTAL HYPERAMMONAEMIA IN HEALTHY ADULTS.	107
3.1 INTRODUCTION.....	107
3.2 METHODS	111
3.2.1 PRELIMINARY EXPERIMENTATION.....	111
3.2.2 PARTICIPANTS.....	111
3.2.3 EXPERIMENTAL DESIGN.....	111

3.2.3 ANALYSIS.....	113
3.3 RESULTS	113
3.3.1 VARIABLE RATE INFUSION TRIALS.....	113
3.3.2 CONSTANT RATE INFUSION TRIALS.....	115
3.4 DISCUSSION	121
CHAPTER 4: THE EFFECTS OF EXPERIMENTALLY INDUCED HYPERAMMONAEMIA ON COGNITION, MOTOR FUNCTION AND FATIGUE	126
4.1 INTRODUCTION.....	126
4.2 METHODS	128
4.2.1 PARTICIPANTS.....	128
4.2.2 FAMILIARISATION SESSION	128
4.2.3 INFUSION PROTOCOL.....	129
4.2.4 BLOOD COLLECTION AND ANALYSIS	130
4.2.5 STATISTICAL ANALYSIS	130
4.3 RESULTS	130
4.3.1. ARTERIALISED VENOUS PLASMA AMMONIA CONCENTRATIONS	130
4.3.2 SUBJECTIVE RATINGS OF FATIGUE.....	131
4.3.3. PSYCHOLOGICAL TASKS.....	134
4.4. DISCUSSION	138
CHAPTER 5: THE EFFECTS OF EXPERIMENTAL HYPERAMMONAEMIA ON THE HEALTHY BRAIN USING QUANTITATIVE MAGNETIC RESONANCE IMAGING (MRI).	145
5.1 INTRODUCTION.....	145
5.1 METHODS	147
5.1.1 PARTICIPANTS.....	147
5.1.2 PROCEDURE	147
5.3 RESULTS	149
5.3.1 VENOUS PLASMA AMMONIA CONCENTRATION	149
5.3.2 MFSI-SF	150
5.3.3 MRI.....	152
5.3.4 PSYCHOLOGICAL TASK DATA	161
5.4 DISCUSSION	163
CHAPTER 6: SUPPRESSION OF C2C12 MUSCLE CELL PROTEIN SYNTHESIS FOLLOWING INCUBATION WITH AMMONIUM CHLORIDE IS REGULATED VIA INHIBITION OF BOTH TRANSLATION INITIATION AND ELONGATION.	175
6.1 INTRODUCTION.....	175
6.1 METHODS	177
6.1.1 CELL CULTURE.....	177
6.1.2 IMMUNOBLOTTING	178
6.1.3 FRACTIONAL SYNTHETIC RATE OF PROTEIN SYNTHESIS (FSR)	179
6.1.4 REAL-TIME PCR	180
6.1.5 MARKERS OF PROTEIN BREAKDOWN	181

6.1.6 STATISTICAL ANALYSIS	181
6.2 RESULTS	182
6.2.1 MUSCLE CELL PROTEIN SYNTHESIS	182
6.2.2 SPECIFIC RESPONSES OF AMPK ^{Thr172} , ACC6 ^{Ser79} AND eEF2 ^{Thr56} PHOSPHORYLATION TO AMMONIUM CHLORIDE INCUBATION	183
6.2.3 SPECIFIC RESPONSES OF mTOR ^{Ser2448} , Akt ^{Ser473} , p70 ^{S6K Thr389} , 4E-BP1 ^{Thr37/46} AND eIF2 α ^{Ser551} PHOSPHORYLATION TO AMMONIUM CHLORIDE INCUBATION.	184
6.2.4 SPECIFIC RESPONSES OF FOXO 3a ^{Ser253} , p90rsk1 ^{Ser380} AND ERK 1/2 PHOSPHORYLATION TO AMMONIUM CHLORIDE INCUBATION.	187
6.2.5 MUSCLE GROWTH FACTOR AND UBIQUITIN LIGASE EXPRESSION FOLLOWING AMMONIA INCUBATION	187
6.2.6 CELLULAR TYROSINE RELEASE.....	188
6.3 DISCUSSION	188
CHAPTER 7: GENERAL DISCUSSION.....	199
7.1 PRINCIPLE FINDINGS	201
7.2 PRACTICAL APPLICATIONS OF FINDINGS.....	209
7.3 FUTURE RESEARCH DIRECTIONS	213
7.4 CONCLUSIONS.....	214
8. REFERENCES	216
9. APPENDICES.....	242

List of Figures

Page no.

- 23** Figure 1.1. Pathways for ammonia detoxification within the liver. A. Ureagenesis within the periportal hepatocytes. Sections within dotted line occur within the cell mitochondria. B. Glutamine synthesis within the perivenous hepatocytes. Ammonia that is not removed via ureagenesis will be scavenged and converted into glutamine within this pathway. AL, argininosuccinate lyase; Arg, arginine; AS, argininosuccinate synthetase; CPS1, carbamoyl phosphate synthetase 1; GS, glutamine synthetase; HCO_3^- , bicarbonate; OTC, ornithine transcarbamoylase. (Taken from Wilkinson et al., 2010)
- 26** Figure 1.2. The cyclical process of whole body ammonia metabolism at rest in a healthy individual. (Taken from Wilkinson et al., 2010)
- 32** Figure 1.3. Branched Chain Amino Acid (BCAA) metabolism within the skeletal muscle mitochondria.
The branched chain keto-acid dehydrogenase (BCKDH) enzyme complex (A) is the rate limiting enzyme of this pathway. BCAA can be used by muscle to produce additional TCA cycle intermediates for cellular energy metabolism, however, BCAA metabolism also provides additional substrates for ammonia production within skeletal muscle. AAT, alanine aminotransferase (controls conversion of pyruvate to alanine); BCAT, branched-chain aminotransferase; BCKA, branched chain keto-acids; CoA-SH, coenzyme A reduced form; GDH, glutamate dehydrogenase (controls conversion of glutamate to ammonia); Kinase, BCKDH kinase; NAD^+ , nicotinamide adenine dinucleotide; NADH, nicotinamide adenine dinucleotide hydrate; Phos, BCKDH phosphatase; R-CoA, acyl coenzyme A. (Taken from Wilkinson et al., 2010)
- 36** Figure 1.4a. Cerebral ammonia metabolism and glutamatergic neurotransmission. Ammonia can be taken up into the brain either; a. as a substitute for K^+ , b. using an ammonium specific transporter (RhGB or RhGC), or c. via diffusion. It is then consumed within a cycle regulating the production of the excitatory neurotransmitter glutamate. The release of glutamate from the presynaptic neuron activates receptors on the postsynaptic membrane, which depending on the receptor subtype will activate different signalling pathways within the postsynaptic neuron. These pathways help to regulate important cellular functions. Two of these pathways are illustrated; 1. NMDA-NO-cGMP pathway. 2. mGluR G-protein coupled pathway. To prevent excess stimulation of the pathways, once activated the glutamate is removed via transporter proteins in the astrocyte membrane, and the whole cycle is initiated once more.
- 36** Figure 1.4b. Neuronal energy metabolism and the ammonium/alanine shuttle. Ammonia may also be utilised to assist in the maintenance of neuronal energy metabolism. Ammonia within the astrocyte can form alanine with pyruvate via the AAT reaction. This alanine is then shuttled from the astrocyte to the neuron where it is broken back down again to release pyruvate which can be used by mitochondria for oxidative energy metabolism. The ammonia which is also released can then be shuttled back to the astrocyte and utilised once more. AAT, alanine aminotransferase; Ala, alanine; cGMP, cyclic guanosine

monophosphate; Cm, calmodulin; Gln, glutamine; Glu, glutamate; Gluc, glucose; Gluc-6-P, glucose-6-phosphate; GS, glutamine synthetase; GTP, guanosine triphosphate; mGluR, metabotropic glutamate receptor; NH₃, ammonia gaseous form; NH₄⁺, ammonium ion; NMDA, N-methyl-D-aspartate receptor; nNOS, neuronal nitric oxide synthetase; NO, Nitric Oxide; PAG, phosphate activated glutaminase; PDE, phosphodiesterase; PKC, protein kinase C; PKG, protein kinase G; PLC, phospholipase C; Pyr, pyruvate; sGC, soluble guanylate cyclase. (Taken from Wilkinson et al., 2010)

- 50** Figure 1.5. Summary of the neural circuitry involved in the regulation of motor activity extending from the basal ganglia. Approximate anatomical positions of the regions involved are illustrated using the outline of a sagittal section of a rat brain. a. Pathways involved in motor regulation in the brain of a healthy rat. Excitatory pathway extending from the nucleus accumbens (Solid Line). Inhibitory pathway extending from the substantia nigra pars reticulata (Dashed Line). Neural interconnection between nucleus accumbens and substantia nigra pars reticulata (Dotted Line). b. Changes in pathway activation in PCS rats, as observed by Cauli et al. (2007a). The inactive 'normal' excitatory pathway (Dotted Line). The active 'Alternative' excitatory pathway extending via the substantia nigra pars reticulata (Solid Line). NA, nucleus accumbens; MDT, medio-dorsal; PFCx, prefrontal cortex SNr, substantia nigra pars reticulata; VMT, ventro-medial thalamus; VP, ventral Pallidum. (Taken from Wilkinson et al., 2010)
- 56** Figure 1.6. Plasma ammonia concentration after oral glutamine challenge in cirrhosis patients (n=6, open squares) and healthy controls (n=4, closed squares), (taken from Ortiz et al., 2004)
- 60** Figure 1.7. Illustration of absorption linewidths of the free (liquid) and bound (macromolecular) proton pools. An off-resonance rf pulse saturates the bound proton pool. (Taken from Henkelman et al., 2001)
- 67** Figure 1.8. Example ¹H-MRS Spectrum with prominent metabolites labelled. NAA; N-Acetylaspartate, Glx; Glutamine/Glutamate, Cho; Choline, Cr; Creatine Peak 1, Cr(2); Creatine Peak 2, ml; Myoinositol
- 73** Figure 1.9. Illustration of complex molecular signalling relating to mTORC1. Highlights the numerous mechanisms believed to be controlled via mTORC1, including the regulation of protein metabolism. Taken from Laplante and Sabatini (2009).
- 84** Figure 2.1. Mean (±SEM) temperature of Hotbox used for collection of arterialised venous blood over three different days during 1 hour of use.
- 85** Figure 2.2. Example of the Borg CR10 Scale Description
- 90** Figure 2.3. Example of screen shot from number connection test.
- 102** Figure 2.4. Reading variability produced by spectrophotometer at 340nm (recommended wavelength) and 365nm (alternative wavelength) at different concentrations of NADH; the light absorbing reagent used for ammonia analysis.

- 103** Figure 2.5: NADH Spectrophotometer Extinction Spectra at 240 and 120 μ M NADH Concentrations
- 114** Figure 3.1. Effect of variable rate infusion of ammonium chloride on arterialised plasma ammonia concentrations. * indicates significant change in concentration from previous time point ($p < 0.05$). A. Peak plasma ammonia concentration range reported during exercise of varying rate and durations. B. Peak plasma ammonia concentration range reported after induction of hyperammonaemia in liver disease. Data are presented as mean \pm SEM.
- 115** Figure 3.2. Effect of variable rate infusion of ammonium chloride on subjective feelings of fatigue, discomfort and nausea. Data are presented as mean \pm SEM. The equivalent verbal expressions of intensity for the CR10 scores are provided along the right hand side of the figure.
- 116** Figure 3.3. Comparison of arterialized plasma ammonia concentrations during the constant rate infusion trials at 100ml/hr (unsuccessful) and 90ml/hr. * indicates significant difference in ammonia concentration between the two trials at this time point ($p < 0.05$). † At 30 minutes in 100ml/hr trial $n = 5$, at 60 minutes $n = 4$, beyond 60 minutes $n = 3$ due to participant drop out. $n = 5$ at all time points for 90ml/hr trial. Data are presented as mean \pm SEM.
- 117** Figure 3.4. Difference in peak subjective feelings of fatigue, discomfort and nausea for the two constant rate trials. Data are presented as mean \pm SEM. The equivalent verbal expressions of intensity for the CR10 scores are provided along the right hand side of the figure.
- 119** Figure 3.5. Relationships between peak CR10 scores and BM/BMI. A. BM and Peak Fatigue CR10 Scores. B. BM and Peak Discomfort CR10 Score. C. BM and Peak Nausea CR10 score. D. BMI and Peak Fatigue CR10 Scores. E. BMI and Peak Discomfort CR10 Score. F. BMI and Peak Nausea CR10 score
- 120** Figure 3.6. Relationships between peak arterialised plasma ammonia concentrations and BM/BMI. G. BMI and peak arterialised plasma ammonia concentrations. H. BM and peak arterialised plasma ammonia concentrations
- 129** Figure 4.1. Schematic of infusion protocol for each testing trial
- 131** Figure 4.2. Arterialised venous plasma ammonia concentrations during AMM (Dashed Line) and PLA (Solid Line) infusion trials. Shaded area represents infusion period. * indicates significant difference in concentration between infusion trials (AMM vs. PLA; $p \leq 0.009$). Data are presented as mean \pm SD.
- 132-133** Figure 4.3. A) Comparison of MFSI-SF total score between PLA and AMM infusion trials. Total scores at 2hrs show significantly higher sensations of fatigue in the AMM trial. Breakdown of total MFSI-SF score into individual subscales shows higher levels of; B) General Fatigue, C) Physical Fatigue, and lowers levels of D) Vigour in the AMM trial. Data are presented as boxplots with median scores, IQR and total range shown
- 135** Figure 4.4. ICT task performance; A) Total number of errors made at each time

point per trial. B) Target reaction time at each time point per trial. C) Lure reaction time at each time point per trial. AMM (Dashed Line), PLA (Solid Line). Data are presented as mean \pm SEM.

- 136** Figure 4.5. COMPTRACK task target displacement error at each time point during the AMM (Dashed Line) and PLA (Solid Line) infusion trials. Data are presented as mean \pm SEM.
- 137** Figure 4.6. A) AVL test raw scores for both AMM (Dashed Line) and PLA (Solid Line) infusion trials. B) Calculated memory and learning scores for AMM (No Fill) and PLA (Solid Fill) infusion trials. Data are presented as mean \pm SEM
- 148** Figure 5.1 Schematic of testing procedure for each infusion trial
- 150** Figure 5.2 Venous plasma ammonia concentrations during PLA (red line) and AMM (black line) infusion trials. Shaded area represents period inside scanner. * significantly different between infusion trials , $p \leq 0.007$
- 151** Figure 5.3. A) Comparison of MFSI-SF total score between PLA and AMM infusion trials. Breakdown of total MFSI-SF score into individual subscales shows higher levels of; B) General Fatigue in the AMM trial post infusion. C) Physical Fatigue and D) Vigour showed a trend towards an increase and a decrease respectively in the AMM trial post infusion, but did not reach significance. Data are presented as boxplots with median scores, IQR and total range shown. NS = not significant.
- 152** Figure 5.4 Mean MTR histograms for A. Gray Matter (GM) B. White Matter (WM)) and C. Whole Brain (WB). pu : percent units.
- 154** Figure 5.5 Example of images from MTR analysis. A. Transverse slice taken from T1 MPRAGE structural image. This image is then segmented into Gray matter (B), White matter (C) and CSF (D). These images are then used to produce MTR masks (E), to determine MTR values within WM, GM and WB (WM+GM) respectively.
- 156** Figure 5.6: Mean DTI histograms for A. FA grey matter, B. FA white matter, C. FA whole brain, D. MD grey matter, E. MD white matter and F. MD whole brain. Enlarged sections illustrate statistically significant change in histogram parameters.
- 158** Figure 5.7 Example of MRS spectrum preprocessing. A. Spectra prior to removal of prominent water peak. B. Spectra immediately following filtering of water peak using HSLVD filter. C. Spectra following all preprocessing ready for analysis.
- 159** Figure 5.8 Graphical output from SPID spectral analysis. Green line represents metabolite database used to model data. Blue line represents original spectrum. Red line represents modelled and analysed data. Important metabolite peaks labelled.
- 162** Figure 5.9 Comparison of NCT data between AMM and PLA infusion trials. $n = 7$, due to joystick failure for one participant.
- 182** Figure 6.1. Changes in FSR in response to incubation with A) 1mM NH_4Cl and B)

10mM NH₄Cl. ***represents a significant decrease in FSR from control, p<0.0001, **p<0.01. Data are presented as Mean ± SEM, n=3.

183-184 Figure 6.2. Changes in phosphorylation of eEF2^{thr56}, AMPK^{Thr172} and ACCβ^{Ser79} in response to incubation with 1mM and 10mM NH₄Cl. ***represents a significant change in phosphorylation from control, p<0.0001. Data are presented as Mean ± SEM, n=6.

185-186 Figure 6.3. Changes in phosphorylation of mTOR^{ser2448}, Akt^{ser473}, p70^{S6K Thr389}, 4E-BP1^{Thr37/46}, eIF2α^{Ser551}, FOXO 3a^{Ser253}, p-p90rsk1^{Thr359/Ser363} and p-ERK1/2^{Tyr202/204} in response to incubation with 1mM and 10mM NH₄Cl. ***represents a significant change in phosphorylation from control, p<0.0001, ** p<0.01, *p<0.05. Data are presented as Mean ± SEM, n=6.

187 Figure 6.4. Expression of muscle growth factors A) Myostatin and B) IGF-1, and Ubiquitin Ligases C) MuRF1 and D) MAFbx in response to 1mM NH₄Cl. All values remained unchanged from controls. Data are presented as Mean ± SEM, n=6.

188 Figure 6.5. Extracellular Tyrosine absorbance at 380nm following incubation with 1mM NH₄Cl. All values remained unchanged from controls. Data are presented as Mean ± SEM, n=6.

208 Figure 7.1. Illustration of proposed signalling pathways regulated by ammonia in skeletal muscle which could lead to the observed depression in MPS.

List of Tables

Page no.

- 56** Table 1.1. Summary of oral amino acid challenge studies in cirrhosis patients where cognitive measures have been collected.
- 98** Table 2.1: Benefits and Weaknesses of different plasma ammonia analysis techniques commonly used in published literature.
- 104** Table 2.2: Variation in calculated concentration from actual concentration when calculated using Kun and Kearney (1974) equation. Variation due to difference in molar extinction coefficient from that expected
- 105** Table 2.3: Interference to absorption provided by assay reagent solution.
- 110** Table 3.1. Summary of Previous Human Intravenous Ammonium Salt Infusion Studies and Ammonium Salt Infusion Information
- 153** Table 5.1 Calculated MTR histogram values for white matter (WM), gray matter (GM), and whole brain (WB). Red type represents not normally distributed data analysed using a Wilcoxon Signed Ranks Test
- 157** Table 5.2 Calculated DTI histogram values. * represents significant difference between trials. Red type represents not normally distributed data analysed using Wilcoxon Signed Rank test. All other data analysed using paired samples t – tests.
- 160** Table 5.3 MRS metabolite data normalised to creatine metabolite peak. Red type represents not normally distributed data analysed using Wilcoxon Signed Rank test. All other data analysed using paired samples t – tests.
- 161** Table 5.4 Comparison of mean ICT parameters between AMM and PLA infusion trials.

Acknowledgements

Firstly, special thanks needs to go to all the volunteers who gave up their spare time for these projects. Without their interest and patience, this thesis would not have been possible. I would also like to thank Peter and Nick for all their help and support over the (many!!) years. Particularly putting up with my endless knocking on office doors with questions, and the numerous coffee, donut and Staropramen breaks to discuss study design, recruitment and statistics. The informal nature of their PhD supervision was very well suited to my style of working, and I have enjoyed working alongside them over the years. I am sure that post-doctoral collaboration on projects will continue. A big thanks must also go to Phil and Kenny (Drs. Atherton and Smith) at the School of Graduate Entry Medicine, University of Nottingham. Without their input, funding and hospitality during the numerous weeks I spent at the labs in Derby, the work contained within the final chapter would not have been possible. Thanks to Nick Medford, Nick Dowell, Jan and all the staff at the Clinical Imaging Sciences Centre, for their help with MRI acquisition, analysis and data collection. Thank you should also go to the C2C12 cell line for putting up with all the experimental treatments so well. Finally, I would like to say a big thank you to my family; my Mum and Dad, Sue and Bill, and my two brothers Matt and Sam. Thank you for your patience and support over the years, it has been stressful at times, but your strong support has helped me get through it. I would like to add a special mention to Rach, thank you, without you this PhD would not have happened.

Author Declaration

I declare that the research contained in this thesis, unless otherwise formally indicated within the text, is the original work of the author. The thesis has not been previously submitted to this or any other university for a degree, and does not incorporate any material already submitted for a degree. Parts of this thesis have been peer reviewed and published as articles, a list of which is outlined in appendix 6.

Signed

Dated

Abbreviations List

AAT, alanine amino transferase

ADP, adenosine diphosphate

ADC, apparent diffusion coefficient

AK, adenylate kinase

AL, adenylosuccinate lyase

Ala, alanine

ALC, acetyl-L-carnitine

AMP, adenosine Monophosphate

AMPA, α -amino-3-hydroxy-5-methyl-4-isoxazole propionate

AMPD, AMP deaminase

AMPK, AMP-activated protein kinase

AMM, Ammonia

Arg, arginine

AS, adenylosuccinate synthetase

ATP, adenosine triphosphate

a-v diff, arterio-venous difference

AVL, auditory verbal learning test

BBB, blood brain barrier

BCAA, branched Chain Amino Acid

BCAT, branched-chain amino transferase

BCKDH, branched chain keto-acid dehydrogenase

BCKA, branched chain keto-acids

CBF, cerebral blood flow

cGMP, cyclic guanosine monophosphate

Cho, choline containing compounds

Cm, calmodulin

CNS, central nervous system

CoA-SH, coenzyme A reduced form

COMPTRACK, continuous compensatory tracking task

CPCCOEt, 7-hydroxyiminocyclopropan[*b*]chromen-1a-carboxylic acid ethyl ester

CPF, cerebral plasma flow

CSF, cerebrospinal fluid

Cr, creatine

DHPG, (5)-3,5-dihydroxyphenylglycine

DTI, diffusion tensor imaging

EAA, essential amino acid

eEF2, eukaryotic elongation factor 2

EEG, electroencephalogram

eIF2 α , eukaryotic initiation factor 2 alpha

ERP, event-related brain potential

FOXO3a, forkhead box O 3a

FA, fractional anisotropy

fMRI, functional magnetic resonance imaging

GABA, gamma-aminobutyric acid

GDH, glutamate dehydrogenase

GDP, guanosine diphosphate

GI Tract, gastrointestinal tract

Glu, glutamate

Gluc, glucose

Gluc-6-P, glucose-6-phosphate

Gln, glutamine

Glx, glutamine/glutamate

GM, gray matter

GS, glutamine synthetase

GTP, guanosine triphosphate

^1H -MRS, ^1H -magnetic resonance spectroscopy

HCO_3^- , bicarbonate ion

HE, hepatic encephalopathy

ICT, inhibitory control test

IMP, inosine monophosphate

K^+ , potassium ion

LTP, long term potentiation

MD, mean diffusivity

MDT, medio-dorsal thalamus

mGluR, metabotropic glutamate receptor

ml, myoinositol

MPT, mitochondrial permeability transition

MRI, magnetic resonance imaging

mTORC1, mammalian target of rapamycin complex 1

MTR, magnetization transfer ratio

NA, nucleus accumbens

NAA, N-acetylaspartate

NAD^+ ; nicotinamide adenine dinucleotide

NADH, nicotinamide adenine dinucleotide hydrate

NCT, number connection test

NH_3 , ammonia gaseous form

NH_4^+ , ammonium ion

NMDA, N-methyl-D-aspartate

NO, nitric oxide

NOS, nitric oxide synthetase

nNOS, neuronal nitric oxide synthetase

OP, l-ornithine phenylacetate

OTC, ornithine transcarbamoylase

p70S6K, 70kDa protein S6 kinase

p90^{RSK1}, 90kDa ribosomal protein S6 kinase

PAG, phosphate activated glutaminase

PCS, portacaval shunt

PDE, phosphodiesterase

PET, positron emission tomography

PFCx, prefrontal cortex

Phos, BCKDH phosphotase

PKG, protein kinase G

PKC, protein kinase C

PLA, Placebo

PLC, phospholipase C

PNC, purine nucleotide cycle

Pyr, pyruvate

R-CoA; acyl coenzyme A

RhB(C)G, rhesus non-erythroid glycoprotein B (C)

ROS, reactive oxygen species

SNr, substantia nigra pars reticulata

sGC, soluble guanylate cyclase

SNAP, S-nitroso-N-acetyl-pencillamine

VMT, ventro-medial thalamus

VP, ventral pallidum

WB, whole brain

WM, white matter

CHAPTER 1: INTRODUCTION

1.1 AMMONIA

1.1.1 AMMONIA PRODUCTION IN THE BODY.

Ammonia is an important metabolic end product and intermediate of several biochemical pathways in the body, its appearance in the systemic circulation stems from a number of sources (gut, muscle, kidney, brain; Olde Damink *et al.*, 2002a). Under normal physiological conditions, the majority of systemic ammonia is released from the gut or gastrointestinal (GI) tract (Summerskill and Wolpert, 1970, Romero-Gómez *et al.*, 2009). Here nitrogenous compounds, primarily glutamine and urea, in addition to epithelial and bacterial debris, are broken down through a combination of proteases, urease containing bacterial flora and ammonia liberating enzymes such as glutaminase, of which activity in the GI tract is very high (James *et al.*, 1998, Olde Damink *et al.*, 2002a). This bacterial and enzymatic activity releases large amounts of ammonia, which is transported across the mucosal epithelia into the portal circulation where it is metabolised by the liver (Olde Damink *et al.*, 2009). Of the ammonia liberated from nutritional sources, as little as 1% is believed to remain unused and excreted in the faecal matter (Summerskill and Wolpert, 1970).

It was known for several decades that ammonia transport occurred bidirectionally between the GI tract and systemic circulation (Summerskill and Wolpert, 1970), however, the exact mechanisms involved in this transport remained unclear until recently (Handlogten *et al.*, 2005). Ammonia is present in the body as two forms. In its gaseous form, NH_3 , it is freely diffusible across membranes, making transport dependent on diffusible concentration or pH gradients (Ott and Larsen, 2004). However, due to the chemical properties of ammonia and the physiological conditions in the body (e.g. pH and temperature), a large proportion

(greater than 98%) of the ammonia is in its ionic form; NH_4^+ (Felipo and Butterworth, 2002). This form cannot cross membranes easily due to its charged state and low lipid solubility (Summerskill and Wolpert, 1970). Therefore, transport mechanisms must be present for it to cross effectively into the circulatory system from the GI tract. Ammonium specific transporter proteins have been identified as contributing to this, in particular the human nonerythroid Rhesus Glycoprotein B (RhBG) and C (RhCG). These proteins are expressed throughout the GI tract from stomach to colon (Handlogten *et al.*, 2005), and they may function cooperatively with other transporters (K^+ - Cl^- cotransporters; Bergeron *et al.*, 2003; K^+ channels; Nagaraja and Brookes, 1998; Hall *et al.*, 1992; and NH_4^+/H^+ exchangers; McDougal *et al.*, 1995), for efficient inter-organ exchange of ammonia (Handlogten *et al.*, 2005).



Figure 1.1. Pathways for ammonia detoxification within the liver. **A.** Ureagenesis within the periportal hepatocytes. Sections within dotted line occur within the cell mitochondria. **B.** Glutamine synthesis within the perivenous hepatocytes. Ammonia that is not removed via ureagenesis will be scavenged and converted into glutamine within this pathway. AL, argininosuccinate lyase; Arg, arginine; AS, argininosuccinate synthetase; CPS1, carbamoyl phosphate synthetase 1; GS, glutamine synthetase; HCO_3^- , bicarbonate; OTC, ornithine transcarbamoylase. (Taken from Wilkinson *et al.*, 2010)

The hepatic portal vein delivers ammonia to the liver, where it may be incorporated into either urea via ureagenesis within the periportal hepatocytes (hepatocytes present around the portal vein), or glutamine via the glutamine synthetase (GS) reaction within the perivenous hepatocytes (hepatocytes present around the hepatic vein) (Haussinger, 1983, Haussinger et al., 1992, Olde Damink et al., 2009). This compartmentalised system of detoxification (Figure 1.1) is highly efficient, with the resting healthy adult liver able to remove all ammonia delivered by the portal circulation in a single pass, even with normal fluctuations in nutritional state and variability in protein content of meals (Yang *et al.*, 2000).

Once ammonia has been converted to urea and glutamine they re-enter the circulation via the hepatic vein. Between 20 and 25% of the urea produced by the liver will return to the GI tract, where it will be reabsorbed and, through the action of bacterial urease, be recycled into amino acids to maintain whole body nitrogen balance (Patterson et al., 1995, Yang et al., 2000, Hamadeh and Hoffer, 1998). The remainder of the urea, will either be added to the whole body urea pool, estimated at approx. 200mM (Yang *et al.*, 2000), or taken to the kidneys with the glutamine. Here the urea will be excreted from the body in the urine, whereas the glutamine will be used by the kidneys for further metabolism (van de Poll et al., 2004, Olde Damink et al., 2009).

Glutamine produced by the liver is metabolised by a phosphate activated glutaminase in the kidney, releasing ammonia and glutamate, glutamate can be metabolised to release a further ammonia moiety and α -ketoglutarate (DuBose et al., 1991, van de Poll et al., 2004), α -ketoglutarate may then be used to provide two bicarbonate ions through its role as a TCA cycle intermediate and these can be used to replace those consumed by liver ureagenesis (Stanton and Koeppen, 1998). The amount of ammonia released back into the circulation,

or excreted by the kidneys in urine, is important in acid-base balance of the body (Pitts *et al.*, 1972, Simpson and Adam, 1975). For example, release of ammonia, in the form of ammonium, into the circulation provides hydrogen ions (through ureagenesis) which can be utilised to titrate any excess bicarbonate ions (DuBose *et al.*, 1991). In contrast, excretion of ammonia in the urine, in the form of ammonium, will remove excess hydrogen ions from the system, preventing their titrating effect, thereby helping to restore bicarbonate ion levels (Stanton and Koeppen, 1998). Under normal physiological conditions approximately 70% of the ammonia produced from glutamine metabolism in the kidneys is released back into the circulation (van de Poll *et al.*, 2004). However this decreases considerably (to approximately 30%) under acidosis where there is a greater urinary ammonia excretion to provide additional hydrogen ion removal and restoration of bicarbonate levels (van de Poll *et al.*, 2004).

This efficient system of detoxification and inter-organ exchange ensures that plasma ammonia concentrations are maintained within a low range of no greater than 50 - 100 $\mu\text{mol/L}$ (Felipo and Butterworth, 2002). Exchange between the GI tract, liver and kidneys maintain most of ammonia homeostasis, however, other tissues and organs, such as the brain and skeletal muscle also contribute to ammonia metabolism and regulation (Olde Damink *et al.*, 2002a, Olde Damink *et al.*, 2009). Skeletal muscle makes up approximately 40% of total body mass (Shimomura *et al.*, 2006), and has a large potential capacity for the production, uptake and metabolism of ammonia. Some early tracer studies estimated that approximately 50% of ammonia may be metabolised in muscle to form glutamine, via the GS reaction (Lockwood *et al.*, 1979). However, GS activity (Lund, 1970) and ammonia uptake is low in resting muscle (Bangsbo *et al.*, 1996, Eriksson *et al.*, 1985) and there are large differences in uptake between skeletal muscle groups in the body (Webster and Gabuzda, 1958, Ganda and Ruderman, 1976). More recently it has been estimated that, in

healthy humans, ammonia uptake by skeletal muscle at rest may be close to zero, indicating that muscle may not contribute significantly to ammonia metabolism in the healthy resting adult (Olde Damink et al., 2002a). Even so, muscle may become more important under conditions when other methods of removal deteriorate, as is the case for liver disease (Clemmesen *et al.*, 2000), and when production far exceeds the capacity for removal, such as in exercise (Banister and Cameron, 1990, Bangsbo et al., 1996).

Ammonia metabolism in a healthy adult at rest is a cyclical process (Figure 1.2), with several input and output points. Even the most minor of alterations to any part of this process may affect ammonia homeostasis, leading to the need for changes in the system to cope with this perturbation. Liver dysfunction and exercise act to provoke a change in homeostasis either by diminishing capacity for removal or increasing production of ammonia.



Figure 1.2. The cyclical process of whole body ammonia metabolism at rest in a healthy individual. (Taken from Wilkinson et al., 2010)

1.2 HYPERAMMONAEMIA; an accumulation of systemic ammonia above the physiological norm.

1.2.1 PATHOLOGICAL HYPERAMMONAEMIA

Pathological hyperammonaemia is primarily a consequence of both acute and chronic liver failure, however there are other less common pathological complications which can lead to hyperammonaemia, including; bacterial infection, haemato-oncological disorders, in born errors of metabolism (urea cycle enzyme deficiencies) and drug-induced side effects (Laish and Ben Ari, 2011). Acute liver failure is caused by drug-induced injury or viral infection, leading to a sudden and severe deterioration in liver function (Larson, 2008). It leads to extremely high levels of ammonia accumulating within the body (up to 350 μ mol/L; Clemmesen et al., 1999), which can progress rapidly to the onset of cerebral herniation, hepatic coma and even death (Clemmesen et al., 1999). As such, acute liver failure and the other complications listed above are not complicit with the type and levels of hyperammonaemia being investigated in this thesis, so will not be discussed further.

1.2.1.1 CHRONIC LIVER DISEASE AND CIRRHOSIS

Chronic insult or injury to the liver, which in the case of cirrhosis takes the form of; persistent alcohol abuse, chronic hepatitis B or C infection, non-alcoholic fatty liver disease resulting from obesity or diabetes, biliary obstruction, or drug induced liver injury (Heidelbaugh and Bruderly, 2006), leads to the formation of fibrotic scar tissue (fibrosis) within the liver lobule, damaging the functional architecture of the liver (Svegliati-Baroni et al., 2008). This in turn prevents efficient exchange of metabolites, such as ammonia, between the blood and hepatocytes reducing urea synthetic capacity (Schuppan and Afdhal, 2008, Rudman et al., 1973). The level by which urea synthetic capacity is reduced seems to vary due to severity of condition, with decompensated or end stage cirrhosis

patients reported to have anything up to 90% impairment (Rudman et al., 1973, Shargraw and Jahoor, 1999). Whilst stable cirrhosis patients can present with near normal arterial ammonia concentrations ($43 \pm 13 \mu\text{mol/L}$), which suggests adequate functional hepatic reserve (Clemmesen et al., 1999). In addition, fibrosis is a major factor in the development of portal hypertension through the resistance to flow caused by microstructural changes to the tissues (Bosch and García-Pagán, 2000). In an attempt to compensate for this increased portal pressure, the formation of portal-systemic collateral veins occurs (Fernandez et al., 2005), in addition to the opening of pre-existing vascular channels (Colle et al., 2008). Although this helps to alleviate some of the increase in pressure, it also causes portal blood to bypass the liver altogether meaning that normal hepatic metabolite extraction cannot be performed (Mínguez et al., 2006). Finally, the impairment to normal function within the liver caused by cirrhosis can also have knock on effects to other organs such as the kidneys. Recent evidence has shown that cirrhosis patients have significantly altered renal metabolism, releasing 6 times more ammonia from the kidneys into the renal vein than normal (Olde Damink et al., 2003).

Pathological hyperammonaemia is therefore a multifaceted phenomenon, caused by significant alterations to normal ammonia handling. Fibrosis causes hepatocellular impairment reducing functional capacity, whilst also altering liver microcirculation leading to portal hypertension, and portal systemic shunting. Ammonia provided to the liver either bypasses hepatic metabolism altogether, or saturated capacity of the liver prevents efficient metabolism. In addition, alterations in the amount of ammonia released by the kidneys ensures that the kidneys become net ammonia producers contributing to significant hyperammonaemia.

1.2.2 PHYSIOLOGICAL HYPERAMMONAEMIA

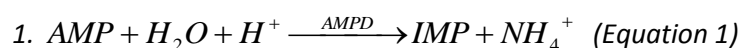
Pathological hyperammonaemia implicates insufficient removal processes in the accumulation of ammonia. In contrast physiological hyperammonaemia, described in the following section, develops as a result of increased ammonia production at a rate greater than can be removed via normal metabolism. This is a process which takes place in skeletal muscle, with ammonia production a result of chemical reactions necessary to maintain the ATP/ADP ratio for efficient contraction, and occurs during certain forms of exercise stress.

1.2.2.1. MUSCLE AMMONIA PRODUCTION DURING CONTRACTION/EXERCISE

The discovery of ammonia production by muscle was first reported by Parnas and colleagues in the late 1920s (Parnas and Mozolowski, 1927). They found a close relationship between ammonia formation in muscle, anaerobic work and adenine nucleotide degradation (Parnas, 1929). It was discovered that the reaction,



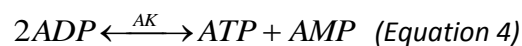
controlled via the enzyme AMP deaminase (AMPD), was responsible for the observed ammonia production in muscle (Parnas, 1929, Schmidt, 1928). This reaction was later identified as part of a process called the purine nucleotide cycle (PNC) which involves three interlinked reactions controlled by the enzymes AMPD, adenylosuccinate synthetase (AS) and adenylosuccinate lyase (AL).



(Lowenstein, 1990).

Metabolic flux through this pathway is tightly regulated by the cell to maintain adequate levels of adenine nucleotides and TCA cycle intermediates for cell energy production (Tullson and Terjung, 1990, Hisatome et al., 1998).

Under a resting physiological state, i.e. no muscle contraction, approximately 90% of the skeletal muscle AMPD is in a sarcoplasmic position and as an inactive form (Rundell *et al.*, 1992). However, a significant change occurs as intense muscle contraction begins, when approximately 50 – 60% of this AMPD becomes bound to the myofibril (Rundell *et al.*, 1992). Binding of the enzyme increases its activity causing an increased rate of degradation of AMP to IMP, and an increased release of ammonia as a result. This increased breakdown of AMP will affect the equilibrium of the adenylate kinase (AK) reaction creating additional ATP from ADP



to increase the cellular energy charge and maintain contraction under conditions of increasing stress (Hisatome *et al.*, 1998).

The amount of ammonia produced by the muscle which is released during exercise has been estimated within the range of 10 – 25% (Katz et al., 1986, Graham et al., 1990). This is due to the large proportion (approx. 99%)¹ of this ammonia being present as NH₄⁺, which without a specific transport mechanism cannot cross the cell membrane. Ammonium

¹ The proportions of ammonia in solution, as gaseous (NH₃) or ionic (NH₄⁺), are dependent on pH. The quantities of each may be calculated using the Henderson-Hasselbalch equation;

$$\log_{10}([NH_3]/[NH_4^+]) = pH - pK_a \text{ (Equation 5; Marcaggi and Coles, 2001)}$$

The pK_a of ammonia is reported to be between 9.01 and 9.25 (Bromberg et al., 1960, Katz et al., 1986, Marcaggi and Coles, 2001) and the pH range of exercising muscle lies between 7.1 and 6.6 (Sahlin et al., 1976). Using equation 5 approximately 99% of all ammonia inside skeletal muscle at rest or during exercise will be in the form of ammonium ions (NH₄⁺).

specific transporters RhBG and RhCG remain to be identified in skeletal muscle, yet NH_4^+ may substitute for K^+ , due to their similar size and charge, and exit via K^+ channels and transporters (Ott and Larsen, 2004, Nagaraja and Brookes, 1998). However NH_4^+ will have to compete with the high intramuscular K^+ concentrations for these routes (Payne *et al.*, 1995), hence the limited release.

The observation of ammonia production in 1:1 stoichiometry with IMP production during exercise, suggested to many early researchers that the PNC was the sole pathway for ammonia production within muscle during exercise (Katz *et al.*, 1986, Meyer and Terjung, 1979). The discovery of the activation of the BCKDH enzyme complex by exercise in both rat (Kasperek *et al.*, 1985) and human muscle (Wagenmakers *et al.*, 1989) questioned this however. The BCKDH complex is the rate limiting step in BCAA catabolism. Through this process (figure 1.3) the BCAAs are broken down via two reactions; branched chain aminotransferase (BCAT) and branched chain alpha keto acid dehydrogenase (BCKDH), to form coenzyme A compounds which can be utilised in the TCA cycle for oxidative energy production (Shimomura *et al.*, 2006, Shimomura *et al.*, 2004). At the primary BCAT reaction, the amino group from the BCAA is utilised to form glutamate from 2-oxoglutarate, after which this glutamate can then either form glutamine via GS, or alanine through combination with pyruvate. In some cases glutamate may react with the co-factor NAD^+ via the glutamate dehydrogenase (GDH) reaction leading to the formation of ammonia, identifying that AMPD is not the only pathway in muscle by which ammonia generation may take place (Wagenmakers *et al.*, 1990). With sufficient pyruvate available the amino group provided by the glutamate will be preferentially incorporated into alanine, due to the near equilibrium state of the alanine aminotransferase reaction (Wagenmakers *et al.*, 1990, Wagenmakers, 1998). The majority of the ammonia produced via this pathway is

only likely to occur when the availability of pyruvate is reduced, as glycogen stores are depleted (Wagenmakers *et al.*, 1990).

The consensus view is that the production of ammonia during exercise occurs via a combination of both AMP deamination and BCAA metabolism, which are activated in an intensity and duration dependent manner. The production of ammonia can lead to significantly elevated systemic ammonia levels being observed of anything between 90 and 200+ $\mu\text{mol.l}^{-1}$ (Hellsten *et al.*, 1999, Dalsgaard *et al.*, 2004, Nybo *et al.*, 2005, Mohr *et al.*, 2006). This is a 3 – 10 fold increase on levels commonly observed in healthy individuals at rest (20 - 80 $\mu\text{mol.l}^{-1}$; van Hall *et al.*, 1995; Bangsbo *et al.*, 1996).

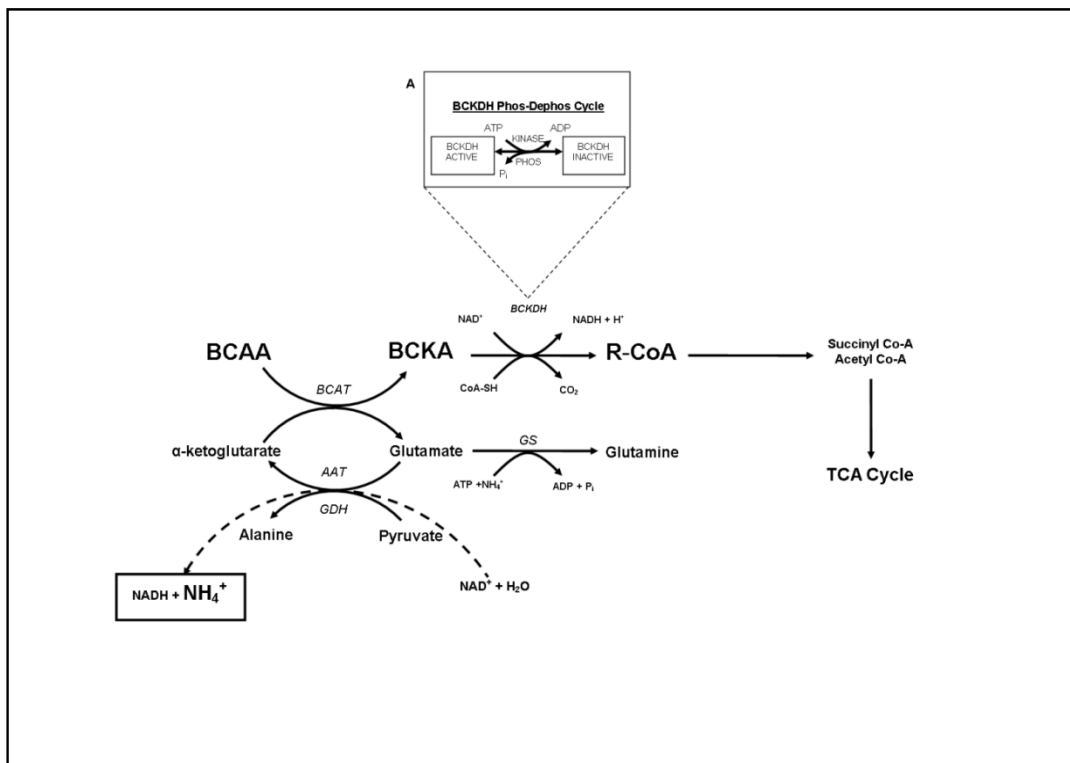


Figure 1.3. Branched Chain Amino Acid (BCAA) metabolism within the skeletal muscle mitochondria.

The branched chain keto-acid dehydrogenase (BCKDH) enzyme complex (A) is the rate limiting enzyme of this pathway. BCAA can be used by muscle to produce additional TCA cycle intermediates for cellular energy metabolism, however, BCAA metabolism also provides additional substrates for ammonia production within skeletal muscle. AAT, alanine aminotransferase (controls conversion of pyruvate to alanine); BCAT, branched-chain aminotransferase; BCKA, branched chain keto-acids; CoA-SH, coenzyme A reduced form; GDH, glutamate dehydrogenase (controls conversion of glutamate to ammonia); Kinase, BCKDH kinase; NAD^+ , nicotinamide adenine dinucleotide; NADH, nicotinamide adenine dinucleotide hydrate; Phos, BCKDH phosphatase; R-CoA, acyl coenzyme A. (Taken from Wilkinson *et al.*, 2010)

This relationship between the presence of large amounts of ammonia in both muscle and blood at maximal exercise and exhaustion, provided many researchers, in particular Banister and colleagues, to suggest a link between ammonia and the onset of fatigue. Using evidence provided by the link between exercise and ammonia derived from muscle metabolism, in combination with that of hyperammonaemia associated pathologies namely hepatic encephalopathy (see following sections of this chapter for further details), they presented their interpretation of ammonia associated fatigue (Mutch and Banister, 1983, Banister and Cameron, 1990). The proposed effects of ammonia on the CNS, such as the involvement in the onset of convulsions in rats (Singh and Banister, 1981, Banister et al., 1976) and other neurological disturbances (McDermott Jr. and Adams, 1954). In addition to the observation that isolated muscle decreased its contractility in the presence of increasing ammonia concentration (Heald, 1975). Indicated the potential for a direct causal role for ammonia in CNS and neuromuscular dysfunction. Banister and colleagues argued that the increased production, accumulation and distribution of ammonia during exhaustive exercise could lead to either or both mechanisms occurring, hence contributing to the onset of fatigue and an inability to sustain efficient or maximal performance (Mutch and Banister, 1983, Banister and Cameron, 1990). Although plausible, the ammonia fatigue theory lacks any direct empirical evidence to support it. The main body of work used by Banister and colleagues to provide support for this theory was one which identified that reduction in blood ammonia during exercise was accompanied by an increase in exercise performance, in the form of increased exercise duration, without consideration for other related effects associated with such intervention (see Mutch and Banister, 1983 and Wilkinson et al., 2010 for further discussion). Since the publication of these ideas by Banister and colleagues, few researchers have gone beyond the findings of the early research and attempted to provide more direct, conclusive evidence in support of this theory. Of the studies which have been performed, the majority have either investigated

the production and metabolism of ammonia within the periphery (Spodaryk et al., 1990, Graham et al., 1993, Graham et al., 1995, Rush et al., 1995, Esbjornsson-Liljedahl and Jansson, 1999, Snow et al., 2000, Mohr et al., 2006), or investigated the link between attenuation of ammonia production during exercise and performance (Denis et al., 1991, Eto et al., 1994, Carvalho-Peixoto et al., 2007, Bassini-Cameron et al., 2008). In light of this, it is unsurprising that questions still remain regarding the ammonia and its influence on fatigue development. Recent evidence to support the uptake and accumulation of ammonia in the cerebral compartments during exercise by Nybo and colleagues (Dalsgaard et al., 2004; Nybo et al., 2005), suggests for the first time that ammonia has the capability to impair brain tissue function during exercise through its proposed neurotoxic actions. There is also evidence from animal models that cerebral ammonia levels during prolonged exercise are associated with interference in neurotransmitter metabolism, i.e. excitatory and inhibitory neurotransmitters glutamate and GABA concentrations (Guezennec *et al.*, 1998). However, there is no evidence for this in humans yet, and no evidence of associated neurological and performance impairments.

1.3 PATHOGENIC MECHANISMS OF HYPERAMMONAEMIA

Brain tissue, unlike the liver, has no urea cycle, and blood-borne ammonia taken up across the blood brain barrier (BBB) is detoxified by a different process, incorporation into glutamine through the GS reaction, in the same way as in the skeletal muscle and perivenous hepatocytes (Butterworth, 2003, Felipo and Butterworth, 2002). In the brain, this process takes place primarily in the astrocyte cells, as these cells are the first point of contact for any substances entering the brain tissues from the blood (Wang and Bordey, 2008). Astrocyte cells provide protection to the neuron and perform important metabolic functions to assist in the process of neurotransmission and neuronal energy metabolism, of which ammonia forms a vital part (Wang and Bordey, 2008). Some of these functions are

illustrated in Figures 1.4a and b. Ammonia, through its incorporation into glutamine, plays an important role in the glutamatergic neurotransmitter system, assisting in affecting, regulating and maintaining levels of the excitatory neurotransmitter glutamate (Felipo and Butterworth, 2002). Glutamate is an important neurotransmitter and also acts as a precursor for production of the inhibitory neurotransmitter, gamma-aminobutyric acid (GABA), through the action of the enzyme glutamic acid decarboxylase (Bak *et al.*, 2006). In addition, a small proportion of the ammonia may be involved in the maintenance of neuronal energy metabolism, through an alanine/ammonium shuttle (Coles *et al.*, 2008). This recently proposed mechanism suggests that ammonia can be utilised along with pyruvate, provided via astrocyte glucose metabolism, to create alanine through the alanine aminotransferase (AAT) reaction (Tsacopoulos *et al.*, 1997, Coles *et al.*, 2008). Alanine may then be shuttled from the astrocyte to the neuron where it is broken down releasing pyruvate for the oxidative metabolism of neuronal mitochondria (Coles *et al.*, 2008). The ammonia which is also released from the breakdown of alanine in the neuron is then returned to the astrocyte where it can be utilised once again (Coles *et al.*, 2008; Figure 1.4b). Ammonia, therefore, is implicated in both excitatory and inhibitory pathways through its role in the synthesis of glutamate and GABA, whilst also being important in the maintenance of neuronal energy metabolism through the alanine/ammonium shuttle. Consequently its presence should not always be considered as having a pathological effect.

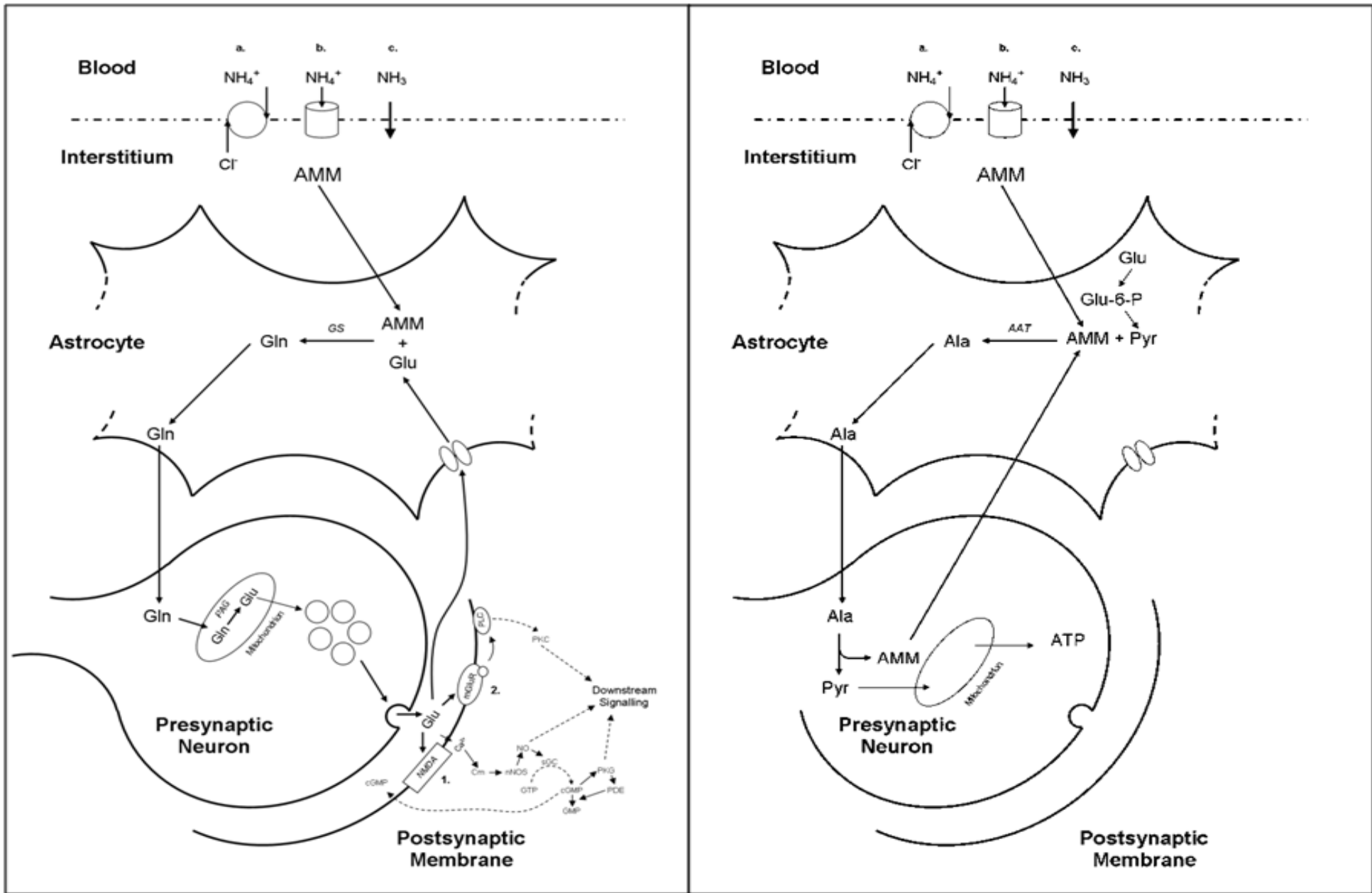


Figure 1.4a. Cerebral ammonia metabolism and glutamatergic neurotransmission. Ammonia can be taken up into the brain either; **a.** as a substitute for K^+ , **b.** using an ammonium specific transporter (RhGB or RhGC), or **c.** via diffusion. It is then consumed within a cycle regulating the production of the excitatory neurotransmitter glutamate. The release of glutamate from the presynaptic neuron activates receptors on the postsynaptic membrane, which depending on the receptor subtype will activate different signalling pathways within the postsynaptic neuron. These pathways help to regulate important cellular functions. Two of these pathways are illustrated; **1.** NMDA-NO-cGMP pathway. **2.** mGluR G-protein coupled pathway. To prevent excess stimulation of the pathways, once activated the glutamate is removed via transporter proteins in the astrocyte membrane, and the whole cycle is initiated once more.

Figure 1.4b. Neuronal energy metabolism and the ammonium/alanine shuttle. Ammonia may also be utilised to assist in the maintenance of neuronal energy metabolism. Ammonia within the astrocyte can form alanine with pyruvate via the AAT reaction. This alanine is then shuttled from the astrocyte to the neuron where it is broken back down again to release pyruvate which can be used by mitochondria for oxidative energy metabolism. The ammonia which is also released can then be shuttled back to the astrocyte and utilised once more. AAT, alanine aminotransferase; Ala, alanine; cGMP, cyclic guanosine monophosphate; Cm, calmodulin; Gln, glutamine; Glu, glutamate; Gluc, glucose; Gluc-6-P, glucose-6-phosphate; GS, glutamine synthetase; GTP, guanosine triphosphate; mGluR, metabotropic glutamate receptor; NH_3 , ammonia gaseous form; NH_4^+ , ammonium ion; NMDA, N-methyl-D-aspartate receptor; nNOS, neuronal nitric oxide synthetase; NO, Nitric Oxide; PAG, phosphate activated glutaminase; PDE, phosphodiesterase; PKC, protein kinase C; PKG, protein kinase G; PLC, phospholipase C; Pyr, pyruvate; sGC, soluble guanylate cyclase. (Taken from Wilkinson et al., 2010)

As with many other systems in the body, the glutamatergic, GABA-ergic and neuronal metabolic systems are closely regulated (Bak et al., 2006, Coles et al., 2008). Under normal conditions these systems function efficiently to maintain adequate neuronal processing (Cauli et al., 2009c, Coles et al., 2008). A major imbalance may arise when blood ammonia levels start to increase, due to a failure of the main detoxification systems, as is the case in liver pathology, or an increase in production levels such as during exercise. Initially any increases may be offset by increases in the production of alanine (Tsacopoulos *et al.*, 1997) and glutamine (Tanigami et al., 2005, Jayakumar et al., 2006) which may act as metabolic sinks within the astrocyte. Astrocytes, however, may only have a limited capacity and may reach saturation levels quickly (Cooper *et al.*, 1985). In addition, the beneficial role of these compounds as sinks for ammonia may be questionable, as increases in glutamine concentrations in the brain have been found to have significant toxic effects (Rama Rao et al., 2003, Jayakumar et al., 2004b). Eventually, ammonia concentrations will start to increase in the brain, which may lead to impairment at several sites in the cellular and subcellular processes of the astrocytes and neurons (Felipo and Butterworth, 2002, Cauli et al., 2009c). This thereby indicates that ammonia may influence brain function in positive

ways at low concentration, by providing necessary substrate for neuronal metabolism and neurotransmission, and negative ways at high concentration by impairing normal cellular function.

The flux of water and other molecules from the blood into the brain is regulated by the BBB (Hawkins *et al.*, 2006) and the movement of ammonia across cellular membranes is limited by chemical form and/or the presence of appropriate transport mechanisms (Ott and Larsen, 2004). Increased levels of ammonia in the blood above the physiological norms leads to an increase in cerebral uptake across the BBB (Nybo *et al.*, 2005, Dalsgaard *et al.*, 2004, Keiding *et al.*, 2006b, Lockwood *et al.*, 1991). This seems to be the case in healthy and diseased states (Lockwood *et al.*, 1991, Keiding *et al.*, 2006b, Nybo *et al.*, 2005, Dalsgaard *et al.*, 2004). Healthy individuals performing exercise which induces significant hyperammonaemia, show a shift from a net balance of ammonia flux at rest, to a significant positive cerebral uptake during exercise (Nybo *et al.*, 2005). Similarly in cirrhosis researchers have reported an increased flux of ammonia into the brain of individuals with hyperammonaemia (Keiding *et al.*, 2006b).

Increased levels of ammonia in brain tissues will, in turn, lead to an increase in glutamine formation in the astrocytes via an increase in flux through the GS reaction, in an attempt to remove and detoxify the excess ammonia (Cooper, 2001). Although glutamine is a non-toxic carrier of ammonia there is evidence to suggest that accumulation of glutamine in brain tissues may impact on cellular function, through activation of secondary mechanisms and its link to osmoregulation of astrocytes (Cooper, 2001).

1.3.1 GLUTAMINE

A common observation in experimental animal models of HE and in acute liver failure (ALF) patients, is evidence of cerebral oedema and cell morphological changes, which can lead to cerebral herniation (Clemmesen et al., 1999, Tofteng et al., 2002, Master et al., 1999, Blei and Larsen, 1999). It has been hypothesised that the process of cellular swelling is due to the increase in intracellular glutamine, evidenced by a correlation between increased brain glutamine (which itself is correlated with arterial ammonia concentrations) and intracranial pressure in ALF patients (Tofteng *et al.*, 2005). Increases in cellular glutamine concentration will draw additional water into the cell, increasing cell volume by osmosis (Bjerring *et al.*, 2008). Under normal conditions this would be counteracted via a process of cellular volume regulatory transport, whereby the mediated cellular release of inorganic ions (K^+ , Na^+ , Cl^-) and organic osmolytes (myoinositol and taurine) assist in reducing or normalising cell swelling (Strange, 1992, Schliess et al., 2006). Such processes are energy dependent and therefore, in the case of pathological conditions such as liver disease, efficient energy provision for these processes may be lacking (Lockwood et al., 2002, Weissenborn et al., 2007), hence contributing to increased cellular swelling (Bjerring *et al.*, 2008). Further evidence to support a glutamine induced swelling hypothesis is provided by studies where inhibition of glutamine synthesis via the GS antagonist methionine sulfoximine (MSO) leads to a reduction of ammonia induced astrocyte swelling in rats (Willard-Mack et al., 1996, Tanigami et al., 2005). Glutamine administered to retinal glial (Müller) cells *in vitro* has been shown to induce rapid swelling, which is accelerated under hypoosmotic conditions, whereas addition of ammonia alone to these cells, showed no significant effect on cell swelling (Karl et al., 2011). The absence of any effect of ammonia on cell volume was attributed to the low intracellular levels of glutamate in these cell types, preventing formation of glutamine (Karl et al., 2011). Co-administration of glutamate and ammonia to the glial cells led to similar levels of cell swelling as observed with glutamine alone (Karl et al., 2011). Taken together, these results highlight the important role of

glutamine in ammonia related cell volume regulation. The mechanisms via which glutamine leads to this cellular swelling are still unclear. Although it may act as an osmolyte as described above, a large body of evidence does provide support for glutamine induced impairment to mitochondrial function via the dissipation of the inner mitochondrial membrane potential and the onset of the mitochondrial permeability transition (mPT; Albrecht and Norenberg, 2006, Pichili et al., 2007, Karl et al., 2011). This will in turn impair cellular energy metabolism and the induction of oxidative stress, interfering with cell volume regulatory mechanisms. In addition or alternatively, more recently it was also identified that glutamine downregulates the expression of astrocyte Kir4.1 potassium channels in culture (Obara-Michlewska et al., 2011). These channels are thought to play a vital role in preventing hyposmotic cell swelling, via potassium efflux (Pannicke et al., 2004), therefore the downregulation via the action of increased glutamine will prevent the regulation of normal cell volume thereby contributing to the induction of cellular swelling (Obara-Michlewska et al., 2011).

Unlike ALF, there are usually no clinical signs of cerebral oedema in patients with cirrhosis and low grade HE². However, using *in vivo* ¹H-magnetic resonance spectroscopy (¹H-MRS) studies, an increase in glutamine/glutamate signal strength and a decrease in the myoinositol signal can be observed in brain slices from a rat model of chronic liver disease (Moats *et al.*, 1993) and in cirrhosis patients with HE (Rovira et al., 2001, Haussinger et al., 2000). This provides some evidence for a glutamine induced cellular oedema mechanism within these more moderate chronic conditions in the absence of overt clinical signs. This is supported by results from some other MRI techniques commonly utilised to monitor water content, such as magnetisation transfer ratio (MTR) imaging (Rovira *et al.*, 2001),

² A re-grading of HE has recently been proposed in order to simplify the process and reduce subjectivity (Haussinger and Schliess, 2008). High grade HE represents patients presenting with severe neurological symptoms such as confusion or coma. Low grade HE categorises patients who are cooperative and present with either no neurological symptoms or mild neurological symptoms. This group consists of those who have previously been categorised as having minimal HE, HE I or HE II (see Haussinger and Schliess, 2008 for further information).

and the recently developed quantitative cerebral water content mapping method (Neeb et al., 2006, Shah et al., 2008), which also identify evidence of cellular oedema in cirrhosis (see section 1.6 for further discussion). Although, the nature of this type of oedema is not likely to lead to such serious complications as increases in intracranial pressure, astrocyte swelling *in vitro* has been found to lead to the production of reactive oxygen species (ROS), which are known to have a number of deleterious effects on cell function (Stewart et al., 2000, Schliess et al., 2004, Schliess et al., 2006, Reinehr et al., 2007). In addition, ROS themselves can augment astrocyte swelling (Sharma, 1996, Brahma et al., 2000, Norenberg et al., 2009), therefore introducing a self-amplifying cycle of ROS production and cellular swelling, which will further increase any associated dysfunction (Schliess et al., 2006, Haussinger and Schliess, 2008). Both ROS production and cellular swelling have been shown to contribute significantly to increases in extracellular glutamate concentrations, through increased efflux of glutamate from the astrocytes (Mongin and Kimelberg, 2002, Kimelberg, 2004, Kimelberg et al., 1990). Whilst ammonia can also directly impair extracellular glutamate uptake rates by astrocytes *in vitro* (Bender and Norenberg, 1996), associated with reduced expression of the membrane glutamate transporters GLAST and GLT-1 (Knecht et al., 1997, Zhou and Norenberg, 1999), in addition to initiating a pH-calcium dependent mechanism of astrocyte glutamate exocytosis (Rose, 2006, Bosoi and Rose, 2009). Such increases in extracellular glutamate levels may lead to impaired glutamatergic neurotransmission through glutamate excitotoxicity.

1.3.2 GLUTAMATERGIC NEUROTRANSMISSION

Glutamate can interact with two types of membrane receptors on the postsynaptic neuron when released into the synaptic cleft;

- Ionotropic receptors: *N*-methyl-*D*-aspartate (NMDA), α -amino-3-hydroxy-5-methyl-4-isoxazole propionate (AMPA), and Kainate
- Metabotropic receptors: metabotropic glutamate receptor (mGluR) (Monfort *et al.*, 2005b)

These receptors once activated initiate a cascade of cellular events which dependent on the type of receptor will assist in regulating normal functioning within the brain. The controlled release of glutamate by the neuron accompanied by the removal and metabolism of extracellular glutamate by the surrounding astrocyte, maintains neurotransmission under normal conditions. However, ammonia has been shown to significantly interfere with the processes of re-uptake when in high concentration within the brain (Cauli *et al.*, 2009c, Rose, 2006). Of the different receptor subtypes, the effects of ammonia on NMDA receptor functioning has been the most widely studied to date (Rodrigo *et al.*, 2009, Montoliu *et al.*, 2010).

When glutamate activates NMDA receptors there is an influx of calcium ions into the postsynaptic neuron. Calcium then binds to calmodulin and activates the calcium dependent enzyme nitric oxide synthetase (NOS) causing an increase in nitric oxide (NO) production (Madhusoodanan and Murad, 2007). NO is an important intracellular messenger which at low concentrations activates soluble guanylate cyclase (sGC), initiating the conversion of GTP to cGMP (Fedele and Raiteri, 1999, Madhusoodanan and Murad, 2007). cGMP, like NO, is also an important intracellular signal, which, depending on the downstream cascade it stimulates, can have a number of different functional roles (Madhusoodanan and Murad, 2007). Therefore, control and tight regulation of its production and the pathways controlling its production within the neuron is essential for normal cellular function (Madhusoodanan and Murad, 2007). For example, alterations in the NMDA receptor-NO-cGMP pathway are evident in a number of pathological disease

states, such as Alzheimer's and Parkinson's Disease (Madhusoodanan and Murad, 2007). One method of regulating this pathway is via degradation of cGMP once its downstream target has been activated, via cGMP-degrading phosphodiesterases (PDE), which are regulated by protein kinase G (PKG), and also via the controlled release of cGMP into the extracellular space (Pepicelli *et al.*, 2004). Extracellular release of cGMP is a useful regulatory mechanism, as it allows for *in vivo* monitoring of intracellular function of this pathway using microdialysis, as changes in extracellular cGMP should represent corresponding changes in the function of the NO-cGMP pathway intracellularly (Pepicelli *et al.*, 2004).

Ammonia affects NMDA receptors in a concentration dependent manner. *In vitro* and animal models of acute ammonia intoxication representative of acute liver conditions, where brain and cellular ammonia concentrations can often exceed 1mM, have been found to lead to overstimulation of NMDA receptors and the NO-cGMP pathway, inducing increased reactive oxygen species (ROS) production in the brain (Kosenko *et al.*, 1999, Hermenegildo *et al.*, 2000). This overstimulation may be caused by a combination of direct stimulation by ammonia (Fan and Szerb, 1993, Hermenegildo *et al.*, 2000), and ammonia induced disruption to astrocyte glutamate handling, leading to increased extracellular glutamate concentrations and glutamate excitotoxicity (Kimelberg *et al.*, 1990, Bender and Norenberg, 1996, Michalak *et al.*, 1996, Zhou and Norenberg, 1999, Hilgier *et al.*, 1999, Chan *et al.*, 2000, Rose *et al.*, 2005b). This increased ROS production initiates a self-amplifying chain of events which may in turn impair mitochondrial function, energy production and eventually lead to coma or death (Kosenko *et al.*, 1999, Kosenko *et al.*, 2003, Kosenko *et al.*, 2007, Hermenegildo *et al.*, 2000). In contrast, the more moderate levels of hyperammonaemia associated with chronic liver conditions, seem to have a rather

different effect on the NMDA receptor, impairing it at levels beyond receptor activation (Hermenegildo et al., 1998b).

Cultured neurons exposed to different moderate ammonia doses (0.01 – 0.1mM) and durations of 15mins, 24hrs and 6 days, showed a reduced formation of cGMP compared to controls when NMDA receptors were stimulated by glutamate (Hermenegildo et al., 1998b). The effect on cGMP production was time and ammonia concentration dependent, therefore the greater the length of ammonia exposure, the greater impairment of the NMDA receptor-NO-cGMP pathway. However, only 15 minutes exposure was needed to produce a significant decrease in cGMP production (Hermenegildo et al., 1998b). In an attempt to assess where ammonia has its effect, the NO generating agent, S-nitroso-N-acetyl-pencillamine (SNAP), was added to the culture medium. If ammonia influenced the pathway before NO-generation, then it should be possible to reverse the reduction of cGMP via SNAP. However, cGMP formation after addition of SNAP was still significantly reduced indicating that ammonia affects the events after NO generation, possibly at sGC activity (Hermenegildo et al., 1998b, Monfort et al., 2001). However, there is some evidence that may indicate effects of ammonia on earlier stages of this signalling pathway. Recent evidence points to a reduction in neuronal NOS (nNOS) activity in brain slices of hyperammonemic rats, by increased phosphorylation of nNOS, potentially implicating interference by ammonia prior to NO generation (El-Mlili *et al.*, 2008).

These *in vitro* findings have been supported by further *in vivo* work. Hermenegildo *et al.*, (1998) used brain microdialysis to stimulate the NMDA receptors in the rat cerebellum through the administration of NMDA. cGMP levels were significantly reduced by up to 60% in hyperammonemic rats, compared to control rats. Basal activity of cGMP, prior to stimulation by NMDA, was also found to be significantly reduced by up to 54% in the

hyperammonemic rats (Hermenegildo et al., 1998b). How this mechanism of impaired cGMP synthesis occurs, remains uncertain, however there is evidence of an indirect mechanism of ammonia in the dysregulation of the NMDA receptor-NO-cGMP pathway, through actions of neurosteroids. Synthesised in mitochondria from cholesterol taken up via the peripheral type benzodiazepine receptors (PTBR), neurosteroids are powerful regulators of neurotransmission in the brain, acting on a multitude of different receptors depending on the type of neurosteroid involved (Zheng, 2009). Evidence has shown that there are increased levels of the allopregnanolone and pregnenolone in the autopsied brain of patients who had died from hepatic coma, and in patients with HE (Ahboucha et al., 2006). With increases in levels of allopregnanolone and tetrahydrodeoxycorticosterone (THDOC) in the cerebral cortex, and increased levels of THDOC and pregnenolone in the cerebellum of hyperammonemic rats also being observed (Cauli et al., 2009a, Zielinska et al., 2011). These neurosteroids have been found to have significant effects on the regulation of cGMP levels within the cerebellum of rats, with pregnenolone, allopregnanolone and THDOC acting as antagonists to the function of the NMDA receptor-NO-cGMP pathway, preventing NMDA induced increases in extracellular cGMP (Cauli et al., 2011). It is this effect of ammonia either directly or indirectly on the NMDA receptor-NO-cGMP pathway, which is believed to contribute to some of the cognitive and neurological disturbances often observed in those with liver disease and other hyperammonemia related disorders.

1.3.2.1 IMPAIRMENTS IN LEARNING AND MEMORY

There is mounting evidence to suggest that regulation of the NMDA receptor-NO-cGMP pathway is essential for control of learning and memory and that disruption to this pathway may lead to impairments in cognitive function (Bernabeu et al., 1996, Bernabeu et al., 1997, Monfort et al., 2009). Blocking the activation of the NMDA receptor-NO-cGMP

pathway using a NMDA antagonist, dizocipine, results in a dose dependent impairment in performance of a Y maze conditional discrimination learning task in mice (Yamada *et al.*, 1996). This impairment was associated with a reduction in cGMP levels in the cerebellum of the mice and after administration of Br-cGMP, a cGMP analogue, the dizocipine induced impairment was reversed (Yamada *et al.*, 1996). The effect on the NMDA receptor-NO-cGMP pathway, by dizocipine, was similar to that reported by Hermenegildo *et al.*, (1998b) in hyperammonemic rats. cGMP was reduced by approximately 50% in the cerebellum compared to controls (Yamada *et al.*, 1996). Therefore, it may be expected that memory and learning would be disrupted in a similar manner in these animal models of hyperammonaemia. Erceg *et al.*, (2005a; 2005b) found a significant impairment in the same Y maze task in rats with chronic hyperammonaemia or portacaval shunting (PCS), which was accompanied by a significant reduction in extracellular cGMP levels in the cerebellum. When these levels of cerebellar cGMP in the hyperammonemic or PCS rats were artificially manipulated via the administration of cGMP or zaprinast/sildenafil (pharmacological agents which prevent cGMP degradation via inhibition of its PDE), cGMP levels significantly increased and this was paralleled by significant improvements in Y maze task learning ability (Erceg *et al.*, 2005a, Erceg *et al.*, 2005b). In contrast increases in cGMP via zaprinast or cGMP administration in control animals resulted in a decreased learning ability (Erceg *et al.*, 2005a). A similar finding was not observed after administration of sildenafil in control rats however, indicating that different types of PDE inhibitors may act in different ways in the restoration of cGMP (Erceg *et al.*, 2005b). These results may imply that under normal conditions the functioning of the NMDA receptor-NO-cGMP pathway in the cerebellum is close to its optimum. Therefore, any perturbation to these normal conditions, such as that provided by ammonia, will impact on the functioning of this pathway, contributing to associated impairments in learning and memory.

Further evidence for the importance of regulation of the NMDA receptor-NO-cGMP pathway in the brain for optimising learning and memory can be observed through its involvement in hippocampal long-term potentiation (LTP). LTP is believed to represent the neurophysiological mechanisms underlying increased synaptic efficiency and plasticity associated with long term memory formation and learning (Lynch, 2004). It has been established that LTP in the CA1 region of the hippocampus is dependent on NMDA receptor activation, and that proper induction and maintenance of the LTP in this area relies upon sequential activation of the NMDA receptor-NO-cGMP pathway (Monfort *et al.*, 2002). Inhibition of this pathway at various stages from the activation of sGC, to the degradation of cGMP by PDE, leads to an impaired tetanus induced LTP in rat hippocampal slices (Monfort *et al.*, 2002). Since ammonia can significantly disrupt this pathway, this is a potential route by which hyperammonaemia could impair LTP and may contribute to deficits in learning and memory in models of hyperammonaemia and liver disease (Aguilar *et al.*, 2000, Mendez *et al.*, 2009).

Hippocampal slices from hyperammonemic rats show impaired induction of LTP, via tetanic stimulation, when compared to controls, with the magnitude of the LTP reduced by almost half (Muñoz *et al.*, 2000). In healthy controls in order to induce and maintain hippocampal LTP there must be sequential activation of the NMDA receptor-NO-cGMP pathway, which first initiates a rapid rise in cGMP, followed immediately by a sustained decline to below basal levels (Monfort *et al.*, 2002). Hippocampal slices treated acutely with ammonia (1mM), however, do not show this sustained decline in cGMP levels and levels remain elevated (Monfort *et al.*, 2004). This demonstrates that hyperammonaemia may impair LTP induction by interfering with the processes controlling regulation of cGMP content. It seems evident from further investigation that ammonia disrupts the efficient degradation of cGMP by preventing the activation of the cGMP degrading PDE through an inhibition of

cGMP PKG (Monfort *et al.*, 2004). This impairment is not restricted to *in vitro* conditions, a study using rat models of chronic hyperammonaemia showed similar, yet less severe impairment of hippocampal LTP (difference in severity likely due to differences in tissue ammonia concentrations; 1mM *in vitro*; 0.1mM *in vivo*), again associated with disruption to the control of cGMP levels through alterations in PKG and PDE activities (Monfort *et al.*, 2005a).

This disruption to the control of cGMP levels will likely impact on aspects of learning and memory associated with the hippocampus, in particular spatial learning, which has been observed to be reduced after pharmacological blockade of hippocampal LTP in rats (Morris, 1989). Furthermore, this type of learning was also found to be significantly disrupted in rat models of chronic liver disease, and as with chronic hyperammonaemia, LTP was impaired (Monfort *et al.*, 2007). However, this impairment was greater than that observed in the rat models of hyperammonaemia alone, suggesting contribution from other precipitating factors to LTP impairment in chronic liver disease additive to ammonia (Monfort *et al.*, 2007).

To summarise, *in vitro* and in animal models, moderate levels of ammonia can directly affect the molecular mechanisms believed to be involved in forms of learning and memory. These effects of ammonia seem to be brain area specific. In the cerebellum for example, evidence points towards a disruption at the level of cGMP synthesis arising from either NOS inhibition (El-Mlili *et al.*, 2008), or a reduced activation of sGC (Hermenegildo *et al.*, 1998b, Monfort *et al.*, 2001), which leads to reduced cGMP synthesis. This reduction in cGMP synthesis in turn, impacts on aspects of learning associated with cerebellar function, such as conditional discrimination learning (Yamada *et al.*, 1996, Erceg *et al.*, 2005a). In contrast, in the hippocampus, ammonia seems to prevent the efficient degradation of

cGMP, via inhibition of PKG activated PDEs (Monfort et al., 2004, Monfort et al., 2005a), impairing both the induction and maintenance of hippocampal LTP. Consequently, hippocampal associated spatial learning abilities are disrupted (Morris, 1989, Monfort et al., 2007). Taken together these actions are likely to contribute to the observed overall learning deficits in animal models of liver disease and hyperammonaemia (Aguilar et al., 2000, Mendez et al., 2009). Another mechanism for disruption to the production of cGMP, and hence impaired learning, has recently been identified in rat cerebral cortical tissue (Zielinska et al., 2011). It has been suggested that increased amounts of glutamine accumulating in extracellular compartments due to ammonia, may lead to increased uptake by astrocytes via the γ^+ LAT2 transporters, which exchange glutamine for arginine (Zielinska et al., 2011). This reduction in intracellular arginine, reduces the availability of the precursor for NO synthesis, and hence impaired cGMP production (Zielinska et al., 2011). Further investigation is required, but this again highlights how delicately balanced the control of this important pathway for regulation of learning and memory is.

Similar disruption at a molecular level in humans as a result of liver disease and associated pathological hyperammonaemia has not been well researched. In one study, however, autopsied brain slices from patients with cirrhosis have shown disruption in the activation of sGC compared to that of healthy brain slices, with increases in sGC activity in the frontal cortex and reductions in activity in the cerebellum (Corbalán *et al.*, 2002). Similar regional alterations in sGC activity can be observed in rat models of liver disease (Monfort et al., 2001, Corbalán et al., 2002), and in cultured neurons exposed to ammonia levels equivalent to chronic hyperammonaemia animal models (Rodrigo *et al.*, 2005). This identifies that similar changes in the brain occur in both rat models of chronic liver disease and patients with cirrhosis. Consequently, the mechanisms constituting cognitive dysfunction in these

rat models may also be present in patients with cirrhosis where significant hyperammonaemia is present.

1.3.2.2 DISTURBANCES IN MOTOR ACTIVITY.

Disruptions to glutamatergic neurotransmission by ammonia are not purely limited to the molecular mechanisms proposed to be involved in learning and memory. Their impact may also extend to the neural circuitry regulating motor output. Normal motor control requires functional connectivity between a number of cerebral areas. However, it is well established that neural projections provided via the basal ganglia are highly involved in the regulation of motor output (Hauber, 1998). Neuroanatomical studies have identified that efferent projections from the nucleus accumbens (NA) innervate the prefrontal cortex (PFCx) via the ventral pallidum (VP) and thalamic nuclei (Churchill et al., 1996b, Churchill et al., 1996a, Churchill and Kalivas, 1999, Mogenson et al., 1983). Artificial activation at the various junctions of this circuit have found an increase in motor activity or excitatory responses in the PFCx (Pirot et al., 1995, Attarian and Amalric, 1997, Meeker et al., 1998, Churchill and Kalivas, 1999). It seems evident that activation of this circuitry is dependent on the release of dopamine in the NA after activation of the metabotropic mGluR group 1 glutamate receptors (Attarian and Amalric, 1997). A number of studies have demonstrated that NA activated locomotion in rats is highly dependent on dopamine release, depletion of dopamine and the action of dopamine receptor inhibitors attenuate mGluR activated locomotion (Attarian and Amalric, 1997, Meeker et al., 1998). Dopamine receptors are known to facilitate the release of GABA from GABAergic terminals (Aceves *et al.*, 1995), which project densely from the NA to the VP (Jones and Mogenson, 1980). The VP provides efferents extending via the medio-dorsal thalamus (MDT) to the PFCx (Churchill and Kalivas, 1999), which are again GABAergic in nature (Churchill et al., 1996b, Churchill et al., 1996a, Churchill and Kalivas, 1999). The PFCx, in turn, provides dense projections to a

number of pre-motor areas which allows this circuit direct access to the areas implicated in movement selection and initiation, and a direct link to the cortico-spinal tract (Lu *et al.*, 1994). Although the neural interactions within these areas are numerous and highly complex *in vivo*, the proposed control provided by this circuitry has been simplified for the purposes of this review and is summarised in Figure 1.5a.

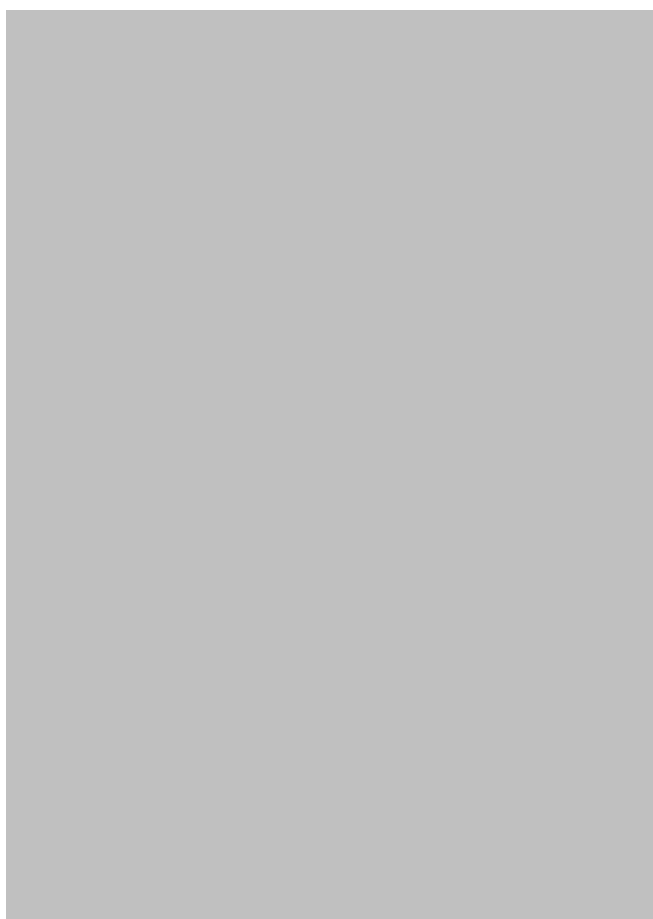


Figure 1.5. Summary of the neural circuitry involved in the regulation of motor activity extending from the basal ganglia. Approximate anatomical positions of the regions involved are illustrated using the outline of a sagittal section of a rat brain. **a.** Pathways involved in motor regulation in the brain of a healthy rat. Excitatory pathway extending from the nucleus accumbens (Solid Line). Inhibitory pathway extending from the substantia nigra pars reticulata (Dashed Line). Neural interconnection between nucleus accumbens and substantia nigra pars reticulata (Dotted Line). **b.** Changes in pathway activation in PCS rats, as observed by Cauli *et al.* (2007a). The inactive 'normal' excitatory pathway (Dotted Line). The active 'Alternative' excitatory pathway extending via the substantia nigra pars reticulata (Solid Line). NA, nucleus accumbens; MDT, medio-dorsal; PFCx, prefrontal cortex SNr, substantia nigra pars reticulata; VMT, ventro-medial thalamus; VP, ventral Pallidum. (Taken from Wilkinson *et al.*, 2010)

To regulate this stimulatory pathway, neural projection from the substantia nigra pars reticulata (SNr), provides inhibitory input to the prefrontal cortex via the ventral medial thalamus (VMT) (Kemel *et al.*, 1988, Miyamoto and Jinnai, 1994, Timmerman and Westerink, 1997). In addition to this, a direct neural connection between the NA and the SNr, is believed to allow the NA to, when stimulated, regulate the inhibitory input from the SNr to the PFCx (Montaron *et al.*, 1996). The complex interaction of these pathways extending from the basal ganglia to the PFCx assist in maintaining appropriate levels of motor output. It is these pathways which have recently been identified as those which may

be compromised under conditions of hyperammonaemia and liver disease (Cauli et al., 2009c, Monfort et al., 2009).

Using rats treated with a portacaval shunt (PCS), to produce a model of chronic liver disease with HE, it was noted that there was a significant decrease in locomotor activity observed in these rat models compared to the control rats (Cauli *et al.*, 2006). This hypolocomotion was found to be significantly correlated to levels of extracellular glutamate in the SNr, suggesting that excess stimulation of the SNr inhibitory pathway may be responsible for decreasing locomotor activity (Cauli *et al.*, 2006). To assess this, the PCS rats were administered a mGluR antagonist, CPCCOEt, which blocked mGluR activation in the SNr. Administration of the antagonist led to an 85% increase in motor activity in the PCS rats, but no effect in the controls (Cauli *et al.*, 2006). These results suggest that biochemical changes which accompany liver disease may directly impair gross motor activity via disruption of the neural pathway extending from the SNr. Because this disruption is associated with an increased level of extracellular glutamate, it may implicate ammonia as a causal factor in the disruption to locomotor activity, due to its effects on astrocyte glutamate handling (Rose, 2006).

Other disruption to the neuronal circuits implicated in motor activity, have recently been identified by the same research group. Using the same model of liver disease, the 'normal' excitatory neuronal circuit regulating motor activity extending from the NA→VP→MDT→PFCx was found to be significantly disrupted in PCS rats (Cauli et al., 2007b). In control rats, stimulation of mGluR receptors in the NA using the mGluR1 agonist (5)-3,5-dihydroxyphenylglycine (DHPG), led to an increase in locomotion and coincided with the activation of the 'normal' neuronal circuit (Cauli et al., 2007b). In PCS rats however, activation of this circuit was absent, due to a blocking of dopamine release. Even so, there

was still a significant stimulatory increase in locomotion in these rats (Cauli et al., 2007b). It was subsequently identified that locomotion in the PCS rats was achieved via an 'alternative' pathway which involves activation of the neural projections between the NA and SNr (Figure 1.5b), providing an excitatory input to the PFCx, via the SNr and VMT, in addition to its inhibitory input (Cauli et al., 2007b). Locomotion via stimulation of this 'alternative' NA→SNr→VMT→PFCx pathway in PCS rats was significantly greater than that stimulated via the 'normal' pathway in controls. This finding suggests that in PCS rats there may be an associative hypersensitivity, contributing to the alterations in normal motor function (Cauli et al., 2007b).

Because ammonia is believed to play a major role in liver disease associated dysfunction, this same research group examined the effects of hyperammonaemia in the absence of liver disease, to assess whether it was the cause of this dysfunction to the 'normal' NA→VP→MDT→PFCx neuronal circuitry (Cauli et al., 2007c). In both control and hyperammonemic rats, locomotion was significantly increased and was associated with activation of the 'normal' circuit (Cauli et al., 2007c). However, in hyperammonaemia, the 'alternative' circuit, identified to be activated in the PCS rats, was also found to be active (Cauli et al., 2007c). The activation of both the 'normal' and 'alternative' neuronal circuits in hyperammonemic rats led to significantly greater levels of motor output compared to controls, again identifying disruptions to normal motor functions (Cauli et al., 2007c). Although, hyperammonaemia was found to activate the 'alternative' circuit, as in PCS rats, it did not completely inhibit the 'normal' circuit. This suggests that either other co-occurring factors in liver disease contribute to the disturbances in the neuronal circuitry observed (Cauli et al., 2007c), as with hippocampal LTP, or the levels of hyperammonaemia reached in rat models of chronic hyperammonaemia, are not great enough to provide the complete inhibition of the 'normal' circuit (Cauli et al., 2007c). Both explanations are

plausible, recently PCS rats were reported to have three fold greater ammonia levels in their brain tissues than in rats with chronic hyperammonaemia (PCS rats, $1.8\mu\text{mol/g}$ tissue; Hyperammonaemia rats, $0.55\mu\text{mol/g}$ tissue; Cauli *et al.*, 2007b). Such increases in brain ammonia levels could be causing the additional dysfunction within the basal ganglia. However, in addition to this, the co-occurrence of inflammation in liver disease could also influence motor activity, as it has been observed that a reduction in inflammation, via the administration of the non-steroidal anti-inflammatory ibuprofen, helps to restore motor function in PCS rats (Cauli *et al.*, 2009d). Consequently, the direct effect of ammonia on neuronal function may not be the only precipitating factor behind motor dysfunction in liver disease states. Despite the implication of other precipitating factors these results demonstrate that mechanisms associated with hyperammonaemia can significantly influence the regulation of motor activity in animals, by interfering with the neural control of the basal ganglia-thalamo-cortical pathways.

Similar impairment to the motor-cortical drive as reported in animal models is believed to translate into humans. Timmerman and colleagues have recently demonstrated using magnetoencephalography, significant impairment to the coupling of thalamic and motor cortical activity in patients with cirrhosis (Timmerman *et al.*, 2003). Whilst also showing reduced cortical-muscular coupling between primary motor cortex activity and EMG of the extensor digitorum longus muscle in patients with cirrhosis and HE (Timmermann *et al.*, 2008). This reduced cortico-muscular coupling was found to be significantly correlated with HE severity as assessed by standardised computer based psychometric test batteries, with higher levels of cortico-muscular impairment observed with increasing HE grades (Timmerman *et al.*, 2008). These findings demonstrate a significant dysfunction to the thalamo-cortical neural drive in these patients, and although it is not possible to measure in intact human brain, these findings suggest that this impairment may be due to the neural

disruption of the basal-ganglia-thalamo-cortical circuitry observed within animals described previously and linked with hyperammonaemia.

1.4 EVIDENCE OF PSYCHOLOGICAL IMPAIRMENT DUE TO HYPERAMMONAEMIA.

Impairment in learning and memory, cognition, and motor activity are evident throughout the whole spectrum of HE severity (Weissenborn et al., 2005). Although the exact aetiology of these neuropsychological disturbances remain unresolved. The *in vitro* and *in vivo* evidence provided in section 1.3.2 helps to explain some of the molecular and neural mechanisms behind the functional deficits in learning and memory, and motor processes associated with liver disease and other such hyperammonaemia related disorders. As such, it is generally accepted that ammonia toxicity is a primary precipitating factor in the development of these neuropsychological disturbances and HE symptoms (Haussinger and Schliess, 2008). This link is further strengthened by a number of recent elegant studies utilising the induction of hyperammonaemia via oral amino acid challenge in liver disease patients. Due to the impaired function of the liver and associated metabolism in these patients, gut derived ammonia, provided by the breakdown of the orally administered amino acid solutions, cannot be metabolised as efficiently as in a healthy control (See figure 1.6 from Ortiz et al., 2004). This leads to transient hyperammonaemia, where plasma concentrations can be increased by anything up to 1.5 to 2.5 fold basal concentrations, peaking at between 105 – 240 $\mu\text{mol/L}$, and lasting up to 1-4 hours in duration. Table 1.1 summarises recent studies which have involved this method of investigation.



Figure 1.6. Plasma ammonia concentration after oral glutamine challenge in cirrhosis patients (n=6, open squares) and healthy controls (n=4, closed squares), (taken from Ortiz et al., 2004)

Table 1.1. Summary of oral amino acid challenge studies in cirrhosis patients where cognitive measures have been collected.

Ref	Oral AA Load	Basal Ammonia Conc	Peak Ammonia Conc	Measures
<i>Oppong et al., (1997)</i>	20g L-glutamine	58µmol/L	120µmol/L	Psych: Digit Symbol Substitution Test, NCT, Information Processing Task A, CRT, EEG
<i>Masini et al., (1999)</i>	20g L-glutamine	83ug/dl	210ug/dl	Psych: NCT, Posner's Attention Test, Sternberg Paradigm.
<i>Rees et al., (2000)</i>	20g L-glutamine	Mean not provided	Increase of 48±7µmol/L	Psych: NCT, CRT, EEG
<i>Douglass et al., (2001)</i>	40g AA mixture	68µmol/L	120µmol/L	Psych: PHES battery, Digit Span Test, CRT, EEG
<i>Romero-Gomez et al., (2002)</i>	10g L-glutamine	70ug/dl	127ug/dl	Psych: Block Design Test, Digit Symbol Test, NCT
<i>Jalan et al., (2003)</i>	75g Haemoglobin AA Solution	87µmol/L	105µmol/L	Psych: Immediate Story Recall Test, SPECT; Cerebral Perfusion Measures
<i>Masini et al., (2003)</i>	20g L-glutamine	79ug/dl	211ug/dl	Psych: NCT, Covert Visual Attention Orienting Test, Scan Test
<i>Balata et al., (2003)</i>	75g Haemoglobin AA Solution	76µmol/L	121µmol/L	Psych: Trails B Test, Digit Symbol Substitution Test, Immediate Story Recall Memory Test, CRT, MRI: MRS and MTR
<i>Olde Damink et al., (2003)</i>	75g Haemoglobin AA Solution	75µmol/L	122µmol/L	Splanchnic Metabolism
<i>Shawcross et al., (2004a)</i>	75g Haemoglobin AA Solution	73.5µmol/L	115µmol/L	Psych: Same as Balata et al., (2003) MRI: MRS
<i>Ortiz et al., (2004)</i>	20g L-glutamine	110µmol/L	240µmol/L	Psych: Subsets of WAIS-III, MRI: MRS
<i>Mardini et al., (2008)</i>	108g AA solution	63µmol/L	126µmol/L	Psych: CDRS, PHES.
<i>Mardini et al., (2011)</i>	18g Each of Ser, Thr and Gly	Mean not provided	Increase of 58±41µmol/L	Psych: CDRS MRI: DTI and MRS.
<i>Bersagliere et al., (2011)</i>	54g Haemoglobin AA Solution	202ug/dl	~ 325 ug/dl	Psych: PHES, Subjective Scales EEG

Using this method for inducing hyperammonaemia, it has been observed that there is significant impairment in immediate memory recall (Balata et al., 2003b, Jalan et al., 2003, Shawcross et al., 2004a), delayed memory recall (Jalan et al., 2003), episodic memory (Mardini et al., 2008), and reaction time (Oppong et al., 1997, Rees et al., 2000, Douglass et al., 2001) after oral amino acid challenge in liver disease patients. Taken together these results highlight deterioration in behavioural components of cognition, and learning and memory associated with the onset of hyperammonaemia, and thereby support the hypothesis that ammonia toxicity is a significant component in causing neuropsychological impairment and HE symptoms in liver disease. Findings from these studies are not consistent however, although the aforementioned studies reported significant deterioration in neuropsychological task performance; Masini et al., (2003), Mardini et al., (2011) and Bersagliere et al., (2011) were unable to find significant impairment in any of the neuropsychological tasks performed after induction of hyperammonaemia (Masini et al., 2003, Mardini et al., 2011, Bersagliere et al., 2011). Whilst the number connection test (NCT), a test which has been commonly used in the diagnosis of mHE in liver disease patients (Weissenborn, 2008, Weissenborn et al., 2001, Weissenborn et al., 1998), consistently showed no appreciable performance decrement after hyperammonaemia (Oppong et al., 1997; Rees et al., 2000; Douglass et al., 2001; Masini et al., 2003). The inconsistent findings from these studies may be due to methodological issues; differences in AA challenge, dosage and neuropsychological tasks used, which does make comparison difficult. However it also raises doubts in the importance and contribution of ammonia to impairment in liver disease and onset of HE.

It has often been believed that in disease the determining factor behind ammonia toxicity is the integrity of the blood brain barrier (BBB). Lockwood et al., (1991) identified a significantly higher BBB permeability surface area (PS) product in liver disease patients

compared to healthy controls using ^{13}N -ammonia positron emission tomography (PET). This helped to explain the inconsistencies often observed between HE severity and arterial ammonia levels (Ong et al., 2003, Kundra et al., 2005), suggesting that the effects of hyperammonaemia in liver disease were perhaps due to impaired function of the BBB rather than the levels of peripheral hyperammonaemia (Lockwood et al., 1991). This would suggest that even with similar levels of hyperammonaemia occurring in physiological conditions such as exercise, the same impairment in brain function due to ammonia may not be possible due to the intact BBB preventing accumulation of ammonia within the brain tissues. More recently, however, other ^{13}N PET studies have identified that the cerebral trapping of ^{13}N labelled ammonia, is similar in both cirrhotic patients without HE, cirrhotic patients with HE and healthy controls (Keiding et al., 2006b, Keiding et al., 2006a, Sorensen and Keiding, 2007). This finding suggests that brain ammonia kinetics may be similar in diseased and healthy states and that flux of ammonia into brain tissue may be strongly related to arterial concentrations (Sorensen and Keiding, 2007). In addition, Goldbecker and colleagues have reported that there was no difference in cerebral blood flow, unidirectional transport of ammonia from blood to the brain, permeability surface area product of the BBB for ammonia, or the metabolic rate of ammonia, between patients with liver fibrosis, cirrhosis and healthy controls again using ^{13}N and ^{15}O PET scanning (Goldbecker et al., 2010). Furthermore, studies involving healthy exercising individuals have also reported significant cerebral uptake of ammonia under conditions of exercise induced hyperammonaemia (Dalsgaard et al., 2004; Nybo et al., 2005). Using a-v difference as a measure of cerebral uptake, it was found that at rest there was a net balance of ammonia across the brain, however after 3 hours of exercise there was a significant uptake of ammonia into the brain of $3.7 \pm 1.3 \mu\text{mol}\cdot\text{min}^{-1}$, which again was related to arterial ammonia concentration (Nybo et al., 2005). These more recent findings into the cerebral transport and metabolism of ammonia contradict those originally reported by Lockwood et al., (1991), and there is now more evidence in favour of the BBB being intact in disease, and

ammonia uptake being dependent on arterial concentration, rather than being due to BBB integrity. These findings would therefore suggest that pathological levels of ammonia in healthy individuals may lead to a similar accumulation of ammonia in the brain as observed in disease, where it would be sensible to assume that the ammonia may cause similar neurotoxicity and hence induce reversible impairment in brain function. Even so, this still remains a hotly debated topic (Sorensen and Keiding, 2007, Lockwood, 2007).

1.5 MRI CHANGES DUE TO LIVER DISEASE/HYPERAMMONAEMIA

Since their introduction in the early 1990s, the use of quantitative magnetic resonance imaging techniques in the clinical progression and/or diagnosis of certain pathologies and tissue injuries, in addition to age related structural changes has become increasingly widespread (Rovira et al., 2008, Kantarci and Jack, 2004, Draganski et al., 2011, Li et al., 2010). The specific details regarding the progress and development of quantitative MR are beyond the scope of this thesis, and for more information the reader is guided towards Toft (2003). However the advent of more powerful and sophisticated hardware developments such as ultra high field magnets (Tkac et al., 2001, Harel et al., 2006), along with the development of innovative imaging sequences to elucidate specific biological actions (Neeb et al., 2006), will ensure that the capabilities and application of this technique within the clinical and research setting continues to progress at a rapid rate.

1.5.1 MAGNETIZATION TRANSFER RATIO (MTR)

Magnetization transfer describes the interaction in tissues between protons bound to macromolecules (proteins, cell membranes etc.) and mobile protons (free protons; water). In standard MRI the bound proton pool could be termed 'MR invisible', as they are difficult

to detect directly due to their short (<1ms) T2 relaxation times (Wolff and Balaban, 1994). Figure 1.7 illustrates the absorption linewidths of the free and bound proton pools. The free proton pool has a very narrow absorption linewidth centred around the Larmor frequency, whilst the bound proton pool has a much



Figure 1.7. Illustration of absorption linewidths of the free (liquid) and bound (macromolecular) proton pools. An off-resonance rf pulse saturates the bound proton pool. (Taken from Henkelman et al., 2001)

broader absorption linewidth (Henkelman et al., 2001). Hence the majority of conventional MR signal comes from the free proton pool as the MR excitation frequency is centred around that of the free proton pool (Grover et al., 2006). Although the bound pool contributes little to conventional MR, its coupling with the free proton pool via dipolar coupling or direct chemical exchange allows these bound protons to influence the spin states of the free protons and hence the MR signal through magnetization transfer (Henkelman et al., 2001). This is performed by applying an off-resonance radio frequency excitation pulse which preferentially 'saturates' the bound proton pool so that there is no net longitudinal magnetization (Wolff and Balaban, 1994). The coupling between the two proton pools allows the transfer of this 'saturation' to the free proton pool decreasing the longitudinal magnetization in this pool and therefore reducing the MR signal (Henkelman et al., 2001). Tissues which show little magnetization transfer, due to lack of coupling between proton pools or a lack of macromolecules, lead to the free proton pool being unaffected. In tissues with magnetization transfer, the free proton pool signal is decreased (Wolff and Balaban, 1994).

MT imaging allows properties of more biologically relevant tissues to be investigated (Tofts et al., 2003), and clinically is used in magnetic resonance angiography to improve image contrast, enhancing signal from blood and suppressing the background tissue signal (Henkelman et al., 2001). Another clinical application of MT imaging is in the detection of tissue pathological changes, particularly in brain. The magnetization transfer ratio (MTR) can be used for this:

$$MTR = 100 \frac{(M_0 - M_s)}{M_0} \quad (\text{Equation 6; Tofts et al., 2003})$$

M_0 is the signal in the absence of saturation, and M_s is the signal in the presence of the saturation pulse. MTR describes the % reduction in the MR signal as a result of the saturation rf pulse, and in a simplification of the exact physical mechanisms is the product of; RfT_{1a} , (Equation 7) where R is the exchange rate coupling of the two proton pools, f is the fraction of bound protons, and T_{1a} is the T1 relaxation of the free proton pool (Tofts et al., 2003). Therefore a decrease in MTR could represent a decrease in the bound proton fraction, and hence pathological alterations in the tissue. The application of this in disease has predominantly been used for the characterisation of brain tissue pathologies in multiple sclerosis (MS). There is a significant decrease in MTR values in MS patients compared to healthy controls, which is believed to represent lesional changes in normal appearing white matter (van Buchem et al., 1996), and it is commonly used in this disease as a marker of demyelination and axonal loss (Giacomini et al., 2009a). Its application can extend to other cerebral pathologies, and recently alterations in MTR have been described in cirrhosis (Iwasa et al., 1999), hyperammonaemia (Balata et al., 2003b), and hepatic encephalopathy (Miese et al., 2006).

Studies utilising MT imaging in chronic liver disease patients consistently report decreased brain region MTR values compared to that of healthy controls (Iwasa et al., 1999, Rovira et

al., 2001, Cordoba et al., 2001, Miese et al., 2006, Miese et al., 2009, Poveda et al., 2010). These MT imaging findings suggest some pathological alteration in the brains of patients which affects the MTR value, however there is some debate as to what is exactly causing this change. Unlike MS patients where MTR values can decrease by anything up to 50% of that of normal appearing white matter (Rovira et al., 1999), in cirrhosis the decrease in MTR values is far more subtle ranging from 8 (Iwasa et al., 1999) to 15% (Cordoba et al., 2001). As such, this has led authors to suggest that, rather than being due to pathological disruption to tissue structure in the form of axonal loss or demyelination, the MTR changes may be related to cerebral oedematous changes via an increase in the free proton pool (Rovira et al., 2001). This hypothesis is supported by correlations between decreases in MTR and changes in MRS metabolite ratios believed to represent alterations in cell osmolarity (Cordoba et al., 2001, Miese et al., 2006, Miese et al., 2009, Poveda et al., 2010). Whilst changes in water content are related to changes in T_1 relaxation times (Fatouros et al., 1991, Neeb et al., 2006), therefore according to equation 7 above, changes in T_1 will lead to changes in overall MTR. This is supported by more recent observations showing that MTR can be significantly affected by changes in cerebral water, oedema and inflammation, with significant correlations between water content in MS brain tissues and decreases in MTR values (Vavasour et al., 2011). Although uncertainty remains as to the specific brain tissue pathological changes relating to decreases in MTR values in cirrhosis, there is evidence to suggest that these changes may be a direct result of hyperammonaemia induced cerebral impairment. Firstly reductions in MTR values in cirrhosis patients are normalized post liver transplant, suggesting that MTR changes are a direct result of altered liver metabolism, potentially that of ammonia (Cordoba et al., 2001). In addition, non-cirrhotic patients with extrahepatic portal vein obstruction, which leads to increased porta-caval shunting and hyperammonaemia, showed equivalent subtle yet significant reductions in MTR as in liver disease patients (Goel et al., 2010). Whilst induction of hyperammonaemia via oral AA feeding in cirrhosis patients has been found to

lead to a significant reduction in MTR values (Balata et al., 2003b), with similar reductions in MTR values seen in non-cirrhotic portal vein thrombosis patients, after induction of hyperammonaemia (Mínguez et al., 2006)

1.5.2 DIFFUSION WEIGHTED IMAGING

Diffusion weighted MRI utilises the diffusion characteristics of water (or other molecules in tissues) to probe tissue structure at a cellular level (Le Bihan et al., 2001). Molecular diffusion in an unrestricted environment or pure liquid, describes a random path (Brownian motion), which is dependent only on the molecular weight, intermolecular interactions and temperature, which can be described using a diffusion coefficient, which represents the root mean square displacement over time (Beaulieu, 2002). Molecular diffusion is complicated somewhat within an enclosed environment such as tissues, barriers provided by cell membranes, macromolecules etc.. restrict random motion (Beaulieu, 2002). Diffusion weighted MRI uses this interaction between diffusing molecules and their environment to probe tissue structure and related pathological changes (Wheeler-Kingshott et al., 2003). Over a normal diffusion time of 100ms or less, a water molecule within brain tissue will interact with a number of structures which will impede its motion, decreasing its overall diffusion distance and displacement (Le Bihan, 2003). In biological tissues, the apparent diffusion coefficient (ADC), describes this interaction between diffusing water molecules and the surrounding biological environment (Grover et al., 2006). This ADC value can be measured using diffusion weighted MRI, high ADC values where there is minimal impedance to the molecular diffusion, e.g CSF, result in a greater reduction in the signal produced in the diffusion weighted (DW) image, than those with more restricted motion and lower ADC values, such as white matter, where there are more barriers to diffusion in the form of membranes and organelles (Sotak, 2004, Mori and Zhang, 2006). Diffusion is however, a 3 dimensional process, and depending on the tissue

structures involved will not be the same in all directions, and is termed *anisotropic*, ADC being a scalar property can only describe diffusivity along either the x, y or z axis (Le Bihan et al., 2001). To gain a better insight into the diffusion of water using DW imaging, a diffusion tensor (DT) can be applied, which is a mathematical model which describes water mobility in all directions and the correlations between these directions (Le Bihan et al., 2001). Analysis of this DT imaging, provides additional information regarding tissue microstructure via two measures: Mean Diffusivity (MD), this value predominantly describes the same measure of diffusion as ADC, however ADC is dependent on subject orientation in the scanner and the direction of the imaging gradients applied (Wheeler-Kingshott et al., 2003), whereas the use of the diffusion tensor to calculate the MD minimises the influence of the direction of magnetic field gradients on the measurement. Although $ADC \approx MD$, the presence of imaging gradients effects the calculation of the ADC, therefore ADC and MD do not always represent one and the same thing, and this should be taken into consideration where interpreting diffusion imaging findings. The other measure provided by the application of the DT is Anisotropy (Fractional; FA or Relative; RA; Le Bihan et al., 2001). MD is the overall mean squared displacement of water molecules, and can be affected by obstacles to displacement; e.g increased obstacles such as cell membranes or other molecules, reduces overall MD. Whilst anisotropy describes the amount to which these displacements vary in space, and will depend on size, shape and integrity of any physical barriers to diffusion, such as nerve fibres (Grover et al., 2006). FA will be low in environments where water diffusion is not restricted, such as free pools of water, whereas in highly structured tissues such as white matter, diffusion is likely to be highly restricted in certain directions due to physical barriers such as membranes and organelles, therefore here FA values will be high reflecting this structured environment (Heiervang et al., 2006).

The application of DW and DT MR imaging to describe pathological changes relating to neurological diseases is becoming more widespread. As with MTR, DTI has been found to be useful to describe microstructural tissue damage in MS, with decreases in MD and reductions in FA reported in MS patients compared to healthy controls (Cercignani et al., 2001). Demyelination is a consequence of MS, and as myelin contributes to the high anisotropy of brain white matter (Wheeler-Kingshott et al., 2003), these changes, in particular reductions in FA, may be representative of MS histopathology through a breakdown of myelin and overall loss of fibre organisation (Hasan et al., 2005).

Animal and cell models of liver disease, and hyperammonaemia show characteristic changes in brain water content, astrocyte structural changes and resultant mild cerebral oedema (see section 1.3). The nature of diffusion weighted imaging to describe the diffusivity of water in relation to microstructural tissue changes could allow this imaging technique to probe such changes *in vivo* and act as a useful monitoring/diagnostic tool. The findings from studies which have utilised diffusion weighted imaging for this purpose to date are somewhat contradictory. Whilst the hypothesis surrounding ammonia induced cerebral water content changes and low grade cerebral oedema proposes that changes in osmolyte concentration draws water into the cell, leading to a cytotoxic cellular oedema (see section 1.3.1). ADC values have been repeatedly found to be increased in patients with cirrhosis compared to healthy controls (Lodi et al., 2004, Miese et al., 2006, Sugimoto et al., 2008) with one study showing no change in ADC values (Poveda et al., 2010). This increase in ADC does not represent changes indicative of cytotoxic cellular oedema, induction of experimental cytotoxic oedema in rats leads to significant reduction in ADC values (Sevick et al., 1992), whilst in stroke patients where water diffusion is believed to be restricted due to ischaemia, ADC values are normally reduced post stroke and then gradually normalise with time (Lansberg et al., 2001). Similar changes in ADC values were

also seen after induction of hyperammonaemia in cirrhosis patients, with a significant increase in ADC of 9% following hyperammonaemia (Mardini et al., 2011), and using animal models of hyperammonaemia, where increases in ADC values were observed in five brain regions (Cauli et al., 2007a). However there was a decrease in ADC in the hippocampus, suggesting regionally selective actions of ammonia on brain water diffusivity. Using DTI, both Kale et al., (2006) and Kumar et al., (2008) found increased MD in cirrhosis patients with HE, which again points towards increases in extracellular/interstitial oedema rather than the proposed intracellular oedema in line with the ammonia detoxification theory. Similar MD data were also reported in non-cirrhotic portal vein obstruction patients with significant hyperammonaemia (Goel et al., 2010). Few studies have reported data regarding FA characteristics in cirrhosis patients or under hyperammonaemia, of those which have FA is generally unchanged (Kale et al., 2006; Goel et al., 2010), which suggests that cirrhosis/HE only induces changes in cellular water distribution, rather than causing lesional damage and breakdown of the tissue integrity. This may explain the reversible nature of HE symptoms following treatment (Shawcross et al., 2004b). However, Kumar et al., (2008) did report slightly contrasting findings, with significant decreases in FA in frontal and occipital WM, which suggests damage to tissues. The authors concluded that this may have been due to the cause of cirrhosis in the patients studied being Hepatitis C virus (Kumar et al., 2008), however the chronic nature of cirrhosis may eventually lead to more permanent lesional brain tissue changes, and hence observed decreases in WM FA. This literature provides a rather unclear picture with regards to the proposed mechanisms behind ammonia induced cerebral changes in cirrhosis, the hypothesis of mild cytotoxic oedema as a consequence and cause of HE is not supported by DW imaging findings, with interstitial water accumulation more commonly observed. It may be the case that cytotoxic oedema is only prevalent in more severe forms of the disease, and cases of acute liver failure, where DW imaging findings support the presence of this form of oedema (Ranjan et al., 2005, Nath et al., 2008, McKinney et al., 2010).

1.5.3 ^1H -MAGNETIC RESONANCE SPECTROSCOPY (^1H -MRS)

^1H -Magnetic Resonance Spectroscopy was the first quantitative MR tool to be utilised in an attempt to describe cerebral impairments in cirrhosis and hyperammonaemia. MRS uses the fundamental properties of nuclear magnetic resonance of certain nuclei, in this case ^1H , to measure signals of different metabolites within a sample (Cousins, 1995). A hydrogen nucleus has a specific resonant frequency (Larmor) when placed in a magnetic field. When a rf is applied to this nucleus it is excited, and during the relaxation period following excitation, a voltage signal can be detected which contains information about the environment or chemical make-up in which the ^1H nucleus is contained (Cox, 1996). This signal is transformed into a frequency spectrum, and the frequency is dependent on the chemical make-up of the molecule, therefore different metabolites will be placed at different points along the spectral axis (see figure 1.8), and the intensity of the signal is proportional to its concentration (Cox, 1996). The application of MRS therefore allows alterations in the chemical environment of tissues to be monitored non-invasively, which is a useful tool for both research and clinical applications (Taylor-Robinson, 2001). One of the major problems with ^1H -MRS in particular is the effects of the water signal. The high concentrations of water in tissues means it dominates the spectra affecting the signal to noise ratio for smaller concentration metabolites, however techniques to suppress water signals during MRS acquisition can improve resolution (Tofts and Waldman, 2003).

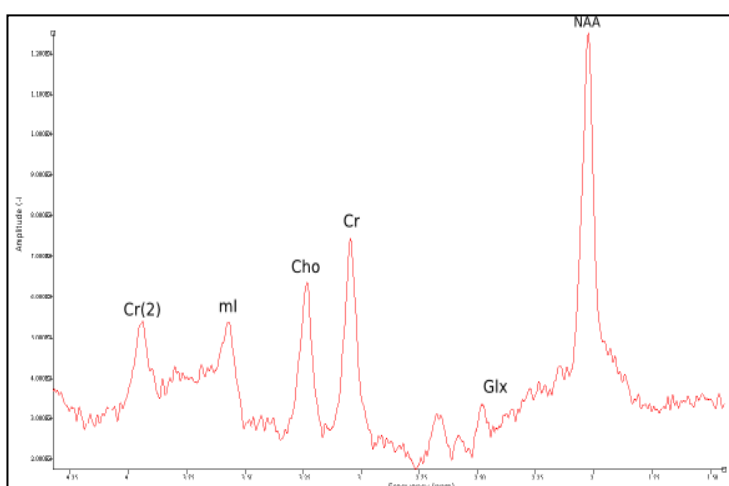


Figure 1.8. Example ^1H -MRS Spectrum with prominent metabolites labelled. NAA; N-Acetylaspartate, Glx; Glutamine/Glutamate, Cho; Choline, Cr; Creatine Peak 1, Cr(2); Creatine Peak 2, ml; Myoinositol

Kreis and colleagues were the first to observe changes in metabolites in the parietal cortex of cirrhosis patients using ^1H -MRS (Kreis et al., 1991). Showing increased signal intensities for glutamine (however we can assume that by this the authors actually mean glx, which represents both glutamine and glutamate, these are complex overlapping multiplets which at short echo times and low power magnets, are difficult to definitively separate in most MRS spectra; Tofts and Waldman, 2003), with a reduction in myoinositol signal intensities in cirrhosis patients compared to controls (Kreis et al., 1991, Kreis et al., 1992). At the time the significance of such changes in metabolite concentrations was uncertain. However, the glutamine (or glx) signal increase can be attributed to the increased metabolic role of brain tissue in the detoxification of ammonia in cirrhosis patients (Kreis et al., 1991). Haussinger and colleagues, a few years later, proposed a mechanism relating to these changes (Haussinger et al., 1994). Applying MRS in patients with hypo-osmolarity and HE, it was found that ml signal intensity was vastly reduced in patients with hypo-osmolarity, but normalised after treatment, suggesting osmoregulatory properties of ml in cell volume homeostasis (Haussinger et al., 1994). With decreases in ml signal intensity in HE also observed, it was proposed that this represents cell volume changes in HE patients and cirrhosis which could act as mechanisms in developing neurological impairment in these patients (Haussinger et al., 1994). Increases in glutamine within brain tissue have been shown to be related to changes in cell volume and oedema; cerebral concentrations of glutamine correlate with increases in intracranial pressure in acute liver failure patients (Bjerring et al., 2008), whilst inhibition of GS with MSO in astrocytes *in vitro* attenuates levels of glutamine whilst also returning cellular oedema to control levels (Tanigami et al., 2005). Using astrocytes incubated with ammonium chloride *in vitro*, NMR spectral changes replicate those observed with *in vivo* MRS, glutamine and glutamate levels increased significantly with a concomitant decrease in ml levels (Zwingmann et al., 1998). Therefore

not only could *in vivo* MRS changes in glx and ml signals be indicative of the onset of cell volume changes within brain, these changes indicate a mechanism regulated by ammonia.

Unlike the inconsistencies reported with some other quantitative MR measures in cirrhosis and hyperammonaemia, the findings of increases in glx signal combined with reductions in ml signal have been consistently reproduced in studies over the years (Kreis et al., 1991, Kreis et al., 1992, Haussinger et al., 1994, Geissler et al., 1997, Huda et al., 1998, Ross et al., 1994, Tarasow et al., 2003, Sawara et al., 2004, Binesh et al., 2006, Lee et al., 1999, Miese et al., 2006, Singhal et al., 2009), to reference but a few of these studies. Increase in glx and decreases in ml, have also been shown to correlate with increases in plasma ammonia levels and increases in ammonia cerebral uptake rate in cirrhosis patients, in addition to correlating with impairment in neuropsychological test scores (Weissenborn et al., 2007). Whilst normalisation of MRS changes can be observed after liver transplant (Cordoba et al., 2001). Not only this, but the actions of ammonia in inducing these MRS changes *in vivo* are only the more evident in studies which have generally reported the characteristic increases in glx and reduction in ml in response to orally induced hyperammonemia in cirrhosis (Balata et al., 2003; Shawcross et al., 2004a), with the same MRS changes reported with non-cirrhotic portal venous obstruction patients and hyperammonaemia (Goel et al., 2010). However some discrepancies can be observed in glutamine MRS changes (Mardini et al., 2011). These findings highlight that ¹H-MRS is a useful quantitative MR tool for monitoring of ammonia induced cerebral changes, and shows more reproducible and consistent results compare with other MR techniques. One potential difficulty highlighted recently with the interpretation of MRS data however, is that most MRS data is represented as metabolite ratios, where the metabolite of interest is referenced to a metabolite believed to be relatively stable, in most cases Creatine. Barba et al., (2008) reported that this may introduce error, as it was observed that creatine levels in rat brain decreased with disease

severity. Although this was not found to be statistically significant, this could lead to uncertainty in some reported findings, particularly those of longitudinal studies where treatments and disease progression are being assessed. The use of more sophisticated analysis techniques, such as that of the metabonomic approach used by Barba et al., (2008) could address such issues however (Barba et al., 2008, Williams et al., 2008).

1.6 EFFECTS OF HYPERAMMONAEMIA ON PERIPHERAL TISSUES

Much of the literature to date regarding the effects of hyperammonaemia *in vivo* has concentrated on its impact upon central nervous system function, with peripheral effects largely overlooked. Considering the significant effects hyperammonaemia can have on neuronal and astroglial cell types, it would only be sensible to assume that ammonia may have similar effects on other cell types within the periphery. Ammonia concentrations under hyperammonaemia can reach as high as 200 - 300 μ mol/L depending on the severity of the physiological (Brouns et al., 1990, Nybo et al., 2005) or pathological (Clemmesen et al., 1999, Olde Damink et al., 2002b) stress, allowing high concentrations of ammonia to come into contact, and potentially effect, multiple organs and tissues in the body. There is evidence to suggest that ammonia can impair protein metabolism in both hepatocytes (Hopgood et al., 1977, Seglen, 1975, Seglen and Reith, 1976), and renal cells (Golchini et al., 1989, Franch, 2000). However, the concentrations which induce these changes vastly exceed concentrations normally observed (10mM +), and it seems unlikely that function of these cells would be affected within normal ranges of ammonia concentrations.

In contrast, skeletal muscle serves as an important metabolic sink for ammonia uptake and removal in liver disease, due to reduced functional liver capacity (Olde Damink et al., 2009, Olde Damink et al., 2002b), with skeletal muscle consuming 301 ± 41 nmol/kg/min of

ammonia in chronic liver disease patients compared to 204 ± 55 nmol/kg/min in the liver (Olde Damink et al., 2002b). Highlighting its importance in these conditions for ammonia metabolism. Whereas during hyperammonaemia in exercise, skeletal muscle is the site of ammonia production, with only ~10-25% being released from muscle (see section 1.2.2.2), allowing intramuscular ammonia concentrations to rise as high as 1 – 2mM (Katz et al., 1986, Snow et al., 2000). This accumulation of ammonia within muscle may directly affect contractility. Ammonia has been reported to depolarise neuronal and astroglial cells (Fan and Szerb, 1993, Coles et al., 1996, Allert et al., 1998), and early findings using isolated frog muscle showed a dose dependent depolarisation of muscle fibres when exposed to ammonium ions (Heald, 1975). However, this effect was only observed at supraphysiological ammonium concentrations (30mM – 120mM). No effect has been observed within physiological or pathophysiological concentration ranges of 0.11 – 5mM (Stephenson and Stephenson, 1996, Shanely and Coast, 2002).

More recently ammonia has also been shown to have a significant impact on cellular protein metabolism. Proteins are the building blocks of the cell, careful regulation of protein metabolism is required to ensure optimum cell functioning. Early studies reported that ammonia concentrations (10mM) could inhibit protein degradation pathways in hepatocytes via depression of lysosomal proteolysis (Seglen, 197), inhibit protein synthesis, represented by incorporation of radiolabelled alanine into protein, in neocortical brain slices (Schott et al., 1984), and suppressing protein degradation, without effects on synthesis, in renal NRK-52E epithelial cells (Franch, 2000). These effects of ammonia on cellular protein metabolism could also be significant in skeletal muscle cells. Recently findings using hyperammonaemic rats, showed that whole body protein breakdown (estimated via turnover of ^{14}C -Leucine) was decreased along with protein synthesis in the skeletal muscle after infusion of ammonium acetate to induce hyperammonaemia

(Holecek et al., 2000). Similar findings of suppressed skeletal muscle protein synthesis can also be observed in PCA rats who present with significant hyperammonaemia (Dasarathy et al., 2011). The mechanisms behind these ammonia related alterations in skeletal muscle protein metabolism remain unresolved. It has been proposed that decreased AA availability through increased need for oxidation to glutamate to maintain efficient ammonia removal, may be a factor (Holecek, 2010, Holecek et al., 2000). AA are known to have potent anabolic effects, regulating protein synthesis at a molecular level through the control of intracellular signalling proteins important in the regulation of mRNA translation (Proud, 2007). This intracellular signalling centres around the activation of the mammalian target of rapamycin complex 1 (mTORC1), and the complex nature of the related signalling for the control of protein metabolism is illustrated in figure 1.9. Other factors regulated via ammonia may also be implicit in the control of protein metabolism at a molecular level. Alterations to gene expression, and systemic pH, can be observed with increases in systemic ammonia (Dasarathy et al., 2004, Caso et al., 2004), and have also been found to significantly alter intracellular signalling via mTORC1, and associated skeletal muscle protein metabolism (Evans et al., 2008, Dasarathy et al., 2011).



Figure 1.9. Illustration of complex molecular signalling relating to mTORC1. Highlights the numerous mechanisms believed to be controlled via mTORC1, including the regulation of protein metabolism. Taken from Laplante and Sabatini (2009).

This proposed effect of ammonia on protein metabolism could have important implications in situations of hyperammonaemia. Cirrhosis patients rely heavily on skeletal muscle for ammonia detoxification, therefore if protein metabolism is impaired as a result, muscle wasting may occur affecting the whole body ammonia buffering capacity in these patients. It is well known that during exercise, protein synthesis is depressed (Gautsch et al., 1998, Dreyer et al., 2006, Rose and Richter, 2009), therefore the hyperammonaemia caused by the onset of exercise may be a mechanism by which depression of protein synthesis during exercise is affected.

1.7 QUESTIONS SURROUNDING THE 'TOXIC' EFFECTS OF AMMONIA

Support for the 'toxic' actions of ammonia, particularly on CNS, is widespread in the literature. Much of this literature has stemmed from the need for a better understanding of the aetiology of encephalopathy in liver disease, for the development of therapeutic interventions. As such, ammonia has long been considered the primary precipitating factor in the development of hepatic encephalopathy in liver disease, through its widespread, multiple neurotoxic actions (Felipo and Butterworth, 2002, Cauli et al., 2009c, Monfort et al., 2009, Wilkinson et al., 2010). With many HE treatment strategies primarily aimed at reducing ammonia production, or increasing ammonia removal (Bass, 2007, Phongsamran et al., 2010). Yet questions still remain over its true contribution to hepatic encephalopathy and whether such 'toxic' actions actually occur *in vivo* (Butterworth, 2008, Butterworth, 2011).

Liver failure is highly complex, consisting of a multitude of pathologies and metabolic disturbances. Impaired hepatic and splanchnic metabolism, leads to the accumulation of a number of potential toxins in addition to ammonia;

- Manganese
- Mercaptans
- Phenols
- Octanoic Acid (Butterworth, 2008)

whilst also leaving the patient prone to infection and the systemic inflammatory response. A number of these co-morbidities show many of the neurotoxic effects attributed to ammonia. Manganese has been found to induce astrocyte swelling (Rama Rao et al., 2007), the production of ROS to a greater extent than ammonia (Jayakumar et al., 2004a), whilst also impairing locomotor activity in rats through action on GABAergic neuronal activity in the substantia nigra pars reticulata (Yang et al., 2011). Relationships have also been observed between inflammatory cytokines and HE severity (Odeh et al., 2005), with IL-1 β and TNF-alpha impairing glutamatergic metabolism in astrocytes (Hu et al., 2000), in addition to inducing the mitochondrial permeability transition (mPT) and concomitant oxidative stress (Alvarez et al., 2011).

In a recent study by Shawcross and colleagues, it was identified that hyperammonaemia associated cognitive dysfunction was only observed in the presence of systemic inflammation (Shawcross et al., 2004b). Cirrhosis patients with a systemic inflammatory response syndrome (SIRS) score of 2 or more were fed an oral amino acid feed (75g AA mimicking haemoglobin) to induce hyperammonaemia, a standard neuropsychological battery was performed before the administration of the AAs, and at 2 and 4 hours after administration. The same procedure was

performed after resolution of the infection with antibiotics (Shawcross et al., 2004b).

Hyperammonaemia impaired performance on cognitive, and learning and memory tasks in the inflammatory state, however upon resolution of inflammation there was no impairment in the same neuropsychological tasks even with the same severity of hyperammonaemia being induced (Shawcross et al., 2004b). Similar results were also found using animal models. PCS rats were found to have significantly impaired learning and memory, and slowing of motor activity compared to sham operated controls (Cauli et al., 2007d, Cauli et al., 2009d). After treatment with the anti-inflammatory drug ibuprofen, learning and memory, and motor abilities were restored (Cauli et al., 2007d; Cauli et al., 2009b). It was identified through these studies that ibuprofen treatment in PCS rats is associated with the normalisation of some of the impaired cerebral processes believed to control these cognitive and motor functions highlighted in section 1.3. Treatment with ibuprofen normalises cGMP levels in cerebellum, in association with restored learning in PCS rats (Cauli et al., 2007d), whilst reducing extracellular glutamate in the SNr, in association with restored motor control (Cauli et al., 2009b). An interaction between hyperammonaemia and neuroinflammation has been recently proposed to control these impairments in learning and motor control. The same group showed that chronic hyperammonaemia in rats induced activation of microglial cells (a common marker of neuroinflammation), and subsequent accumulation of inflammatory markers in brain (Rodrigo et al., 2010). Treatment with ibuprofen, again restored learning and motor control in these rats, whilst also eliminating microglial activation and hence neuroinflammation (Rodrigo et al., 2010). These findings were replicated in a bile duct ligation rat model of liver disease using ibuprofen (Rodrigo et al., 2010), and in PCS rats treated with an inhibitor of p38 mitogen-activated protein kinase (p38 MAPK; an intracellular signalling molecule believed to be involved in inflammation, Agusti et al., 2011), suggesting that hyperammonaemia initiates neuroinflammation which in turn leads to cognitive and motor impairment (Rodrigo et al.,

2010, Agusti et al., 2011). This discreet interaction between inflammation and hyperammonaemia in pathology has further been supported in a study by Pederson et al., (2007), where rats administered lipopolysaccharide (LPS) to induce an inflammatory response showed an increase in intracranial pressure, which was significantly increased further by the co-administration of ammonium acetate (Pedersen et al., 2007).

These studies thereby question the role played by ammonia alone in the development of HE symptoms, and also the significance of the proposed neurotoxic actions highlighted from animal and cell culture studies. The findings discussed suggest that HE symptoms may be primarily a neuroinflammatory condition, secondary to hyperammonaemia. Further research by Shawcross and colleagues has identified that ammonia can significantly impair immune function *in vitro* and *in vivo*, by affecting neutrophil phagocytosis (Shawcross et al., 2008). This suggests that ammonia may predispose liver patients to infection/inflammation by impairing the normal immune response which will in turn exacerbate symptoms of HE (Shawcross et al., 2010). More recently it has also been suggested that ammonia may not be indicated in some forms of HE at all, with infection more prominently associated with hospitalised cirrhosis patients with severe onset HE (Shawcross et al., 2011). The pathophysiology of liver disease and HE are clearly highly complex and rely on the interaction between multiple metabolic disturbances brought about by the failing liver. From the evidence presented, it seems ammonia does have a role to play in the development of HE, however the extent of this contribution is questionable and still warrants further investigation. Such findings will have specific implications on therapeutic strategies in chronic liver disease, where at present the reduction of hyperammonaemia is the primary therapeutic aim (Butterworth, 2011). Treatment of hyperammonaemia alone may not be as beneficial as first thought.

1.9 SUMMARY

Ammonia is an important metabolite required by a number of tissues and organs in the body in order to maintain normal function. Problems begin to arise when the normal metabolism of ammonia is perturbed, through either increased production (e.g. exercise), or decreased removal (e.g. liver disease). In such situations, other tissues are recruited in order to compensate for the decreased liver function and assist in metabolising this excess ammonia; two such tissues particularly important for this are brain and skeletal muscle. However, evidence from cell and animal models has highlighted that excess ammonia in these tissues can significantly impair normal function, effecting the control of neurotransmission and cellular energy production in brain cells, and amino acid and protein metabolism in skeletal muscle. In humans, conditions where hyperammonaemia commonly occurs such as exercise or liver disease, can often be associated with impaired cognitive function and motor control, whilst in some cases also showing signs of skeletal muscle wasting and/or altered protein metabolism. Therefore this evidence combined with the effects observed in animals and cells, has led to the proposal that ammonia is a primary cause of these changes, and has guided investigators to develop nutritional or therapeutic interventions aimed at decreasing hyperammonaemia in order to ameliorate such effects (Phongsamran et al., 2010). Yet despite the extensive research performed within this area over the past 50 years, the causal link between ammonia and the effects on brain and muscle function remain uncertain. Hyperammonaemia in humans occurs alongside a number of other metabolic changes, all of which could contribute to these commonly observed functional and metabolic impairments. Thus the initial aims of this thesis were two fold; Firstly using a method developed specifically for this thesis, an acute state of experimental hyperammonaemia was induced in healthy humans at rest to investigate the

effects of ammonia on cerebral functioning using behavioural and quantitative MR imaging techniques. This method isolates the effects of ammonia on the brain from other metabolic changes which are present in exercise or disease, allowing a better understanding as to the causal consequences of hyperammonaemia in humans, and hence its overall contribution to the cerebral impairment often associated with this condition. Secondly, with the high levels of ammonia which can accumulate in skeletal muscle due to hyperammonaemia, and the association between hyperammonaemia and wasting/altered protein metabolism, this thesis aimed to investigate the effects of ammonia on isolated muscle cell protein metabolism, with particular attention paid to the molecular mechanisms which may be controlling these effects in muscle. Collectively these results will allow an expansion of our understanding as to the causal consequences of hyperammonaemia in humans and the mechanisms underlying alterations in cellular function and metabolism. Such knowledge will have wide ranging application in conditions where hyperammonaemia is prevalent, imparting a better understanding for identifying potential therapeutic or nutritional targets, in both clinical and healthy populations where hyperammonaemia may impact.

CHAPTER 2: GENERAL METHODS AND MATERIALS

This section describes the materials and procedures used in all the experimental chapters. Any additional procedures specific to individual experiments are described in chapters concerning those experiments. Data collection took place in the Welkin Laboratories of the Chelsea School, University of Brighton in Eastbourne, the Clinical Imaging Sciences Centre (CISC) of the Brighton and Sussex Medical School (BSMS) in Falmer, or the Division of Clinical Physiology of the Graduate Entry Medical School, University of Nottingham.

2.1 HEALTH AND SAFETY

Ethical approval for all the experimental procedures was granted by the University of Brighton Research and Ethical Governance Committee and the Brighton and Sussex Medical School Ethics Committee, and procedures were performed in accordance with the World Medical Association Declaration of Helsinki (1975) for the use of human research participants. The availability of a qualified first aider or appropriate medical staff was ensured throughout. Sterility of all equipment used was maintained. Any non-reusable items were disposed of in appropriate waste disposal containers for incineration.

Experimental testing was ceased if:

- The participant requested.
- The experimenter deemed that the participant should not continue due to adverse reaction or side effects to experimental treatment.

Inclusion Criteria:

The nature of the testing meant that several inclusion criteria were implemented. All participants had to be:

- Male, due to the significant differences in ammonia metabolism between sexes (Esbjornsson et al., 2006).
- In good general health.
- Free from any history or family history of the following; Cardiac or circulatory conditions (e.g. abnormal ECG, angina, atherosclerosis), Neurological conditions, Kidney or Liver conditions, Diabetes, and other serious medical conditions. If family history of any of the above was uncovered, the condition was discussed with lead supervisor (Dr. Watt). If contraindicated to the experimental treatment, the participant was removed from the testing group.
- Currently not taking any medication or supplementation contraindicated with the administration of ammonium salts.

For the MRI testing in chapter 5, additional inclusion criteria for participants were required due to the nature of the procedure. These criteria are outlined in an example safety questionnaire in appendix 1. Each participant completed a safety questionnaire prior to their first MRI scan, this was reviewed by the resident radiographer, and participants were only included in the study if the radiographer deemed they were safe to do so.

2.2 PARTICIPANTS

All participants were recruited from the undergraduate and postgraduate student populations of the University of Brighton. Participants were recruited via a combination of poster

advertisements, email advertisement and direct recruitment through verbal explanations. Prior to participation, the procedures and risks involved in the testing were explained in detail both verbally and in writing, before written informed consent was obtained. In addition to this, each participant was required to fill in a detailed health/medical questionnaire (see appendix 2) and participants were only included in the studies if they fulfilled the criteria described above. Each participant was informed that they were free to withdraw from testing at any point, even after data collection was complete, and that if they did decide to withdraw their data would be disposed of in accordance with the data protection act (1992).

2.3 STANDARDISATION

Prior to testing each participant was required to abstain from caffeine, alcohol and strenuous exercise for 24 hours. An overnight fast of 12 hours was also implemented to ensure that they were in a post-absorptive state, so that dietary protein had minimal influence on basal plasma ammonia concentration. Any fasting greater than 8 hours in duration is effective in ensuring this (Bisschop et al., 2003).

2.4 EXPERIMENTAL PROCEDURES FOR CHAPTERS 3, 4 AND 5

The procedure utilised in all human studies (Chapters 3,4 and 5) for the administration of the intravenous infusions will now be described.

Each participant was requested to arrive at approximately 8.45am for testing. The participants were made comfortable in a seated position and two 18 gauge cannulae were inserted

(Biovalve PTFE, Vygon, France). The cannula for the dominant side was inserted antegrade into the antecubital vein, and was used for the infusion of the assigned solution. On the non-dominant side the cannula was inserted retrograde into a digital vein on the dorsum of the hand (in later studies, chapters 4 & 5, both cannulae were placed in the same non-dominant arm to free up the dominant arm for performance of tasks). This cannula was used for the collection of arterialised blood samples, and was kept patent via a continuous slow flow of sterile 0.9% sodium chloride (Baxter, UK). The non-dominant hand was then placed in a temperature controlled hot box (University of Brighton), which maintained a consistent temperature range of between 48 and 52°C through a continuous flow of hot air (mean \pm SD over 1hr; $50.4 \pm 1.8^\circ\text{C}$, see figure 2.1). This method of heating the hand was performed to allow the collection of arterialised venous blood through the opening of anastomoses in the hand. Arterialised venous blood is preferred to venous blood in studies of metabolism as venous blood can be influenced by local tissue metabolism. Conversely, arterialised venous blood has been found to be almost indistinguishable from arterial blood for analysis of metabolites (Frayn and Macdonald, 1992), and has been validated for the investigation of ammonia metabolism (Greenhaff et al., 1991, Lambert et al., 1993). After approximately 15 minutes with the hand in the Hotbox, a 10 ml basal blood sample was drawn from the cannula. Once the basal sample had been collected the intravenous (iv) administration line for the infusion was attached to the other cannula and the infusion was started. The infusion administration rate was controlled via a Volumed VP5000 Infusion Pump (Arcomedical Infusion LTD, Essex, UK). The rate of infusion and duration of infusion was dependent upon the experimental chapter and is described in detail within each experiment.

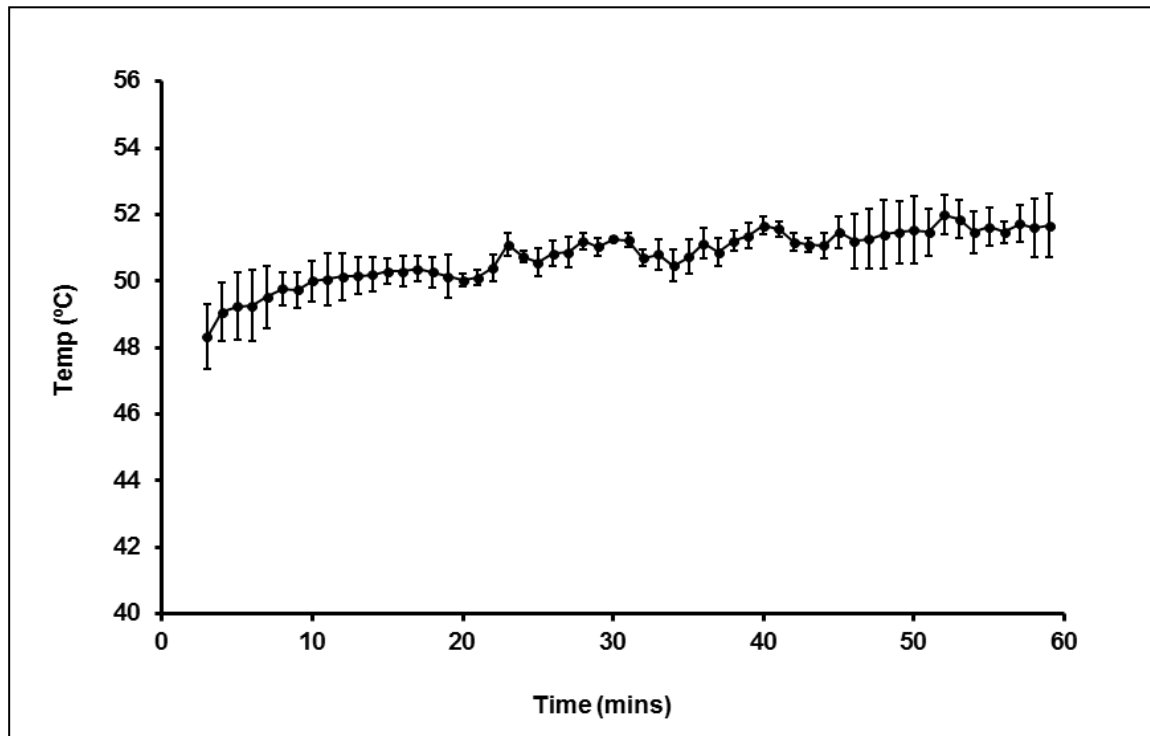


Figure 2.1. Mean (\pm SEM) temperature of Hotbox used for collection of arterialised venous blood over three different days during 1 hour of use.

Throughout the course of each infusion 10ml whole blood samples were obtained at regular intervals (Chapter 3; 10 and 30 minute intervals, Chapter 4; 60 minute intervals, Chapter 5; 15 minute intervals). In addition to this sampling, every 10 minutes a measure of subjective rating scores of perceptions of fatigue, discomfort and nausea were collected (Chapters 3 only). The subjective scores were performed using Borg's Category Ratio (CR10) scale (Borg, 1998), which is a general intensity scale that can be used to identify how strong an individual's perception of a certain attribute is (see figure 2.2; Borg, 1998). In the case of these experiments it was implemented with these categories to monitor each participant's responses and levels of tolerance to the infusions. The CR10 scale has been implemented for the investigation of each of these attributes previously (Borg, 1998, Dederling et al., 1999, Hager, 2003, Thorburn et al., 2006)

0	Nothing at all	“No P”
0.3		
0.5	Extremely Weak	Just noticeable
1	Very Weak	
1.5		
2	Weak	Light
2.5		
3	Moderate	
4		
5	Strong	Heavy
6		
7	Very Strong	
8		
9		
10	Extremely Strong	“Max P”
11		
●	Absolute Maximum	Highest Possible

Figure 2.2. Example of the Borg CR10 Scale Description

In chapters 4 and 5 the Multi-Dimensional Fatigue Severity Index-Short Form (MFSI-SF) questionnaire (Stein et al., 1998, Stein et al., 2004) was administered to rate changes in subjective sensations of fatigue in the participants during the infusions. The MFSI-SF is a multi-dimensional tool for measuring levels of fatigue. It has been extensively validated using cancer patients (Stein *et al.*, 2004), however it is not disease specific and hence is applicable to measure fatigue in many different situations, for example in; non-medical healthy populations (Bardwell *et al.*, 2006), patients with sleep apnoea (Yue *et al.*, 2009), and patients with muscle and joint pain (de Leeuw *et al.*, 2005). This questionnaire requires the participants to rate the severity of a list of 30 statements designed to assess the multi-dimensional nature of fatigue. They each rated their responses using a standard 5-point Likert scale (0 = not at all; 4 = extremely) to each of the 30 statements as to how they were feeling at that moment. For each completed MFSI-SF, five subscale scores were obtained for different dimensions of fatigue;

general fatigue, physical fatigue, emotional fatigue, mental fatigue and vigour. A total score of the overall sensation of fatigue can then be calculated from the sum of the first four subscales minus the vigour score. An example of a questionnaire can be observed in Appendix 3.

At the end of the assigned infusion duration, the infusion was stopped and each participant was monitored for a further 20 minutes, during which blood collection was continued at 10 and 15 minute intervals. Both cannulae were then removed, and this marked the end of the testing.

2.4.1 PSYCHOLOGICAL TASKS

The following describes the psychological tasks used in chapter 4 of this thesis.

2.4.1.1 CONTINUOUS COMPENSATORY TRACKING (COMPTRACK) TASK (Makeig and Jolley, 1996)

This task was downloaded from the authors website (<http://sccn.ucsd.edu/~scott/>; no longer available for free download) and is programmed using C and administered via a computer through the MS DOS interface. The task required participants to keep a randomly moving disc as close as possible to a bullseye in the centre of the computer screen by correcting the position of the disc using a joystick. The position of the disc on the screen is a function of the perturbation forces applied to the disc by the program (the sum of six sine waves with different frequencies, amplitudes and random phase angles), and that of the force provided by the action of the participant through the joystick. The x and y Cartesian coordinates of the disc are

sampled approx. 14 times per second and these are saved as a text file with the velocity and force data once the task is complete. Each performance of this task lasted 4 minutes.

2.4.1.2 INHIBITORY CONTROL TASK (ICT: Garavan et al., 1999)

This task was programmed using DMDX (www.u.arizona.edu/~kforster/dmdx/dmdx.htm) according to the original task description provided in Garavan et al., (1999). The task required participants to recognise and respond when the target letters X and Y were presented on a computer screen. The target letters X and Y were randomly embedded within strings of consecutive letters presented in the centre of the computer screen at a rate of one every 500ms. When the target letters were presented, the participant responded as quickly as possible by releasing the spacebar key (at all other times the participant was asked to keep the spacebar depressed). Participants were only to respond to the targets when they were presented in alternating order (e.g. **X** n a m b u **Y**), when one target letter was followed by the same target letter (e.g. **X** n a m b u **X**) participants were told not to respond. If they did respond, this counted as an error. The task recorded number of errors and reaction time (ms) for each correct target response and each incorrect target response.

2.4.1.3 AUDITORY VERBAL LEARNING (AVL) TEST (Lezak, 2004)

The auditory verbal learning test is a paper pencil task used to assess learning, short term and long term memory. The test consists of eight trials in total and lasts approximately 15 minutes. For trial 1 the experimenter reads a list of 15 words (example word list provided in Appendix 4) to the participant at a rate of one per second. The participant is then asked to repeat back as many words from this list as they can remember. The experimenter notes down the words on

a response sheet as they are repeated back. Any errors are also noted down, these may be any of the following;

- The same word repeated twice.
- The same word repeated twice but corrected.
- The same word repeated twice but questioned.
- Any words which were not on the original list.

Once the participant can remember no more words, the experimenter repeats the list again for trial 2 and the participant is asked to do the same again and repeat back as many words from the list as they can remember. The same is repeated again for trials 3, 4 and 5. On completion of trial 5, the experimenter then reads a new list of 15 words to the participant, and they are again asked to repeat back as many words as they can remember from this new list.

Immediately after this, the participant is asked to remember as many words from the original list as possible. 45 minutes later the participant was asked again to repeat back as many words from the original list as possible. Scores for each trial are the total number of words correctly remembered. Learning, short-term memory and long term memory as well as error scores can also be calculated.

2.5 Magnetic Resonance Imaging (MRI)

MRI was used to quantify structural and functional changes to the brain in chapter 5. All scanning was performed using a Clinical Siemens Magnetom AVANTO 1.5T Scanner (Siemens AG, Erlangen, Germany), with a conventional head coil. Each scan was performed in the following order:

1. MP RAGE (structural t1w image)
 2. 3D GRE MTR (with MTC)
 3. 3D GRE MTR (without MTC)
 4. T2w TSE localizer in transaxial plane (wikus)
 5. T2w TSE localizer in sagittal plane (wikus)
 6. T2w TSE localizer in coronal plane (wikus)
 7. Spectroscopy
 8. DTI
-

The total scan time ranged between 1h 10mins and 1h 30mins, depending on the length of time required to collect spectroscopy measurements. Throughout the scan radiographers and experimenters were in regular contact with the participant to explain procedures and scan times.

2.5.1 SCAN TASKS

The tasks performed during the MRI study are described in more detail below. Presentation of the tasks were performed using code written in-house (Dr. Marcus gray, BSMS) using the Cogent tool box for MATLAB (www.fil.ion.ucl.ac.uk/cogent).

2.5.1.1 ICT Task

This task follows the same protocol as that described above. The only difference being that the participant was required to respond via button press rather than lifting of keyboard spacebar. Each performance of the task was preceded by a practice session for familiarisation. The task lasted 10 minutes in total.

2.5.1.2 NUMBER CONNECTION TASK

This task is commonly used in the literature for diagnosis of minimal hepatic encephalopathy in cirrhosis patients (Weissenborn et al., 1998). It is traditionally performed as a paper pencil task, however for this study it has been computerised for ease of administration whilst in the scanner.

Participants were presented with numbered circles ranging from 1 to 10 on a screen in a random order (see Figure 2.3). Using an MR compatible joystick they were required to move a cursor on the screen from circle to circle in numerical order, clicking on each circle using a button on the joystick with the aim of reaching circle number 10 within a time period of 25

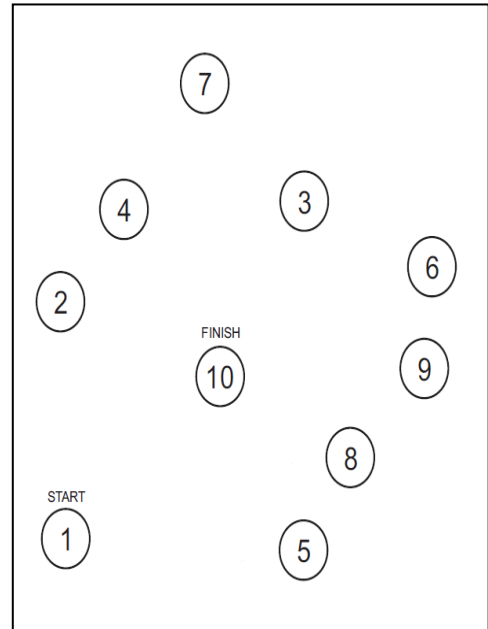


Figure 2.3. Example of screen shot from number connection test.

seconds. Once the time had elapsed, whether the participant had reached circle number 10 or not, the

next sequence of circles was presented, and the same was repeated. A total of ten sequences were presented for the participant to complete, interspersed with control sequences where the participant was required to repeatedly move the cursor back and forth between two circles. The task lasted approximately 10 minutes.

2.5.2 SCANNING ACQUISITION AND PARAMETERS

Described below are the scanning parameters for each of the scanning sequence listed above.

2.5.2.1 MTR

After acquisition of a T1 weighted MP-RAGE structural scan (TR/TE=1160/4.44ms, TI=600ms, FOV=230 x 230 mm, Slice Thickness=0.9 mm, Acquisition Matrix=256 x 256, Flip Angle = 15°, scan time: 4m 58s), two 3D gradient echo images were obtained (TR/TE=30/5ms, Slabs=1, Slices=64, Slice Thickness=2.5 mm, Flip Angle=5°) using a matrix of 256 x 192 pixels with a field of view of 220 x 220 mm. The first images were acquired with magnetization contrast (MTC) on, and the second with MTC off. Scan time: 12m 20s.

2.5.2.2 ¹H- MRS

Short T2 weighted localisers were initially performed in the coronal, sagittal and transverse planes for positioning of the voxel (Scan time: 3m 45s). Following localised shimming and water suppression until the line width of the water signal was between 9 and 14hz, single voxel spectra were obtained from a volume of interest (2cm³) in the frontal white matter of the right hemisphere using the PRESS acquisition method. Parameters were as follows; TR/TE = 1500/30ms, Voxel Size = 2 cm², Averages = 192, Flip Angle = 90° (Scan time: 3m 18s).

2.5.2.3 DTI

DTI was acquired using a standard echo planar imaging with 30 diffusion directions and 2 diffusion weightings (b-values of 0 and 1000 s.mm⁻², scan time: 6m 45s). Parameters were set as: TR/TE=6.4 /0.11s, Slices=34, Slice Thickness=5mm, FOV=220x220mm.

2.5.3 ANALYSIS

Prior to analysis the raw MRI files (Dicom format) were converted to NIfTI (.nii) file format using MRI convert 2.0 (Lewis Centre for Neuroimaging, University of Oregon) for MTR analysis, or FSL NIfTI file format for DTI analysis. During this process the MRS data file was identified and filed ready for analysis.

2.5.3.1 MTR

Segmentation of the T1 MP-RAGE was performed using SPM 8 (Wellcome Centre for Neuroimaging, London UK) to create gray matter (GM), white matter (WM) and cerebral spinal fluid (CSF) probability maps. The magnetisation transfer contrast images (MTC on and MTC off) were then transformed into the same image space as the structural scan using the SPM co-registration option. Using these transformed MTC on and MTC off images MTR maps were created using the application beckmtr2 (written in-house, Dr. Nicholas Dowell, BSMS). The resulting MTR map was smoothed in image (<http://rsb.info.nih.gov/ij/>) by adding a specified noise at a standard deviation of 50. MTR masks were then created using the application beckmask4 (Dr. Nicholas Dowell, BSMS). The smoothed MTR map was loaded in as the source image, along with the GM, WM and CSF probability maps. Threshold values were set at 0.70 for CSF and 0.95 for GM and WM, and masking was applied to the source image to create GM, WM and whole brain (WB) MTR masks. From each of these masks a MTR histogram was created using the application beckhist2 (Dr. Nicholas Dowell, BSMS) and the following parameters (Bins:350, Min:60, Max:7060, Smoothing factor:20), each was saved as a text file and exported into a MS excel spreadsheet. Histogram analysis not only allows the extent of changes in MTR within brain to be assessed but also the severity of any changes (Della Nave et

al., 2007). Each histogram produced is normalised, so that the total AUC was equal to 100, this ensures that the parameters measured by the histogram for MTR will be independent of any effect of participant brain size (Pagani et al., 2007). From each histogram the following parameters can be obtained; peak height (maximal normalised pixel count value), peak location (modal MTR value), and the mean histogram MTR (average MTR value across whole brain section). Comparisons can then be made of these MTR histogram parameters between trials for WM, GM and WB, to quantify any changes.

2.5.3.2 DTI

To correct for any movement distortions in the images, eddy current correction is performed using the FSL eddy correct package. Using these corrected images Fractional Anisotropy (FA) and Mean Diffusivity (MD) probability maps were calculated using dtifit (FMRIB Software Library FSL, www.fmrib.ox.ac.uk). Following extraction of the T2 weighted images, these were segmented using SPM8 in the same way as for MTR to create T2 GM, WM and CSF probability maps. FA and MD brain masks were then created using beckmask4. The FA and MD maps were loaded in as the source images, along with the GM, WM and CSF T2 probability maps. Threshold values were set at 0.70 for CSF and 0.8 for GM and WM, and masking was applied to the source images to create GM, WM and whole brain (WB) FA and MD masks. From each of these masks a histogram was created using beckhist2 and the following parameters:

	MD			FA		
	GM	WM	WB	GM	WM	WB
No. of Bins	360	240	360	200	200	200
Min	2e-4	2e-4	2e-4	0.01	0.01	0.01
Max	2e-3	1.4e-3	2e-3	1.01	1.01	1.01
Smoothing	5e-6	7.5e-6	7.5e-6	0.005	0.00875	0.0075

Each was saved as a text file and exported into a MS Excel spreadsheet. Histogram analyses techniques are similar to that described for MTR, each histogram produced is normalised to remove any effects of brain size, for DTI measures total AUC was normalised equal to 1000. Peak height, peak location and mean histogram values were then obtained for FA and MD in WM, GM and WB, and compared between trials to quantify any changes.

2.5.3.3 ¹H-MRS

The MRS file was loaded into jMRUI (www.mrui.uab.es/mrui/), after visual checking of the spectra for errors or anomalies, the x axis was scaled by referencing the prominent water peak to 4.7ppm and reversing the spectrum. This spectrum was then saved as a .txt file for exporting into the MATLAB based spectral analysis program, **Simulation Package based on In vitro Databases (SPID v0.3; Katholieke Universiteit Leuven)**. The SPID program uses the AQSES quantitation technique to process spectra, this models the spectra to a database of known metabolites collected using the same scanning sequence (in this case PRESS at 1.5T) stored in the program, to obtain information regarding metabolite intensity. To ensure accurate processing, the MRS spectra to be analysed first needs to be preprocessed. The metabolite database used for quantitation may not always be aligned with the MRS spectra to be analysed

due to chemical shifts caused by temperature and pH variations. Therefore the two spectra should be aligned using a reference peak, in this case NAA was used (as this is most prominent peak in the filtered spectrum), this was shifted from 2.06ppm to 2.01ppm using the align function to match the metabolite database. Following this the signal to noise ratio was improved using the apodization function, and the water peak was removed using a HSLVD-PRO filter pack, model order was set at 25, with the filter passband set from 0.25 – 4.0 ppm ensuring that all peaks to the right of the water peak (< 4.7ppm) remain whilst the water peak is removed. The spectra were then inspected visually by producing a 2D plot. The spectra was then ready to process using AQSES. The metabolite database used for quantitation contained the following metabolites: NAA, Myoinositol, Phosphorylcholine, Creatine, Glutamate, Glutamine and Glucose. As the spectra had already been aligned in preprocessing the allowed frequency shift was set at 0.005Hz to prevent any shift in the spectra during calculation, and damping variation was set at 0.005Hz to prevent broadening and overlapping of metabolite peaks. Iterations were set at 25, and plot at each iteration was selected so real time visual inspection of the calculation could be performed. Once processed results were saved as a .mat file, which contained the amplitude of each of the fitted metabolite peaks (in arbitrary units), and plots representing each metabolite peak. This data was exported into excel where glutamate and glutamine peaks were combined to give a glx peak (the low signal to noise ratio at 1.5T means that glutamate and glutamine multiplets often overlap and therefore quantitation of individual components is difficult, and they are often reported as combined glx peaks), all metabolite peaks were then normalised to Cr (as this is considered not to change) to create metabolite ratios for comparison. There was no difference in Cr peak intensity between the AMM and PLA trials (data not shown), confirming that normalisation to creatine was appropriate for analysis.

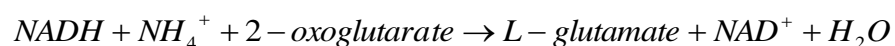
2.6 PREPARATION OF AMMONIUM CHLORIDE INFUSION FOR ADMINISTRATION

All intravenous ammonium chloride (NH₄Cl) solutions were prepared in accordance with standard laboratory procedures for research and development.

2% concentration NH₄Cl solutions were prepared by dissolving either 5 g (for 250ml volumes) or 10g (for 500ml volumes) of NH₄Cl salt (Ph.Eur Grade, Sigma Aldrich, UK) in a sterile sodium chloride solution (0.9% w/v, Baxter, UK). NH₄Cl was weighed out in sterile 30ml containers using laboratory scales accurate to 0.0001g. 20ml of the sodium chloride solution was then added to the container via a sterile 10ml syringe, it was sealed and left to dissolve. The solution was then drawn into a new syringe and injected back into the remaining volume of sodium chloride solution through a sterile 0.2µm antibacterial and antipyrogen filter. Each bag of NH₄Cl solution was passed through a second 0.2µm antibacterial filter to ensure sterility of the solution prior to administration. Solutions prepared via this method have been checked in Eastbourne District General Hospital laboratories and discovered to be pyrogen and bacteria free.

2.7 PLASMA AMMONIA CONCENTRATION ANALYSIS

Plasma was analysed for ammonia (NH₃ and NH₄⁺) concentrations using the enzymatic method described by Kun & Kearney (1974). This involves the amination of 2-oxoglutarate to glutamate via the catalyst glutamate dehydrogenase (GDH).



The oxidation of NADH to NAD⁺ is stoichiometric for the amount of ammonia present, therefore the change in concentration of NADH, as measured via its spectrophotometric change in extinction at 339, 334 or 365nm, represents the concentration of ammonia present in the sample. This method of ammonia analysis is the most widely used application for determining biological plasma ammonia concentrations in research. However, there are a number of other techniques which are occasionally utilized to analyse ammonia, such as:

- Flow injection analysis (Svensson & Anfalt, 1982).
- Microdiffusion Method (Conway & Byrne, 1933).
- Colorimetric Method; Berthelot Reaction (Chaney and Marbach, 1962).
- Ion exchange Methods (Dienst, 1961).
- Automated Analysis (Huizenga and Gips, 1983).

Because of this, there can be a lack of standardisation in plasma ammonia analysis across studies. However, unlike some of the other techniques, the enzymatic reaction involving GDH is specific to ammonia, and hence minimal interference or loss of accuracy was expected. In addition, the enzymatic analysis method is relatively inexpensive to perform and requires minimal equipment, whereas some other methods require expensive equipment and preparatory materials. Therefore, they tend to be less popular as analytical techniques in the literature compared with the enzymatic technique presented here. The pros and cons of the above ammonia analysis techniques are presented in table 2.1 below.

Table 2.1: Benefits and Weaknesses of different plasma ammonia analysis techniques commonly used in published literature.

Analytical Technique (Reference)	Brief Description	Pros	Cons
Flow Injection Analysis (Svensson & Anfalt, 1982)	Sample is alkalised. Ammonia diffuses through membrane and reacts with an indicator which is monitored by a photometer. This procedure is performed using a piece of automated equipment call a flow injection analyser	<ul style="list-style-type: none"> • Can analyse whole blood, plasma or precipitated plasma • Once running analysis can be rapid, up to 60 samples per hour 	<ul style="list-style-type: none"> • Expensive equipment is required for analysis • Potential for other volatile amines to interfere
Microdiffusion Method (Conway & Byrne, 1933)	A two chamber system is used, whereby the outer chamber contains the sample and the inner chamber contains an indicator. After alkalisation of the sample in the outer chamber, it is left for 90 mins and ammonia gas which is produced diffuses into the inner chamber reacting with the indicator.	<ul style="list-style-type: none"> • simple apparatus and set-up with few reagents needed. 	<ul style="list-style-type: none"> • Dated technique • Again potential for interference from other compounds such as amines
Colorimetric Method: Berthelot Reaction (Chaney & Marbach, 1962)	Ammonia reacts with phenol and hypochlorite to form indophenol blue. The intensity of which can be measured spectrophotometrically allowing ammonia concentrations to be determined.	<ul style="list-style-type: none"> • Simple and quick procedure • Can be modified to be performed using a multi-well plate reader allowing a large number of samples to be analysed at once 	<ul style="list-style-type: none"> • Primary, secondary and tertiary amines, thiols and ascorbic acid can all interfere
Ion Exchange Methods (Dienst, 1961)	This method captures ammonium ions after acidification of the sample through a cation-exchange resin, separating the ammonium from all other substances in the sample. The ammonium ions are then eluted from the resin using a salt solution and the sample can then be analysed using a number of different methods.	<ul style="list-style-type: none"> • removes any substances which may interfere with the analysis 	<ul style="list-style-type: none"> • Adds additional steps to the analysis procedures increasing time for analysis • Additional consumables are required, thereby increasing costs.
Automated Analysers (Huizenga & Gips, 1983)	Methods vary depending on which analyser is being used. See manufacturers instructions for details	<ul style="list-style-type: none"> • Rapid analysis • Some methods require no sample preparation 	<ul style="list-style-type: none"> • Analysers and consumables tend to be very expensive • Requires accurate calibration of equipment prior to each use
Enzymatic Method (Kun & Kearney, 1974)	Method described in main document	<ul style="list-style-type: none"> • GDH is specific for ammonia and does not react with volatile amines unlike some other methods. • Minimal sample preparation time is required • Uses standard laboratory equipment for analysis such as spectrophotometer and fluorimeter • Accurate within a large range 	<ul style="list-style-type: none"> • Other NADH consuming reactions may interfere (this is removed however if pre-incubation performed or NADPH is utilised instead) • Time-consuming procedure

2.7.1 PROCEDURE

All reagents used were purchased from Sigma-Aldrich (Poole, UK) unless otherwise stated.

2.7.1.1 PREPARATION OF REAGENTS

Tris-hydroxymethyl-aminomethane (TRIS) Buffer Solution; 25ml of 2M TRIS solution (Fisher Chemicals, New Jersey, USA) was added to 50ml of distilled water. After mixing, pH was adjusted to 8.0 using 3M hydrochloric acid solution via a drop by drop technique. pH was measured using a Hydrus 300 Benchtop pH Meter (Fisherbrand, New Jersey, USA). Once stable at pH 8.0, distilled water was added until a 100ml volume was achieved. The final solution was then dispensed into 5ml tubes and immediately frozen at -20°C.

2-oxoglutarate; 40ml of distilled water was added to 0.7305g of 2-oxoglutaric acid and dissolved by gently mixing. This solution was then adjusted to pH 7.4 using 1M sodium hydroxide solution using the same method as previously described. Once stable this was diluted to 50ml with distilled water and dispensed into 5ml tubes and frozen at -20°C.

Reduced nicotinamide-adenine dinucleotide (NADH); 70mg of NADH was dissolved in 10ml of 1% Potassium Bicarbonate (KHCO_3) solution and was immediately frozen in individual microtubes at -20°C.

Potassium hydrogen carbonate (KHCO_3); 20g of KHCO_3 was dissolved in 100ml of distilled water (20% Solution). 1g of KHCO_3 was dissolved in 100ml of distilled water (1% solution)

Glutamate Dehydrogenase (GDH); This was stored as a powder at -20°C and prepared fresh for each assay. 3mg of GDH enzyme powder was dissolved in 1ml of distilled water prior to each assay to create an enzyme concentration of ~90 Units/ml

2.7.1.2 ANALYSIS PROCEDURE

First a stock reagent solution was created; 12ml of TRIS (100mM), 6ml of 2-oxglutarate (10mM), 9.36ml of distilled water and 1.8ml of NADH (120 μ M) were mixed in a 30ml sterile container (stock solution for up to 60 samples). This was then stored at 0 - 4 $^{\circ}$ C until needed.

Ammonium chloride standards were then created. 26.75mg of ammonium chloride salt was dissolved in 100ml of distilled water to create a 5mM ammonium chloride solution. Because this is such a small amount of ammonium chloride, it is difficult to repeatedly obtain the exact same amount for each solution prepared. Therefore, the solution concentration was slightly different each time, but it was always accurately calculated and was as close to 5mM as possible. This 5mM solution was then diluted 1:100 to create a 500 μ M standard. This was then diluted by $\frac{1}{2}$ in stages until a range of standards covering 30 - 500 μ M were created. This process was repeated each time an assay was performed.

2.7.1.3 SAMPLE PREPARATION AND ANALYSIS

500 μ l of plasma was added to an equal volume of ice cold 2.8% perchloric acid in 1.5ml microtubes. This was vortex mixed for a few seconds using a Reax Top benchtop mixer (Heidolph, GmbH), and it was then left for 20 minutes at 0 - 4 $^{\circ}$ C to ensure that the sample was fully deproteinised, after which it was cold centrifuged (0 - 4 $^{\circ}$ C at 5000rpm) for 10 minutes. The supernatant (700 μ l) was then transferred into a new microtube and 800 μ l of KHCO₃ (20%) was added to neutralise it. The ratios of PCA to KHCO₃ required for neutralisation were predetermined in a separate experiment. The sample was then cold

centrifuged again for 10 minutes, after which 500 μ l of the neutral supernatant was transferred to a spectrophotometer cuvette (1.5ml volume).

To each sample cuvette 471 μ l of the reagent stock solution was added and then mixed. The sample was then incubated at room temperature for 15 minutes to eliminate any endogenous NADH consuming reactions from the sample (Bruce et al, 1978). The sample was then placed in the spectrophotometer and absorbance 1 (A_1) was read using a reference standard containing the same solutions minus NADH and the sample (replaced with distilled water to avoid volumetric interference). A_1 was recorded in triplicate at 365nm and each sample was prepared in duplicate. Once measured, 50 μ l of GDH was added to the sample, which was then mixed again and left to incubate at room temperature for 90 minutes. After 90 minutes absorbance 2 (A_2) was read as before. After a further 15mins A_2 was read again to ensure that the reaction was complete. If the reaction was not complete, A_2 was re-read at 10 minute intervals until no change in A_2 was observed.

Alongside each biological sample, ammonium standards were prepared in the same way as the samples (inclusive of PCA and neutralisation), so that their dilutions were equal, and analysed in the same way to create a standard curve of known concentration. The concentration of ammonia present in each sample was calculated from this standard curve using the value of change in absorbance ($A_2 - A_1$ corrected for the change in absorbance of a blank standard).

2.7.2 STANDARDISATION OF ANALYTICAL TECHNIQUE

Practice analysis with known standards and plasma samples prior to initial analysis allowed for standardisation of the analysis technique and the reduction of any measurement errors; including pipetting errors, interference errors.

The peak absorption wavelength for NADH is 339-340nm (Kun and Kearney, 1974), and it is recommended that analysis using NADH oxidation be performed at this wavelength. It was discovered that the spectrophotometer used for these experiments was not stable at this wavelength, high reading variability at this wavelength produced a level of concentration error (see figure 2.4). Therefore as suggested by Kun & Kearney (1974), the wavelength was increased to 365nm, a wavelength at which the spectrophotometer was found to be more reliable.

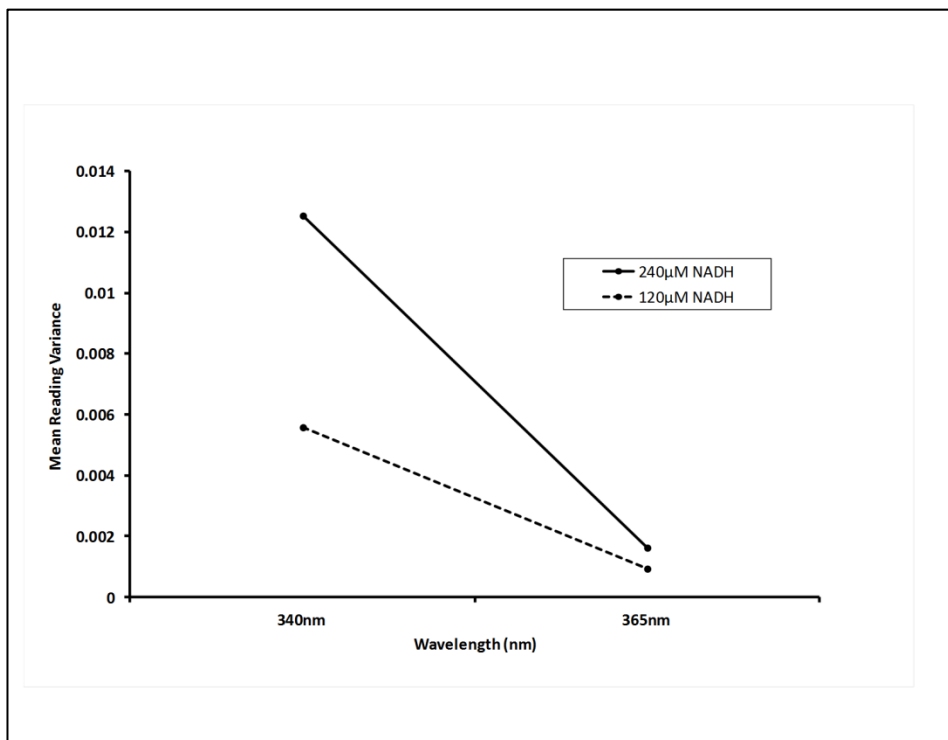


Figure 2.4. Reading variability produced by spectrophotometer at 340nm (recommended wavelength) and 365nm (alternative wavelength) at different concentrations of NADH; the light absorbing reagent used for ammonia analysis.

In the method described by Kun & Kearney (1974) it recommends using 240 μ M NADH in the assay, however spectral analysis of NADH performed in our laboratory, showed that 240 μ M NADH gave a lower peak extinction coefficient from that expected, on our spectrophotometer (see figure 2.5). When the concentration of NADH was reduced (from the recommended concentration of 240 μ M) the peak molar extinction coefficient began to rise, reaching close to its accepted value of 6270 $M^{-1}.cm^{-1}$ at 120 μ M (figure 2.5). It was difficult to determine what could be causing such a large error in the extinction coefficient at this concentration, however, it could have been due to the same instrumental error which caused the lack of reading accuracy at 340nm. From these findings it was therefore deemed necessary to reduce the concentration of NADH in the assay from 240 to 120 μ M to maintain instrument accuracy throughout each analysis. In support of our preliminary findings, research by Bruce *et al.* (1978) also identified that values between 80 - 160 μ M of NADH were the most accurate concentrations for use in the GDH method of ammonia analysis.

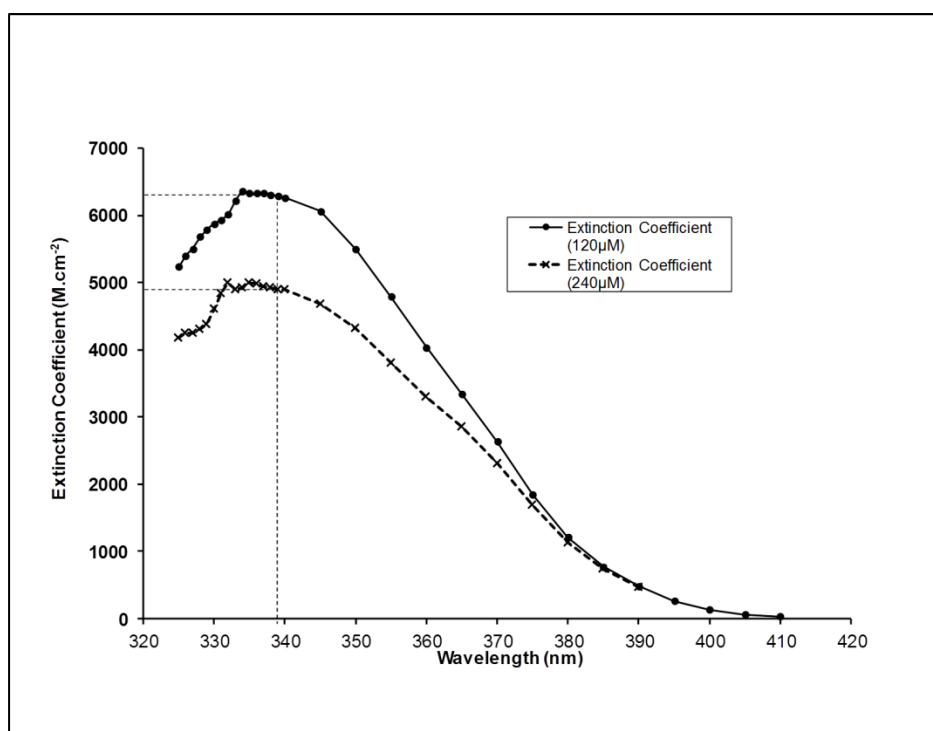


Figure 2.5: NADH Spectrophotometer Extinction Spectra at 240 and 120 μ M NADH Concentrations

Standard curves were utilised instead of the recommended equation due to the lack of agreement between known concentrations and their theoretical values (See table 2.2). An acceptable level of agreement is considered as being within 5%, the equation here produces values which are $16.8 \pm 5.1\%$ different from the known concentration.

Table 2.2: Variation in calculated concentration from actual concentration when calculated using Kun and Kearney (1974) equation. Variation due to difference in molar extinction coefficient from that expected

Assay number	Actual Concentration (μM)	Equation Calculated Concentration (μM)	Concentration Difference	% Difference
1	132.25	110.5	21.7	16.4
2	132.25	102.8	29.4	22.2
3	132.25	110.5	21.7	16.4
4	132.25	118.2	14.01	10.6
5	132.25	118.2	14.01	10.6
6	132.25	108.8	23.4	17.7
7	132.25	101.1	31.1	23.5
		Mean	22.2	16.8
		SD	6.7	5.1

Producing a standard curve with each assay removes the effect of any pipetting or preparatory errors, which may influence the accuracy of the values produced from the equation, as each standard is treated in exactly the same way as each sample. It was also noted from other preliminary experiments that depending on how NADH standards were prepared for calculation of absorption spectra and extinction coefficients, the values seemed to differ when using the spectrophotometer in our laboratory (see table 2.3).

Table 2.3: Interference to absorption provided by assay reagent solution.

NADH Conc (µM)	Absorbance Assay Reagent Sol.	Ext Co	Absorbance Water Dilutions	Ext Co	Diff in Abs	Diff in Ext Co	% Error
117.5	0.352	3002.12	0.407	3466.66	0.0545	464.54	13.4
109.6	0.332	3036.04	0.376	3430.65	0.0432	394.62	11.5
94.02	0.286	3047.22	0.348	3704.88	0.0618	657.66	17.75
78.35	0.237	3029.81	0.298	3808.30	0.0609	778.49	33.8
				Mean	0.0551	573.83	19.1
				<i>SD</i>	0.0085	176.04	8.7

Extinction coefficient values produced with NADH standards in distilled water dilutions were $19.1 \pm 8.7\%$ higher than those produced with NADH standards in GDH assay reagent stock solution. These findings suggest that there is interference in NADH absorption produced by the stock assay reagent solutions. This interference most likely contributed to the error in concentration calculation via the equation from the method of Kun and Kearney (1974) creating the observed lack of agreement between the calculated and actual concentrations. Therefore in order to maintain accurate readings throughout repeated assay analysis, calculation from a standard curve was always performed. The accuracy of the assay was checked regularly using samples containing spikes of known ammonia concentration. The recovery of these spikes ranged from 96 – 100%, indicating high accuracy of the assay.

2.8 STATISTICAL ANALYSIS

All statistical analysis was performed using SPSS for windows (version 16.0, SPSS inc.) or GraphPad Prism 5.0 (GraphPad Software Inc.). Descriptive statistics were produced for all data sets and checked for normal distribution using a Shapiro-Wilk or Kolgomorov-Smirnov

tests of normality. Normal distribution was accepted if $p > 0.05$. All experimental data is expressed as mean and standard error of the mean (SEM), unless otherwise stated. All biochemical, psychological, physiological and subjective data at multiple time points were analysed using a one-way ANOVA for repeated measures to assess for changes over time. Differences between trials were analysed with a two-way ANOVA for repeated measures, using a Bonferroni correction to avoid type 1 errors unless otherwise stated. Differences between trials for individual time points or single measures were analysed using a paired samples t – test. Differences between trials for MFSI-SF data were analysed using a Wilcoxon Signed Rank Test. Equivalent non-parametric tests were utilised where normal distribution of data was not observed. Linear relationships between variables were analysed using Pearson’s Product Moment Correlation Coefficients. The alpha level of significance was set at $p < 0.05$.

CHAPTER 3: DEVELOPING A SIMPLE HUMAN MODEL OF ACUTE EXPERIMENTAL HYPERAMMONAEMIA IN HEALTHY ADULTS.

3.1 INTRODUCTION

Healthy humans could constitute a useful model for the study of *in vivo* ammonia metabolism and its effects on normal function. Ammonia has long been considered toxic to the central nervous system, yet certain factors remain unresolved as to its true contribution to such toxicity. Many conditions where hyperammonaemia is prevalent are highly complex, and constitute a number of metabolic perturbations which accompany the increases in ammonia. For example, liver disease patients present with, amongst other things; gastrointestinal bleeding, electrolyte imbalance and systemic infection, whilst also being prescribed several medications (Dong and Saab, 2008), all of which may have their own impact on normal metabolism and function. Whilst extremes of exercise lead to depletions in plasma and muscle metabolites (Clausen and Nielsen, 2007, Ferreira and Reid, 2008), changes in cerebrovascular responses (Ide and Secher, 2000), amongst other significant changes.

Current models of hyperammonaemia which have been developed to understand better the changes and mechanisms associated with this condition have either utilised animal models; which although provide useful insight into physiology and metabolism, translation of findings to humans is complicated by inter-species variation. A number of physiological and biological systems show differences between animals and humans, for example protein synthesis (Rennie *et al.*, 2010), and drug pharmacological responses (Easton and Marsden, 2006). Therefore, findings from animals in hyperammonaemia may not accurately represent that which occurs in humans. Alternatively other studies have used the

induction of hyperammonaemia in stable chronic liver disease patients through oral amino acid administration (Oppong et al., 1997, Douglass et al., 2001, Balata et al., 2003b, Shawcross et al., 2004a, Mardini et al., 2008, Mardini et al., 2011). Although this acts as a clinically relevant model of hyperammonaemia in liver disease, it is not possible to determine the causal influence of ammonia on any observed psychological or physiological derangements, due to the interaction between ammonia, amino acids themselves and the other co-morbidities involved in this condition. This was highlighted in an elegant study by Shawcross et al., (2004b), where it was found that the neuropsychological impairment observed in liver disease patients under hyperammonaemia could be resolved after the treatment of systemic inflammation and infection with antibiotics (Shawcross *et al.*, 2004b). To control for these other influencing factors, therefore, and to provide a better understanding of the true contribution of ammonia toxicity under conditions of hyperammonaemia, we aimed to examine a state of hyperammonaemia in the absence of any associated pathology or other physiological stresses. This is where the use of healthy human subjects is beneficial. It can be assumed that any changes as a result of hyperammonaemia in a resting healthy adult will be due to ammonia alone, as all other physiological systems should be in equilibrium, unless influenced directly by the actions of ammonia. The aim of this initial experimental chapter was to develop and standardise a method for investigating hyperammonaemia in healthy adult males. The method of oral amino acid administration to induce hyperammonaemia is generally inconsistent in healthy individuals (Ortiz et al., 2004; Bersagliere et al., 2011) due to the efficiency of the healthy liver to remove much of the ammonia provided to it in a single pass (Yang et al., 2000, Olde Damink et al., 2009). Moreover, studies where control (healthy) subjects have been fed amino acids orally can show no appreciable increase in plasma ammonia as a result (Ortiz et al., 2004; See figure 1.6, Chapter 1), whilst on other occasions showing significant increases above basal levels (Bersagliere et al., 2011). To ensure consistent development of significant hyperammonaemia in healthy individuals, which is both physiologically and

pathologically relevant, an alternative route of administration, such as intravenous (iv) infusion would be necessary.

Table 3.1. Summary of Previous Human Intravenous Ammonium Salt Infusion Studies and Ammonium Salt Infusion Information

<u>Reference/Source</u>	<u>Subjects (n)</u>	<u>Study Aim</u>	<u>Infusion Concentration</u>	<u>Infusion Time Course</u>	<u>Infusion Rate or equivalent</u>	<u>Tolerance Data</u>
Summerskill et al., (1957)	Liver Disease Patients (5); Healthy Controls (4)	To investigate the disturbances between ammonia, blood pyruvate and alpha-ketoglutarate in liver disease	2% solution (374mmol/L)	45 mins	~75mM/hr (200ml/hr)	None Reported
Tyor and Wilson (1958)	Hospitalised Males without Liver Disease (9)	To investigate the peripheral metabolism of ammonia following iv infusion of ammonium salts.	155mmol/L	1 hour	0.007-0.018mM/kg/min (for 70kg adult ~29.4mM/hr – 105mM/hr)	Vomiting Reported in one Subject
Owen et al., (1960)	Hospitalised Males without Liver Disease (9)	To investigate the effects of hyperammoniaemia on renal ammonia metabolism	155mmol/L	45 mins	30-45mEq/hr	None Reported
Fleshler and Gabuzda (1965)	Hospitalised in-patients without liver disease (7)	To investigate the effects of blood ammonia on gastric ammonia levels	2.14% Solution (400mmol/L)	2 hours	60 – 79ml/hr (48 – 60mM/hr)	None Reported
Furst et al., (1969)	Healthy Adults (9)	To investigate the nutritional value of ammonium nitrogen	80 – 200 mmol/L	3 hours	No information provided	Mild nausea and vomiting
Kisch et al., (1976)	Sodium-depleted subjects (6)	To look at the different iv salts on renin secretion	75mM	1 hour	75mM/hr	None Reported
Hospira Inc. Ammonium Chloride Injection Solution	n/a	n/a	2% solution (374mmol/L)	3 hours recommended	300ml/hr (112mM/hr) max	n/a

3.2 METHODS

3.2.1 PRELIMINARY EXPERIMENTATION

Initial test dosages of ammonium chloride (NH_4Cl) were prepared and administered according to information obtained from Hospira Inc (see table 5). Hospira Inc., produce NH_4Cl for sale in the pharmaceutical market for the treatment of metabolic alkalosis. It is recommended that a 1-2% ammonium chloride solution is prepared and administered at a maximum infusion rate of 5ml/min or 300ml/hr over a period of 3 hours. Attempts were made to infuse a 2% ammonium chloride solution at a rate of 1.25ml/min (75ml/hour), doubling the rate after each hour for 3 hours. Although the first hour of infusion was tolerated, in the second hour when the rate was increased to 2.5ml/min (150ml/hr), adverse reaction often rapidly set in (e.g. nausea, vomiting), and infusions were ceased (Data not shown). Due to the severe nature of the reactions beyond 75ml/hr, rates were drastically reduced for follow-up testing with the maximum rate set at 100ml/hr in an attempt to improve tolerance to the protocol.

3.2.2 PARTICIPANTS

Nine healthy male participants (Age: 25 ± 5 yrs, BM: 80.7 ± 11 kg, Height: 181.8 ± 7.1 cm, Mean \pm SD) volunteered for this study. Prior to each testing session, participants were asked to abstain from caffeine, alcohol and strenuous exercise for 24 hours.

3.2.3 EXPERIMENTAL DESIGN

3.2.3.1 PART 1: VARIABLE RATE INFUSION

For the variable rate infusion trials eight participants received a continuous iv infusion of a 2% NH₄Cl (5g per 250ml volume; 374mM) solution over a period of 240 minutes (4 hours), which followed the procedures described in the general methods. The infusion rate was varied hourly. The starting rate was set at 25ml/hr (0.5g ammonium chloride/hr; 9.34mM/hr) and this rate was increased by 25ml/hr until a maximum rate of 100ml/hr (1.98g/hr; 37.4mM/hr) was reached within the final hour. Blood and CR10 subjective scores were collected every ten minutes and all the other procedures for infusion follow those in general methods section.

3.2.3.2 PART 2: CONSTANT RATE INFUSION TRIALS

100ml/hr (1.98g/hr) Trial

The second part of this study required five volunteers to return for one further infusion trial. This return trial consisted of a constant rate infusion of the 2% NH₄Cl solution performed over the same 240 minute (4 hour) period. Due to a high incidence (40% of participants) of adverse reaction (nausea and vomiting), attempts to use an infusion rate of 100ml/hr were abandoned.

90ml/hr (1.8g/hr; 33.7mM/hr) Trial

Four of the same participants (one of whom responded badly to the previous trial), plus one additional new participant, performed another constant rate infusion trial at 90ml/hr, to assess whether this was more tolerable whilst still providing sufficient blood ammonia elevation to mimic a pathologically and physiologically relevant level. Due to the fact that the adverse reactions to the previous rate occurred within the first hour of the infusion, it

was only deemed necessary to perform these final infusions for a total of two hours, so that the participants were not inconvenienced any further. Subjective scores for fatigue, discomfort and nausea were collected as before, with blood collected every 30 minutes.

3.2.3 ANALYSIS

Biochemical and statistical analysis follows that described in the general methods.

3.3 RESULTS

3.3.1 VARIABLE RATE INFUSION TRIALS

3.3.1.1 PLASMA AMMONIA CONCENTRATIONS

There was a significant increase in plasma ammonia concentration from baseline after only 10 minutes of administration of the NH_4Cl solution ($55 \pm 2 \mu\text{mol/L}$ to $84. \pm 7 \mu\text{mol/L}$; $F(1,6) = 19.873$, $p = 0.004$, $\eta_p^2 = 0.768$; Figure 3.1). Further significant increases in plasma concentration occurred at the beginning of each hour when the infusion rate was increased, peaking at $224 \pm 17 \mu\text{mol/L}$ within the final hour (Figure 3.1). Immediately upon cessation of the infusion at 240 minutes, there was a rapid decrease in ammonia concentration of $84 \pm 12 \mu\text{mol/L}$ ($F(1,6) = 40.261$, $p = 0.001$, $\eta_p^2 = 0.870$) within 10 minutes, continuing to decrease further up to 20 minutes.

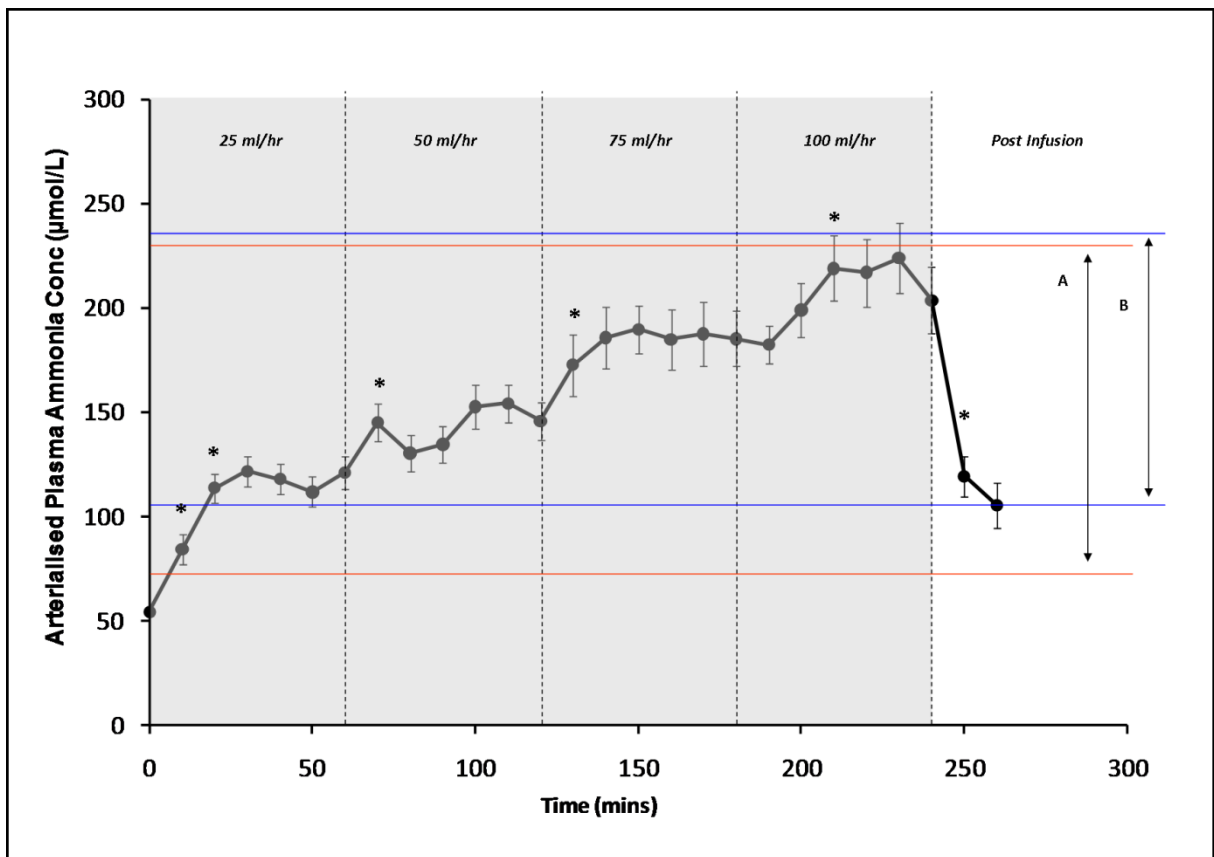


Figure 3.1. Effect of variable rate infusion of ammonium chloride on arterialised plasma ammonia concentrations. * indicates significant change in concentration from previous time point ($p < 0.05$). A. Peak plasma ammonia concentration range reported during exercise of varying rate and durations. B. Peak plasma ammonia concentration range reported after induction of hyperammonaemia in liver disease. Data are presented as mean \pm SEM.

3.3.1.2 TOLERANCE

The NH_4Cl infusion administered at a variable rate was tolerated well by the majority of participants. One participant dropped out due to discomfort experienced from the positioning of the iv cannula. There were no significant increases measured in mean subjective scores for fatigue, nausea or discomfort (Figure 3.2).

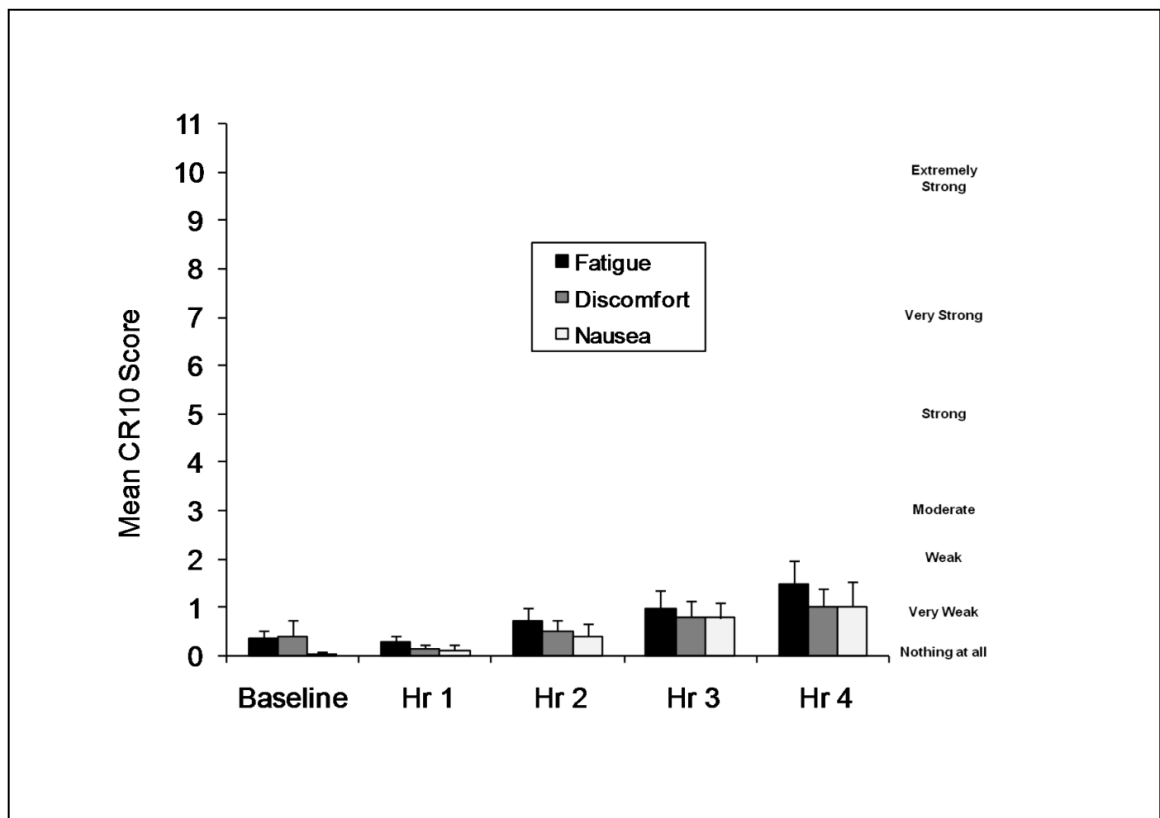


Figure 3.2. Effect of variable rate infusion of ammonium chloride on subjective feelings of fatigue, discomfort and nausea. Data are presented as mean \pm SEM. The equivalent verbal expressions of intensity for the CR10 scores are provided along the right hand side of the figure.

3.3.2 CONSTANT RATE INFUSION TRIALS

The results from the variable rate infusions provided a profiling of blood ammonia concentrations during iv infusion as the rate was gradually increased each hour. This data was then used to determine the appropriate constant rate of infusion which would provide a level of hyperammonaemia representative of both physiological and pathophysiological norms. Analyses of exercise studies where changes in plasma ammonia concentration were determined, identified that peak ammonia concentration can range from 67 – 235 $\mu\text{mol/L}$ depending on the type, duration and intensity of the exercise (see appendix 5, meta-analysis of ammonia concentration). In chronic liver disease patients, peak plasma ammonia concentrations range from 105 - 240 $\mu\text{mol/L}$ after induction of hyperammonaemia via oral amino acid feeding (see Table 1, Chapter 1). Therefore the

infusion rate chosen should produce hyperammonaemia which falls within both these ranges.

In order to ensure that any changes relating to hyperammonaemia were captured using this model, no matter how subtle, it was decided to attempt to induce the highest level of tolerable and physiologically relevant hyperammonaemia possible. The first infusion rate attempted for the constant rate trials was therefore 100ml/hr (1.98g/hr), the highest infusion rate administered during the variable rate trials. However, this was found to be poorly tolerated in 2 of the 5 participants, with a sudden onset of vomiting observed within 40 – 60 minutes. Therefore, the infusion rate was reduced to 90ml/hr (1.8g/hr) to observe whether an improvement in tolerance could be seen. This decrease in the infusion rate led to a significant increase in mean plasma ammonia concentration from $55 \pm 3 \mu\text{mol/L}$ to $191 \pm 13 \mu\text{mol/L}$ within 30 minutes ($F(1,4) = 88.097, p = 0.001, \eta_p^2 = 0.957$; Figure 3.3), which was $57 \pm 20 \mu\text{mol/L}$ lower than at the same time point in the 100ml/hr trial ($t = 2.746, p = 0.027$). However, it was still within the appropriate reference ranges.

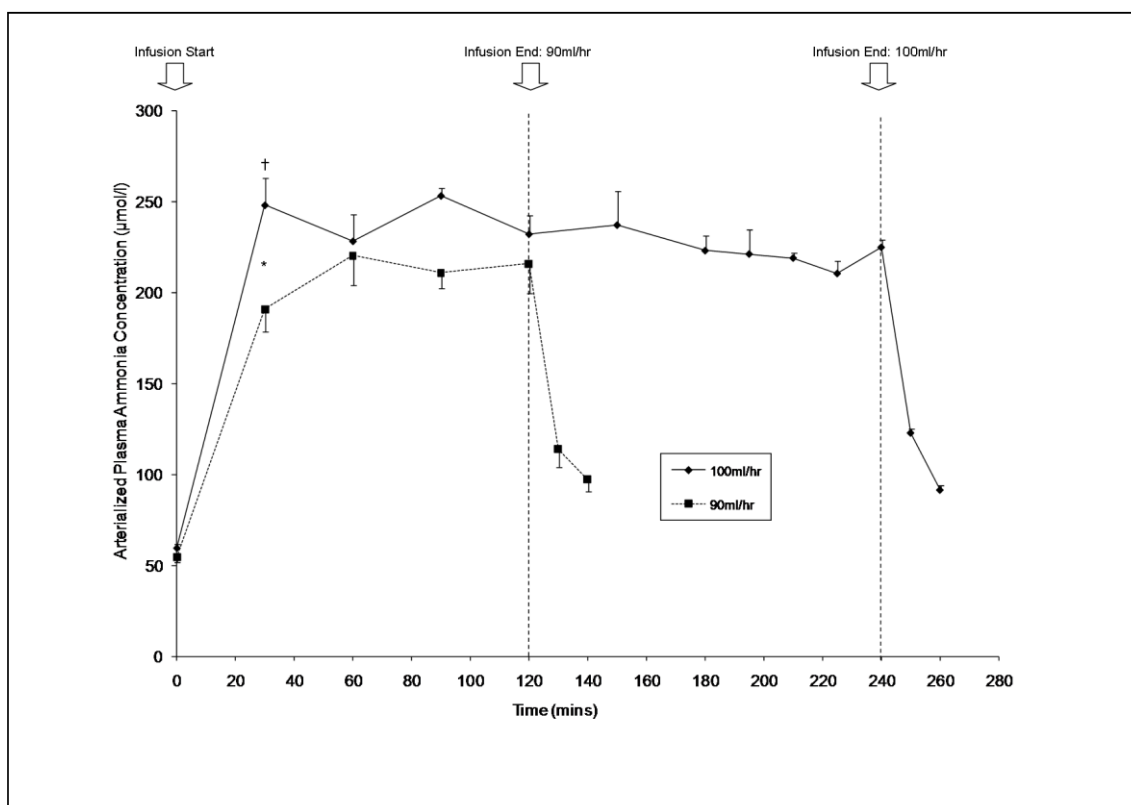


Figure 3.3. Comparison of arterialized plasma ammonia concentrations during the constant rate infusion trials at 100ml/hr (unsuccessful) and 90ml/hr.

* indicates significant difference in ammonia concentration between the two trials at this time point ($p < 0.05$). † At 30 minutes in 100ml/hr trial $n = 5$, at 60 minutes $n = 4$, beyond 60 minutes $n = 3$ due to participant drop out. $n = 5$ at all time points for 90ml/hr trial. Data are presented as mean \pm SEM.

3.3.2.1 TOLERANCE

The main benefit of this reduced rate of infusion was the overall tolerance by all participants. Anecdotally the participant who performed both constant rate infusions reported that feelings of discomfort and nausea were reduced at the lower dose, and although this was reflected in a reduction in mean peak subjective scores, it was not significant (Figure 3.4).

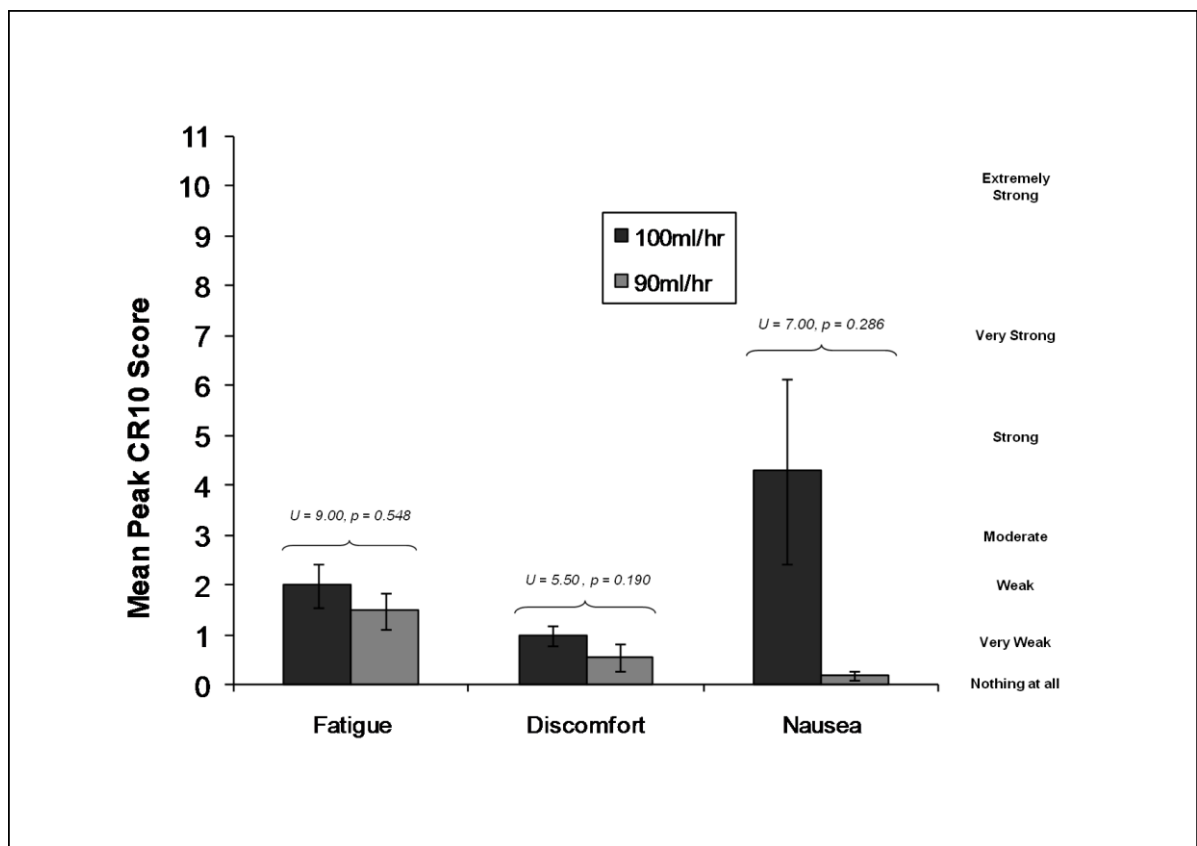


Figure 3.4. Difference in peak subjective feelings of fatigue, discomfort and nausea for the two constant rate trials. Data are presented as mean \pm SEM. The equivalent verbal expressions of intensity for the CR10 scores are provided along the right hand side of the figure.

3.3.2.2 CORRECTION FOR BM

In many infusion protocols rates of delivery are often corrected for patient/participant body mass. The present experiment had participants ranging in BM from 68.8 to 103 kg. Theoretically one may expect that those participants with larger body mass would be able to buffer ammonia to a greater extent than those with smaller body mass, due to the capacity of skeletal muscle (Olde Damink et al., 2009) and adipose tissue (Esbjornsson et al., 2006) to act as sinks for ammonia removal, therefore requiring a correction for body mass when calculating rates for infusion. However, the present results showed no relationship between participant BM or BMI and peak plasma ammonia concentrations and measures of tolerance (see figure 3.5 and 3.6). It was therefore decided not to correct for BM when calculating infusion rates, and to use a constant infusion rate for all participants.

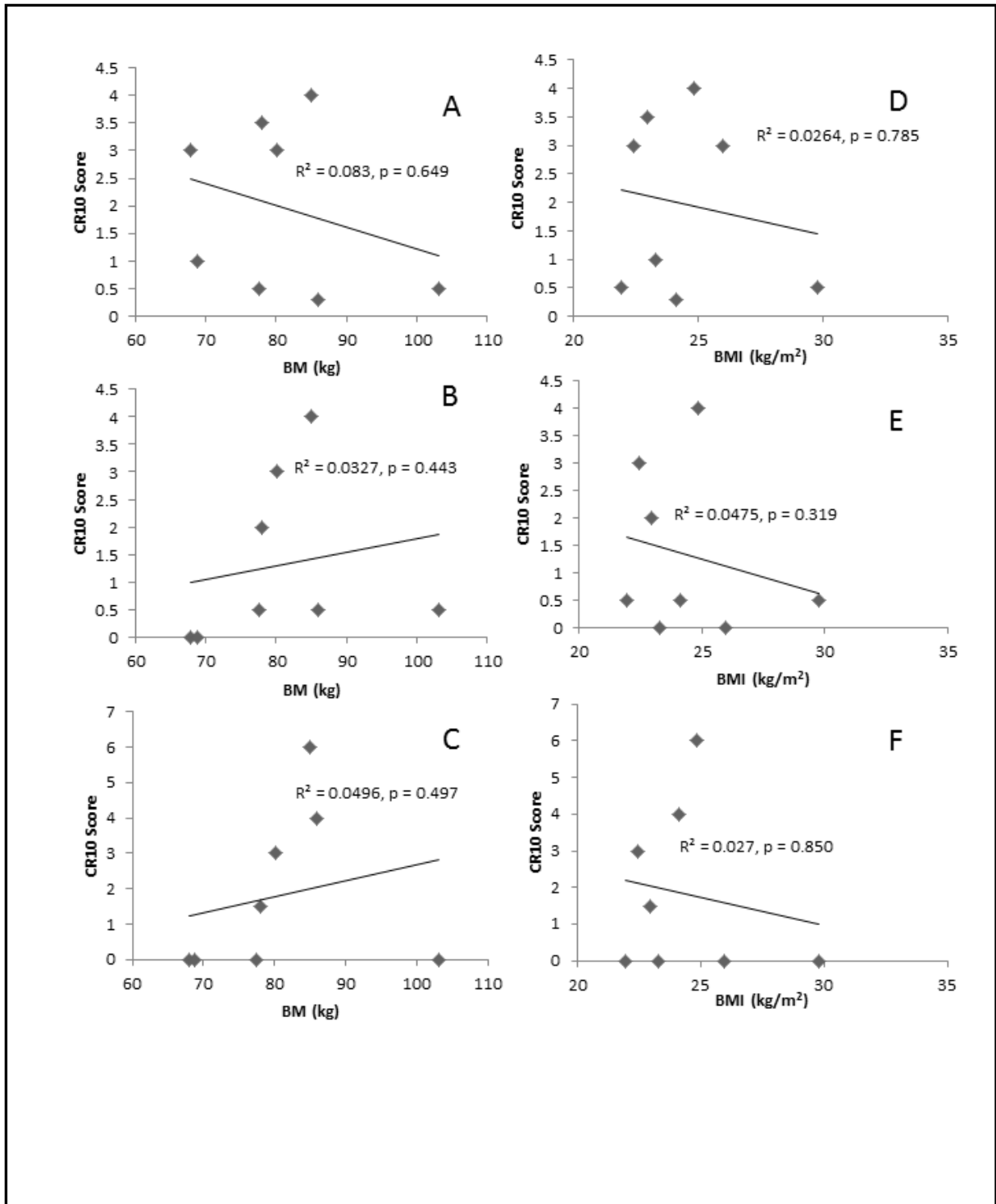


Figure 3.5. Relationships between peak CR10 scores and BM/BMI. A. BM and Peak Fatigue CR10 Scores. B. BM and Peak Discomfort CR10 Score. C. BM and Peak Nausea CR10 score. D. BMI and Peak Fatigue CR10 Scores. E. BMI and Peak Discomfort CR10 Score. F. BMI and Peak Nausea CR10 score

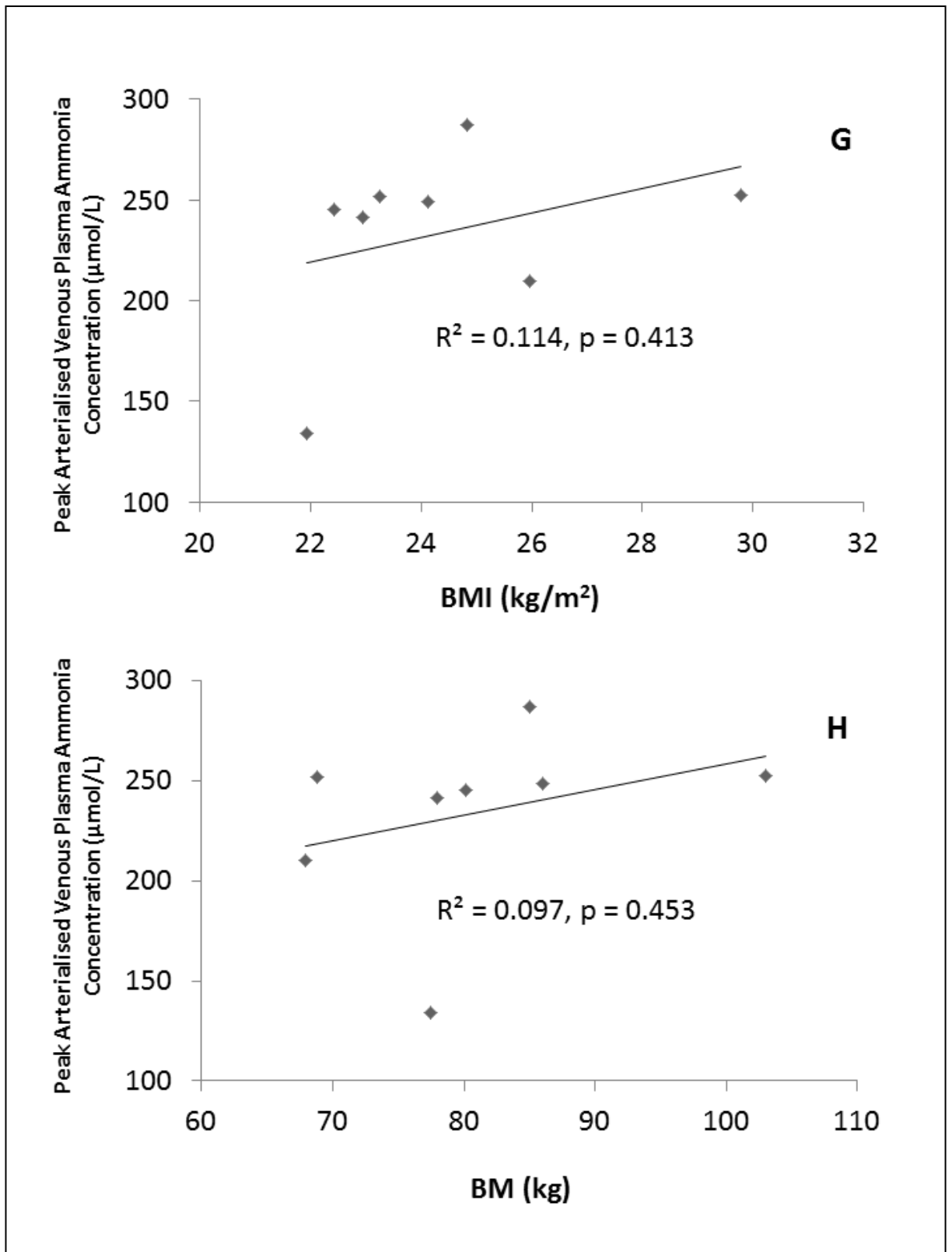


Figure 3.6. Relationships between peak arterialised plasma ammonia concentrations and BM/BMI. G. BMI and peak arterialised plasma ammonia concentrations. H. BM and peak arterialised plasma ammonia concentrations

3.3.2.3 POST INFUSION RECOVERY

Upon cessation of the infusion, there was a rapid decrease in plasma ammonia concentration from 204 to 105 μ mol/L for the variable rate infusion (Figure 3.1), and 216 to 97 μ mol/L for the 90ml/hr constant rate infusion (Figure 3.3), within 20 minutes.

3.4 DISCUSSION

The data presented here shows that a sustained, tolerable, physiologically and pathologically relevant state of hyperammonaemia can be achieved in healthy adults via the continuous iv infusion of a 2% NH₄Cl solution, at a maximum rate of 90ml/hr (1.8g/hr; 33.65mM/hr). Few previous studies exist which have implemented the use of iv NH₄Cl infusion techniques before, however of those which have, administration rates and dosages have varied greatly between studies, with some in excess of the maximum which was able to be tolerated in the present study (e.g. Summerskill et al., (1957), see table 3.1). The results in this chapter make it seem unlikely that these higher infusion rates would be tolerated in most individuals. In the participants investigated, severe adverse reactions were observed in some at infusion rates of 100ml/hr (1.98g/hr; 37.4mM/hr). At a rate of 90ml/hr, a 2% NH₄Cl solution can be administered comfortably in most individuals for extended periods of time, allowing the acute effects of hyperammonaemia to be assessed *in vivo*. With the alleviation of any associated adverse reaction, it could therefore be assumed that any functional or metabolic changes observed during such an infusion, should be due to the effects of the increases in systemic ammonia alone, as all other systems should be in equilibrium unless directly influenced by the ammonia.

It is important to note however, that the administration of ammonium chloride is used as a research tool to study acid base changes. Significant reduction in the base excess and induction of acidosis has been observed after oral NH_4Cl administration in humans (van de Ven *et al.*, 1999) and animals (Caso *et al.*, 2004). NH_4Cl is also listed for this purpose within the European Pharmacopoeia with commercial preparations available from pharmaceutical companies as a clinical treatment for the correction of metabolic alkalosis (Hospira Inc, Forest Lake, USA).

Acidosis accompanies a number of clinical conditions, which are associated with significant muscle wasting (Caso *et al.*, 2004). Therefore, acidosis has also been investigated as a potential mechanism of this wasting, and NH_4Cl administration represents one of the more common methods for inducing acidosis experimentally. A number of animal and human studies have shown significant alterations in protein metabolism in response to NH_4Cl induced acidosis, with increased proteolysis (Mitch *et al.*, 1994) and decreased skeletal muscle protein synthesis (Caso *et al.*, 2004) in rats, and altered leucine metabolism in humans (Reaich *et al.*, 1992). It is therefore also possible that the iv infusion of NH_4Cl used here could have similar impact on acid base balance, and any observed effects as a result of such an infusion could, in part, be related to this metabolic change, rather than solely the increases in ammonia. However, it remains uncertain as to whether iv NH_4Cl infusions in humans induce an acidosis in a similar way as oral administration. Reports from early iv infusion studies show that arterial pH is not affected during the infusion of ammonium chloride, acetate or lactate salts in healthy humans (Tyor and Wilson, 1958, Furst *et al.*, 1969). These conflicting findings regarding NH_4Cl induced acidosis may be time dependent. Studies where changes in protein metabolism have been observed, involve chronic administration of NH_4Cl over periods ranging from 24hrs (Caso *et al.*, 2004) to 5 days (Mitch *et al.*, 1994). Therefore significant effects of acidosis may take time to develop only being

prevalent under chronic acidotic conditions, and acute administration of ammonium may not provide sufficient time for any significant associated changes to become apparent. Additionally any significant effects may also be dependent on the condition severity. Studies in rats showed severity specific effects of HCl induced acidosis in excised gastrocnemius muscle (Safránek *et al.*, 2003). A decrease in pH by 0.1 pH units showed no effect on protein metabolism, yet a more severe change of 0.4 pH units decreased protein turnover significantly (Safránek *et al.*, 2003), whilst *in vivo* alterations in whole body protein turnover were only found with a decrease in pH of 1.6 pH units (Safránek *et al.*, 2003). To obtain equivalent severity of pH changes via iv NH₄Cl administration in pigs, NH₄Cl must be infused at a minimum rate of 9.7µmol/kg/min (Nordgren *et al.*, 2006). If the same were infused in a 70kg human, this would equate to 37.6mM/hr of ammonium chloride, which is in excess of that being used here (33.7mM/hr; 90ml/hr). Even so, when rates higher than this were performed in humans, there was no significant change in arterial pH observed (Tyor and Wilson, 1958). Again highlighting the difficulties in inferring findings from animals studies to human populations. Furthermore, oral administration requires a bolus of 1.7 – 2.6g of NH₄Cl to be consumed to induce significant acidosis in a healthy adult (van de Ven *et al.*, 1999). Whereas an individual administered an iv infusion of a 2% solution at 90ml/hr will only be receiving 1.8g of NH₄Cl over that 1 hour period. Therefore with administration of NH₄Cl at a continuous slow rate rather than as a large bolus, compensatory acid-base regulation may be possible to counter any ammonium induced acidosis occurring at this rate. In addition to this, clinical administration of NH₄Cl for the treatment of metabolic alkalosis is recommended at rates far in excess of what was performed in this study; 5ml/min (300ml/hr), suggesting that significant acidosis may only be achieved at such high rates, and therefore may explain the initial adverse reaction to test infusions at these higher clinical rates.

Whilst the effects observed in NH_4Cl induced acidosis experiments are attributed to the accompanying acid base changes, few recognise the potential accompanying hyperammonaemia which may also occur. Rats fed ammonium containing diets chronically show significant hyperammonaemia (Hermenegildo et al., 1998a), yet authors fail to acknowledge this in acidosis studies. One study which reported altered protein synthesis due to NH_4Cl induced acidosis did perform an additional experiment with H^+ ion exchange resin as an alternative for inducing acidosis to highlight that the findings were similar between the two treatments, and hence must be due to the acidosis, rather than the ammonia (Caso *et al.*, 2004). Yet a more robust method of performing this would have been to administer ammonium salts, and control pH levels such as through the infusion of ammonium acetate rather than chloride. Although the onset of a metabolic acidosis cannot be ruled out in the present experiment as arterial pH was not measured, it should be possible to make the assumption that any effect of acidosis may be minimal, if present at all, compared to that of hyperammonaemia due to the large increases in plasma ammonia observed with this iv model, and slow rate of infusion. For future uses of this infusion outside this thesis, pH measures would complement any findings, these were not possible to perform here due to an absence of appropriate analytical equipment.

In conclusion, this model of hyperammonaemia was tolerated well and will allow the study of ammonia metabolism in isolation from other potentially conflicting variables (inflammation, metabolite changes, drug interactions, exercise stresses). Furthermore, it is logical to suggest that the unpleasant sensations associated with the higher infusion rates previously reported as tolerable could significantly influence research findings, yet this model removes the risk of these responses, and so may show the underlying effects of ammonia on function more clearly. Numerous perturbations to metabolic function within cerebral and peripheral tissues have been implicated to the direct action of ammonia using

in vitro and animal models, yet these actions have yet to be investigated in humans *in vivo*. The current findings open up a potentially useful, yet currently underused tool for investigating the metabolic, physiological and neurological consequences of systemic hyperammonaemia in isolation. This will help to identify the extent of its contribution to toxicity and neurological derangements in hyperammonaemic conditions, clearly distinguishing it from the effects of the other potentially conflicting precipitating factors. This infusion rate of NH_4Cl was used throughout the remainder of the thesis.

CHAPTER 4: THE EFFECTS OF EXPERIMENTALLY INDUCED HYPERAMMONAEMIA ON COGNITION, MOTOR FUNCTION AND FATIGUE

4.1 INTRODUCTION

Hepatic encephalopathy is a neurological condition which occurs commonly in liver disease patients. Ranging in severity, mild forms of this condition, also known as minimal hepatic encephalopathy (mHE), can often go undetected in patients due to the lack of clinical symptoms shown. It is only evident through detailed neuropsychological examination, where subtle impairments to cognition, motor control and learning and memory may be measured (Ortiz et al., 2005, Weissenborn et al., 2005, Butz et al., 2010a). Or alternatively via information reported about an individual's change in behaviour; such as increased tiredness, altered sleep-wake cycle and decreases in attention, from the patient, their families and/or work colleagues (Dhiman and Chawla, 2009). Effective treatment of this condition is paramount because it has been shown that up to 80% of cirrhosis patients with mHE will go on to develop the more severe form; overt HE (Romero-Gomez *et al.*, 2001), which can lead to cerebral oedema, coma or even death (Clemmesen *et al.*, 1999). The aetiology of mHE remains unclear, however it is generally accepted that the onset of hyperammonaemia plays a major role in its development (Haussinger and Schliess, 2008). Both a reduced capacity of the liver to remove gut derived ammonia from the blood and presence of portal hypertension causing portal blood to bypass the liver, leads to the onset of hyperammonaemia and an increased uptake of ammonia into the brain (Olde Damink *et al.*, 2009). Once in the brain, ammonia is believed to cause disturbances to a number of cellular and subcellular processes important in the control of normal brain function (Felipo and Butterworth, 2002, Monfort *et al.*, 2009, Montoliu *et al.*, 2010, Cauli *et al.*, 2009b, Wilkinson *et al.*, 2010). Supporting evidence for the importance of hyperammonaemia in HE symptom development is found in studies where the induction of hyperammonaemia

via oral amino acid challenge in liver disease patients leads to impairment in immediate memory recall (Shawcross et al., 2004a, Balata et al., 2003b, Jalan et al., 2003), delayed memory recall (Jalan *et al.*, 2003), episodic memory (Mardini *et al.*, 2008), and a slowing of reaction times (Oppong et al., 1997, Douglass et al., 2001, Rees et al., 2000).

Such findings in liver disease have led to the proposal that similar dysfunction could also be present in other physiological states where hyperammonaemia is prevalent, such as exercise, where it is reported to contribute to the onset of developing fatigue (Wilkinson et al., 2010). Yet the direct effects of ammonia on metabolic and functional capacity remain uncertain. For example, the pathophysiology of chronic liver disease is complex, a number of co-morbidities exist alongside hyperammonaemia; increased manganese levels, proinflammatory cytokines and hyponatraemia have all been linked with impaired function in liver disease and the onset of mHE symptoms (Butterworth et al., 1995, Odeh et al., 2005, Butterworth, 2008, Shawcross et al., 2008), whilst drug interactions with other physiological systems should also not be ruled out. In addition, the complex metabolic and energetic costs associated with exercise could also be highly influential in any functional impairment attributed to hyperammonaemia, such as fatigue (Secher et al., 2008, Ament and Verkerke, 2009, Ferreira and Reid, 2008).

Therefore, the aim of this second experimental study was to assess the effects of hyperammonaemia on healthy human adults in isolation from other pathological or physiological variables, to determine whether hyperammonaemia leads to the commonly observed alterations in cognition, motor function and fatigue often attributed to this condition. The iv infusion method developed in the previous experimental chapter was used for this experiment. Three psychological tasks were used to assess motor control, learning and memory, reaction time and motor inhibition. These tasks were selected

because they represent areas of psychological deterioration commonly observed in patients with mHE that are often attributed to the effects of ammonia in the brain (Ortiz et al., 2005, Weissenborn et al., 2005, Butz et al., 2010a). Questionnaires were used to assess perceived levels of fatigue because it is also often reported by mHE patients and can be the first signs of impairment (Cordoba et al., 1998, Dhiman and Chawla, 2009, Malaguarnera et al., 2011b). If ammonia is a direct cause of these proposed changes in function and sensation, experimental induction of hyperammonaemia in a healthy human adult to typical levels found in exercisers or those with disease would lead to impairment in performance of neuropsychological tasks and increased sensations of fatigue.

4.2 METHODS

4.2.1 PARTICIPANTS

Ten healthy right hand dominant males (Age: 25 ± 5 yr, BM: 76.3 ± 7.1 kg, Height: 178.6 ± 4.5 cm, mean \pm SD) volunteered for this study. Prior to each testing session, participants were asked to abstain from caffeine, alcohol and strenuous exercise for 24 hours.

4.2.2 FAMILIARISATION SESSION

Prior to the initial testing trial, each participant attended a familiarisation session.

Participants familiarised themselves with each of the psychological tasks and subjective scales to be performed during the main testing trials. Motor control, cognition, and learning and memory were assessed using the Continuous Compensatory Tracking Task (COMPTRACK), the Inhibitory Control Test (ICT), and Auditory Verbal Learning Task (AVL) respectively. The Multi-Dimensional Fatigue Symptom Inventory-Short Form (MFSI-SF) was administered to assess fatigue sensation. All tests are described in detail in the general

methods section. Each participant performed five 2-minute trials of the COMPTRACK, and three 2-minute trials of the ICT. They were not asked to perform the AVL test or MFSI-SF at this time, but were provided with a verbal description of both.

4.2.3 INFUSION PROTOCOL

Testing was performed on two days, with each day separated by at least 1 week. On each day the participant received a continuous iv infusion of either a sterile 2% ammonium chloride (NH₄Cl) solution (AMM trial) or a sterile placebo 0.9% sodium chloride solution (PLA trial), over a period of 240 minutes (4 hours). This was administered at a rate of 90ml/hr, as determined from chapter 3, using a double blind cross over design. The procedures follow those in the general methods, with psychological tasks and subjective scales administered at the intervals outlined in figure 4.1 below.

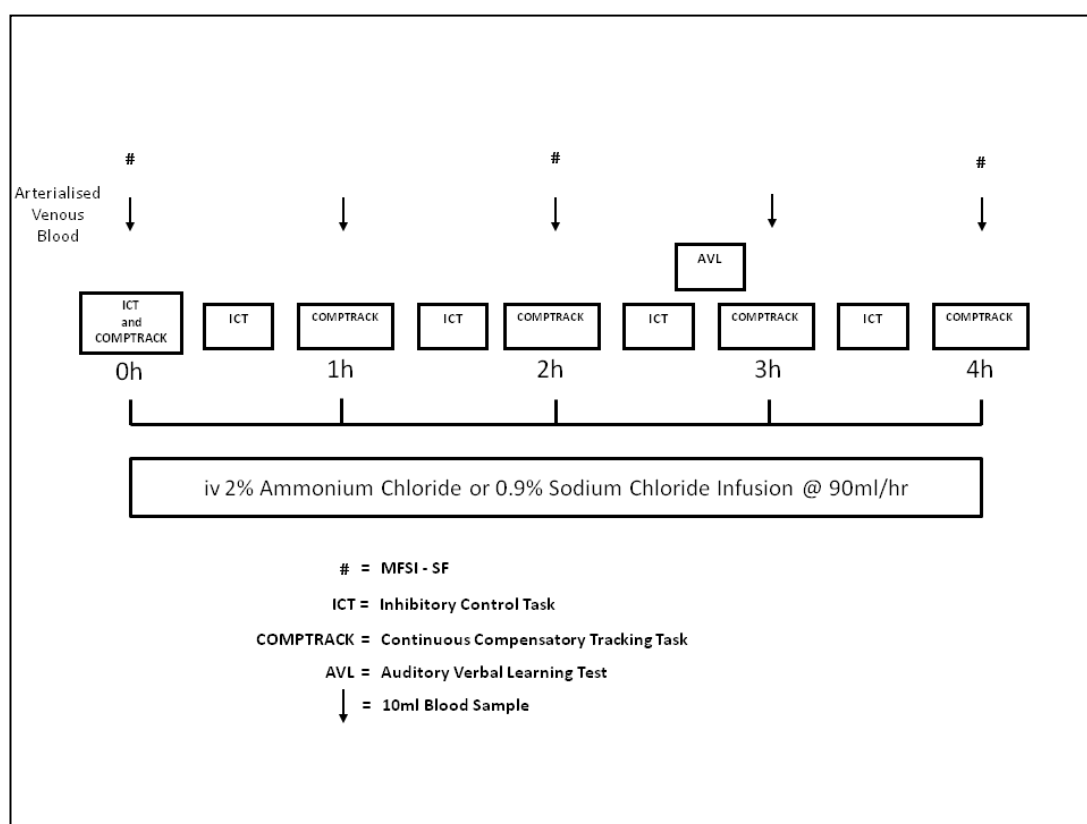


Figure 4.1. Schematic of infusion protocol for each testing trial

4.2.4 BLOOD COLLECTION AND ANALYSIS

Arterialised venous blood was collected at baseline, and every hour during the infusion. It was processed and analysed for plasma ammonia concentration as described in the general methods section.

4.2.5 STATISTICAL ANALYSIS

All statistical analysis was performed as described within the general methods.

4.3 RESULTS

4.3.1. ARTERIALISED VENOUS PLASMA AMMONIA CONCENTRATIONS

At baseline there was no difference between arterialised venous plasma ammonia concentration in the AMM and PLA trials ($52 \pm 4 \mu\text{mol/L}$ PLA; $48 \pm 7 \mu\text{mol/L}$ AMM; Mean \pm SD, $p = 0.667$). There was a main effect of time ($F(6,54) = 151.391$, $p < 0.001$, $\eta_p^2 = 0.94$), and an interaction effect of time and infusion ($F(6,54) = 119.810$, $p < 0.001$, $\eta_p^2 = 0.93$).

There was a significant increase in plasma ammonia concentration from baseline at all time points during the AMM trial infusion (see figure 4.2, $p < 0.002$), with a small increase in plasma ammonia concentration from baseline at 2 hrs ($+5 \mu\text{mol/L}$, $p = 0.009$) and 3 hrs ($+11 \mu\text{mol/L}$, $p = 0.004$) during the PLA trial infusion (figure 4.2). The plasma ammonia concentrations were significantly higher at all time points during the infusion in the AMM trial compared to the PLA trial ($p \leq 0.009$). Post infusion plasma ammonia concentrations in the AMM trial decreased rapidly from $210 \pm 15 \mu\text{mol/L}$ to $86 \pm 11 \mu\text{mol/L}$ within 15 minutes.

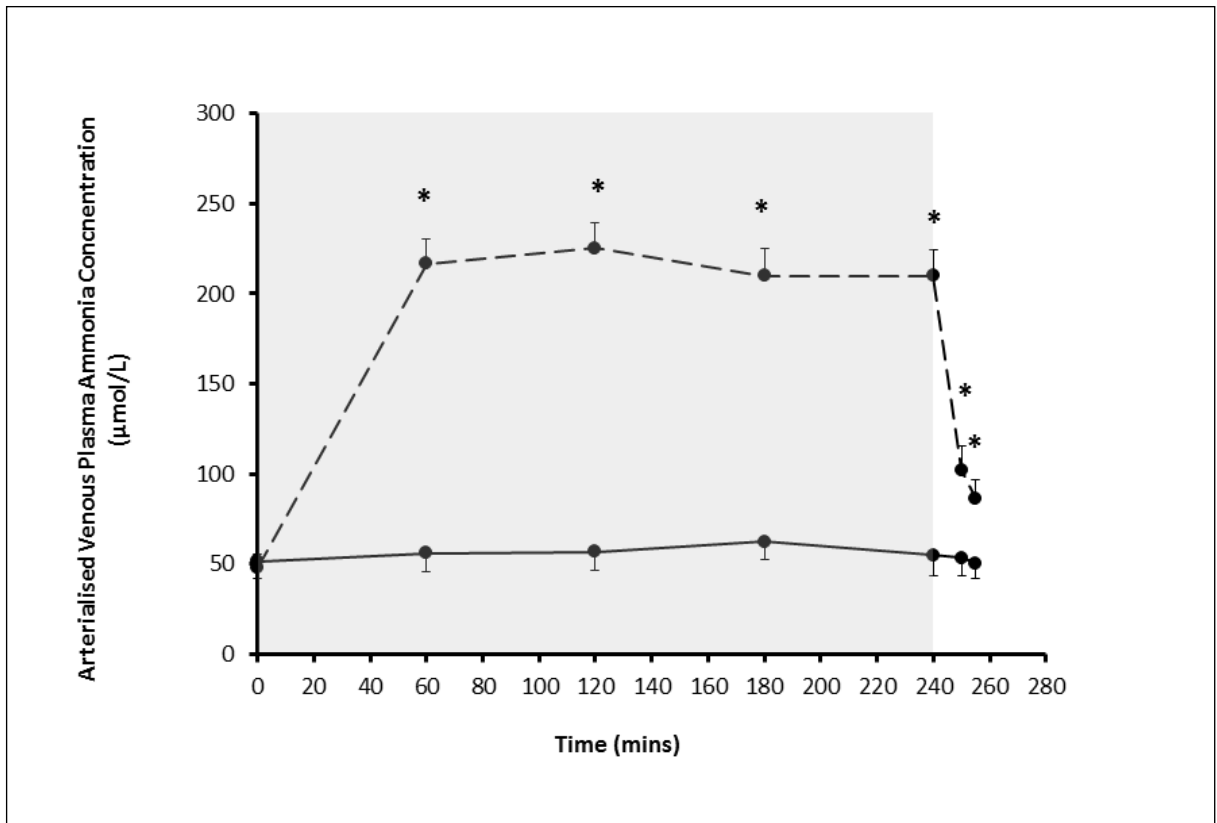
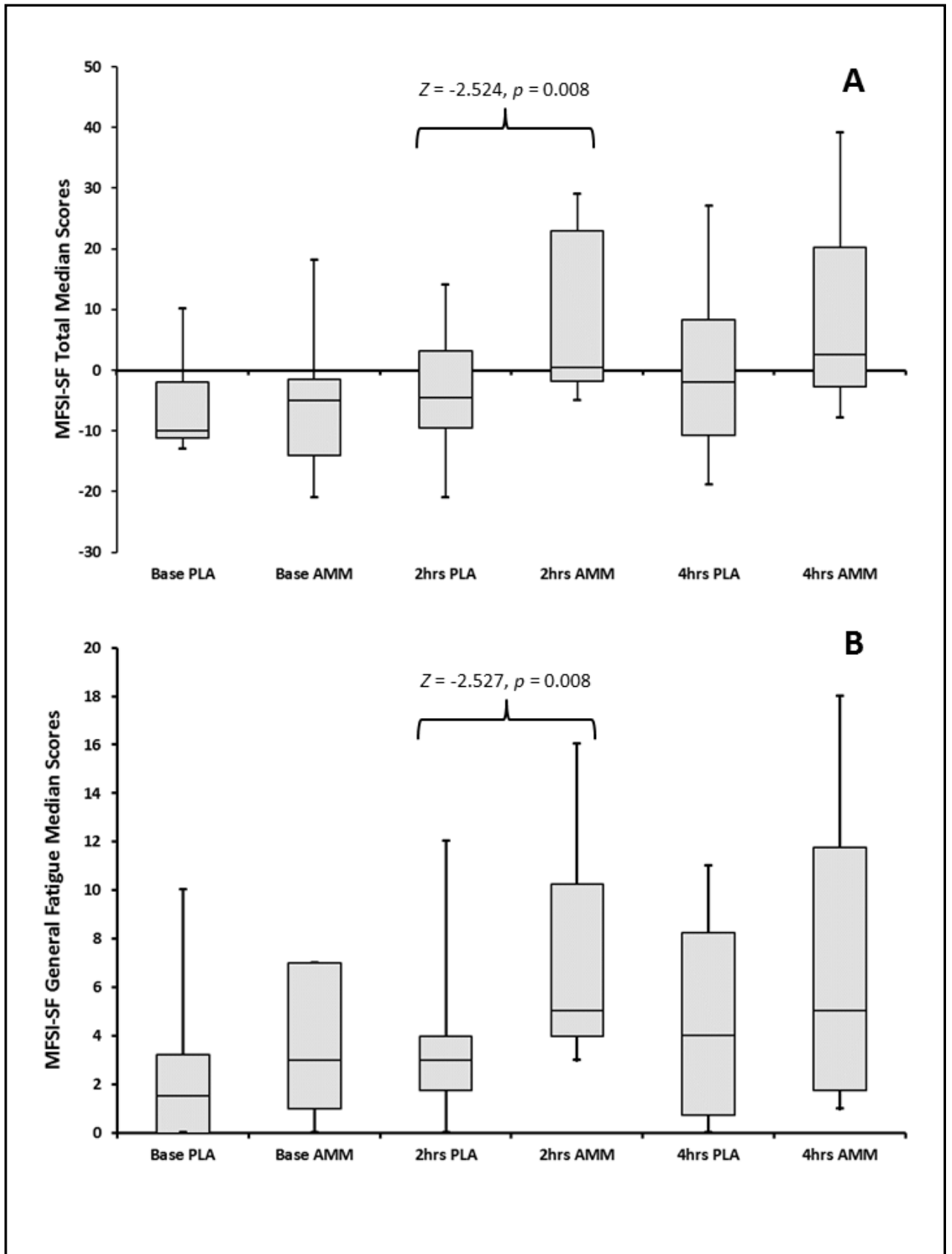


Figure 4.2. Arterialised venous plasma ammonia concentrations during AMM (Dashed Line) and PLA (Solid Line) infusion trials. Shaded area represents infusion period. * indicates significant difference in concentration between infusion trials (AMM vs. PLA; $p \leq 0.009$). Data are presented as mean \pm SD.

4.3.2 SUBJECTIVE RATINGS OF FATIGUE

At baseline there were no significant differences in MFSI-SF total or subscale scores between trials. At 2 hours there was a significantly higher total MFSI-SF score in the AMM trial compared to the PLA trial ($Z = -2.524$, $p = 0.008$, 2 tailed; Figure 4.3), indicating overall that there were increased sensations of fatigue associated with the AMM trial. When the individual subscales were analysed, they showed significantly higher sensations of general fatigue ($Z = -2.527$, $p = 0.008$, 2 tailed) and physical fatigue ($Z = -2.156$, $p = 0.027$, 2 tailed), and lower sensations of vigour ($Z = -2.456$, $p = 0.012$, 2 tailed) for the AMM trial. There were no differences observed between trials in the remaining two subscales of mental ($Z = -1.849$, $p = 0.082$, 2 tailed) or emotional fatigue ($Z = -0.184$, $p = 1.000$, 2 tailed). At 4 hours there were no longer any significant differences in MFSI-SF total or subscale scores between trials.



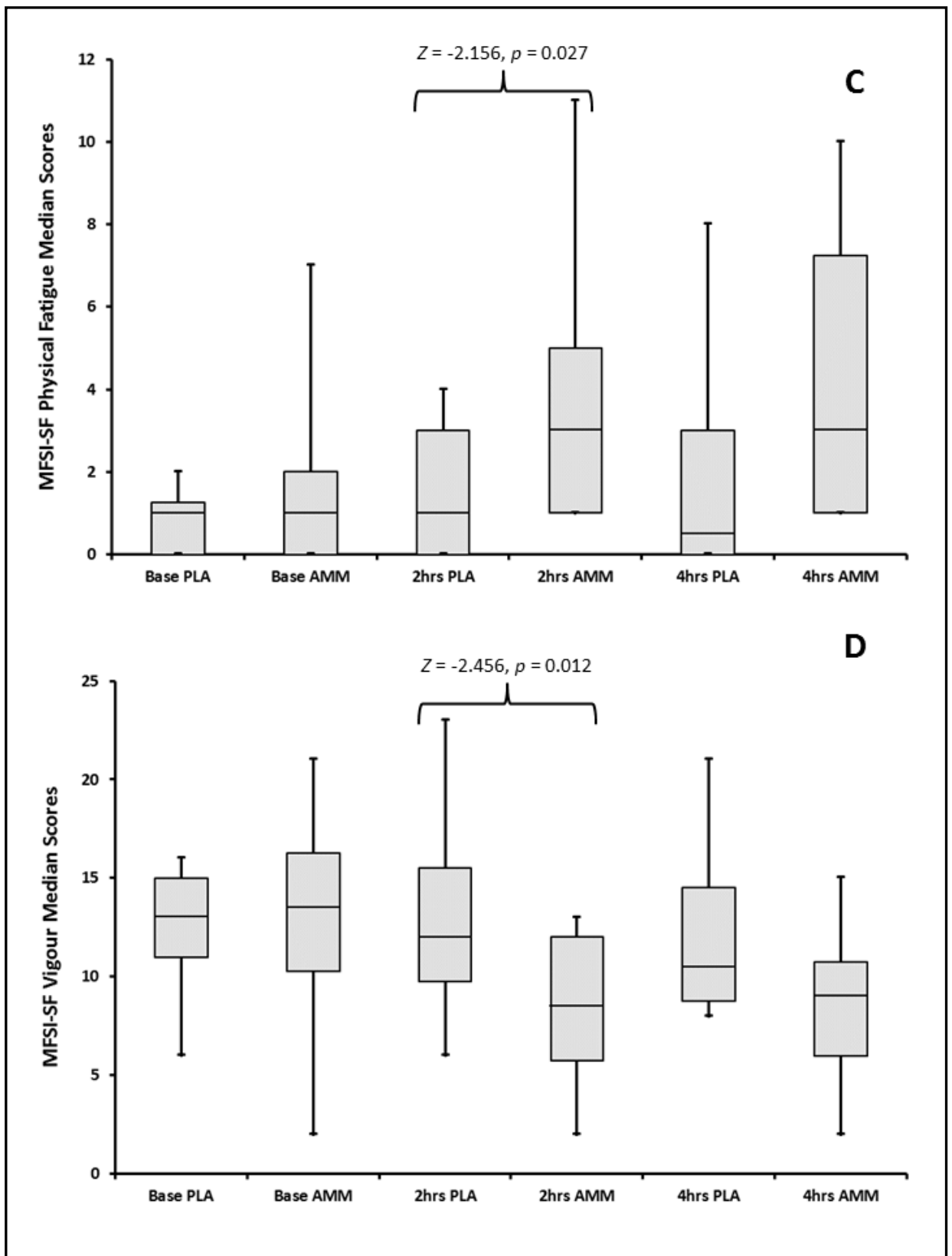
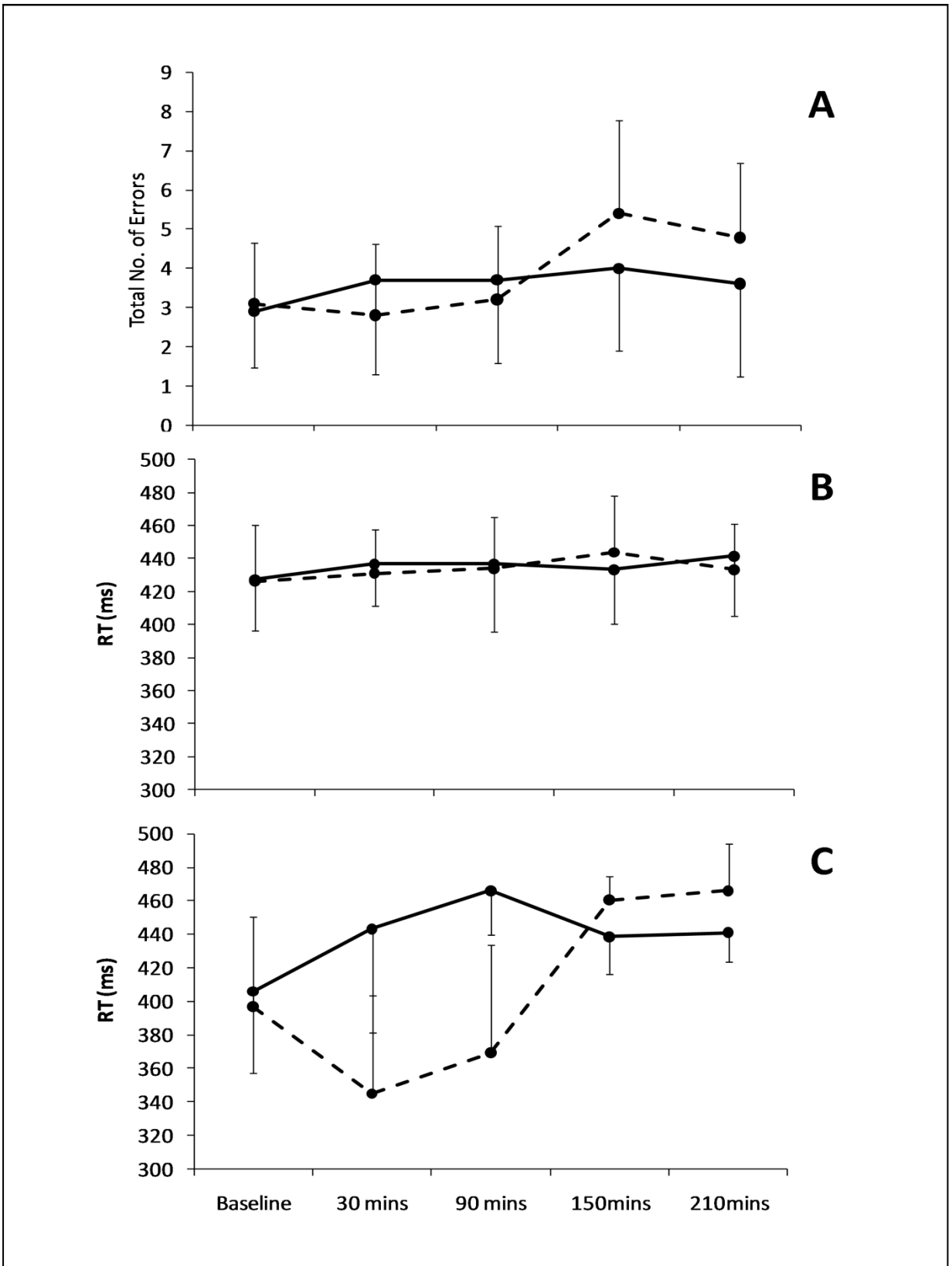


Figure 4.3. A) Comparison of MFSI-SF total score between PLA and AMM infusion trials. Total scores at 2hrs show significantly higher sensations of fatigue in the AMM trial. **Breakdown of total MFSI-SF score into individual subscales shows higher levels of; B) General Fatigue, C) Physical Fatigue, and lowers levels of D) Vigour in the AMM trial.** Data are presented as boxplots with median scores, IQR and total range shown

4.3.3. PSYCHOLOGICAL TASKS

ICT task

There was a main effect of time on total number of errors for the ICT task ($F(4,32) = 3.450$, $p = 0.019$, $\eta_p^2 = 0.301$), suggesting an increase in number of errors with time, however this did not survive after correction for a type one error using a Bonferroni correction. Figure 4.4 illustrates that there was a trend towards a higher number of total errors at 150 minutes ($p = 0.457$) and 210 minutes ($p = 0.357$; Figure 4.4A), as well as a decrease in lure reaction time (RT) at 30 ($p = 0.161$) and 90 minutes ($p = 0.161$) in the AMM trial compared to the PLA trial (Figure 4.4C), however these did not reach statistical significance.



COMPTRACK Task

There was no significant effect of time or infusion on measures of COMPTRACK task performance (Figure 4.5)

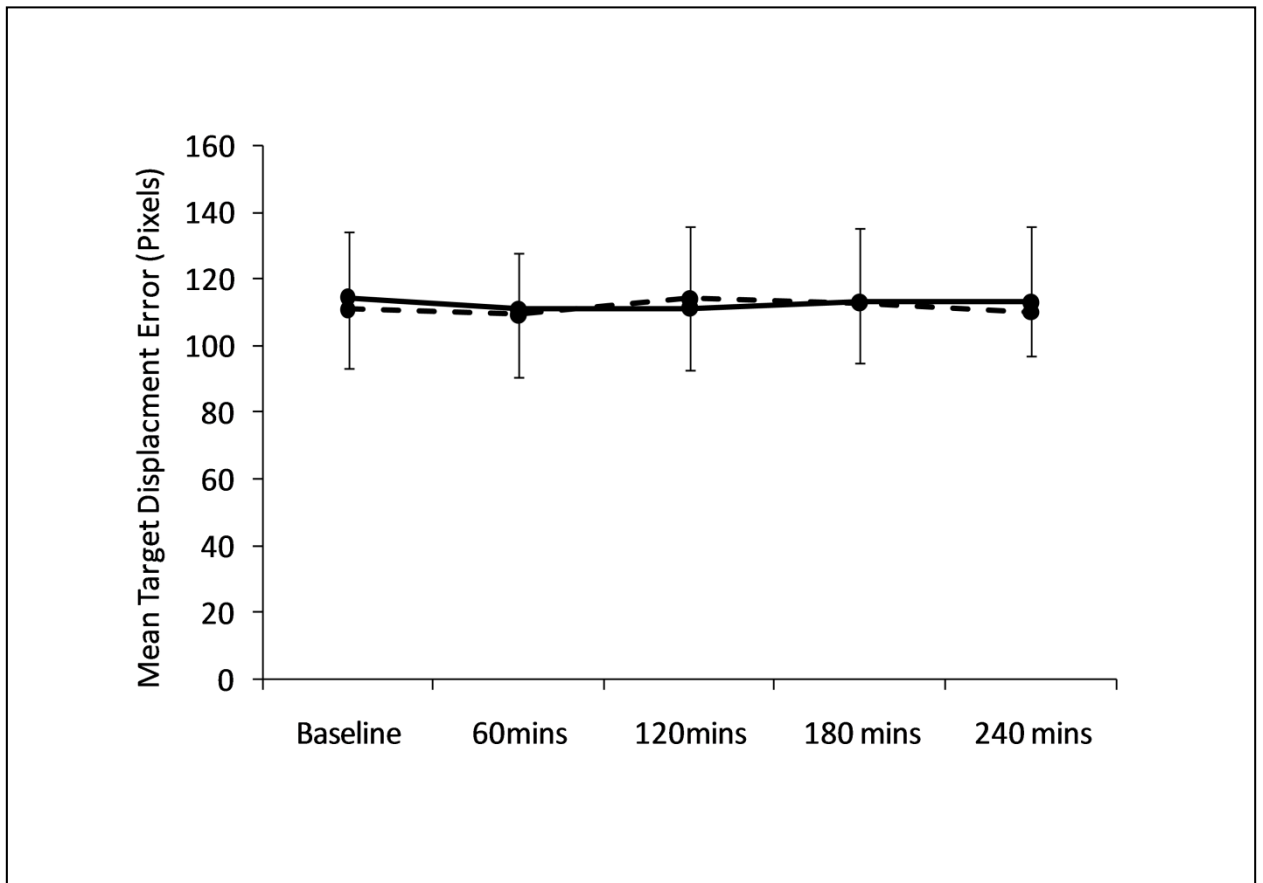


Figure 4.5. COMPTRACK task target displacement error at each time point during the AMM (Dashed Line) and PLA (Solid Line) infusion trials. Data are presented as mean \pm SEM.

AVL Test

As with both the ICT and COMPTRACK tasks, there was no significant effect of ammonium infusion on AVL task performance (Figure 4.6)

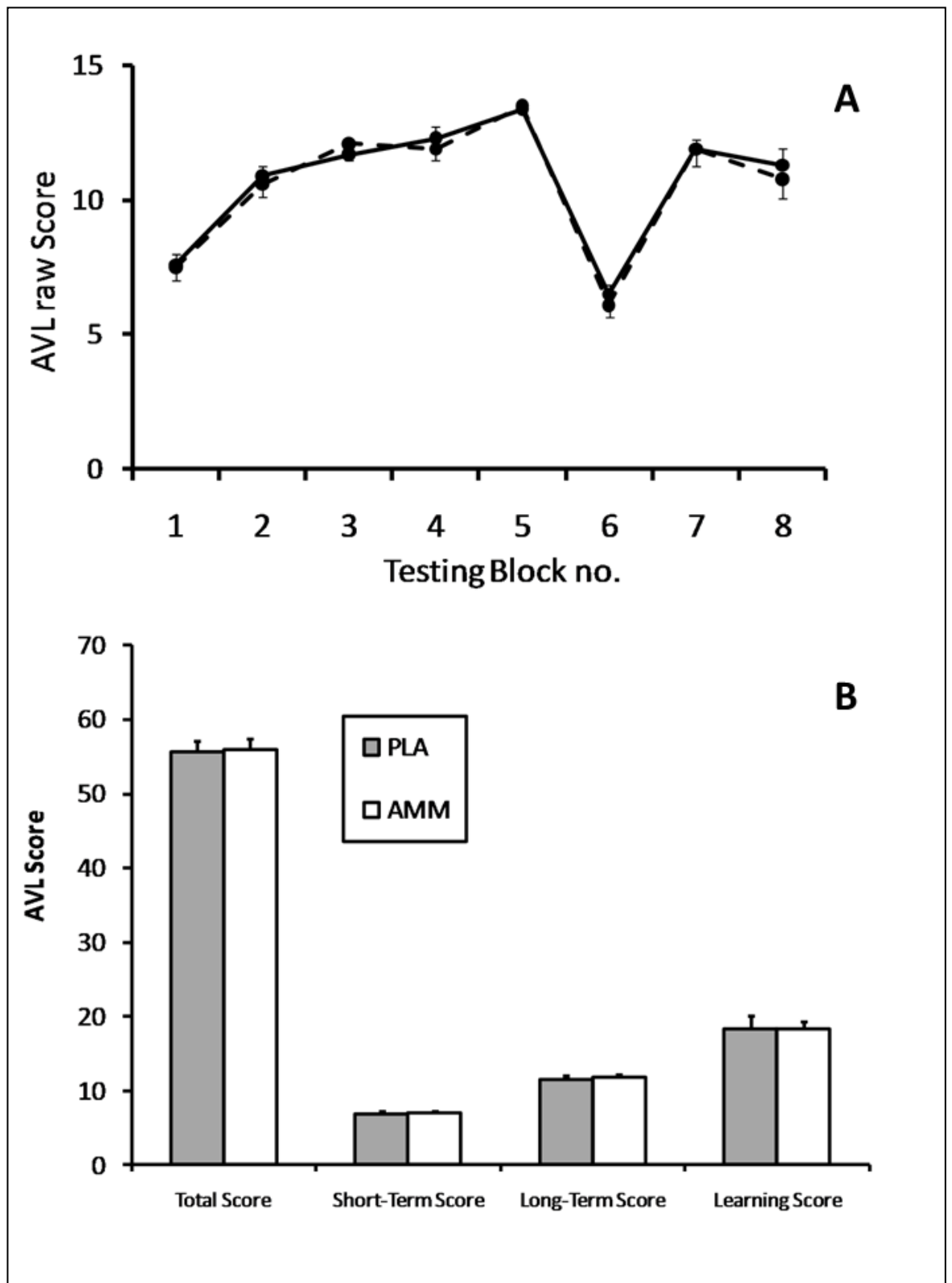


Figure 4.6. A) AVL test raw scores for both AMM (Dashed Line) and PLA (Solid Line) infusion trials. B) Calculated memory and learning scores for AMM (No Fill) and PLA (Solid Fill) infusion trials. Data are presented as mean \pm SEM

4.4. DISCUSSION

The aim of this second experimental study was to identify whether hyperammonaemia in isolation from other physiological or pathological variables in healthy human adults has a direct effect on brain function and leads to the commonly observed alterations in cognition, motor function and fatigue associated with this condition. These results show that acute hyperammonaemia in healthy human adults induces significant sensations of fatigue but there was no impairment in the performance of psychological tasks designed to assess; motor control, learning and memory, reaction time and motor inhibition. These results demonstrate that acute hyperammonaemia in the absence of other complications does not cause the typically observed performance impairment which is common in individuals with mHE. Whilst the effects of chronic exposure to ammonia cannot be ruled out, as the repeated exposure to hyperammonaemia experienced in cirrhosis may have a cumulative effect causing chronic damage, the levels of ammonia reached in the blood in the present study match or exceed those found in patients with liver disease, which have been found to result in impairment of psychological task performance after induction of hyperammonaemia (Balata et al., 2003a, Shawcross et al., 2004a). This is the first experiment to directly assess the contribution of ammonia to the impairment of psychological function by using iv infusion of ammonium chloride in healthy human adults in the absence of other pathological variables, and suggests that ammonia alone may not be the primary cause of such impairments observed in liver disease patients.

Rey's AVL test was used to assess for changes in learning and memory. Deficits in learning and memory are consistently observed in animal models of chronic moderate hyperammonaemia and liver disease (Mendez et al., 2009, Erceg et al., 2005a), and have been associated with impaired regulation of the NMDA receptor – Nitric Oxide (NO) – cGMP pathway by ammonia in neurons, leading to alterations in the levels of cGMP within

brain (Erceg et al., 2005a, Monfort et al., 2009). This test has previously been found to be sensitive to impairment in learning and memory in patients with chronic liver disease with significantly lower learning and long term memory scores observed (Ortiz et al., 2006). In contrast, the present findings show no significant impairment in raw scores, learning scores, short term memory scores or long term memory scores associated with the onset of significant hyperammonaemia (Figure 4.6). In fact, scores for both the AMM and PLA trials were markedly similar (Figure 4.6). The COMPTRACK task was used to monitor any induced motor impairment. Rat models of chronic liver failure show impaired motor behaviour associated with alterations to the activation of the basal-ganglia-thalamo-cortical neural pathway (Cauli *et al.*, 2007b), with similar yet less severe alterations also being observed in rats with chronic moderate hyperammonaemia (Cauli *et al.*, 2007c). Impaired thalamo-cortical drive has also been observed in cirrhosis patients with HE who present with motor dysfunction (Timmerman et al., 2003). The required combination of sustained attention and fine motor adjustments for successful COMPTRACK task performance, in combination with the rapid data sampling rate were believed to be sufficient to uncover any subtle changes in motor output which may have been present due to the hyperammonaemia in the present study. Butz et al. (2010), recently highlighted using 3D motion analysis equipment, that subtle alterations in motor control can be observed in cirrhotic patients even prior to the onset of mHE. However, as with the AVL test scores there was no difference in task performance between AMM and PLA trials observed in the present study. The final psychological task was the ICT task, a task designed to assess psychomotor delay and response inhibition (Garavan et al., 1999). This is an area found to be significantly affected in cirrhosis patients (Schiff et al., 2005), and could be related to the alterations in basal-ganglia-thalamo-cortical activation patterns that have been observed in both animals and cirrhosis patients related to ammonia (Cauli et al., 2007b, Timmerman et al., 2003). In addition, the ICT task is increasingly being used as a successful diagnostic tool for distinguishing between the presence of mHE in chronic liver

disease patients (Bajaj et al., 2007). Regardless, this task too showed no significant performance decrement due to hyperammonaemia (Figure 4.4).

The absence of an effect on psychological task performance may suggest that ammonia does not or cannot affect brain function in the same way in healthy individuals as it does in disease states. It has often been believed that in disease, the determining factor behind ammonia neurotoxicity is the permeability of the blood brain barrier (BBB) to ammonia (Lockwood et al., 1991). Lockwood and colleagues suggested that as disease developed, the BBB would deteriorate, allowing more ammonia into the brain, where its toxic actions can develop, and provided evidence for this by showing an increase permeability surface area product and cerebral extraction for ammonia using $^{13}\text{NH}_3$ -PET methods (Lockwood et al., 1991). However, recently this theory has been challenged, as results from further functional $^{13}\text{NH}_3$ -PET scanning has revealed that brain ammonia kinetics are similar in both healthy individuals and those with cirrhosis, and that uptake of ammonia into the brain is more dependent on arterial concentration, rather than disease severity (Keiding et al., 2006b, Keiding et al., 2006a, Sorensen and Keiding, 2007). In addition more recent findings highlight evidence for an intact BBB in liver cirrhosis, with no global or regional differences in cerebral blood flow, unidirectional transport of ammonia into the brain and BBB permeability surface product for ammonia between healthy individuals, liver fibrosis and liver cirrhosis patients (Goldbecker *et al.*, 2010). Studies involving healthy exercising individuals have also reported significant cerebral uptake of ammonia under conditions of exercise-induced hyperammonaemia (Dalsgaard et al., 2004, Nybo et al., 2005). Using arterial-venous difference as a measure of cerebral uptake, Nybo et al. (2005) found there was a net balance of ammonia across the brain at rest. However after 3 hours of exercise there was a significant uptake of ammonia into the brain of $3.7 \pm 1.3 \mu\text{mol}/\text{min}$, which again was significantly correlated to arterial ammonia concentration (Nybo *et al.*, 2005). These

findings would therefore suggest that pathological levels of ammonia in healthy individuals may lead to a similar accumulation of ammonia in the brain as observed in disease, where it would be sensible to assume that the ammonia may cause similar neurotoxicity and hence induce reversible impairment in brain function. The absence of a significant effect in the present findings however may be due to the effects caused by ammonia being too subtle for the psychological tasks to measure any significant change. It can be noted in figure 4.4A that there is a trend towards an increased level of error in the ICT task performance in the AMM trial, however this does not reach significance. This hypothesis is tested in chapter 5 of this thesis where structural and metabolic changes in the brain are measured under hyperammonaemia using quantitative MRI scanning techniques. This will aim to identify whether ammonia does impair or alter structure or metabolism in any areas of the brain and to what severity, which could help to explain the absence of an effect here. The lack of sensitivity of some psychological tasks to show impairment in hyperammonaemia is discussed in section 1.4 of chapter 1 of this thesis. Studies have previously shown an absence of psychological task performance, even in the presence of significantly altered brain quantitative MRI measures (Mardini et al., 2011).

Liver disease is a condition associated with a number of metabolic disturbances besides hyperammonaemia. Other factors such as; manganese, mercaptans, phenols and octanoic acid can all accumulate significantly in liver disease (Butterworth, 2008), whilst inflammation and infection can also be present (Shawcross et al., 2004b, Odeh et al., 2005). All of these factors may impact on HE severity and symptom development. Recently the idea of synergism and interaction between these co-factors and ammonia has been receiving increased interest (Butterworth, 2008, Shawcross et al., 2008, Butterworth, 2011). Alterations in motor behaviour and learning in rat models of liver disease can be reversed with administration of the non-steroidal anti-inflammatory ibuprofen (Cauli et al.,

2009d, Rodrigo et al., 2010). Similar findings have also been identified in liver disease patients. It was reported that worsening of psychological test performance in cirrhosis patients after induction of hyperammonaemia, was only evident in the presence of systemic inflammation (Shawcross et al., 2004b). After the treatment of the systemic inflammation with antibiotic therapy, there was no worsening of psychological task performance, even with the same severity of hyperammonaemia being induced (Shawcross et al., 2004b). In addition, it has recently been identified that ammonia impairs neutrophil function decreasing phagocytosis *in vitro*, and that these impairments are reproduced in rat models of hyperammonaemia, in addition to cirrhosis patients under oral amino acid challenge (Shawcross et al., 2008). The impairment in neutrophil function due to hyperammonaemia, will likely predispose cirrhosis patients to infection and an inflammatory response, leading to an additive effect of hyperammonaemia on normal brain function and associated HE symptom development (Shawcross et al., 2010). These findings confer that it is the interaction between hyperammonaemia and the other metabolic and immunological perturbations in liver disease, which are necessary to induce the psychological and functional impairment associated with HE symptom development. Recently this interaction has been realised in rat models of hyperammonaemia, where neuroinflammation via the activation of microglia in the cerebellum was observed, and related to impaired cognition and motor activity (Rodrigo *et al.*, 2010). Treatment with ibuprofen normalised the inflammatory response in these rats with concomitant restoration of cognition and motor activity (Rodrigo et al., 2010). These findings were replicated in a rat model of liver disease (Rodrigo et al., 2010). This highlights the important interaction of hyperammonaemia and inflammation in HE symptom development, and hence this may be the case for other hyperammonaemic conditions such as exercise as well.

There are, however, some subtle changes associated with the onset of hyperammonaemia in healthy adults, as shown by the appearance of significantly higher sensations of fatigue in the AMM trial than the PLA trial at 2 hours in the present findings (figure 4.3).

Hyperammonaemia has been associated with the onset of fatigue since the early 20th century (see review by Wilkinson *et al.*, 2010). Exercise physiologists highlighted a relationship between the intensity and duration of exercise/muscle contraction, and the accumulation of ammonia (Babij *et al.*, 1983, Snow *et al.*, 2000), and suggested that this accumulation may be significant in fatigue development (Banister and Cameron, 1990, Mutch and Banister, 1983). Whilst early work in animals and humans showed a reduced plasma ammonia concentration was associated with increased exercise capacity (Barnes *et al.*, 1964, Ahlborg *et al.*, 1968), no studies have been able to demonstrate causality between ammonia accumulation and fatigue. Here we show a direct link between the two for the first time, providing support for the role of ammonia in fatigue development.

Cirrhosis patients themselves report fatigue (Malaguarnera *et al.*, 2011b), show reduced muscle strength (Gam *et al.*, 2011) and reduced aerobic capacity (Campillo *et al.*, 1990), whilst they or their family members often report alterations in sleep patterns and increased levels of drowsiness as some of the initial signs of developing mHE (Cordoba *et al.*, 1998, Dhiman and Chawla, 2009). Acute ammonia exposure in rats has shown significant changes in the somatosensory cortex through T_1 , T_2 , and diffusion weighted magnetic resonance imaging (Cauli *et al.*, 2007a), with prolongation of somatosensory evoked potentials commonly being observed in cirrhosis patients (Yang *et al.*, 1998). This may help explain the present findings, by suggesting that exposure to acute hyperammonaemia could differentially and temporally affect certain brain areas. The somatosensory cortex being one of the primary areas to be initially impaired, leading to subtle changes in sensation and hence increases in sensations of fatigue, with more chronic exposures eventually leading to the common psychological impairments associated with minimal hepatic encephalopathy. All neural connections running into and out of the

somatosensory cortex, are relayed via the thalamus (Brodal, 2004). Thalamic neural pathways have shown altered regulation due to hyperammonaemia (Cauli et al., 2007b), therefore this may play a role in interrupting normal sensory output from the somatosensory cortex contributing to the onset of increased fatigue sensation. Regionally selective effects of ammonia in brain have been proposed, sGC activity (an important enzyme in the regulation of the NMDA receptor – Nitric Oxide (NO) – cGMP pathway in neurons, which is impaired by the actions of ammonia; section 1.3, chapter 1) in autopsied brain slices from cirrhosis patients has been found to be increased in the frontal cortex, but decreased in the cerebellum of these patients compared to controls, showing regionally selective behaviour of this enzyme in response to metabolic perturbations (Corbalán *et al.*, 2002).

In conclusion, this experiment identifies for the first time that acute hyperammonaemia is directly associated with increased sensations of fatigue, supporting the commonly held hypothesis that ammonia accumulation leads to the development of fatigue. In contrast however, there were no significant effects on any of the psychological measures, which does not support the hypothesis that ammonia is a major contributory factor to the deteriorations in cognition, motor control, and memory and learning commonly observed in liver disease patients with HE. Based on this data, it remains unclear whether ammonia has a direct effect on brain. The behavioural measures used to assess brain function may not have been sensitive enough to identify any changes relating to ammonia. More sensitive quantitative analysis such as MRI will help to clarify whether ammonia directly affects brain function.

CHAPTER 5: THE EFFECTS OF EXPERIMENTAL HYPERAMMONAEMIA ON THE HEALTHY BRAIN USING QUANTITATIVE MAGNETIC RESONANCE IMAGING (MRI).

5.1 INTRODUCTION

The effects of hyperammonaemia at a cellular level are indicative of changes to cerebral tissue architecture, its metabolism and function (see chapter 1, section 1.3). These effects are believed to cause impairment to normal brain function *in vivo*, which in its mildest form manifest as alterations to mood (Malaguarnera et al., 2011a), cognition (Weissenborn et al., 2005) and fine motor control (Butz et al., 2010b). These changes are observed in cirrhosis patients as symptoms of HE, and are reliably reproduced in rat models of liver disease and hyperammonaemia (Méndez et al., 2011, Erceg et al., 2005a, Cauli et al., 2007b, Monfort et al., 2007, Cauli et al., 2007c). Furthermore, exercise physiologists often attribute decreases in performance and the development of fatigue in extremes of exercise as being directly related to these cerebral actions of ammonia (Banister and Cameron, 1990, Wilkinson et al., 2010).

Ensnuing hyperammonaemia is prevalent in certain forms of exercise, in some cases reaching levels similar to that of pathology (Bangsbo et al., 1996, Nybo et al., 2005, Mohr et al., 2006). It has often been proposed that this increased ammonia may start to accumulate in body tissues such as brain and affect their function thereby contributing to cerebral impairment and the development of fatigue (Wilkinson et al., 2010). This has led to the pursuit of therapies specifically designed to combat hyperammonaemia, in order to reduce these associated impairments, improve patient quality of life (Phongsamran et al., 2010, Bass, 2007, Wright and Jalan, 2007), and maintain optimal performance in athletes for longer (Prado et al., 2011b). The exact consequences of ammonia's actions in the brain *in vivo*, and its overall contribution to impairment in brain function still remain unclear

however (see chapter 1 section 1.8), and findings from chapter 4 of this thesis have only added further questions. It was found that under significant hyperammonaemia, in the absence of other pathological or physiological stress, there was no associated psychological task impairment, however there were increased sensations of fatigue observed. This may suggest that the direct effects of ammonia alone, are in fact more subtle than previously proposed (Bersagliere et al., 2011). In situations such as liver disease ammonia may be reliant on interaction with other physiological changes which commonly occur to induce significant psychological impairment in these patients (Butterworth, 2008, Felipo et al., 2011). The observed changes in fatigue sensation do however suggest that there may be some subtle alterations in brain occurring as a result of hyperammonaemia in healthy individuals, and provide for the first time a direct link between ammonia and fatigue. This is complimented by other recently published data which showed changes in subjective sleepiness and EEG following oral amino acid challenge induced hyperammonaemia in both healthy and liver disease patients (Bersagliere et al., 2011). Such changes therefore may be evidence for some subtle centrally mediated actions of ammonia, which are undetectable using standard psychological task assessment alone. Although commonly used as diagnostic tools in HE patients, psychological measures have been shown previously to be insensitive to certain brain structural alterations related to hyperammonaemia in liver disease patients (Mardini *et al.*, 2011). Therefore, the aim of this next experimental study was to use quantitative MRI techniques to identify and quantify any changes in the brain which may be caused by hyperammonaemia. It was expected that hyperammonaemia would induce increased sensations of fatigue related to changes in brain MRI, in the absence of changes in psychological task performance. MRI is highly sensitive to minor perturbations in normal brain tissue, therefore, if any direct effects of ammonia on the brain are present, MRI will be able to measure these effects. Magnetization transfer ratio (MTR) imaging and Diffusion Tensor Imaging (DTI) were used to quantify any cerebral osmotic changes which may be being caused by the increases in

ammonia. Magnetic Resonance Spectroscopy (MRS) will provide complimentary information to the MTR and DTI, by highlighting changes in brain metabolites, in particular the important osmolytes glutamine, myoinositol and choline containing compounds.

5.1 METHODS

5.1.1 PARTICIPANTS

Eight healthy male right-hand dominant volunteers (Age: 25 ± 5 yrs, BM: 77.7 ± 6.3 kg, Height: 181.4 ± 3.9 cm; Mean \pm SD) attended for testing, which took place at the Clinical Imaging Sciences Centre of the Brighton and Sussex Medical School in Falmer.

5.1.2 PROCEDURE

After completion of appropriate paperwork (see general methods and appendix 1), participants were asked to remove all metal from their person (jewellery, watches, wallet) and then change into MR compatible tunic and trousers. They were made comfortable in a clinical examination room and the infusion was set up as for previous chapters, however, in addition, a 7m infusion line extension was included to ensure infusion was possible during scanning (an MR compatible infusion pump was unavailable, so a standard pump had to be situated outside the scan room). The participant then completed a pre-infusion MFSI-SF questionnaire and the infusion was started at a constant rate of 90ml/hr with venous blood sampling at 15 minute intervals (see figure 5.1). After 1 hour, the participant was transferred to the scan room. To do this, the infusion was stopped and disconnected, it was reconnected and started again at the same rate, once the participant was lying supine on the scanner plinth. The infusion was stopped for no longer than 5 minutes, which although meant plasma ammonia concentrations will likely to have reduced in this period, it will have been only by approximately $40\mu\text{mol/L}$ (see chapter 3), and will have returned to

similar levels rapidly once restarted. Scanning was performed as described in the general methods. Once complete, the infusion was stopped, the participant completed a post infusion MFSI-SF, and was monitored for a further 30 minutes before leaving. The participant returned at least 1 week after the initial trial for their second trial. This followed the same procedure.

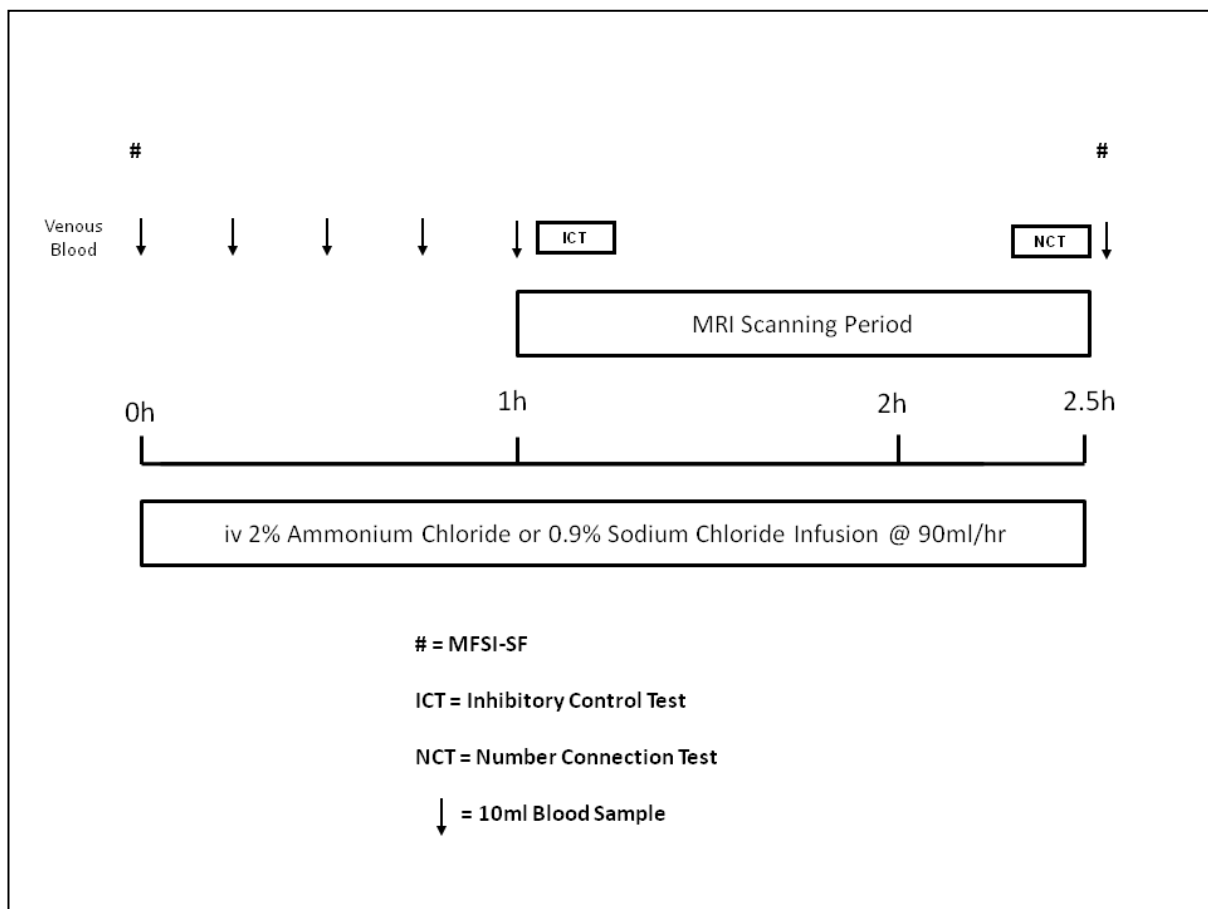


Figure 5.1 Schematic of testing procedure for each infusion trial

5.2.2 ANALYSIS

Venous plasma ammonia concentration

Plasma ammonia analysis followed that outlined in the general methods.

MRI Analysis

All MRI scanning techniques used were analysed as described in the general methods.

Statistical Analysis

Statistical analysis was performed as described in the general methods.

5.3 RESULTS

5.3.1 VENOUS PLASMA AMMONIA CONCENTRATION

At baseline there was no difference between venous plasma ammonia concentration in the AMM and PLA trials ($65 \pm 15 \mu\text{mol/L}$, PLA; $67 \pm 12 \mu\text{mol/L}$ AMM: Mean \pm SD, $p = 0.795$).

There was a main effect of time ($F(5,25) = 17.431$, $p < 0.001$, $\eta_p^2 = 0.777$), and an interaction effect of time and infusion ($F(5,25) = 15.904$, $p = 0.003$, $\eta_p^2 = 0.761$). The plasma ammonia concentrations were significantly higher at all time points during the infusion in the AMM trial compared to the PLA trial (see figure 5.2 all comparisons $p \leq 0.007$).

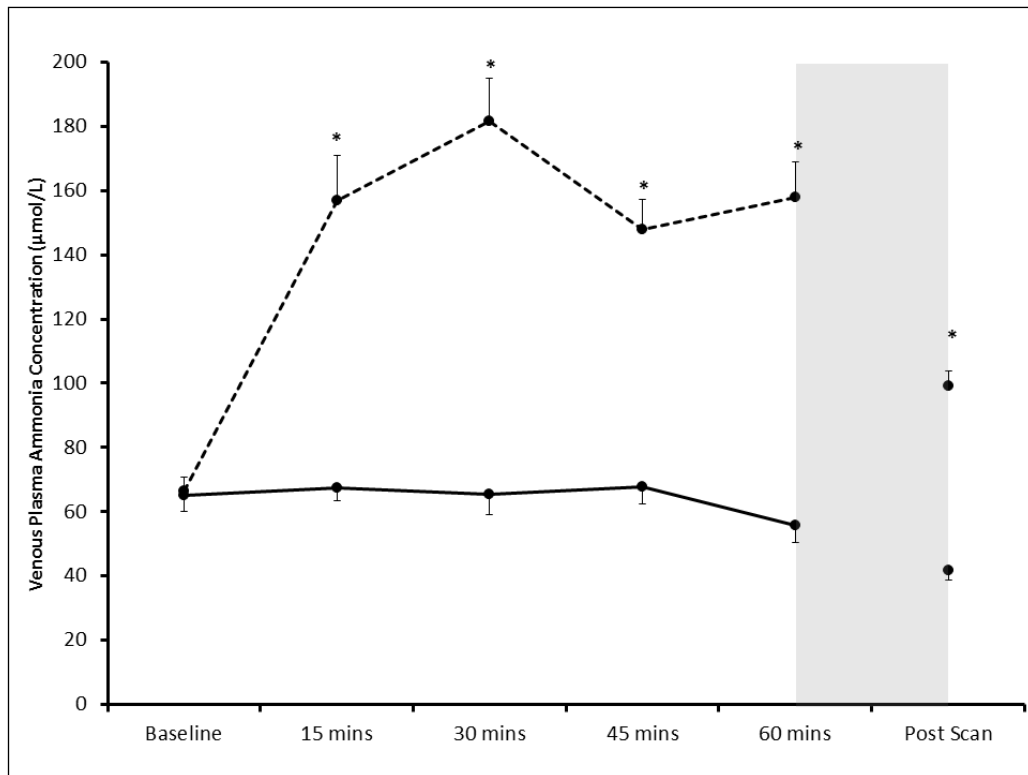


Figure 5.2 Venous plasma ammonia concentrations during PLA (solid line) and AMM (dashed line) infusion trials. Shaded area represents period inside scanner. * significantly different between infusion trials, $p \leq 0.007$

5.3.2 MFSI-SF

Pre-infusion there were no significant differences in MFSI-SF total or subscale scores between trials. Post infusion total MFSI-SF scores were higher in the AMM trial than the PLA trial, however did not quite reach significance ($Z = -1.859$, $p = 0.078$, 2 tailed). When the individual subscales were analysed they showed significantly higher sensations of general fatigue post infusion in the AMM trial ($Z = -2.111$, $p = 0.020$, 2 tailed). There were no significant differences in any of the other subscale scores post infusion (see figure 5.3).

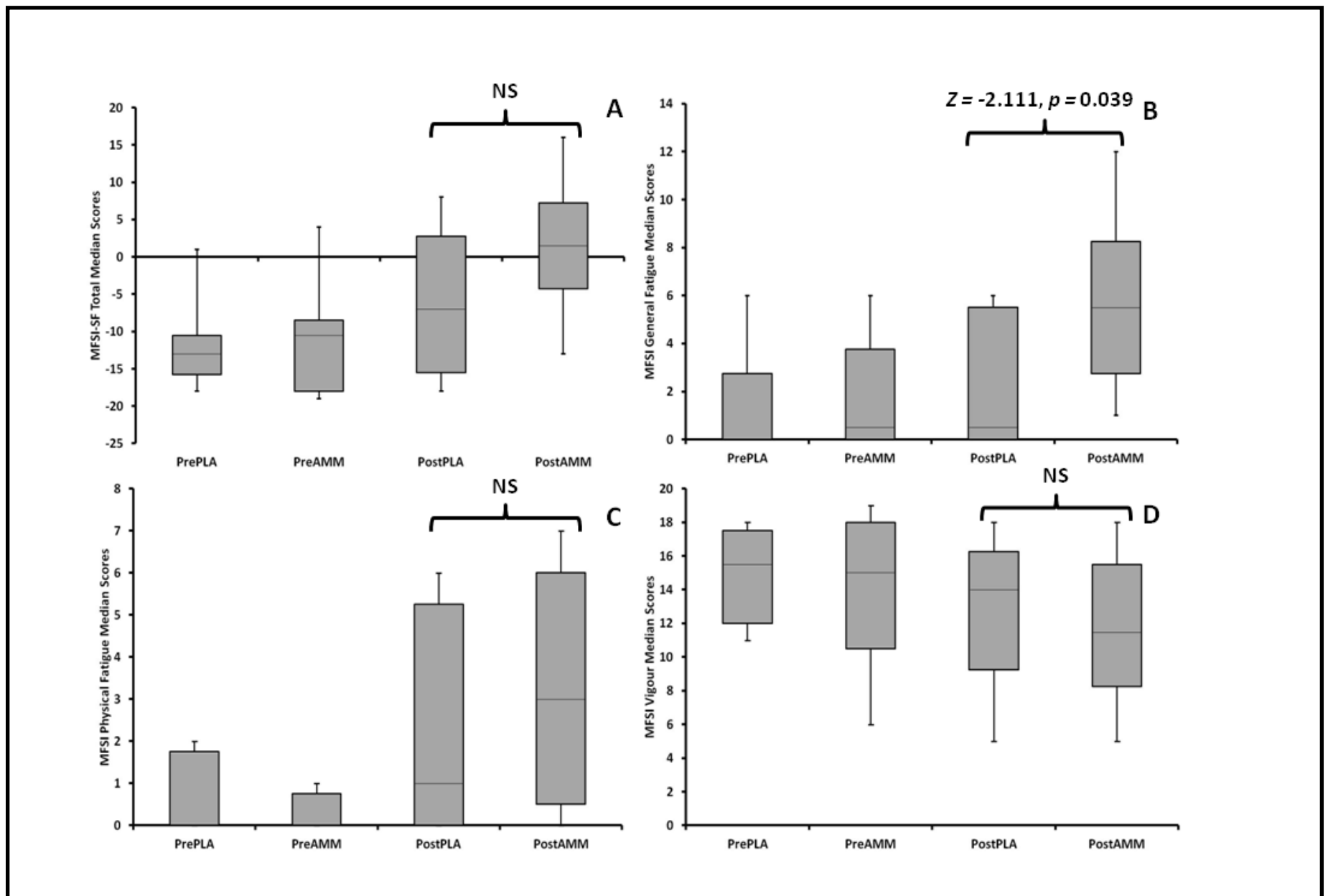


Figure 5.3. A) Comparison of MFSI-SF total score between PLA and AMM infusion trials. Breakdown of total MFSI-SF score into individual subscales shows higher levels of; B) General Fatigue in the AMM trial post infusion. C) Physical Fatigue and D) Vigour showed a trend towards an increase and a decrease respectively in the AMM trial post infusion, but did not reach significance. Data are presented as boxplots with median scores, IQR and total range shown. NS = not significant.

5.3.3 MRI

5.3.3.1 MAGNETIZATION TRANSFER RATIO (MTR).

MTR histograms for white matter (WM), gray matter (GM) and whole brain (WB) are illustrated in figure 5.4. Table 5.1 reports the mean MTR histogram derived parameters for the AMM and PLA trials. There were no significant changes observed in any of the histogram parameters between trials.

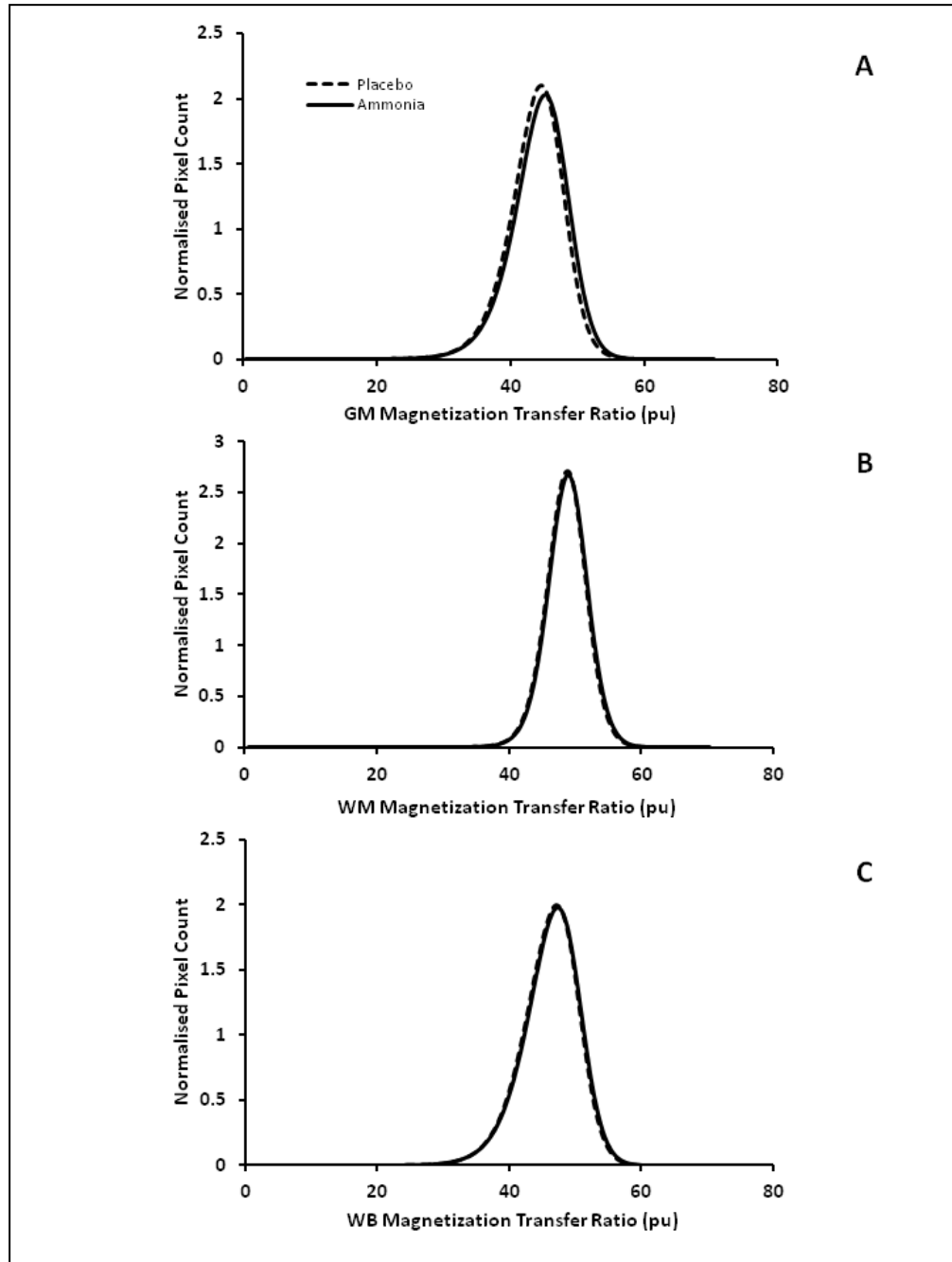


Figure 5.4 Mean MTR histograms for A. Gray Matter (GM) B. White Matter (WM)) and C. Whole Brain (WB). pu : percent units.

Table 5.1 Calculated MTR histogram values for white matter (WM), gray matter (GM), and whole brain (WB). Red type represents not normally distributed data analysed using a Wilcoxon Signed Ranks Test

WM	AMM	PLA	p values
Mean Histogram MTR (pu)	48.82 ± 0.79	48.61 ± 0.52	0.420
MTR Peak Location (pu)	49.08 ± 0.83	48.83 ± 0.57	0.311
MTR Peak Height (pixels)	2.77 ± 0.17	2.74 ± 0.17	0.238
GM			
Mean Histogram MTR (pu)	44.32 ± 1.54	43.78 ± 0.56	0.742
MTR Peak Location (pu)	45.35 ± 1.27	44.65 ± 0.49	0.156
MTR Peak Height (pixels)	2.20 ± 0.27	2.12 ± 0.12	0.467
Whole Brain			
Mean Histogram MTR (pu)	46.28 ± 0.78	46.09 ± 0.56	1.000
MTR Peak Location (pu)	47.50 ± 0.81	47.25 ± 0.61	0.401
MTR Peak Height (pixels)	2.03 ± 0.10	2.02 ± 0.10	0.650

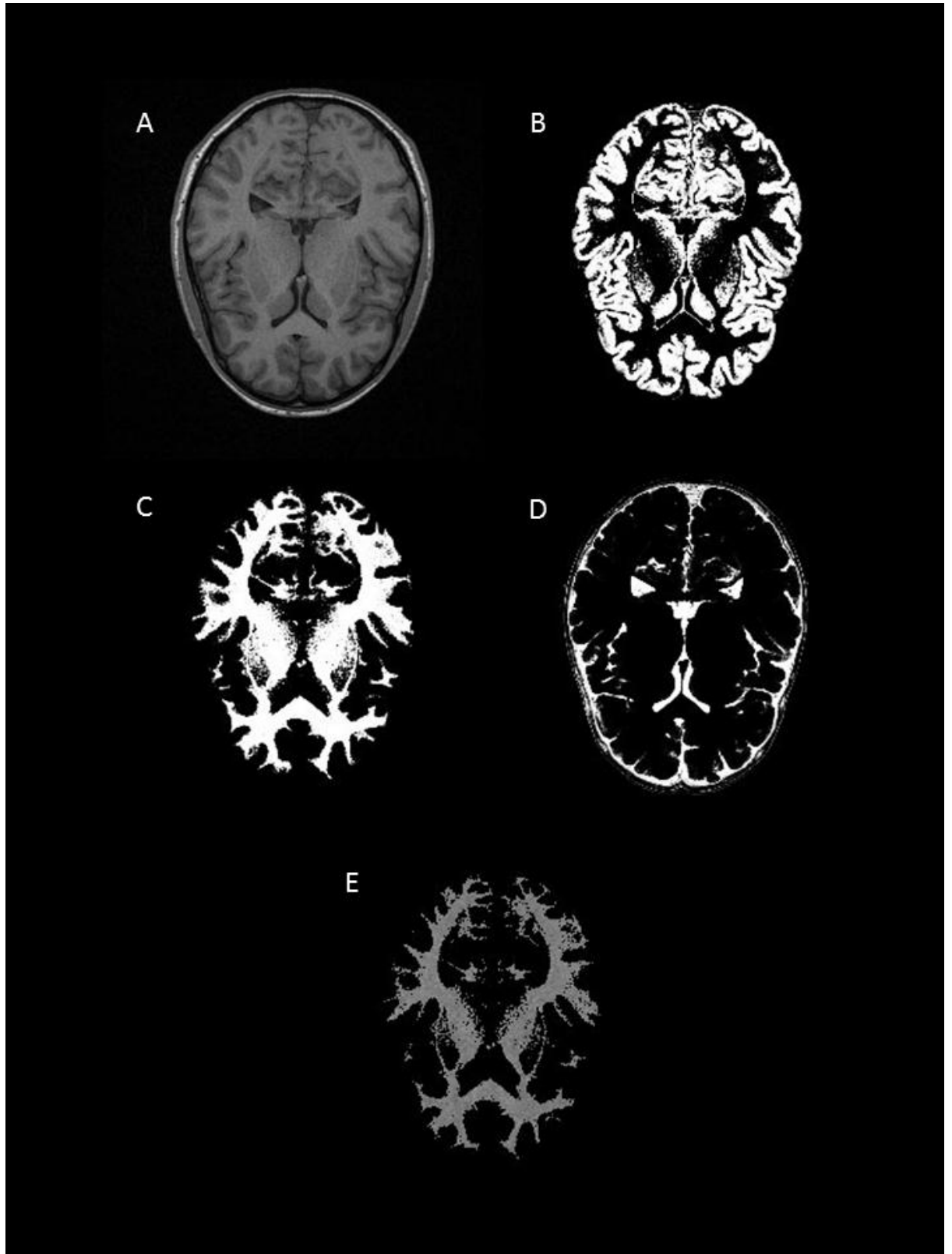


Figure 5.5 Example of images from MTR analysis. A. Transverse slice taken from T1 MPRAGE structural image. This image is then segmented into Gray matter (B), White matter (C) and CSF (D). These images are then used to produce MTR masks (E), to determine MTR values within WM, GM and WB (WM+GM) respectively.

5.3.3.2 Diffusion Tensor Imaging (DTI)

Fractional Anisotropy (FA) and Mean Diffusivity (MD) histograms for WM, GM and WB are illustrated in figure 5.6. Table 5.2 reports the mean FA and MD derived histogram parameters for the AMM and PLA trials. There was a decrease in FA histogram mean in the AMM trial compared to the PLA trial for WM, GM and WB (see table 5.2), however the decrease in WM FA mean did not quite reach significance ($p = 0.056$). This was accompanied by significant increases in FA peak height for GM and WB in the AMM trial, with an increase in the positive skew of the GM (PLA: 1.907, AMM: 1.979) and WB histograms (PLA: 0.964, AMM: 1.061). For MD, there was a decrease in MD peak height for GM in the AMM trial with no change in any of the other MD parameters being observed.

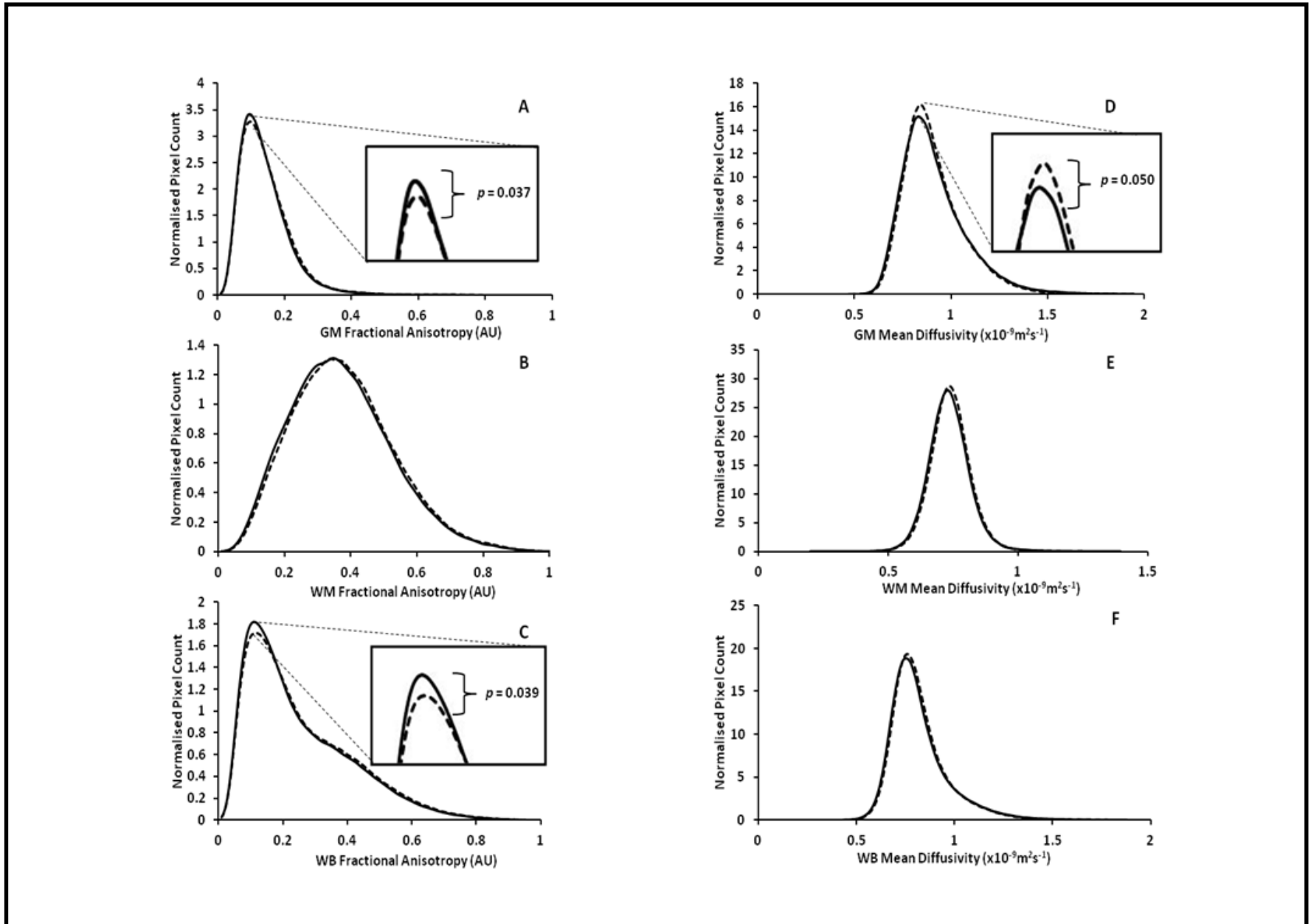


Figure 5.6: Mean DTI histograms for A. FA gray matter, B. FA white matter, C. FA whole brain, D. MD gray matter, E. MD white matter and F. MD whole brain. Enlarged sections illustrate statistically significant change in histogram parameters.

Table 5.2 Calculated DTI histogram values. * represents significant difference between trials. Red type represents not normally distributed data analysed using Wilcoxon Signed Rank test. All other data analysed using paired samples *t* – tests.

DTI FA	WM	AMM	PLA	p values
	Mean Histogram FA (AU)	0.3712 ± 0.0146	0.3790 ± 0.0117	0.056
	FA Peak Location (AU)	0.3463 ± 0.0169	0.3425 ± 0.0255	0.736
	FA Peak Height (pixels)	1.3244 ± 0.0535	1.3187 ± 0.0268	0.714
	GM			
	Mean Histogram FA (AU)	0.1417 ± 0.0075	0.1451 ± 0.0075	0.045*
	FA Peak Location (AU)	0.0956 ± 0.0062	0.0975 ± 0.0065	0.437
	FA Peak Height (pixels)	3.4505 ± 0.2639	3.2956 ± 0.2565	0.037*
	Whole Brain			
	Mean Histogram FA (AU)	0.2493 ± 0.0098	0.2562 ± 0.0094	0.021*
	FA Peak Location (AU)	0.1119 ± 0.0100	0.1188 ± 0.0146	0.164
	FA Peak Height (pixels)	1.8323 ± 0.1724	1.7371 ± 0.1340	0.039*
DTI MD	WM			
	Mean Histogram MD ($\times 10^{-9} \text{m}^2 \text{s}^{-1}$)	0.7359 ± 0.0213	0.7410 ± 0.0144	0.252
	MD Peak Location ($\times 10^{-9} \text{m}^2 \text{s}^{-1}$)	0.7306 ± 0.0235	0.7388 ± 0.0158	0.109
	MD Peak Height (pixels)	29.6114 ± 1.7872	29.3588 ± 3.0682	1.000
	GM			
	Mean Histogram MD ($\times 10^{-9} \text{m}^2 \text{s}^{-1}$)	0.9155 ± 0.0294	0.9139 ± 0.0259	0.828
	MD Peak Location ($\times 10^{-9} \text{m}^2 \text{s}^{-1}$)	0.8381 ± 0.0212	0.8388 ± 0.0175	0.937
	MD Peak Height (pixels)	15.3950 ± 1.4063	16.3327 ± 1.4380	0.05*
	Whole Brain			
	Mean Histogram MD ($\times 10^{-9} \text{m}^2 \text{s}^{-1}$)	0.8214 ± 0.0196	0.8232 ± 0.0167	0.663
	MD Peak Location ($\times 10^{-9} \text{m}^2 \text{s}^{-1}$)	0.7525 ± 0.0224	0.7563 ± 0.0162	0.578
	MD Peak Height (pixels)	19.3079 ± 1.0701	19.4429 ± 1.6416	0.714

5.3.3.3 ^1H -MAGNETIC RESONANCE SPECTROSCOPY (^1H -MRS)

Magnetic resonance spectroscopy was performed using a 2cm^3 voxel placed in the WM of the right hemispheric frontal lobe. Figures 5.7 illustrates examples of the spectra produced from each MRS measurement. Note the prominent water peak at 4.7ppm in figure 5.7A, this is common to all ^1H -MRS spectrum, due to the high abundance of $^1\text{H}_2\text{O}$ found in brain tissue, this signal can only be suppressed by so much during signal acquisition, therefore processing is performed offline to enable a more accurate quantification of the lower concentration metabolites (see figure 5.7C following filtering of water peak).

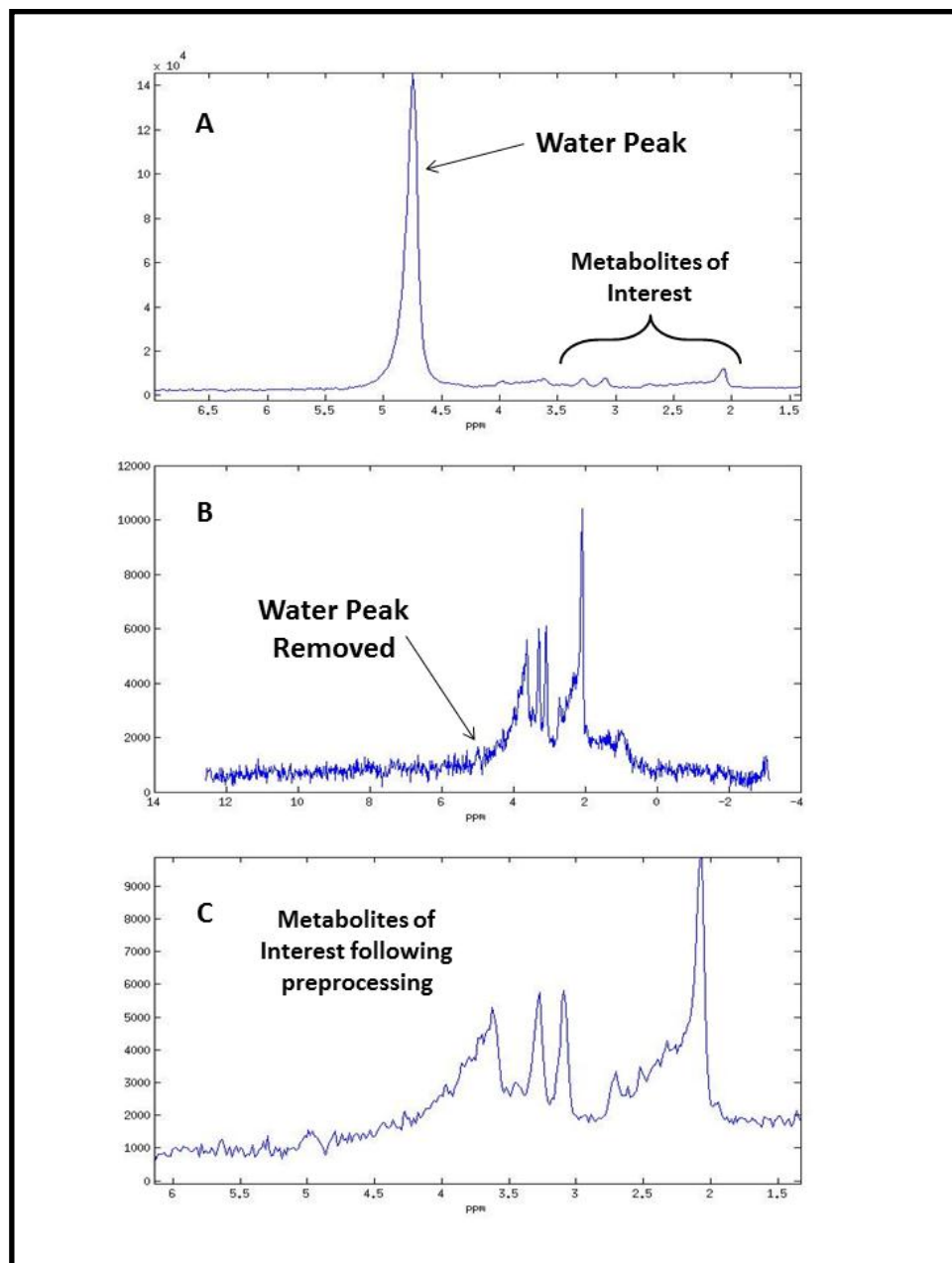


Figure 5.7 Example of MRS spectrum preprocessing. A. Spectra prior to removal of prominent water peak. B. Spectra immediately following filtering of water peak using HSLVD filter. C. Spectra following all preprocessing ready for analysis.

Figure 5.8 illustrates the signal processing performed by the SPID analysis program. The pre processed metabolite spectrum (Blue Line) was modelled against known *in vitro* metabolites peaks collected by the program developers using the PRESS scanning sequence (Green Line). This allowed quantification of Glx, ml, Cr, Cho and NAA peaks from the *in vivo* spectrum (Red Line), providing peak amplitudes for the individual metabolites in arbitrary units, which were then normalised as a ratio to the Cr peak.

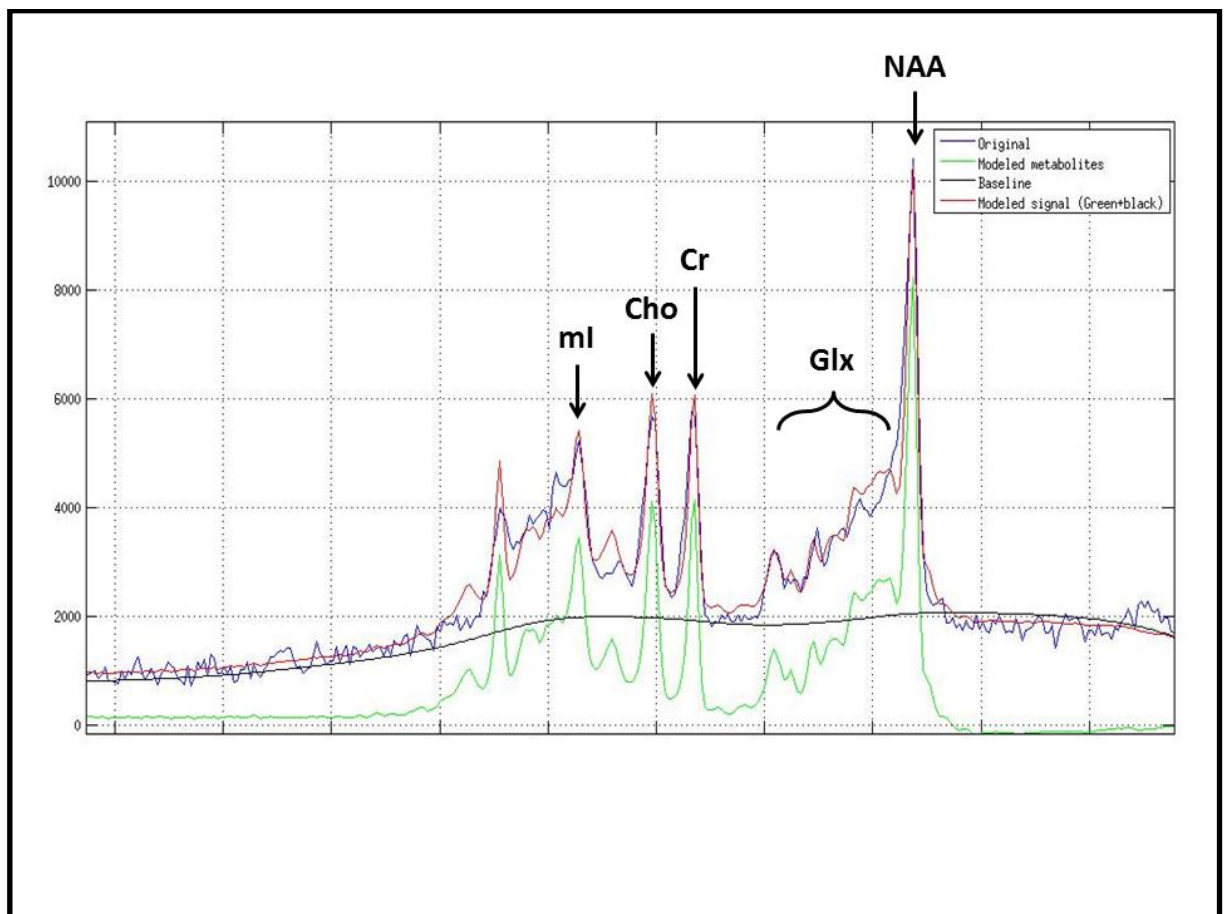


Figure 5.8 Graphical output from SPID spectral analysis. Green line represents metabolite database used to model data. Blue line represents original spectrum. Red line represents modelled and analysed data. Important metabolite peaks labelled.

The MRS metabolite ratios for Glx/Cr, ml/Cr, Cho/Cr and NAA/Cr are presented in table 5.3.

At 1.5T the resolution of individual peaks representing glutamine is poor, therefore it is normal to quantify glutamine together with glutamate as glx. There were no differences in

the Glx/Cr or the ml/Cr ratios between the AMM and PLA trials. The ml/Cr ratios were lower than those normally reported in the literature for the healthy human brain; 0.50 – 0.61 (Cordoba et al., 2001, Geissler et al., 1997), this is likely to have been caused by the poor signal to noise ratio observed around the position of the ml peak in the present spectra (see figure 5.8). In addition to Glx/Cr and ml/Cr, there were no differences observed for the NAA/Cr or Cho/Cr ratios (see table 5.3).

Table 5.3 MRS metabolite data normalised to creatine metabolite peak. Red type represents not normally distributed data analysed using Wilcoxon Signed Rank test. All other data analysed using paired samples *t* – tests.

Metabolite	AMM	PLA	p value
Glx/Cr	1.65 ± 0.31	1.49 ± 0.26	<i>0.468</i>
ml/Cr	0.15 ± 0.05	0.14 ± 0.05	<i>0.868</i>
NAA/Cr	1.64 ± 0.20	1.66 ± 0.22	<i>0.794</i>
Cho/Cr	0.89 ± 0.18	0.94 ± 0.09	0.250

5.3.4 PSYCHOLOGICAL TASK DATA

ICT

The findings from the ICT task were similar to those reported previously in chapter 4 of this thesis. There were no significant differences in the ICT task performance between the AMM and PLA trials (see table 5.4).

Table 5.4 Comparison of mean ICT parameters between AMM and PLA infusion trials.

	AMM	PLA	p value
Mean No. Targets Hit	235.0 ± 36.8	227.9 ± 39.3	0.476
Mean No. Targets Missed	53.0 ± 36.8	60.1 ± 39.3	0.476
Mean Lure Responses	6.4 ± 3.2	5.4 ± 3.4	0.121
Mean Errors	38.6 ± 26.4	47.6 ± 32.3	0.274
Mean Target RT (ms)	400.9 ± 23.7	400.2 ± 27.7	0.870
Mean Lure RT (ms)	403.8 ± 24.3	401.8 ± 26.2	0.692

NCT

There were no significant differences between the AMM and PLA trials (see figure 5.9).

Problems were encountered with joystick calibration for this task, which may have contributed to the low number of targets hit per trial overall (below 50%; 5 out of 10 targets).

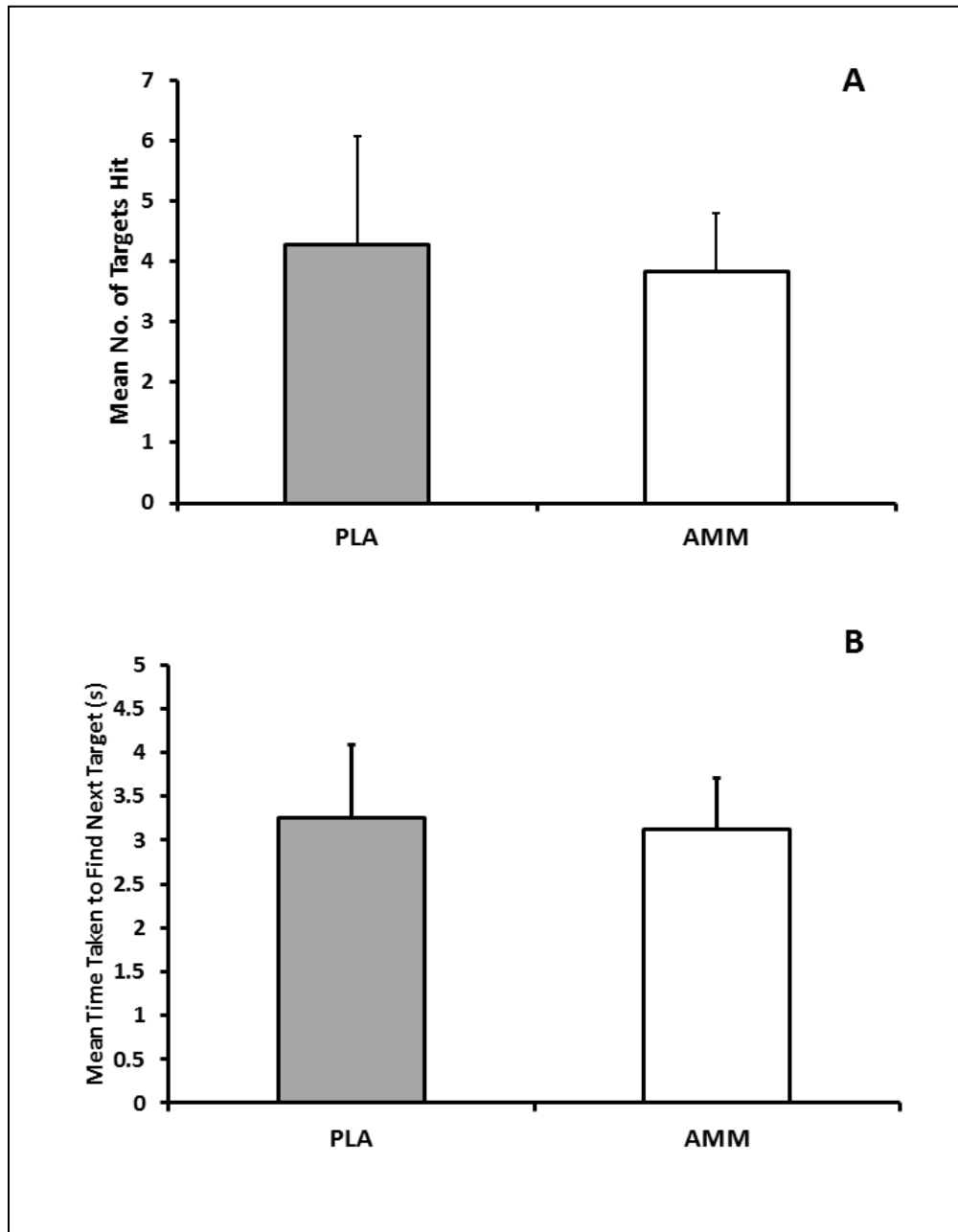


Figure 5.9 Comparison of NCT data between AMM and PLA infusion trials. n = 7, due to joystick failure for one participant.

5.4 DISCUSSION

The aim of this 3rd experimental study was to quantify the *in vivo* structural, functional and metabolic changes that occur in brain in response to acute experimental hyperammonaemia in healthy humans. Ammonia is often reported to cause disturbances in normal brain tissue function (Felipo and Butterworth, 2002, Haussinger and Schliess, 2008), which in turn lead to reversible cognitive and behavioural impairment (Balata et al., 2003b, Shawcross et al., 2004a, Méndez et al., 2011). However, much of this evidence derives from animal models (Cauli et al., 2009c, Monfort et al., 2009), or in the study of patients with chronic disease (Balata et al., 2003b). No studies have investigated the effects of ammonia in humans in isolation from other confounding variables in order to determine its effects on brain. This study is the first to use non-invasive neuroimaging techniques to quantify the effects of ammonia on the healthy brain *in vivo*.

The intravenous infusion of ammonium chloride led to a significant hyperammonaemia in all participants peaking at $181 \pm 38 \mu\text{mol/L}$. This was $\sim 50 \mu\text{mol/L}$ lower than the peak concentrations observed in previous chapters (see figure 4.2, chapter 4), however, due to the nature of this testing it was only possible to obtain venous blood rather than arterialised venous blood. This may account for the difference, as venous ammonia concentrations are often reported as lower than arterial ammonia concentrations when sampled from the same individual (Bessman and Bessman, 1955, Ong et al., 2003, Clemmesen et al., 1999). As with the findings from chapter 4 there were no significant effects of hyperammonaemia on the performance of the psychological tasks, highlighting discordance between systemic hyperammonaemia and psychological function. Similar changes in fatigue sensation were observed in hyperammonaemia, with significantly higher sensations of general fatigue reported post AMM trials compared with the PLA trials (see figure 5.3). As previously discussed in chapter 4 these results suggest that

hyperammonaemia may be causing some subtle effects on brain function, however consistent absence of psychological impairment with hyperammonaemia questions the significance of ammonia to such cerebral dysfunction in disease states. Hence in order to confirm the effects of ammonia on brain structure, function and metabolism, non-invasive *in vivo* neuroimaging using MRI was performed in the present study.

Astrocytes perform many important metabolic functions within the brain tissues; assisting in the maintenance of efficient neural activity, whilst also acting to protect the neuron from damage as they are the first point of contact for any substance crossing the blood brain barrier (BBB) into the brain (Wang and Bordey, 2008). However, astrocytes *in vitro* can show disturbances in morphology, through increased cell volume/swelling, when ammonium salts are added to their medium (Jayakumar *et al.*, 2009). These disturbances within the astrocyte may lead to an opening of membrane channels and an efflux of substances into the extracellular space (Kimmelberg *et al.*, 1990, Haskew-Layton *et al.*, 2008). If neurotransmitters such as glutamate start to accumulate in the extracellular space, excitotoxicity may occur, altering neurotransmission and associated neural signalling mechanisms, impairing many important cellular processes, including motor activation, memory and learning (Cauli *et al.*, 2009c, Monfort *et al.*, 2009). In addition, astrocyte swelling is also found to be linked to the production of ROS/RNOS. Hypoosmotic induced swelling of astrocytes *in vitro* leads to rapid production of ROS/RNOS, which is mimicked by ammonia induced astrocyte swelling (Reinehr *et al.*, 2007). ROS/RNOS have damaging effects on neuronal function; NO generating astrocytes have been shown to effect the level of the mitochondrial respiratory chain complexes, in turn affecting neuronal energy metabolism (Stewart *et al.*, 2000), whilst also causing RNA oxidation (Görg *et al.*, 2008, Nunomura *et al.*, 2006) and protein tyrosine nitration (Schliess *et al.*, 2004), which may affect BBB integrity (Haussinger and Schliess, 2008). ROS themselves can augment

astrocyte swelling (Sharma, 1996, Brahma et al., 2000, Norenberg et al., 2009), which will therefore introduce a self amplifying cycle of ROS production and swelling, exacerbating any associated impairment (Schliess *et al.*, 2006). Such effects of astrocyte swelling due to hyperammonaemia are proposed as major factors in the development of the psychological disturbances which are characteristic of patients with chronic liver disease and HE, through the cascade of cellular and subcellular mechanisms which can be disturbed as a result. Therefore the *in vivo* monitoring of cerebral cellular water and markers of cell swelling under such conditions as hyperammonaemia and disease are useful to determine the presence and contribution of such mechanisms to these cognitive disturbances.

Diffusion tensor imaging (DTI) describes the diffusion of water molecules within brain tissues, and changes in the DTI indices FA or MD represent alterations in the diffusion characteristics of water in the brain and hence will be related to alterations in the local tissue environment regulating the distribution of this water, such as cell membranes integrity (Wheeler-Kingshott *et al.*, 2003). Decreases in diffusivity (as represented by ADC or MD) are believed to represent changes in intracellular volume related to the onset of cellular swelling/oedema (Sotak, 2004). Global ischaemia in rat brain which led to decreases in the extracellular space volume and cellular swelling were related to decreases in the ADC (van der Toorn *et al.*, 1996). Therefore, according to what has previously been discussed regarding the effects of ammonia on astrocyte morphology, one may have expected to have observed a decrease in the MD indices following the induction of hyperammonaemia in the present study. In contrast, there were no significant changes in MD reported following the AMM infusion trials, beyond a decrease in GM MD histogram peak height. The lack of change in diffusivity parameters due to hyperammonaemia tends to suggest that ammonia may not be acting to influence cell volume regulation to such an extent *in vivo* as has been found *in vitro*.

Whilst there was only minimal change in the diffusivity measures, a decrease in the mean histogram FA was observed in WM, GM and WB during the AMM trials, although this did not quite reach significance for WM ($p = 0.056$). The mean histogram FA value represents the average FA value over that entire section of brain (Leung et al., 2004). This combined with a significant increase in FA histogram peak height for both GM and WB suggests that the distribution of the FA within the tissues is shifting from a high FA to low FA values, which can be observed through the increase in the positive skew for both the GM and WB histograms, and overall is representative of a reduction in FA in brain during the AMM trials. FA is generally related to tissue integrity and organisation. Highly structured tissues such as WM will typically have the highest FA as water mobility will be restricted in certain directions dependent on the tissues, whereas environments with few structures such as CSF will have low FA values (Heiervang *et al.*, 2006). Changes in FA will therefore represent alterations to tissues and/or other structures which may impede the diffusion of water in certain directions. Decreases in FA are commonly reported in multiple sclerosis (MS) patients (Cercignani et al., 2001), and have been related to the breakdown of myelin associated with this condition and hence an overall loss of fibre organisation in the tissues (Hasan et al., 2005). Yet this explanation of pathological alteration to tissue integrity is unlikely to be the case in the present study, as the decrease in FA due to ammonia was reversible. Three of the eight participants were randomly allocated the AMM infusion as their first trial, and each showed an increased FA value in their second PLA trial, thereby suggesting that any decrease in FA due to ammonia was only transient in nature, and was therefore not due to long term tissue breakdown from the first trial.

Whilst being representative of tissue integrity, FA values can also be significantly influenced by the accumulation of intra/extracellular fluid within the tissue. Following a stroke,

diffusion anisotropy is found to increase in brain, and this is thought to be due to cell swelling causing a decrease in the extracellular compartment thereby restricting water movement between fibres (Sotak, 2004). In addition, the induction of vasogenic (extracellular) oedema in cats, show characteristic reductions in FA through enlargement of the extracellular space and disorganisation of the brain fibre tract thereby decreasing the anisotropy of water diffusion (Zhao et al., 2006). In contrast, interpretation of FA changes in response to oedema and/or cellular swelling can differ. Cell swelling has also been suggested to be characterised by reductions in FA, rather than increases (Wheeler-Kingshott et al., 2003). Furthermore, a recent study of alcoholic men has identified that low FA values are associated with the accumulation of excess fluid within brain (Pfefferbaum and Sullivan, 2005). Whether extracellular or intracellular fluid build up was the main contributor to these low FA values, was thought to be difficult to directly confirm from the DTI findings alone. Yet the authors did suggest that the relationship between the change in diffusivity and FA could act as a good predictor; with high MD and low FA indicating extracellular contribution, and vice versa (Pfefferbaum and Sullivan, 2005). Therefore, although it is difficult to interpret the precise cellular mechanism responsible for the present findings, the evidence of decreased FA values may indicate signs of ammonia dependent changes in cell and tissue morphology through the regulation of either excess intra or extracellular water. This should be interpreted with caution however, as one may expect parallel changes in diffusivity to accompany these FA changes if this was the case. It is generally considered that cellular oedema would have a larger effect on MD than FA (Rashid et al., 2004). It could be possible that these changes in FA reflect the early stages of ammonia's effect on brain water regulation. A recent study in early stage MS patients using DTI uncovered only small changes in FA histogram peak height at this early stage of the disease, and suggested that FA may be a more sensitive DTI parameter than MD to subtle early pathological change (Rashid et al., 2004). Therefore, could the changes in FA presented here also reflect subtle initial changes in cell water regulation by ammonia,

which would develop into more prominent alterations in brain water with chronic exposure, such as in disease? Evidence of a significant decrease in GM MD peak height in the present study could be indicative of these subtle early effects of ammonia beginning to take place.

Although intriguing to speculate such mechanisms, the interpretation of this DTI data is made all the more difficult by the lack of comparative data available from other studies involving hyperammonaemia and its associated conditions. Mardini et al. (2011) performed diffusion imaging following induction of hyperammonaemia in cirrhosis patients, but only reported ADC data, which was found to increase with hyperammonaemia (which in itself does not fit the proposed theory of ammonia-induced cellular swelling, because increased diffusivity is indicative of interstitial oedema), and not FA data. Whilst in liver disease or portal hypertension patients with significant hyperammonaemia, FA values can be found to be unchanged (Kale et al., 2006) or decreased (Kumar et al., 2008) compared to healthy controls. However, this reported decrease in FA by Kumar et al., (2008) was thought to be due to the cause of the liver cirrhosis in the patients, hepatitis C, which may have led to lesional tissue damage in the brain, decreased structural tissue organisation and hence the associated decrease in FA (Kumar et al., 2008).

Other quantitative MR techniques such as MTR and MRS are routinely used to describe osmotic shifts and the quantification of changes in brain tissue water in pathological and experimental conditions. MTR is more commonly used for the detection of brain pathological changes due to disease such as MS. A decrease in MTR is observed in the brains of MS patients, which is related to a decrease in bound proton fraction and hence representation of tissue pathology e.g axonal loss or lesional demyelination (Giacomini et al., 2009b). Decreases in MTR have also been reported in cases of cirrhosis and

hyperammonaemia (Cordoba et al., 2001, Balata et al., 2003b), however these decreases are far milder than those observed in MS patients, therefore it has been proposed that MTR change in hyperammonaemia or cirrhosis may represent changes in cerebral water through alterations in T1 relaxation times, and/or a decrease in the ratio of bound to free proton pools (see lit review section 1.6.1). Induction of hyperammonaemia in cirrhosis patients and non-cirrhotic portal vein thrombosis patients show significant decreases in MTR, which therefore implicate an ammonia induced mechanism as a cause of these MTR changes (Balata et al., 2003b, Mínguez et al., 2006). Accompanying ¹H-MRS data reported no change in NAA levels (Minguez et al., 2006), whilst normal appearing white matter is observed on T2 weighted imaging in these patients (Rovira *et al.*, 2001), therefore the decrease in MTR under these conditions have been described in terms of changes to brain water, rather than neuronal or tissue damage (Minguez et al., 2006), and provide support for the ammonia induced swelling hypothesis in the development of HE. Although significant hyperammonaemia was induced in the present study, and reflecting the minimal change observed in diffusivity measures, MTR was unaffected, with strikingly similar MTR values observed in WM, GM and WB for both AMM and PLA trials. MTR is heavily influenced by other metabolic disturbances which may be present in disease, such as brain tissue deposition of manganese, whose paramagnetic properties can affect T1 relaxation times (Kuo *et al.*, 2005). Therefore changes in MTR following hyperammonaemia in cirrhosis may be due to the presence of other interacting co-morbidities, rather than the ammonia alone.

¹H-MRS on the other hand provides the opportunity to investigate a number of metabolites within brain tissue related to ammonia metabolism (glutamine/glutamate; Glx), in addition to important organic osmolytes which may be involved in the control of cell volume regulation and cellular swelling (ml and Cho). This compliments findings from diffusion

imaging and MT imaging, by potentially providing mechanistic information as to the cause of such brain water changes. Mammalian cells mainly control cell volume via the cross membrane transport of osmotically active inorganic ions such as Na⁺, K⁺ and Cl⁻ (Lang et al., 1998, Strange, 2004). However, many important cell functions rely on the maintenance of appropriate cell membrane transport and gradients of these ions, therefore many cells, contain additional organic osmolytes which act to control cell volume in addition to inorganic ions, in order to prevent excess disturbances to cell function associated with displacement of these ions (Lang *et al.*, 1998; Strange, 2004). The change in the levels of these osmolytes can be monitored via NMR/MRS techniques *in vivo*. Of these, glutamine/glutamate (glx) and myoinositol (ml) are most commonly measured. In conditions associated with hyperammonaemia, and after induction of hyperammonaemia, it is almost always consistently shown using ¹H-MRS that Glx/Cr signal is increased and the ml/Cr signal is decreased in multiple brain areas (see lit review section 1.6.3). It is also common that decreases in the Cho/Cr ratio are observed to accompany these changes (Grover et al., 2006), as part of the Cho signal represents glycerophosphocholine (GPC), a methylamine which acts as an organic osmolyte like ml (Strange et al., 2004). This response in brain tissue provides additional support for the ammonia induced swelling hypothesis in cirrhosis. Increased ammonia taken up into the brain will be incorporated into glutamine via GS, increasing the Glx MRS signal. This in turn will induce astrocyte swelling, initiating cell volume regulation via the efflux of ml and choline containing compounds from the cell, hence leading to decreases in ml and Cho MRS signals. In the present findings there were no changes in Glx/Cr, ml/Cr or Cho/Cr between the two trials. The reasons behind these MRS finding remain unclear, the absence of any change in the Glx/Cr was not predicted. Ammonia can readily cross the BBB with flux of blood ammonia into glutamine significantly related to arterial ammonia concentrations (Keiding et al., 2006b). Therefore one might expect that with significant hyperammonaemia, there would be an increased flux of ammonia into brain glutamine, which would be reflected by an

increase in the ^1H -MRS Glx/Cr signal. Even with significant hyperammonaemia in the present study, there was no accompanying increase in Glx/Cr. It is suggested that there are regional differences in ammonia extraction by the brain, with significantly higher ammonia uptake in the basal ganglia and cerebellum compared with the cortical regions in cirrhosis (Ahl *et al.*, 2004), with a similar non-significant trend in healthy individuals also (Keiding *et al.*, 2006b). The voxel in the present study was placed in the frontal white matter, where uptake of ammonia may not have been as rapid, reflecting the MRS findings. Different findings may have been observed if additional voxels had been placed in the basal ganglia or cerebellum, however time constraints prevented this. It is also possible that ammonia trapped as glutamine was immediately lost back into the blood. Early studies using animal models of cirrhosis suggested that there may be significant efflux of gln from brain in exchange with aromatic amino acids, and a mechanism for this was observed with isolated cerebral microvessels (Cangiano *et al.*, 1983). However, more recently backflux of glutamine into blood from brain has not been identified in ^{13}N PET studies *in vivo*, suggesting such a mechanism may not be present (Keiding *et al.*, 2006). The glx signal in MRS is essentially the combination of glutamate and glutamine, as these complex multiplets overlap within the same region of the MR spectra (Glx; 2.03-2.35ppm, Gln; 2.10-2.45ppm), and with the strength of the magnet used (1.5T) are difficult to separate due to the low signal to noise ratio. Therefore the lack of Glx/Cr change observed, may have been due to a lack of sensitivity. Yet other studies have been able to observe changes in Glx at 1.5T (Miese *et al.*, 2006), and hence changes should have been measurable in the present study if they were occurring. Finally, it may be the case that the ammonia is not actually reaching the brain tissue, or the uptake is not sufficient to influence glutamine metabolism (Maddock *et al.*, 2011). Great debate exists as to the ability of ammonia to cross the BBB, with suggestions that in cirrhosis ammonia may cross more readily due to an increase in the BBB permeability surface area product for ammonia (Lockwood *et al.*, 1991, Lockwood, 2007, Sorensen and Keiding, 2007), and hence healthy individuals would be less

susceptible to ammonia due to increased integrity in the BBB (Lockwood *et al.*, 1991). However, there is sufficient evidence that the healthy brain does take up significant ammonia (Keiding *et al.*, 2006b, Goldbecker *et al.*, 2010) and that it is increased with increased arterial concentration (Keiding *et al.*, 2006b, Nybo *et al.*, 2005). Therefore this explanation of the MRS findings also seems unlikely. Without further investigation using radiolabelled isotope tracers to measure cerebral ammonia metabolism under experimental hyperammonaemia in healthy individuals, the cause of this Glx/Cr MRS finding remains uncertain. However, this finding combined with no change in ml/Cr or Cho/Cr, and the lack of change in MTR and diffusivity measures, tends to imply that the onset of ammonia-induced cellular oedema may not be present following hyperammonaemia in healthy adults. Furthermore it does not support the idea that the decrease in FA reported in the AMM trials is a consequence of subtle cell morphological changes due to ammonia-induced cellular swelling, and as such it remains uncertain as to what is causing these FA effects.

The minimal effects of ammonia in the brains of healthy individuals, reflects the lack of functional or behavioural change observed. It may therefore mean that the development of psychological impairment in hyperammonaemic disorders such as cirrhosis is a consequence of chronic adaptations in response to continual failure to remove ammonia and/or other compounds, rather than acute changes. Furthermore, the effects observed in cirrhosis after hyperammonaemia induced by oral AA challenge, may be due to the additive nature of this hyperammonaemia to the already underlying diffuse impairment caused by the chronic nature of the disease or vice versa. Recent evidence has pointed towards ammonia acting to 'prime' the brain, increasing its sensitivity to other co-morbidities such as infection/inflammation, which once present lead to the onset of cerebral dysfunction and HE symptom development (Marini and Broussard, 2006, Wright *et al.*, 2011b). Despite

the absence of significant psychological impairment in the present study, a significant effect of ammonia on the development of fatigue sensation was observed replicating the findings in chapter 4. Although one of the aims of this experimental chapter was to determine what may be causing this increase in fatigue sensation due to ammonia, this has proven somewhat difficult as minimal structural or metabolic changes could be observed from the use of the quantitative MRI techniques. The significant decrease in FA found in the AMM trial using DT imaging, could represent subtle microstructural changes to the brain due to hyperammonaemia, which may be related to the onset of fatigue. However, it is difficult to infer a mechanism for this change, with the absence of any other quantitative MR changes, in particular changes in diffusivity. Alternatively, the effects of increased fatigue may be due to hyperammonaemia related alterations in neural activation patterns, rather than structural or metabolic changes to the brain tissue. Cauli and colleagues have highlighted altered neural activation in hyperammonaemic rats (Cauli et al., 2007), whilst more recently EEG patterns were found to be significantly affected in both cirrhosis patients and healthy controls following oral AA challenge, which were related to increased subjective sleepiness (Bersagliere et al., 2011). fMRI data would evidence this. Despite this limitation the findings of this and the previous chapter suggests that hyperammonaemia alone causes minimal effects to brain acutely, beyond that of alterations in perceived sensations of fatigue through an, as yet, unidentified mechanism. Highlighting that ammonia, although a contributing factor to HE symptom development in hepatic disease, its impact may be minimal in the absence of other chronic metabolic alterations relating to the disease. Therefore, it would likely be beneficial to investigate more diverse therapeutic options in liver disease; for example combination therapies treating a diverse range of complaints including inflammation and immune function, as many current methods remain aimed at ameliorating hyperammonaemia. These acute findings, however, are not trivial, the measurement of fatigue could prove useful as a early indicator of impending progression to more overt and severe symptom development, particularly if the actions of

ammonia are to 'prime' the brain to the deleterious actions of other co-morbidities as proposed. Treatment at an early stage to relieve this hyperammonaemia, may prevent ensuing impairment.

The present findings of increased sensations of fatigue could prove more significant to other forms of hyperammonaemia, such as that related to extreme exercise. Ammonia has for many years been suggested as a cause of fatigue, and the findings here and in chapter 4 provide the first evidence for a direct link between the two within the time frame for exercise. The effects of ammonia are mild, inducing increased sensations of fatigue. Therefore they are unlikely to directly impair exercise performance. However as with disease, it can be proposed from the findings here that the additive nature of these ammonia related changes to other metabolic and functional changes which occur during exercise, may provide significant contribution to eventual performance decrement and the cessation of volitional exercise.

CHAPTER 6: SUPPRESSION OF C2C12 MUSCLE CELL PROTEIN SYNTHESIS FOLLOWING INCUBATION WITH AMMONIUM CHLORIDE IS REGULATED VIA INHIBITION OF BOTH TRANSLATION INITIATION AND ELONGATION.

6.1 INTRODUCTION

Efficient inter-organ exchange between muscle, liver, kidneys and GI tract, and metabolism of ammonia nitrogen therein, ensures maintenance of low systemic ammonia concentrations whilst also regulating the availability of ammonia nitrogen for non-essential amino acid production (Patterson *et al.*, 1995), urea metabolism (Yang *et al.*, 2000), brain cell metabolism (Marcaggi and Coles, 2001), and the maintenance of acid-base balance (van de Poll *et al.*, 2004). Perturbation to any part of this system, forces the other organs and tissues to increase ammonia uptake accordingly in order to compensate for these changes. One tissue important in this process, due to its large size (approximately 40% total body mass; Shimomura *et al.*, 2006) and capacity for ammonia metabolism, is skeletal muscle. For example, impaired liver function due to injury or disease leads to skeletal muscle taking up 0.5 times more ammonia per minute than the liver (Olde Damink *et al.*, 2002b). Furthermore, during exercise skeletal muscle produces and releases large amounts of ammonia as a result of increasing energy demand for maintenance of efficient contraction (Katz *et al.*, 1986, Snow *et al.*, 2000, Zhao *et al.*, 2000). This in turn causes resting/less active muscle to increase uptake of ammonia up to 60 fold basal levels (Bangsbo *et al.*, 1996). Under such conditions plasma ammonia concentrations can increase 5 – 10 fold (Brouns *et al.*, 1990, Bangsbo *et al.*, 1996, Nybo *et al.*, 2005), with intramuscular concentrations approaching $6\text{mmol}\cdot\text{kg}\cdot\text{dw}^{-1}$ (Katz *et al.*, 1986, Zhao *et al.*, 2000).

There is evidence to suggest that tissues exposed to mM ammonia concentrations show significant impairment to normal cellular function; in particular cellular protein metabolism,

suppressing protein synthesis in hepatocytes (Seglen, 1978) and fibroblasts (Jessup *et al.*, 1983), and proteolysis in renal tubular cells (Franch, 2000). With these significant effects of ammonia on protein metabolism being observed in other cell types, it seems sensible to hypothesize that large intramuscular ammonia concentrations, could also affect the regulation of skeletal muscle protein metabolism. If this was shown to be the case, this could highlight potential mechanisms contributing to altered protein metabolism and associated muscle wasting in liver disease (McCullough *et al.*, 1998, Dasarathy *et al.*, 2011), in addition to the commonly observed alterations to protein synthesis during exercise (Gautsch *et al.*, 1998, Dreyer *et al.*, 2006, Rose and Richter, 2009).

Recently it has been shown that the administration of ammonium salts in rats leads to a significant decrease in whole body protein turnover and skeletal muscle protein synthesis (Holecek *et al.*, 2000). Whilst, portacaval shunted rats presenting with significant hyperammonaemia show a reduction in rates of skeletal muscle protein synthesis compared to sham operated controls (Dasarathy *et al.*, 2011). Whether these *in vivo* effects on skeletal muscle protein turnover are directly related to the actions of ammonia remains uncertain, as treatment of excised skeletal muscle with 0.5mM ammonia did not show any significant effects on either protein synthesis or proteolysis (Holecek *et al.*, 2011). Therefore, the aim of this final experimental chapter was to investigate the effects of ammonium chloride treatment on muscle cell protein synthesis using a C2C12 murine myotube cell culture model. Protein synthesis is regulated by the rate of messenger RNA translation, which is formed of three stages; initiation, elongation and termination (Proud, 2007). Each of these stages is controlled by groups of proteins termed eukaryotic initiation, elongation and release factors (Rose and Richter, 2009), whose activity is regulated via a complex molecular signalling network centred around the mammalian target of rapamycin complex 1 (mTORC1; Proud, 2007). Therefore in an attempt to elucidate some of the

mechanisms surrounding the proposed suppression of protein synthesis with ammonia, the phosphorylation states of a number of target proteins involved in the control of mRNA translation were assessed. Furthermore, the expression of atrogenes involved in the control of proteolysis were measured along with markers of proteolysis to determine any accompanying effects of ammonia on protein breakdown, enabling an overall effect of ammonia on skeletal muscle protein metabolism to be established.

6.1 METHODS

6.1.1 CELL CULTURE

All cell culture experiments and analyses were performed at the Department of Clinical Physiology of the School of Graduate Entry Medicine and Health, University of Nottingham. Murine C2C12 myocytes were seeded and cultured in Dulbeccos modified eagle's medium (DMEM) containing 10% (v/v) foetal calf serum, amphotericin (250ng/ml), penicillin (100units/ml) and streptomycin (100µg/ml), at 37°C in a 5%CO₂/95% air atmosphere. Once 80% confluency of myoblasts was reached, serum concentration was reduced to 2% to induce differentiation into multinucleated myotubes in 6 well plates.

Experiments were performed 24h post media change, 5-9 days post differentiation. Cells were treated with two different concentrations of ammonium chloride; 1mM and 10mM, for 1 and 4 hours. 50% APE [¹³C]-Proline was added to the media (final conc: 100µg/ml) for the last 30 minutes of each incubation to allow for the measurement of protein synthesis. Two control conditions were included, tracer control (no ammonium with 50% ¹³C-Proline added for 30 minutes) and a no tracer control (no ammonium and no tracer added). Following incubations, 1ml of media was collected from each well and frozen at -20°C. The

remaining media was discarded and the cells were washed twice with 1ml ice cold phosphate buffered saline. Cells were scraped and harvested into 200µl of homogenization buffer (50mM Tris-HCl pH 7.5, 1mM EDTA, 1mM EGTA, 10mM glycerophosphate, 50mM NaF, 1 complete protease inhibitor tablet [Roche Diagnostics Ltd, Burgess Hill, UK]) for immunoblotting and determination of fractional synthetic rate of protein synthesis. For PCR, cells were scraped into Tri-reagent (Sigma Aldrich, Poole, UK) and immediately homogenized via repeated pipetting before freezing. For tyrosine release experiments media was changed prior to treatment to HEPES buffered saline due to the high concentrations of tyrosine present in DMEM (~0.1g/litre).

6.1.2 IMMUNOBLOTTING

Cell lysates were homogenised via repeated pipetting in homogenization buffer, samples were then centrifuged at 10000g at 4°C for 10 minutes to separate the sarcoplasmic fraction (supernatant). Sarcoplasmic protein concentrations were determined after 1 in 3 dilution in homogenization buffer using the Bradford method with a commercially available reagent (B6916, Sigma Aldrich, Poole, UK). Samples were then standardised to 0.3µg/µl by dilution in 3 x Laemmli buffer. After mixing, samples were heated at 90°C for 5 minutes before loading 15µl/lane (4.5µg protein/lane) onto Criterion XT Bis-Tris 12% SDS-PAGE gels (Bio-Rad, Hemel Hempstead, UK) for electrophoresis at 200V for 60 minutes. Gels were equilibrated in western blotting transfer buffer, pH 8.5 for 10 minutes before electroblotting proteins on to a 0.2µm PVDF membrane at 100V for 45 minutes. Following this the membranes were blocked in 2.5% milk in 1% Tris buffered saline with 0.1% tween (TBST) and gentle agitation for 1 hour, to prevent background interference. The membrane was incubated in the appropriate primary antibody (1 in 2000 dilution) at 4°C overnight. The next day membranes were washed x3 with TBST, before incubation in HRP conjugate secondary antibody (specific to each primary antibody) for 1 hour at room temperature.

After washing x3 in TBST, membranes were incubated for 5 minutes with ECL reagents (Millipore Corp, USA), and were imaged and quantified for peak density using the Chemidoc XRS system (Bio-Rad Laboratories Inc., Hercules, CA). Relative phosphorylated protein concentrations of Akt^{ser473}, mTOR^{ser2448}, p70S6K^{Thr389}, 4E-BP1^{Thr37/46}, eEF2^{thr56}, AMPK^{Thr172}, ACC β ^{Ser79}, eIF2 α ^{Ser551}, FoxO 3a^{Ser253}, p90rsk^{Thr259/Ser363} were measured with total Pan Actin and total β -Tubulin as loading control.

6.1.3 FRACTIONAL SYNTHETIC RATE OF PROTEIN SYNTHESIS (FSR)

Cell lysates from two wells were combined to ensure adequate measurement sensitivity (therefore final data is mean of N=3 per treatment). FSR was either measured from mixed muscle or sarcoplasmic protein. Mixed muscle proteins were isolated via precipitation of cell lysates with equal volume 1M PCA. Samples were cold centrifuged (4°C) at 12,000g for 10 minutes to separate the protein pellet from the free AA supernatant (which was discarded). Sarcoplasmic proteins were isolated from supernatant fractions following homogenization of cell lysates. 1M PCA was added to the supernatant fraction to precipitate out the proteins, which were then cold centrifuged (4°C) at 12,000g for 10 minutes to separate the protein pellet from the free AAs. The protein pellets were washed twice with 70% ethanol. Washed pellets were transferred to boiling tubes containing 0.1M HCl/Dowex H⁺ resin and hydrolysed overnight at 110°C. The next day amino acids were isolated on Dowex H⁺ resin, before eluting into 2M NH₄OH. After evaporation of the NH₄OH, samples were converted to their *n*-acetyl, *n*-propyl ester derivatives (Kumar et al., 2009; Atherton et al., 2010). The ¹³C proline incorporation into protein was analysed by gas chromatography-combustion-isotope ratio mass spectrometry (GC-C-IRMS; Meier-Augenstein, 1999). ¹³C proline labelling in the media was determined after isolation of media amino acids on Dowex H⁺ resin, elution into NH₄OH and evaporation to dryness. Amino acids were then converted to their tBDMS derivatives (Mawhinney et al., 1986).

Analysis of ¹³C proline incorporation in media samples was then analysed using GC-MS (MD 800, Thermo Finnigan, Hemel Hempstead, UK) using selective ion monitoring for m/z 286, 287. This was used as a precursor for calculation of protein synthesis via fractional synthetic rate (FSR):

$$\left(\frac{E_{inc}}{E_{media} \times t} \right) \times 100$$

where E_{inc} is the enrichment of protein bound proline, E_{media} is labelling of proline bound media, and t is the time. FSR is expressed as %/hour.

6.1.4 REAL-TIME PCR

RNA was extracted from Tri-reagent homogenate according to the manufacturers' instructions. Following removal of the RNA layer to a new microtube, the remaining DNA layer was stored at -20°C. 1µg of RNA from each sample was separated on a 1% agarose gel and visualised using ethidium bromide on a Chemidoc XRS system to check for DNA contamination. cDNA was synthesised via reverse transcription from 1µg of RNA as a template, using an iScript cDNA synthesis kit (Bio-Rad Laboratories Inc., Hercules, CA). RT PCR was carried out for 40 cycles using a Bio-Rad iCycler (Bio-Rad Laboratories Inc., Hercules, CA). Primer sequences were designed using mouse specific sequencing data for myostatin (Forward: ACCAAGCAAACCCAGAGGCT, Reverse: TGAGCACCCACAGCGGTCTA), muscle ring finger 1 (MuRF-1, Forward: GTGTTTGGGGCTCACCAGGC, Reverse: ACCTGGTGGCTATTCTCCTTGGT), muscle atrophy F-box (MAFbx, Forward: CTTTCAACAGACTGGACTTCTCGA, Reverse: CAGCTCCAACAGCCTTACTACGT), IGF-1 (Forward: GCGAATGTTCCCCAGCTGTT, Reverse: TGCGCAGGCTCTATCTGCTCT), using GAPDH as a housekeeping gene (Forward: CCCAGCAAGGACACTGAGCAAG, Reverse:

AGGCCCTCCTGTTATTATGGGG). Following RT PCR the Ct number for each target gene and the house keeping gene were extracted, and ΔCt values were calculated:

$$\Delta Ct = Ct^{\text{Target}} - Ct^{\text{Housekeeping}}$$

Where Ct^{Target} is the cycle threshold for the target gene, and $Ct^{\text{Housekeeping}}$ is the cycle threshold for the housekeeping gene.

6.1.5 MARKERS OF PROTEIN BREAKDOWN

To estimate whether there was any effect of ammonia on protein breakdown, the net release of tyrosine from the cell was measured by the appearance of tyrosine in the extracellular media. Tyrosine was measured using a colorimetric assay originally described by Chrastil (1975). Following collection of 1ml of HEPES buffered saline (DMEM replacement to prevent interference from high media tyrosine concentrations) from ammonium treated cells, a 0.5ml volume was mixed with 50 μ l of 30% (w/v) hydroxylamine hydrochloride and 250 μ l of 50% (w/w) sulfuric acid. This was mixed, and after 1minute, 250 μ l of 5% (w/v) ammonium cerium (IV) nitrate was added, mixed and incubated at room temperature for 45 minutes. In the presence of hydroxylamine, soluble ceric salts form stable orange coloured complexes with tyrosine. The intensity of the colour is linearly related to the amount of tyrosine present and the absorbance can be read at 380nm on a spectrophotometer.

6.1.6 STATISTICAL ANALYSIS

All statistical analysis was performed using Graph Pad Prism (v.5.0, Graph Pad Software Inc, La Jolla, San Diego, CA). Descriptive statistics were produced for all data sets and checked for normal distribution using a Kolgomorov-Smirnov test. Normal distribution was

accepted if $p > 0.05$. All data are presented as mean \pm SEM. Differences between multiple treatments were assessed using a one-way ANOVA, significant main effects were followed up with a Tukey-Kramer post hoc test. Differences between single treatments were assessed using an unpaired t-test. Equivalent non-parametric statistical tests were used where data were not normally distributed or data variance was unequal. The alpha level of significance was set at $p = 0.05$.

6.2 RESULTS

6.2.1 MUSCLE CELL PROTEIN SYNTHESIS

Incubation of C2C12 cells with 1mM ammonium chloride (NH_4Cl) for 1 hr led to a significant (0.15 ± 0.05 fold, $F(2,6)=53.88$, $p < 0.01$) suppression in muscle cell protein fractional synthetic rate (FSR) compared to controls (see figure 6.1A). The level of suppression in FSR was time dependent with a greater decrease in FSR observed following incubation with 1mM NH_4Cl for 4hrs (0.29 ± 0.05 fold, $p < 0.0001$). To assess whether this response to treatment with NH_4Cl was also concentration dependent, cells were incubated in the presence of a higher (10mM) NH_4Cl concentration.

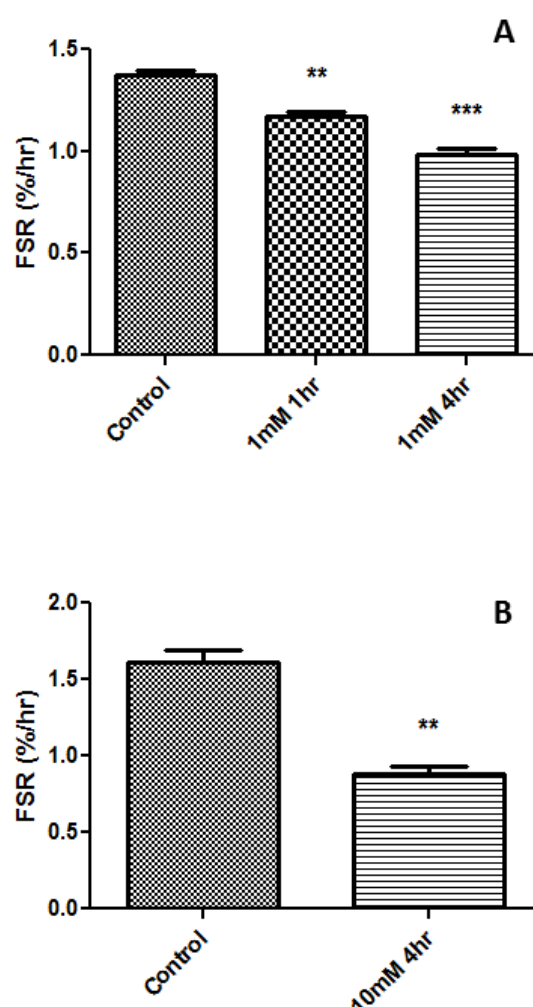


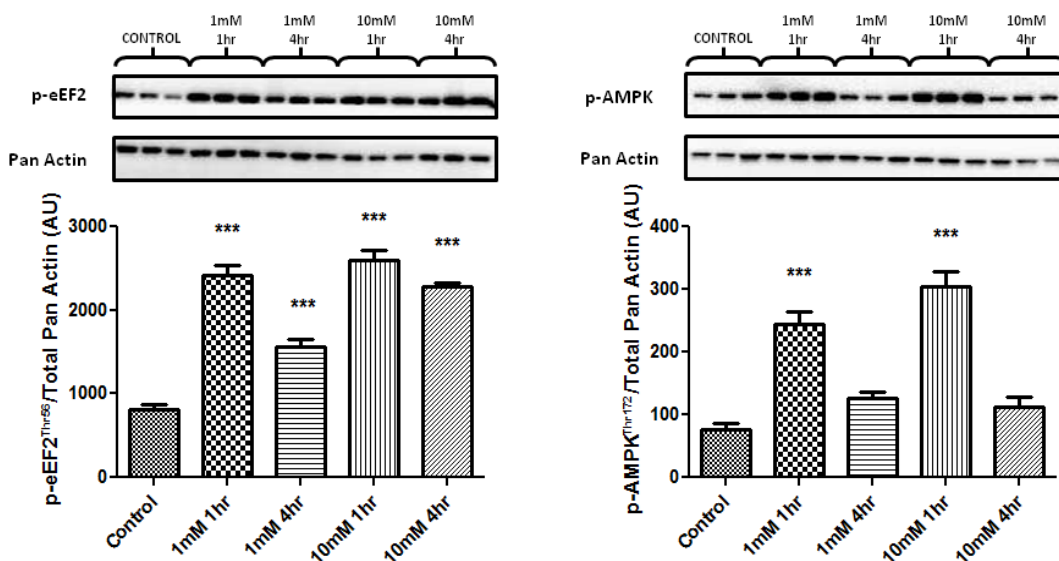
Figure 6.1. Changes in FSR in response to incubation with A) 1mM NH_4Cl and B) 10mM NH_4Cl .

***represents a significant decrease in FSR from control, $p < 0.0001$, ** $p < 0.01$. Data are presented as Mean \pm SEM, $n=3$.

Increasing the NH₄Cl concentration to 10mM led to a greater level of suppression in FSR (0.45±0.1, p<0.01).

6.2.2 SPECIFIC RESPONSES OF AMPK^{Thr172}, ACCβ^{Ser79} AND eEF2^{Thr56} PHOSPHORYLATION TO AMMONIUM CHLORIDE INCUBATION

Incubation of C2C12 cells in 1mM NH₄Cl for 1hr led to a sharp (1.81±0.16 fold, F(4,25)=66.13, p<0.0001) increase in phosphorylation of eEF2 compared to controls (see figure 6.2). This increase in phosphorylation of eEF2 remained after incubation in 1mM NH₄Cl for 4hrs, but was significantly decreased compared to the 1hr incubation (p<0.0001). Incubation with 10mM NH₄Cl showed the same pattern of increased phosphorylation at 1hr (2.01±0.4 fold, p<0.0001), however this increase was more sustained as there was no decrease after 4hrs (see figure 6.2). Phosphorylation of AMPK showed similar responses to ammonium chloride treatment as eEF2 with a pronounced 2.5±1.4 fold (F(4,25)=30.52, p<0.0001) increase in phosphorylation after 1hr incubation at 1mM, however this effect was only transient, returning to near basal levels after 4hrs. Incubation with 10mM NH₄Cl showed the same transient increase in phosphorylation of AMPK increasing by 3.1±0.85 fold (p<0.0001) after 1hr, returning to basal levels after 4hrs. Phosphorylation of ACCβ, followed a similar trend to AMPK, but was not found to be significant.



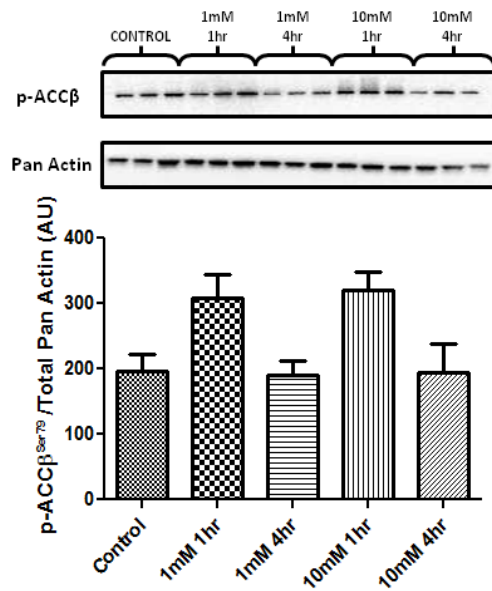
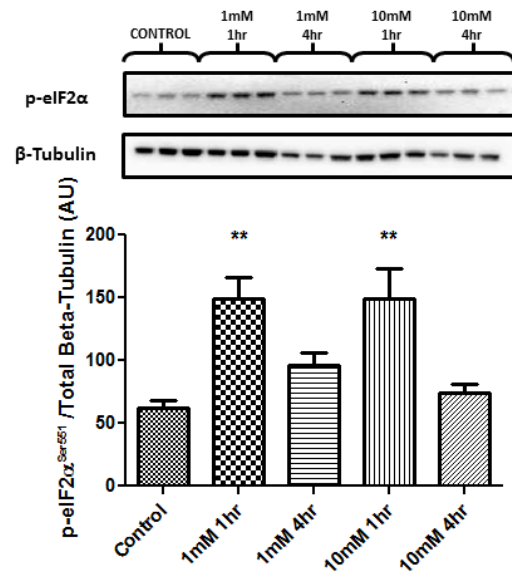
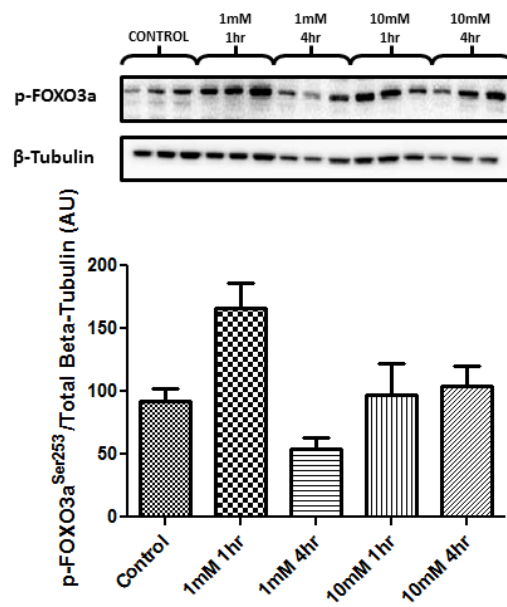
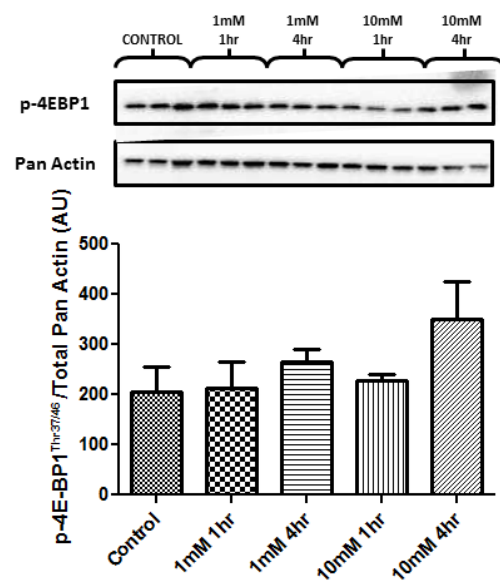
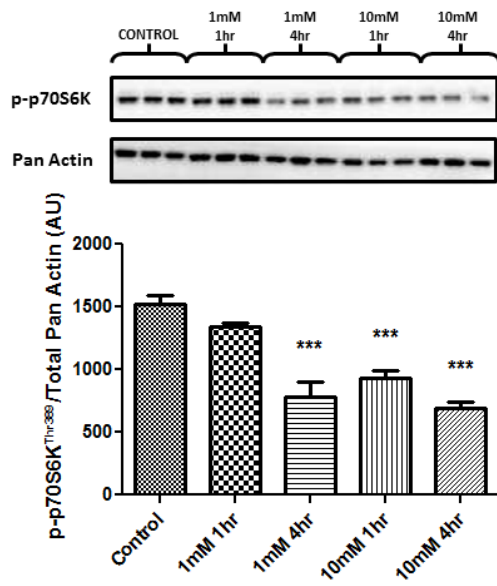


Figure 6.2. Changes in phosphorylation of eEF2^{Thr56}, AMPK^{Thr172} and ACCβ^{Ser79} in response to incubation with 1mM and 10mM NH₄Cl. *represents a significant change in phosphorylation from control, p<0.0001. Data are presented as Mean ± SEM, n=6.**

6.2.3 SPECIFIC RESPONSES OF mTOR^{Ser2448}, AKT^{Ser473}, p70^{S6K Thr389}, 4E-BP1^{Thr37/46} AND eIF2α^{Ser551} PHOSPHORYLATION TO AMMONIUM CHLORIDE INCUBATION.

Following incubation with 1mM ammonium chloride for 1hr there was a 1.4±0.25 fold (F(4,25)=8.231, p<0.01) increase in eIF2α phosphorylation, with a 1.4±0.63 fold (p<0.01) increase at 10mM (figure 6.3). These effects were only transient, returning to basal levels after 4hrs at both 1 and 10mM. Following incubation with 1mM NH₄Cl for 1hr, phosphorylation of p70^{S6K} remained unchanged from controls. However, after 4hr phosphorylation had decreased (0.4±0.14 fold, F(4,25)=25.52, p<0.0001; figure6.3). In contrast to 1mM, incubation at 10mM led to a rapid decrease (0.25±0.16 fold, p<0.0001) in p70^{S6K} phosphorylation after 1hr, which was maintained for up to 4hrs (see figure 6.3). Whilst mTOR, although showing similar trends in phosphorylation to p70^{S6K} following incubation with NH₄Cl, this decrease in phosphorylation was only found to be significant following incubation at 10mM for 4hrs (Figure6.3). Phosphorylation of Akt and 4E-BP1 remained unchanged in all treatments.



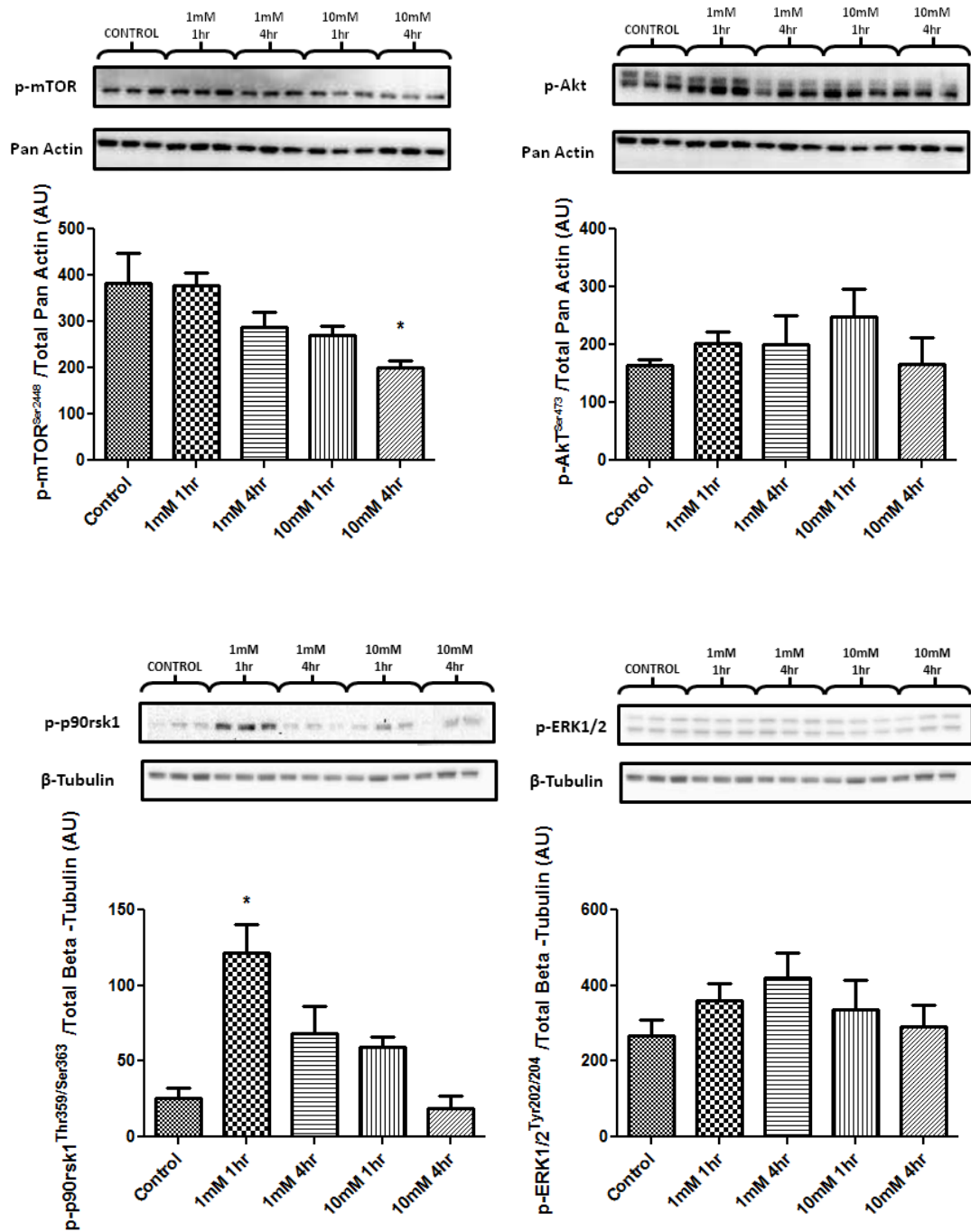


Figure 6.3. Changes in phosphorylation of mTOR^{ser2448}, Akt^{ser473}, p70^{S6K Thr389}, 4E-BP1^{Thr37/46}, eIF2α^{Ser551}, FOXO 3a^{Ser253}, p-p90rsk1^{Thr359/Ser363} and p-ERK1/2^{Tyr202/204} in response to incubation with 1mM and 10mM NH₄Cl. ***represents a significant change in phosphorylation from control, p<0.0001, ** p<0.01, *p<0.05. Data are presented as Mean ± SEM, n=6.

6.2.4 SPECIFIC RESPONSES OF FOXO 3a^{Ser253}, p90rsk1^{Ser380} AND ERK 1/2 PHOSPHORYLATION TO AMMONIUM CHLORIDE INCUBATION.

Incubation with 1mM NH₄Cl led to a transient increase in phosphorylation of p90rsk1 (5.05 ± 2.7 Fold, p<0.05) after 1hr, returning to near basal levels at 4hrs. No change in phosphorylation of p90rsk1 was observed with 10mM NH₄Cl. Phosphorylation of p-FOXO 3a was increased only at 1mM after 1hr incubation (see figure 6.3) and p-ERK1/2 remained unchanged following all treatments.

6.2.5 MUSCLE GROWTH FACTOR AND UBIQUITIN LIGASE EXPRESSION FOLLOWING AMMONIA INCUBATION

There were no changes in the expression of either the muscle growth factors myostatin or insulin like growth factor 1 (IGF-1), or the muscle specific ubiquitin ligases Muscle Atrophy F-box (MAFbx) or Muscle RING Finger 1 (MuRF-1), following incubation of C2C12 cells with 1mM NH₄Cl.

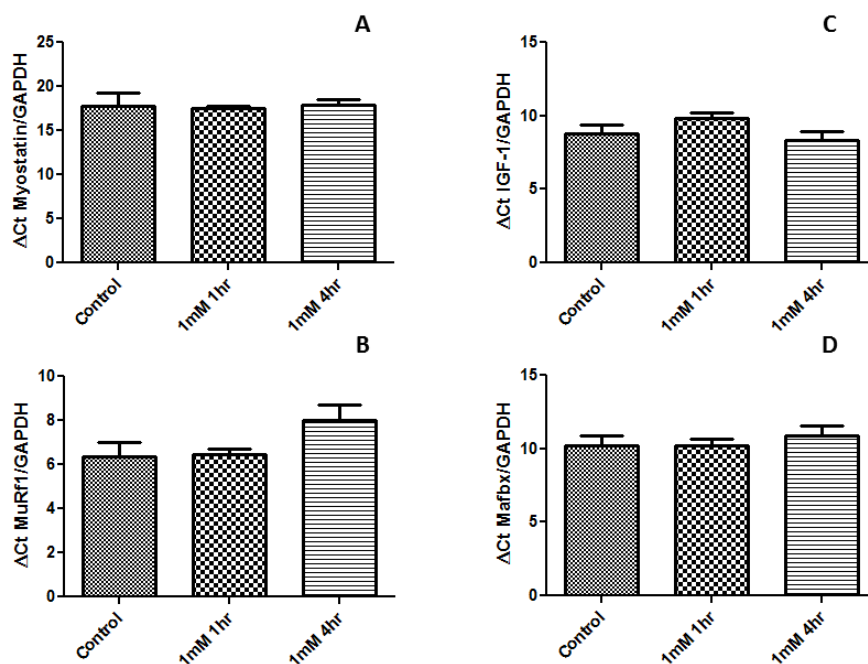


Figure 6.4. Expression of muscle growth factors A) Myostatin and B) IGF-1, and Ubiquitin Ligases C) MuRF1 and D) MAFbx in response to 1mM NH₄Cl. All values remained unchanged from controls. Data are presented as Mean ± SEM, n=6.

6.2.6 CELLULAR TYROSINE RELEASE

There were no differences in absorption observed for extracellular tyrosine in control cells and cells treated with 1mM NH_4Cl . This suggests that there was no increase in net tyrosine release from the cell as a result of the ammonium treatment.

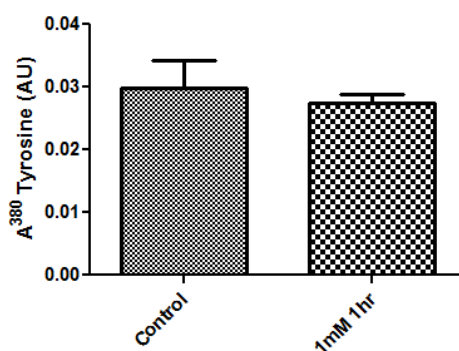


Figure 6.5. Extracellular Tyrosine absorbance at 380nm following incubation with 1mM NH_4Cl . All values remained unchanged from controls. Data are presented as Mean \pm SEM, n=6.

6.3 DISCUSSION

The main findings of this experimental chapter are that treatment of a skeletal muscle cell line with NH_4Cl leads to a suppression in muscle protein synthesis (MPS), without an increase in markers of breakdown. The suppression of MPS appeared to result from altered translational signalling of proteins regulating the control of both the initiation and elongation phases of mRNA translation. Analysis of this information would lead to the conclusion that if the mechanisms observed in cell culture apply to the whole organism, then some of the effects of sarcopenia and muscle wasting in clinical conditions of hyperammonaemia, may arise mainly from suppression of protein synthesis and not increased catabolism. The fact that the effect was concentration and time dependent would suggest that the longer the elevated ammonium concentrations persist, the greater the suppression of protein synthesis and the bigger the impact on lean body mass.

Skeletal muscle acts as a major site for both the production and removal of ammonia. Failure of hepatic and renal ammonia metabolism (Wright et al., 2011a) or increased production and release of ammonia by contracting muscle (Katz et al., 1986, Snow et al., 2000, Zhao et al., 2000), leads to increased skeletal muscle uptake (Bangsbo et al., 1996, Olde Damink et al., 2002b), and intramuscular concentrations approaching 6mmol.kg dw^{-1} (Katz et al., 1986, Zhao et al., 2000). The present findings show that the exposure of skeletal muscle cells to ammonia concentrations within this range causes a significant suppression to skeletal muscle cell protein synthesis. This supports previous findings which have highlighted inhibition of protein synthesis by ammonia in macrophages (Jessup *et al.*, 1983) and hepatocytes (Seglen, 1978), as well as skeletal muscle *in vivo* (Holecek *et al.*, 2000). Yet the causes of this ammonia induced suppression in synthesis remains uncertain.

Protein synthesis may be regulated by the rate of mRNA translation, which at each stage; initiation, elongation and termination, is controlled via the activity, and related upstream translational signalling, of eukaryotic initiation, elongation and release factors (Proud, 2007, Rose and Richter, 2009). Therefore in an attempt to elucidate some of the mechanisms surrounding the suppression of protein synthesis with ammonia, the phosphorylation states of a number of target proteins involved in the translational signalling and the control of mRNA translation were investigated. One of the main findings was the rapid and sustained increase in phosphorylation of the eukaryotic elongation factor; eEF2. Phosphorylation was increased 2 fold even at the lowest ammonia concentrations and shortest incubation time, and remained elevated above basal levels at 4hrs. eEF2 regulates the translocation of the ribosome relative to the mRNA (Browne and Proud, 2002). Phosphorylation of eEF2 at Thr56 by eEF2 kinase provides reversible inactivity of eEF2 inhibiting its ability to bind to the ribosome thereby downregulating translocation of mRNA at the elongation phase (Ryazanov and Davydova, 1989, Kaul et al.,

2011). The rapid phosphorylation of eEF2 in response to ammonium chloride may suggest that the suppression of MPS by ammonia is regulated via inhibition of translation elongation.

Translation elongation consumes large amounts of energy, with each addition of an AA to the nascent chain using the equivalent of 4 ATP moieties (Proud, 2007). The major pathway for ammonia metabolism in skeletal muscle is conversion to glutamine via glutamine synthetase (He *et al.*, 2010), which itself requires consumption of one ATP per molecule of ammonia (Iqbal and Ottaway, 1970, Listrom *et al.*, 1997). Therefore, in times of increased ammonia load, the inhibition of protein synthesis at the elongation phase may help to preserve ATP levels for efficient ammonia metabolism. Alternatively, the reduction of energy charge in relation to the increased metabolism of ammonia to glutamine through the consumption of ATP, may increase concentrations of AMP within the cell activating AMP activated protein kinase (AMPK), which serves as an energy sensor and can in turn activate eEF2 kinase, phosphorylating eEF2 and inhibiting translation elongation (Browne *et al.*, 2004). Exercise and liver disease, conditions associated with increased systemic ammonia, lead to an energy depleted state. Cirrhosis patients present with impaired mitochondrial ATP synthesis rates, significantly reducing intramuscular ATP levels (Jacobsen *et al.*, 2001), whereas certain forms of exercise can rapidly deplete the muscle ATP pool (Zhao *et al.*, 2000). Furthermore, it has been shown that the phosphorylation of AMPK in skeletal muscle can be increased in both of these conditions (Rose *et al.*, 2005a, Dasarathy *et al.*, 2011). Therefore the onset of hyperammonaemia may lead to an additive effect, further increasing AMPK phosphorylation and inhibition of synthesis via AMPK dependent eEF2 phosphorylation. The present findings reveal that the rapid increase in eEF2 phosphorylation following 1hr incubation at both 1mM and 10mM NH₄Cl concentrations was accompanied by a concomitant increase in AMPK phosphorylation. This suggests a

linear pathway for control of protein synthesis by ammonia through AMPK-eEF2K-eEF2. However after 4hrs incubation, although the phosphorylation of eEF2 remained elevated, AMPK had returned to basal levels. Therefore changes in eEF2 due to ammonia outlast that of upstream changes in AMPK. Dissociation between phosphorylation of AMPK and eEF2 has been observed before, with phosphorylation of eEF2 occurring well in advance of AMPK during exercise, suggesting alternative regulation of eEF2 phosphorylation via mechanisms independent of AMPK (Rose et al., 2005a). Using muscle specific AMPK knockdown (KD) mice, Rose et al., (2009) showed that the eEF2 related suppression in synthesis during contractions, was not related to AMPK signalling, as synthesis and eEF2 phosphorylation were unchanged between wild type and KD AMPK mice (Rose *et al.*, 2009).

Phosphorylation of eEF2 can be regulated by multiple molecular targets in addition to that of AMPK. The 70kDa protein S6 kinase (p70^{S6K}) and the 90kDa ribosomal protein S6 kinase (p90^{RSK1}), regulate phosphorylation of eEF2 via signalling through mTOR dependent and mTOR independent pathways respectively (Fenton and Gout, 2011, Anjum and Blenis, 2008). p70^{S6K} has been shown to regulate eEF2 activity via phosphorylation and inactivation of eEF2K (Wang et al., 2001). These actions of p70^{S6K} on eEF2K were found to be downstream of mTOR as treatment of cells with rapamycin (an inhibitor of mTOR) blocks phosphorylation of eEF2K by p70^{S6K} and dephosphorylation of eEF2 (Wang et al., 2001, Wang and Proud, 2002). The present findings show that phosphorylation of p70^{S6K} is reduced following incubation with 1mM NH₄Cl for 4hrs, and 10mM NH₄Cl for 1 and 4hrs. This suggests that p70^{S6K} may be a component in the ammonium induced phosphorylation of eEF2. A decrease in p70^{S6K} would prevent phosphorylation and inactivation of eEF2K, allowing increased phosphorylation of eEF2 and hence downregulation of mRNA translation. This mechanism could explain the presence of sustained eEF2 phosphorylation at 4hrs in the absence of AMPK phosphorylation. The reduced phosphorylation at 1mM

and 10mM 4hrs may sustain phosphorylation of eEF2 once AMPK phosphorylation has returned to basal levels. Although this pathway is mTOR dependent, there were no accompanying changes in mTOR except a significant reduction in phosphorylation at 10mM for 4hrs. This absence of change in phosphorylation of mTOR in the presence of significant changes in the phosphorylation of its downstream substrates has been reported previously, and it has been suggested that Ser2448 phosphorylation may not be a critical component in regulating mTOR activity (Atherton *et al.*, 2010).

In contrast p90^{RSK1} regulates eEF2 phosphorylation independent of mTOR via the MEK/ERK signalling pathway (Das *et al.*, 2010). As with p70^{S6K}, phosphorylation of p90^{RSK1} phosphorylates and inactivates eEF2K, dephosphorylating eEF2 thereby promoting elongation (Wang and Proud, 2002, Das *et al.*, 2010). The present findings showed a transient increase in p90^{RSK1} phosphorylation at 1mM NH₄Cl for 1hr, with phosphorylation not significantly different from basal after 4hrs and at both 10mM incubations. This was accompanied by no change in phosphorylation of its upstream regulator p-ERK1/2. This clearly shows that there is no regulation of eEF2 activity through MAPK/ERK/p90^{RSK1} pathway, as although there was an increase in phosphorylation at the 1mM 1hr incubation, this is in the wrong direction to be a component in the increase in eEF2 phosphorylation. One would expect a decrease in p90^{RSK1} phosphorylation to suggest regulation of increases in eEF2 phosphorylation via p90^{RSK1}. The increase in p90^{RSK1} phosphorylation could be interpreted as aiding to promote eEF2 activity and elongation, yet this is not the case as there is a marked and sustained increase in eEF2 phosphorylation in the present study. Therefore it seems that if p90^{RSK1} is acting to regulate phosphorylation of eEF2, other signalling mechanisms (e.g. AMPK, p70S6K) are overriding this action. Translational signalling via p90^{RSK1} is not solely through a linear MEK/ERK/eEF2K pathway however. p90^{RSK1} has also been shown to regulate mTORC1 signalling via phosphorylation of TSC1,

preventing its inhibition of mTOR (Roux *et al.*, 2004). Whereas it can also directly regulate mTORC1 activity via phosphorylation of raptor (Carriere *et al.*, 2008). Furthermore direct phosphorylation of eIF2B by p90^{RSK1} assists in promoting translation initiation (Shahbazian *et al.*, 2006). Whilst p90^{RSK1} is also known to phosphorylate IκBα, which subsequently activates the transcription factor Nuclear Factor Kappa B (NF-κB; Ghoda *et al.*, 1998). NF-κB performs a diverse number of roles within the cell from regulating the immune/inflammation response (Bakkar and Guttridge, 2010), to the control of muscle wasting (Cai *et al.*, 2004). Therefore any changes to phosphorylation of p90^{RSK1} by NH₄Cl may not only be related to suppression of synthesis through control of eEF2.

Whilst the evidence provided by changes to eEF2, and its upstream regulators, suggests strong support for the control of synthesis by ammonia through inhibition of elongation. Evidence of downregulation of translation initiation can also be observed through the increase in phosphorylation of the eukaryotic initiation factor 2 (eIF2) alpha subunit. The initiation of protein synthesis is composed of several stages, the first of which involves binding of the initiator tRNA with the eIF2•GTP binary complex to form a ternary Met-tRNA•eIF2•GTP complex (Pain, 1996). This in turn binds to the 40s ribosome to form the 43s preinitiation complex, on to which the mRNA strand binds (Pain, 1996). Once initiation is complete the hydrolysis of GTP to GDP releases eIF2 from the ribosomal subunit (Kimball *et al.*, 1998b). The eIF2•GDP complex must be recycled back to eIF2•GTP for initiation to continue, this is performed by the guanosine exchange factor eIF2B (Pain, 1996).

Phosphorylation of eIF2 at its alpha subunit inhibits eIF2B by binding to it and preventing it from performing guanosine exchange (Kimball *et al.*, 1998a). This increased eIF2α phosphorylation and reduced eIF2B activity leads to a decrease in synthesis due to impaired initiation (Kimball *et al.*, 1998b). eIF2B concentration is small compared to eIF2α, therefore even a small increase in phosphorylation of eIF2α will significantly inhibit

synthesis (Schmitt *et al.*, 2010). The increase in phosphorylation of eIF2 α observed in the present findings following incubation with 1mM and 10mM NH₄Cl for 1hr suggests that ammonia regulates the suppression in MPS through translational signalling regulating both elongation and initiation. eIF2 α again showed only transient increase in phosphorylation, returning to near basal levels after 4hrs. Therefore impaired initiation is likely to be most pronounced at 1hr.

Recently it has been identified that PCA rats with significant hyperammonaemia and signs of muscle wasting have altered expression of both myostatin and insulin like growth factor 1 (IGF-1), important muscle growth factors involved in the regulation of muscle mass (Dasarathy *et al.*, 2004, Dasarathy *et al.*, 2011), and it may be this altered gene expression which contributes to the impaired muscle protein metabolism observed with ammonia (Dasarathy *et al.*, 2011). Both IGF-1 and myostatin have been shown to be potent regulators of muscle mass (Rommel *et al.*, 2001, Taylor *et al.*, 2001). Increased expression of myostatin significantly inhibits cell proliferation and protein synthesis in C2C12 muscle cells (Taylor *et al.*, 2001). In contrast increased IGF-1 expression induces hypertrophy in muscle cells via upregulation of translational signalling via Akt/mTOR pathways (Rommel *et al.*, 2001). Expression of myostatin is upregulated in PCA rats, with IGF-1 expression decreased (Dasarathy *et al.*, 2004, Dasarathy *et al.*, 2011), and these rats also show significantly suppressed skeletal muscle protein synthesis compared to sham operated controls (Dasarathy *et al.*, 2011). Administration of follistatin, a functional antagonist of myostatin, normalised protein synthesis in the PCA rats so they were not different from controls (Dasarathy *et al.*, 2011). It was suggested that ammonia may be a common factor in regulating the expression of these genes, as increased myostatin expression has been reported following exposure to ammonium acetate in muscle cells, and that this may be a route through which ammonia regulates MPS (Dasarathy *et al.*, 2010). There were no

changes in the expression of either myostatin or IGF-1 following incubation with 1mM NH₄Cl in the present study, indicating that MPS changes are independent of altered gene expression and are purely regulated through control of mRNA translation. The differences in findings between those of the present study and those of Dasarathy and colleagues may be related to the length of exposure, changes in myostatin expression following exposure to ammonium acetate peaked after 24hrs (Dasarathy *et al.*, 2010). Therefore chronic changes relating to ammonia may be due to alterations in gene expression, yet more acute conditions may be related to control of mRNA translation.

With the absence of changes in gene expression, precisely how ammonium chloride initiates these alterations in translational signalling remains to be determined. However, one mechanism may be through ammonium induced changes in pH. eEF2 kinase is a calcium-calmodulin dependent kinase, whose activity is increased in the presence of calcium (Nairn and Palfrey, 1987). *In vitro* incubation of cells with ammonium leads to a rapid transient intracellular alkalinisation (Thomas, 1984). In astrocytes this ammonium induced intracellular alkalinisation leads to an increase in intracellular calcium concentration (Rose *et al.*, 2005b). If the same occurs in muscle, such an increase in intracellular calcium may increase the activity of eEF2 kinase, thereby increasing phosphorylation of eEF2 and inhibiting elongation (Rose *et al.*, 2005a). However, such ammonium induced alkalinisation is only transient, returning to baseline within 10 minutes, with a concomitant reduction in intracellular calcium back to baseline (Rose *et al.*, 2005b). Therefore this mechanism is unlikely to greatly affect rates of protein synthesis over the long incubation periods used here, in fact following the rapid intracellular alkalinisation with ammonium chloride there is an overshoot and a plateau phase intracellular acidification occurs (Thomas, 1984). Metabolic acidosis has been shown to significantly impair skeletal muscle protein synthesis (Caso *et al.*, 2004) and skeletal muscle proteolysis

(May et al., 1986, Evans et al., 2008). *In vivo*, contributions made by secondary mechanisms such as increased proinflammatory cytokines (Franch *et al.*, 2004) and glucocorticoids (May *et al.*, 1986), are believed to play a major role in metabolic acidosis induced alterations in skeletal muscle protein synthesis. Yet other authors have also suggested a more direct effect of pH on mRNA translation (Caso et al., 2004). Decreased extracellular pH causes an impairment in the function of the system A (SNAT2) amino acid transporter in L6 rat skeletal muscle cells (Bevington *et al.*, 2002). This inhibition of SNAT2 by decreased pH is coupled to impaired mTOR translational signalling, with decreased p70^{S6K} activity and 4E-BP1 phosphorylation (Evans *et al.*, 2007), which may inhibit mRNA translation at both the initiation and elongation phases. Inhibition of SNAT2 causes depletion of intracellular amino acids, even those not directly transported via SNAT2 (Evans et al., 2007). This decrease in amino acid availability may lead to decreased mTOR signalling, and hence altered protein metabolism due to acidosis (Evans et al., 2007). However, a more recently proposed mechanism also suggests that SNAT2 transporters may act independently of AA levels, directly signalling intracellular pathways related to protein metabolism through mTOR (Hundal and Taylor, 2009). Therefore, the intracellular acidosis which may be evident with ammonium chloride incubations in the present study, may regulate the suppression of synthesis through a SNAT2 transporter initiated mechanism and decreased phosphorylation of p70^{S6K}. The SNAT2 acidosis mechanism is observed with extracellular acidosis of the culture media, and therefore it is uncertain whether similar mechanisms may be present with decreases in intracellular pH.

Further to its effects on cell protein synthesis, ammonia has also been found to influence the control of proteolysis in other cell types (Franch, 2000). Evidence from the present findings, however, does not support the role of ammonia in the regulation of proteolysis in muscle cells. Net tyrosine release was used as an estimate of protein breakdown, and

showed no change following incubation with 1mM NH₄Cl. Previous studies which have used this method for estimating breakdown, tend to pre-incubate cells with cycloheximide to prevent reincorporation of tyrosine (Hobler *et al.*, 1998). Cycloheximide was not included in the present study, therefore it cannot be confirmed that reincorporation of tyrosine didn't take place, however tyrosine reincorporation is much slower than other amino acids (Ballard, 1982). Moreover, cycloheximide can affect both synthesis and breakdown within cells, therefore will have impacted the results (Ballard, 1982). Overall, net tyrosine release should act as a reasonable estimate of breakdown if major changes are occurring. To add to this, expression of the ubiquitin E3 ligases MuRF1 and MAFbx were unchanged following NH₄Cl incubations. MuRF1 and MAFbx show increased expression associated with the onset of skeletal muscle atrophy (Bodine *et al.*, 2001, Gomes *et al.*, 2001, Sandri *et al.*, 2004, Reed *et al.*, 2011). Expression of these atrophy related genes is related to the activity of the forkhead box O (FOXO) transcription factors (Sandri *et al.*, 2004). Dephosphorylation of FOXO 3a via upstream regulation through Akt (Zhao *et al.*, 2007) increases its activity, promoting expression of atrophy related genes and skeletal muscle atrophy (Sandri *et al.*, 2004). In support of the findings of no changes in MuRF1 and MAFbx, Akt phosphorylation was unchanged with FOXO3a phosphorylation increased at 1mM 1hr but unchanged for the remaining incubations, which suggests an absence of effect of NH₄Cl on control of proteolysis in skeletal muscle cells. More recently however, it has been purported that atrogene expression may not be a good marker of proteolysis in muscle, as although MuRF-1 knockout mice show attenuation in muscle atrophy, this attenuation is associated with maintenance of synthesis, rather than inhibition of proteolytic pathways (Baehr *et al.*, 2011). Therefore, conclusions on ammonia's true effects on protein breakdown in muscle warrant further investigation.

In conclusion, incubation of C2C12 muscle cells with NH_4Cl suppresses MPS, with no associated changes in markers related to protein breakdown. This suppression in MPS is mediated via a downregulation of mRNA translation both at the initiation and elongation phases, as evidenced by the increased phosphorylation of eIF2 α and eEF2. However the most potent regulator seems to be elongation, as phosphorylation of eEF2 remains elevated at all incubations, whilst eIF2 α phosphorylation returns to basal levels at 4hrs. Upstream signalling of eEF2 by ammonia is complex involving actions of AMPK and possibly p70^{S6K} pathways. Yet further research is needed for better understanding into the regulation of these pathways by ammonia. These findings do however suggest that ammonia could be a major factor in altered protein metabolism in both disease and exercise where hyperammonaemia is prevalent, and provides evidence for the mechanisms through which these effects may be regulated. Furthermore, it also shows that although the effects of ammonia are often believed to be confined to cerebral action, findings from this thesis suggest a more pronounced effect of ammonia within peripheral tissues, therefore further investigation within this area is warranted.

CHAPTER 7: GENERAL DISCUSSION

Ammonia is an essential intermediate in a number of metabolic processes important to normal function in the mammalian system. Renal ammonia handling, ensures maintenance of acid-base balance (van de Poll *et al.*, 2004). Ammonia provides nitrogen for the amidation of glutamine in several tissues, which is believed to be essential for the maintenance of immune function (Holecek, 2002). Whilst in cerebral tissues, its incorporation into glutamine in astrocytes provides substrates for glutamatergic neurotransmission (Felipo and Butterworth, 2002, Bak *et al.*, 2006), in addition to also acting as an important substrate in the alanine-pyruvate shuttle helping to maintain neuronal energy metabolism (Coles *et al.*, 2008). Ammonia however, can act as both 'friend' and 'foe'. Maintenance of systemic ammonia levels within a narrow low concentration range (no greater than 50 – 100 μ mol/L) through efficient inter-organ exchange, is believed to be vital to ensure normal function (Olde Damink *et al.*, 2009, Olde Damink *et al.*, 2002a). Failure of organs, such as the liver, to efficiently metabolise ammonia leads to an increase in systemic ammonia concentrations and the onset of neurological complications in the form of hepatic encephalopathy (Wright *et al.*, 2011a), believed to be a direct consequence of ammonia's actions on brain tissue function (Felipo and Butterworth, 2002, Haussinger and Schliess, 2008, Monfort *et al.*, 2009). Whilst increased production and release of ammonia in exercising muscle, leads to levels of systemic ammonia concentration similar to that of disease (Katz *et al.*, 1986, Bangsbo *et al.*, 1996), which is also accompanied by an increased uptake by the brain (Dalsgaard *et al.*, 2004, Nybo *et al.*, 2005). This has led to the proposal that the cerebral actions of ammonia attributed to disease states may also occur in exercise and contribute to declines in performance and the onset of fatigue (Wilkinson *et al.*, 2010, Banister and Cameron, 1990).

As highlighted in chapter 1, and experimental chapters 4 and 5, although ammonia has been shown to be toxic to certain brain cell functions *in vitro* (Albrecht and Norenberg,

2006, Hermenegildo et al., 1998b, Monfort et al., 2004, Rose et al., 2005b) and in animal models (Erceg et al., 2005a, Cauli et al., 2007c), there are conflicting findings presented by some authors which question the contribution of ammonia to these functional disturbances in brain *in vivo* in humans related to the onset of hyperammonaemia (Shawcross et al., 2004b, Shawcross et al., 2011, Mardini et al., 2011). Thus, the aim of the first three studies presented in this thesis was to investigate the effects associated with the onset of experimental hyperammonaemia in healthy humans. Specifically, these initial studies aimed to: 1) Determine the effects of hyperammonaemia, in isolation from other physiological or pathological variables, on brain function. 2) Investigate the underlying causes of any dysfunction using *in vivo* neuroimaging techniques.

The impairment of brain cell function by ammonia is commonly the focus of much of the research in hyperammonaemic disorders (Cauli et al., 2009b, Monfort et al., 2009, Felipe and Butterworth, 2002). Yet other organs and tissues can be sequestered to take up and metabolise large amounts of ammonia, when normal pathways of metabolism in liver become impaired or the processes become saturated (Olde Damink et al., 2002b, Bangsbo et al., 1996), leading to high concentrations of ammonia building up within these tissues. One such tissue which becomes vital as a metabolic sink for ammonia metabolism under such conditions is skeletal muscle (Olde Damink *et al.*, 2002b). In isolated cell models ammonia has been shown to significantly impair protein metabolism, suppressing both protein synthesis (Seglen, 1978, Jessup et al., 1983) and proteolysis (Franch, 2000). *In vivo*, liver disease patients show significant muscle wasting (McCullough *et al.*, 1998), whilst during exercise protein metabolism is shown to be altered with a significant suppression in synthesis (Gautsch et al., 1998, Dreyer et al., 2006, Rose and Richter, 2009). It has been mooted that ammonia may have a role to play in this altered skeletal protein metabolism, with evidence of suppressed synthesis and whole body protein turnover in

hyperammonaemic rats (Holecek et al., 2000, Dasarathy et al., 2011). Yet the causes and mechanisms of such an effect remain to be resolved. Therefore, with an overall aim to understand better the effects of hyperammonaemia on multiple tissues, the aim of the final experimental chapter was to investigate the effects of ammonia on skeletal muscle cell protein metabolism and the potential mechanisms controlling such effects.

7.1 PRINCIPLE FINDINGS

Chapter 3 describes the development of a tolerable method for inducing physiologically relevant states of systemic hyperammonaemia in healthy adults. Previous methods for studying hyperammonaemia *in vivo* in humans, have used AA feeding methods in patients with compromised liver function (see table 1, Chapter 1). This compromised function prevents efficient first pass metabolism of gut derived ammonia and hence a transient systemic hyperammonaemia develops. This method may be clinically relevant, however, the multiple metabolic and pathological complications associated with liver disease makes it difficult to determine effects due to hyperammonaemia alone, from those due to the interactive effects associated with the other aspects of the disease. The induction of hyperammonaemia via the continuous iv infusion method described here controls for these other conflicting variables present in disease through the use of healthy adult subjects, the assumption can therefore be made that any effects observed following hyperammonaemia using this method are directly due to the actions of the ammonia in the tissues. In addition, it creates a plateau steady state of hyperammonaemia which is maintained via continuous infusion, this allows the temporal effects of hyperammonaemia to also be investigated, something which is not possible using a bolus feeding model. Several studies have previously performed iv ammonium infusions in humans (see table 3.1 Chapter 3 for details). These studies varied greatly in their dosage and design, with some describing dosages which when attempted in the present thesis, were found to induce severe adverse

reactions. The findings provided from chapter 3 therefore describe a useful and tolerable method for inducing controlled experimental hyperammonaemia in humans allowing for its investigation in a wide variety of situations.

In chapter 4, this *iv* method for inducing hyperammonaemia was implemented to assess the effects of hyperammonaemia on cognitive function, motor control and sensations of fatigue in healthy adults. Hyperammonaemia was found to induce significant sensations of fatigue, but did not cause any changes in cognition and motor control. Liver disease patients regularly show impaired memory (Balata et al., 2003b, Jalan et al., 2003, Shawcross et al., 2004a) and a slowing of reaction time (Oppong et al., 1997, Rees et al., 2000, Douglass et al., 2001) associated with the onset of hyperammonaemia. It is therefore generally accepted that ammonia and its actions in the brain are a major cause of this altered psychological function and hence the development of hepatic encephalopathy symptoms in liver disease (Haussinger and Schliess, 2008). This is further supported by multiple animal and *in vitro* studies which show significant detrimental effects of ammonia on brain and neural/astrocytic tissue function (Chan and Butterworth, 2006, Monfort et al., 2009, Cauli et al., 2009b). In contrast, recent *in vivo* human studies have identified a discordance between the induction of hyperammonaemia and impaired psychological function in liver disease patients (Shawcross *et al.*, 2004b), reporting that psychological dysfunction associated with HE and the onset of hyperammonaemia could be normalised with treatment of systemic inflammation (Shawcross *et al.*, 2004b). Furthermore it has also been shown in severe HE patients that symptoms and severity of condition, had a strong relationship with the level of inflammation, rather than the level of systemic hyperammonaemia (Shawcross *et al.*, 2011).

Such findings question the importance of hyperammonaemia alone in the development of impaired brain function and HE symptom development. The interaction of ammonia with

other metabolic perturbations such as inflammation may be critical in disease. Chapter 4 is the first study to investigate the effects of hyperammonaemia in isolation from other potentially conflicting physiological or pathological variables, on the performance of psychological tasks designed to assess motor control, cognition and learning and memory, three areas believed to be most affected by ammonia in the brain (Ortiz et al., 2005, Weissenborn et al., 2005, Butz et al., 2010a). Despite significant hyperammonaemia, there was no impairment in the performance of any of the tasks. These findings provide support to those of Shawcross and colleagues (Shawcross et al., 2004b), that impairment in psychological function in disease is a result of factors other than and/or in addition to the development of hyperammonaemia.

Although no changes in psychological function were observed, a significant increase in the sensation of fatigue was found in response to hyperammonaemia from two separate experiments. Ammonia has been implicated in the development of fatigue for several decades, based primarily upon the findings associated liver disease patients (Banister and Cameron, 1990; Wilkinson et al., 2010). This is the first study to show a direct link between the two. Signs of fatigue are often initial indications of developing HE in liver disease patients (Cordoba et al., 1998, Dhiman and Chawla, 2009, Malaguarnera et al., 2011b), therefore ammonia may lead to initial subtle changes in brain, inducing alterations in somatosensory neural pathways and hence increased sensations of fatigue, which, with chronic disease and interaction with other metabolic changes, leads to the additive effects of observed psychological impairment and more significant symptoms of HE. Such an effect may also be prevalent in exercise, the combination of ammonia induced sensations of fatigue and other metabolic changes occurring as a result of exercise stress may lead to additive impairment in normal function, and eventual exhaustion/performance decrement,

this seems plausible given the multitude of factors implicated in fatigue development over the years (Ament and Verkerke, 2009).

Chapter 5 is the only study to have investigated the effects of acute hyperammonaemia on the structure and function of the brain *in vivo* using non-invasive quantitative MRI, in an attempt to better understand the effects of ammonia on brain, and help describe the results reported in chapter 4. It is proposed that ammonia entering the brain across the BBB is trapped as glutamine in the astrocytes (Keiding et al., 2006b), which, as an active osmolyte, induces the onset of astrocyte swelling and mild intracellular oedema (Willard-Mack et al., 1996, Tanigami et al., 2005). Associated glutamate efflux into the extracellular space (Mongin and Kimelberg, 2002, Kimelberg, 2004, Kimelberg et al., 1990, Rose et al., 2005b), oxidative stress (Stewart et al., 2000, Schliess et al., 2004, Schliess et al., 2006, Reinehr et al., 2007) and impaired mitochondrial function (Albrecht and Norenberg, 2006, Pichili et al., 2007, Karl et al., 2011), amongst other mechanisms (see lit review section 1.3 for more detailed discussion), impairs normal brain function and leads to the observed psychological dysfunction and HE symptoms in liver disease patients and liver disease models (Haussinger and Schliess, 2008, Monfort et al., 2009). Using MRI, a number of different authors have described; changes in brain water/onset of mild oedema highlighted by decreases in MTR (Balata et al., 2003b) and increases in diffusivity measures ADC and MD in WM (Mardini *et al.*, 2011), increases in Glx/Cr ratios and decreases in ml/Cr ratios using MRS (Balata et al., 2003b, Shawcross et al., 2004a, Mardini et al., 2011), following induction of hyperammonaemia in cirrhosis patients. In contrast, the present findings showed far more subtle changes in quantitative MR measures in response to acute hyperammonaemia, with no change in MD, MTR or the MRS metabolites Glx/Cr, ml/Cr and Cho/Cr being observed. There was however, a significant decrease in brain FA due to hyperammonaemia as measured using DT imaging. This change is difficult to interpret on

its own, as changes in other diffusion measures such as MD would often be expected to accompany any FA changes. It could be suggested that the changes in FA may be indicative of initial subtle changes in brain water due to ammonia, which with longer exposure may develop into more profound change. However this remains speculative, particularly because of the absence of significant changes in other quantitative MR measures. This difference between the findings from the quantitative MR measures here and those observed in cirrhosis and hyperammonaemia, suggests ammonia alone is unlikely to be the cause of the more pronounced psychological changes in liver disease patients. The effects of the additional co-morbidities in disease will therefore likely act synergistically with ammonia to induce more prominent cerebral changes, and hence associated psychological impairment and HE symptom development. The lack of change in brain observed from the present findings explain the absence of psychological impairment found in chapter 4 with hyperammonaemia, which were replicated again in chapter 5 with no changes in psychological task performance being observed.

Despite the absence of impaired psychological task performance, increased sensations of fatigue were replicated with hyperammonaemia in chapter 5 supporting the findings of chapter 4. Unfortunately, the minimal structural or metabolic changes found from the MRI measures, makes it difficult to determine what may be causing this increase in fatigue sensation due to ammonia. The decrease in FA could represent subtle microstructural changes in brain due to ammonia which may in turn relate to increased sensations of fatigue. However, it may also be the case that the type of MRI data collected in the present study missed the mechanism to this fatigue entirely. The effects of increased fatigue could be due to alterations in neural activation patterns rather than structural or metabolic changes to the tissues. Cauli and colleagues have reported altered neural activation within the basal ganglia-thalamus-cortical pathway in hyperammonaemic and liver disease rats

(Cauli et al., 2007b, Cauli et al., 2007c), whilst changes in EEG were found to be related to increased subjective sleepiness following hyperammonaemia in both cirrhosis patients and healthy controls (Bersagliere *et al.*, 2011). As discussed in chapter 4, all neural connections running into and out of the somatosensory cortex, are relayed via the thalamus (Brodal, 2004), therefore disruption to neural pathways running via the thalamus may play a role in interrupting normal sensory output from the somatosensory cortex contributing to the onset of increased fatigue sensation. fMRI measures would help to confirm this.

Even so, fatigue during exercise and ammonia has long been linked in the literature. These findings from chapters 4 and 5 provide evidence of a direct causal role of ammonia in inducing feelings of fatigue, albeit without confirmation of a physiological mechanism. Therefore, during exercise where significant hyperammonaemia can develop and ammonia brain uptake is increased (Nybo et al., 2005), it may play a pivotal role in triggering developing sensations of fatigue and exhaustion in response to the exercise stress. The impact such effects of ammonia may have on overall performance in exercise is difficult to determine from the current findings, however, ammonia may act in a similar manner as in liver disease, in synergy with the co-existing metabolic perturbations present in exercise.

The neurotoxic actions of ammonia on the function of astrocytes, glial cells and neurons have been extensively investigated (Albrecht and Norenberg, 2006, Haussinger and Schliess, 2008). However, ammonia is also known to show significant impairment to a number of different cell types in the body (Seglen, 1978, Fan and Szerb, 1993, Franch, 2000). Skeletal muscle through its large metabolic capacity to remove and produce ammonia, can under certain physiological conditions, come into contact with high intracellular ammonia concentrations (Olde Damink et al., 2002b, Bangsbo et al., 1996).

There is increasing evidence that such high ammonia concentrations can in particular lead

to impaired protein metabolism. Animal models of hyperammonaemia show impaired whole body protein turnover in addition to decreased rates of skeletal muscle protein synthesis (Holecek et al., 2000), whilst rat models of liver disease presenting with hyperammonaemia also show a suppression in the rate of skeletal muscle protein synthesis (Dasarathy et al., 2011). Using a C2C12 murine myotube cell line as a model of skeletal muscle, chapter 6 supported these findings of ammonia induced impairment to skeletal muscle protein metabolism, showing a significant suppression in fractional synthetic rate of protein synthesis when cells were incubated with 1 and 10mM ammonium chloride for 1 and 4 hours. In addition, this chapter is the first to describe the molecular events within the cell which may be regulating this ammonia induced impairment in skeletal muscle metabolism.

The ammonia dependent suppression in MPS seems to be related to inhibition at the initiation and elongation phases of mRNA translation. Ammonium chloride treated muscle cells show significantly increased phosphorylation of the eukaryotic initiation factor 2 (eIF2) alpha subunit and the eukaryotic elongation factor 2 (eEF2). eEF2 regulates the translocation of the ribosome relative to the mRNA (Browne and Proud, 2002), and is active in its dephosphorylated state. The rapid and sustained increases in phosphorylation in response to ammonia represents a decrease in the activity of eEF2, which in turn will down regulate translocation of the ribosome relative to the mRNA, thereby suppressing overall rates of synthesis. eIF2 regulates the rate of mRNA translation through the formation of the 43s preinitiation complex which binds the mRNA strand (Pain, 1996). Phosphorylation of eIF2 at its alpha subunit (eIF2 α) impairs this process, inhibiting synthesis at the initiation stage (Kimball et al., 1998a). Although affecting the initiation and elongation mechanisms, the effect of ammonium chloride on eEF2 outlast those of eIF2 α , suggesting that ammonia's influence on the regulation of MPS are likely to be mainly through control

elongation. Furthermore, findings from chapter 6 propose that regulation of eEF2 phosphorylation by ammonia could be through multiple upstream molecular signalling targets, including; AMPK and p70s6K (see figure 7.1). However, the primary control pathway revealed through the present findings seems to be via AMPK. How these pathways are modulated by ammonia remains to be established, however what is clear is that they are not related to the altered gene expression of common muscle growth factors, myostatin or IGF-1, which has been previously suggested (Dasarathy et al., 2011, Dasarathy et al., 2010).

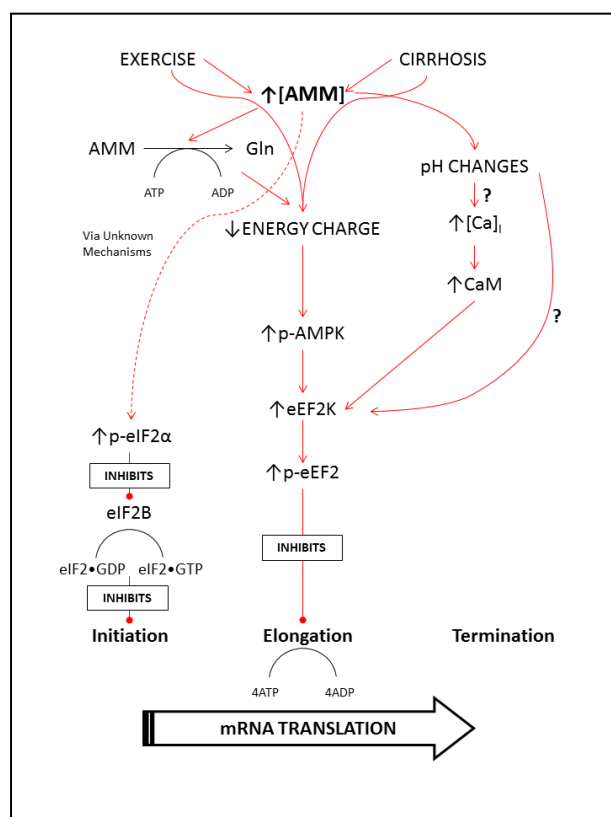


Figure 7.1. Illustration of proposed signalling pathways regulated by ammonia in skeletal muscle which could lead to the observed depression in MPS.

↓ = activates ↓ = inhibits

MPS is depressed during exercise (Gautsch et al., 1998, Dreyer et al., 2006, Rose and Richter, 2009) , whilst muscle wasting is common in liver disease patients (McCullough et al., 1998), and is believed to be associated with reduced MPS (Dasarathy et al., 2011).

Although both situations are highly complex in terms of metabolism, both show significant associated hyperammonaemia. Therefore the findings of ammonia impaired skeletal muscle cell protein synthesis reported in chapter 6, highlight a potential mechanism

through which protein synthesis might, at least in part, be regulated in exercise and disease states. It should be noted that these findings are based on responses to ammonia *in vitro*, and extrapolation to *in vivo* situations is therefore difficult. However it does open up new avenues for investigation with regards to the control of MPS, in addition to potential new therapeutic targets.

7.2 PRACTICAL APPLICATIONS OF FINDINGS

Chapter 3

The findings from chapter 3 demonstrate a reproducible model of hyperammonaemia for use in healthy humans. This model produces a controlled state of systemic hyperammonaemia which can be easily manipulated to alter severity of condition, whilst the continuous iv administration allows temporal effects to also be assessed. It will be possible to use this model in a variety of situations and experimental settings, such as combining it with exercise or other such stressors. In addition, combination administration with LPS to induce a mild inflammatory response, would enable the interaction effects of inflammation/infection and ammonia to be assessed in a controlled environment to investigate the synergistic relationship between co-existing metabolic changes in the development of HE symptoms. Such information could prove vital in the development of combination therapeutic strategies in HE and liver disease for the alleviation of multiple co-morbidities in addition to hyperammonaemia to ensure optimum quality of life for patients. At present many therapies to combat HE are aimed solely at ameliorating hyperammonaemia, which as highlighted in the present thesis, may not be the most appropriate course of action.

Chapters 4 and 5

Ammonia is generally accepted as having multiple neurotoxic actions in the CNS (Felipo and Butterworth, 2002). Hence in conditions such as liver disease, where hyperammonaemia frequently develops alongside cerebral and cognitive impairment in the form of HE, ammonia is thought to be the primary cause (Haussinger and Schliess, 2008). This in turn, has led to proposals for ammonia induced cerebral actions in other hyperammonaemic conditions like exercise, implicating it as a factor in performance regulation and fatigue (Wilkinson et al., 2010). Yet this oversimplifies what are clearly highly complex physiological states, where a multitude of metabolic perturbations are taking place simultaneously, all of which could potentially influence brain function directly or through secondary mechanisms. Liver failure for example, leads to accumulation of plasma manganese, phenols and Mercaptans (Butterworth, 2008). Whilst also leading to impaired immune function (Shawcross *et al.*, 2008). With manganese replicating the effects of ammonia on astrocytes in vitro (Rama Rao et al., 2007, Jayakumar et al., 2004a, Yang et al., 2011), and infection/inflammation showing evidence of significant impact on HE development in liver disease, independent from hyperammonaemia (Shawcross et al., 2004; Shawcross et al., 2011). This questions the true impact of ammonia in causing these symptoms in disease, and now increasing attention has been focused on investigating ammonia independent causes of cerebral dysfunction (Butterworth, 2008). Even with the broadening of knowledge in to the causes of HE symptoms, treatments and therapies still rely heavily on the amelioration of ammonia production (Rifaximin, Neomycin and Lactulose) or increased removal (Ornithine Phenylacetate; OP, L-Ornithine-L-Aspartate; LOLA). The evidence provided from chapters 4 and 5 of this thesis show minimal effect of acute hyperammonaemia on brain metabolism and function. With brain uptake and metabolism of ammonia now suggested to be similar in liver disease and healthy individuals (Keiding et al., 2006). This suggests that ammonia alone is unlikely to be a major cause of developing HE symptoms in disease. The observed response of impaired psychological function in liver disease patients under acute hyperammonaemia is therefore

likely to be reliant on ammonia's interaction with other presenting co-morbidities, as is highlighted in a number of studies (Shawcross et al., 2004b, Shawcross et al., 2008, Wright et al., 2011b). More and more published evidence now recognises the multi-faceted nature of HE development in disease, and how the interaction of ammonia with other metabolic changes is key (Felipo et al., 2011, Wright et al., 2011b). It has recently been proposed that ammonia may 'prime' the brain, increasing its sensitivity to the other factors such as inflammation/infection, which in turn lead to the onset of the classical cerebral dysfunction and HE observed in liver disease. Evidence of this priming effect can be observed from the work of Wright et al., (2011b). When bile duct ligated cirrhotic rats were treated with LPS to induce an inflammatory response, a large proportion showed the onset of brain oedema and subsequent coma. Yet if these rats were pre-treated with OP to reduce hyperammonaemia, brain oedema was significantly reduced and coma onset delayed (Wright et al., 2011b). This result suggests ammonia sensitizes the brain to the effects of other co-morbidities. Therefore therapeutic intervention in liver disease should not only look to alleviate hyperammonaemia, but also aim to control and treat other factors such as immune function, inflammation, manganese levels, and other co-morbidities. This will help to maintain a higher quality of life in these patients for longer.

In addition to this, the finding of increased sensations of fatigue under acute hyperammonaemia could highlight a new method of monitoring impending changes in patients' clinical condition. It is often reported that alterations in sleep-wake cycles and increased levels of tiredness are initial signs of developing mHE (Cordoba et al., 1998, Dhiman and Chawla, 2009, Malaguarnera et al., 2011b). Therefore regular monitoring of subjective fatigue in chronic liver disease, may allow the implementation of early preventative therapy for HE, particularly if ammonia does act as suggested to 'prime/sensitize' the brain to the deleterious actions of other co-morbidities. In addition to

this clinical benefit, this link between ammonia and fatigue could provide the first evidence to support the commonly held belief that ammonia is important in fatigue development during exercise. Prevention of hyperammonaemia during exercise may therefore prove beneficial to optimising performance and delaying the onset of fatigue, and research within this area is already taking place (de Almeida et al., 2010, Prado et al., 2011a). It could be possible that this 'priming' effect present in disease states, could be present during exercise also. Hyperammonaemia alone may not significantly influence deteriorations in performance through the onset of fatigue directly, but 'sensitizes' the brain to the effects of other metabolic perturbations in exercise, which in turn lead to exhaustion and performance impairment.

Chapter 6

The blunting of MPS by ammonia presented in Chapter 6, supports the evidence of previous studies and suggests that systemic ammonia levels could be a major regulator of skeletal muscle protein metabolism. Furthermore, ammonia may at least in part, contribute to the suppression in skeletal muscle protein synthesis observed during exercise, and the muscle wasting present in chronic liver disease. Muscle wasting in liver disease can be potentially devastating to the patient, as it has been shown to be a key predictor of patient survival rates (Alberino et al., 2001). To confirm this link between ammonia and impaired protein metabolism however, future research needs to investigate such mechanisms *in vivo*. However, if confirmed, this could lead to the development of new strategies to ameliorate these effects on muscle, helping to maintain muscle mass and function, and helping to combat wasting due to disease, potentially improving patient survival rates as a consequence. One point which needs to be considered from these *in vitro* results is the physiological relevance of the findings. The skeletal muscle cell line in chapter 6 was treated with an extracellular NH_4Cl concentration of 1mM. Blood ammonia

concentrations in disease and exercise states can reach levels as high as 200-250 μ mol/L (Ortiz et al., 2004, Nybo et al., 2005), yet are never likely to get as high as 1mM. However, the C2C12 cell model is an isolated system, if we consider that intracellular concentrations of ammonia in muscle can reach millimolar levels, whilst also taking into account the mechanisms of cell membrane ammonium transport in muscle (ie lack of ammonium specific transporters). The intracellular concentrations reached within this model system following incubation with 1mM NH₄Cl are likely to reflect physiological ranges, and the methods used in this chapter are therefore justified for understanding physiological responses to ammonia. This does however need confirming with future research into intracellular ammonia metabolism potentially using stable isotope tracers.

7.3 FUTURE RESEARCH DIRECTIONS

Hyperammonaemia in liver disease patients leads to disturbances in cognition and the onset of HE symptoms. Yet findings from chapters 4 & 5 of this thesis show that hyperammonaemia in a healthy adult has minimal effect on brain function and that cognitive disturbances are absent. Therefore in disease the interaction of ammonia with one or many other metabolic disturbances must be key to the onset of these HE symptoms. Future research should therefore aim to investigate these interactions and how they influence the onset of HE, in particular that of ammonia with inflammation and the immune response, which initial reports show, could have major implications in liver disease (Shawcross et al., 2010, Shawcross et al., 2004b, Shawcross et al., 2011, Pedersen et al., 2007). A better understanding of these interactions, particularly relating to the 'priming' hypothesis, and the molecular mechanisms regulating them will assist in developing more effective therapeutic interventions to alleviate HE in cirrhosis and improve patient quality of life. In addition to this, the precise mechanism relating to the increased sensations of fatigue have yet to be resolved. Further research should aim to investigate neural

activation patterns under hyperammonaemic stress using fMRI, EEG, MEG or combinations thereof, to determine what may be regulating these sensational changes.

Furthermore, the evidence of ammonia induced alterations in skeletal muscle protein synthesis opens up a whole new avenue for investigation. Following on from the *in vitro* findings in Chapter 6, future research should focus on, a) understanding the molecular mechanisms which are regulating these responses to ammonia in skeletal muscle, for example through pharmacological manipulation or genetic knockdown. b) Determining the temporal and dose responses relating to these changes, whether there is a “threshold” beyond which ammonia induces such effects on muscle protein metabolism. c) Finally, investigating the translation of these effects of ammonia on MPS from *in vitro* to *in vivo* human studies, and determining whether ammonia is a key mechanism in the development of muscle wasting in cirrhosis. If these effects of ammonia were found to translate to *in vivo* situations, the aim for research within this area would then be to develop effective therapeutic and/or nutritional intervention to counteract these effects on MPS.

7.4 CONCLUSIONS

Taken together, work performed in this thesis has increased current understanding on how and to what extent excess ammonia can impact on brain and muscle metabolism and function. Firstly, despite commonly reported as neurotoxic, ammonia alone seems to have minimal effect on brain. Acute hyperammonaemia induced subtle MR changes (that may be indicative of microstructural change), which are accompanied by increased sensations of fatigue. Yet the psychological and functional disturbances often attributed to ammonia are absent, suggesting that mechanism other than or in addition to those of ammonia are key to inducing these cognitive changes. Secondly, in contrast to the brain, ammonia showed

pronounced effects on skeletal muscle protein synthesis, causing a time dependent suppression in MPS in C2C12 murine myotubes. This effect of ammonia on MPS seems to be caused by the regulation of molecular signalling involved in the control of mRNA translation.

Such findings have wide application to conditions of hyperammonaemia in both athletic and liver disease populations. Evidence provided by these studies can be used in the development of more effective therapeutic intervention in the treatment of HE patients. Whilst also contributing to the understanding of the control of protein synthesis and regulation of muscle mass during both exercise and in disease, through which nutritional or pharmacological interventions can be developed to help maintain optimal skeletal muscle mass and function.

8. References

- ACEVES, J., FLORAN, B., SIERRA, A. & MARISCAL, S. 1995. D-1 receptor mediated modulation of the release of gamma-aminobutyric acid by endogenous dopamine in the basal ganglia of the rat. *Prog Neuropsychopharmacol Biol Psychiatry*, 19, 727-39.
- AGUILAR, M. A., MIÑARRO, J. & FELIPO, V. 2000. Chronic Moderate Hyperammonemia Impairs Active and Passive Avoidance Behavior and Conditional Discrimination Learning in Rats. *Experimental Neurology*, 161, 704-713.
- AGUSTI, A., CAULI, O., RODRIGO, R., LLANSOLA, M., HERNÁNDEZ-RABAZA, V. & FELIPO, V. 2011. p38 MAP kinase is a therapeutic target for hepatic encephalopathy in rats with portacaval shunts. *Gut*.
- AHBOUCHA, S., POMIER-LAYRARGUES, G., MAMER, O. & BUTTERWORTH, R. F. 2006. Increased levels of pregnenolone and its neuroactive metabolite allopregnanolone in autopsied brain tissue from cirrhotic patients who died in hepatic coma. *Neurochemistry International*, 49, 372-378.
- AHL, B., WEISSENBORN, K., HOFF, J. V. D., FISCHER-WASELS, D., KÖSTLER, H., HECKER, H. & BURCHERT, W. 2004. Regional differences in cerebral blood flow and cerebral ammonia metabolism in patients with cirrhosis. *Hepatology*, 40, 73-79.
- AHLBORG, B., EKELUND, L. G. & NILSSON, C. G. 1968. Effect of Potassium-Magnesium-Aspartate on the Capacity for Prolonged Exercise in Man. *Acta Physiologica Scandinavica*, 74, 238-245.
- ALBERINO, F., GATTA, A., AMODIO, P., MERKEL, C., DI PASCOLI, L., BOFFO, G. & CAREGARO, L. 2001. Nutrition and survival in patients with liver cirrhosis. *Nutrition*, 17, 445-50.
- ALBRECHT, J. & NOREMBERG, M. D. 2006. Glutamine: A Trojan Horse in Ammonia Neurotoxicity. *Hepatology*, 44 788-794.
- ALLERT, N., KÖLLER, H. & SIEBLER, M. 1998. Ammonia-induced depolarization of cultured rat cortical astrocytes. *Brain Research*, 782, 261-270.
- ALVAREZ, V. M., RAMA RAO, K. V., BRAHMBHATT, M. & NOREMBERG, M. D. 2011. Interaction between cytokines and ammonia in the mitochondrial permeability transition in cultured astrocytes. *J Neurosci Res*.
- AMENT, W. & VERKERKE, G. J. 2009. Exercise and fatigue. *Sports Medicine*, 39, 389-422.
- ANJUM, R. & BLENIS, J. 2008. The RSK family of kinases: emerging roles in cellular signalling. *Nature Reviews: Molecular Cell Biology*, 9, 747-747-758.
- ATHERTON, P., ETHERIDGE, T., WATT, P., WILKINSON, D., SELBY, A., RANKIN, D., SMITH, K. & RENNIE, M. 2010. Muscle full effect after oral protein: time-dependent concordance and discordance between human muscle protein synthesis and mTORC1 signaling. *Am J Clin Nutr*.
- ATTARIAN, S. & AMALRIC, M. 1997. Microinfusion of the Metabotropic Glutamate Receptor Agonist 1S, 3R–1-Aminocyclopentane-1, 3-dicarboxylic Acid Into the Nucleus Accumbens Induces Dopamine-dependent Locomotor Activation in the Rat. *European Journal of Neuroscience*, 9, 809-816.
- BABIJ, P., MATTHEWS, S. & RENNIE, M. 1983. Changes in blood ammonia, lactate and amino acids in relation to workload during bicycle ergometer exercise in man. *European Journal of Applied Physiology*, 50, 405-411.
- BAEHR, L. M., FURLOW, J. D. & BODINE, S. C. 2011. Muscle sparing in muscle RING finger 1 null mice: response to synthetic glucocorticoids. *The Journal of Physiology*, 589, 4759-4776.
- BAJAJ, J. S., SAEIAN, K., VERBER, M. D., HISCHKE, D., HOFFMANN, R. G., FRANCO, J., VARMA, R. R. & RAO, S. M. 2007. Inhibitory Control Test Is a Simple Method to Diagnose Minimal Hepatic Encephalopathy and Predict Development of Overt Hepatic Encephalopathy. *American Journal of Gastroenterology*, 102, 754-760.

- BAK, L. K., SCHOUSBOE, A. & WAAGEPETERSEN, H. S. 2006. The glutamate/GABA-glutamine cycle: aspects of transport, neurotransmitter homeostasis and ammonia transfer. *Journal of Neurochemistry*, 98, 641-653.
- BAKKAR, N. & GUTTRIDGE, D. C. 2010. NF- κ B Signaling: A Tale of Two Pathways in Skeletal Myogenesis. *Physiological Reviews*, 90, 495-511.
- BALATA, S., DAMINK, S. W. M. O., FERGUSON, K., MARSHALL, I., HAYES, P. C., DEUTZ, N. E. P., WILLIAMS, R., WARDLAW, J. & JALAN, R. 2003a. Induced hyperammonemia alters neuropsychology, brain MR spectroscopy and magnetization transfer in cirrhosis. *Hepatology*, 37, 931-939.
- BALATA, S., OLDE DAMINK, S. W. M., FERGUSON, K., MARSHALL, I., HAYES, P. C., DEUTZ, N. E. P., WILLIAMS, R., WARDLAW, J. & JALAN, R. 2003b. Induced hyperammonemia alters neuropsychology, brain MR spectroscopy and magnetization transfer in cirrhosis. *Hepatology*, 37, 931-939.
- BALLARD, F. J. 1982. Regulation of protein accumulation in cultured cells. *Biochem J*, 208, 275-87.
- BANGSBO, J., KIENS, B. & RICHTER, E. A. 1996. Ammonia uptake in inactive muscles during exercise in humans. *Am J Physiol*, 270, E101-6.
- BANISTER, E. W., BHAKTHAN, N. M. & SINGH, A. K. 1976. Lithium protection against oxygen toxicity in rats: ammonia and amino acid metabolism. *The Journal of Physiology*, 260, 587-596.
- BANISTER, E. W. & CAMERON, B. J. C. 1990. Exercise-induced Hyperammonaemia: Peripheral and Central Effects. *International Journal of Sports Medicine*, 11, S129-S142.
- BARBA, I., CHATAURET, N., GARCÍA-DORADO, D. & CÓRDOBA, J. 2008. A 1H nuclear magnetic resonance-based metabonomic approach for grading hepatic encephalopathy and monitoring the effects of therapeutic hypothermia in rats. *Liver International*, 28, 1141-1148.
- BARDWELL, W. A., BURKE, S. C., THOMAS, K. S., CARTER, C., WEINGART, K. & DIMSDALE, J. E. 2006. Fatigue varies by social class in African Americans but not Caucasian Americans. *International Journal of Behavioral Medicine*, 13, 252-258.
- BARNES, R. H., LABADAN, B. A., SIYAMOGLU, B. & BRADFIELD, R. B. 1964. Effects of Exercise and Administration of Aspartic Acid on Blood Ammonia in the Rat. *Am J Physiol*, 207, 1242-6.
- BASS, N. M. 2007. Review article: the current pharmacological therapies for hepatic encephalopathy. *Alimentary Pharmacology & Therapeutics*, 25, 23-31.
- BASSINI-CAMERON, A., MONTEIRO, A., GOMES, A., WERNECK-DE-CASTRO, J. P. & CAMERON, L. 2008. Glutamine protects against increases in blood ammonia in football players in an exercise intensity-dependent way. *Br J Sports Med*, 42, 260-6.
- BEAULIEU, C. 2002. The basis of anisotropic water diffusion in the nervous system - a technical review. *NMR Biomed*, 15, 435-55.
- BENDER, A. S. & NOREMBERG, M. D. 1996. Effects of ammonia on L-glutamate uptake in cultured astrocytes. *Neurochem Res*, 21, 567-73.
- BERNABEU, R. N., SCHMITZ, P., FAILLACE, M. A. P., IZQUIERDO, I. & MEDINA, J. H. 1996. Hippocampal cGMP and cAMP are differentially involved in memory processing of inhibitory avoidance learning. *NeuroReport*, 7, 585-588.
- BERNABEU, R. N., SCHRODER, N., QUEVEDO, J., CAMMAROTA, M. N., IZQUIERDO, I. N. & MEDINA, J. H. 1997. Further evidence for the involvement of a hippocampal cGMP/cGMP-dependent protein kinase cascade in memory consolidation. *NeuroReport*, 8, 2221-2224.
- BERSAGLIERE, A., RADUAZZO, I., NARDI, M., SCHIFF, S., GATTA, A., AMODIO, P., ACHERMANN, P. & MONTAGNESE, S. 2011. Induced hyperammonaemia may compromise the ability to generate restful sleep in patients with cirrhosis. *Hepatology*.

- BESSMAN, S. P. & BESSMAN, A. N. 1955. The cerebral and peripheral uptake of ammonia in liver disease with an hypothesis for the mechanism of hepatic coma. *J Clin Invest*, 34, 622-8.
- BEVINGTON, A., BROWN, J., BUTLER, H., GOVINDJI, S., M-KHALID, K., SHERIDAN, K. & WALLS, J. 2002. Impaired system A amino acid transport mimics the catabolic effects of acid in L6 cells. *European Journal of Clinical Investigation*, 32, 590-602.
- BINESH, N., HUDA, A., THOMAS, M. A., WYCKOFF, N., BUGBEE, M., HAN, S., RASGON, N., DAVANZO, P., SAYRE, J., GUZE, B., MARTIN, P. & FAWZY, F. 2006. Hepatic encephalopathy: a neurochemical, neuroanatomical, and neuropsychological study. *J Appl Clin Med Phys*, 7, 86-96.
- BISSCHOP, P. H., DE SAIN-VAN DER VELDEN, M. G. M., STELLAARD, F., KUIPERS, F., MEIJER, A. J., SAUERWEIN, H. P. & ROMIJN, J. A. 2003. Dietary Carbohydrate Deprivation Increases 24-Hour Nitrogen Excretion without Affecting Postabsorptive Hepatic or Whole Body Protein Metabolism in Healthy Men. *J Clin Endocrinol Metab*, 88, 3801-3805.
- BJERRING, P., HAUERBERG, J., FREDERIKSEN, H.-J., JORGENSEN, L., HANSEN, B., TOFTENG, F. & LARSEN, F. 2008. Cerebral Glutamine Concentration and Lactate–Pyruvate Ratio in Patients with Acute Liver Failure. *Neurocritical Care*, 9, 3-7.
- BLEI, A. T. & LARSEN, F. S. 1999. Pathophysiology of cerebral edema in fulminant hepatic failure. *Journal of Hepatology*, 31, 771-776.
- BODINE, S. C., LATRES, E., BAUMHUETER, S., LAI, V. K.-M., NUNEZ, L., CLARKE, B. A., POUYMIROU, W. T., PANARO, F. J., NA, E., DHARMARAJAN, K., PAN, Z.-Q., VALENZUELA, D. M., DECHIARA, T. M., STITT, T. N., YANCOPOULOS, G. D. & GLASS, D. J. 2001. Identification of Ubiquitin Ligases Required for Skeletal Muscle Atrophy. *Science*, 294, 1704-1708.
- BORG, G. 1998. *Borg's Perceived Exertion and Pain Scales* Champaign, IL, Human Kinetics.
- BOSCH, J. & GARCÍA-PAGÁN, J. C. 2000. Complications of cirrhosis. I. Portal hypertension. *Journal of Hepatology*, 32, 141-156.
- BOSOI, C. & ROSE, C. 2009. Identifying the direct effects of ammonia on the brain. *Metabolic Brain Disease*, 24, 95-102.
- BRAHMA, B., FORMAN, R. E., STEWART, E. E., NICHOLSON, C. & RICE, M. E. 2000. Ascorbate Inhibits Edema in Brain Slices. *Journal of Neurochemistry*, 74, 1263-1270.
- BROUNS, F., BECKERS, E., WAGENMAKERS, A. J. M. & SARIS, W. H. M. 1990. Ammonia Accumulation During Highly Intensive Long-Lasting Cycling: Individual Observations. *International Journal of Sports Medicine*, 11, S78-S84.
- BROWNE, G. J., FINN, S. G. & PROUD, C. G. 2004. Stimulation of the AMP-activated Protein Kinase Leads to Activation of Eukaryotic Elongation Factor 2 Kinase and to Its Phosphorylation at a Novel Site, Serine 398. *Journal of Biological Chemistry*, 279, 12220-12231.
- BROWNE, G. J. & PROUD, C. G. 2002. Regulation of peptide-chain elongation in mammalian cells. *European Journal of Biochemistry*, 269, 5360-5368.
- BUTTERWORTH, R. F. 2003. Pathogenesis of hepatic encephalopathy: new insights from neuroimaging and molecular studies. *Journal of Hepatology*, 39, 278-285.
- BUTTERWORTH, R. F. 2008. Pathophysiology of hepatic encephalopathy: The concept of synergism. *Hepatology Research*, 38, S116-S121.
- BUTTERWORTH, R. F. 2011. Hepatic encephalopathy: A central neuroinflammatory disorder? *Hepatology*, 53, 1372-6.
- BUTTERWORTH, R. F., SPAHR, L., FONTAINE, S. & LAYRARGUES, G. P. 1995. Manganese toxicity, dopaminergic dysfunction and hepatic encephalopathy. *Metabolic Brain Disease*, 10, 259-267.
- BUTZ, M., TIMMERMAN, L., BRAUN, M., GROISS, S. J., WOJTECKI, L., OSTROWSKI, S., KRAUSE, H., POLLOK, B., GROSS, J., SUDMEYER, M., KIRCHEIS, G., HAUSSINGER, D. & SCHNITZLER, A. 2010a. Motor impairment in liver cirrhosis without and with minimal hepatic encephalopathy. *Acta Neurologica Scandinavica*, 122, 27-35.

- BUTZ, M., TIMMERMANN, L., BRAUN, M., GROISS, S. J., WOJTECKI, L., OSTROWSKI, S., KRAUSE, H., POLLOK, B., GROSS, J., SUDMEYER, M., KIRCHEIS, G., HAUSSINGER, D. & SCHNITZLER, A. 2010b. Motor impairment in liver cirrhosis without and with minimal hepatic encephalopathy. *Acta Neurol Scand*, 122, 27-35.
- CAI, D., FRANTZ, J. D., TAWA JR, N. E., MELENDEZ, P. A., OH, B.-C., LIDOV, H. G. W., HASSELGREN, P.-O., FRONTERA, W. R., LEE, J., GLASS, D. J. & SHOELSON, S. E. 2004. IKK β /NF- κ B Activation Causes Severe Muscle Wasting in Mice. *Cell*, 119, 285-298.
- CAMPILLO, B., FOUET, P., BONNET, J. C. & ATLAN, G. 1990. Submaximal oxygen consumption in liver cirrhosis : Evidence of severe functional aerobic impairment. *Journal of Hepatology*, 10, 163-167.
- CANGIANO, C., CARDELLI-CANGIANO, P., JAMES, J. H., ROSSI-FANELLI, F., PATRIZI, M. A., BRACKETT, K. A., STROM, R. & FISCHER, J. E. 1983. Brain microvessels take up large neutral amino acids in exchange for glutamine. Cooperative role of Na⁺-dependent and Na⁺-independent systems. *J Biol Chem*, 258, 8949-54.
- CARRIERE, A., CARGNELLO, M., JULIEN, L. A., GAO, H., BONNEIL, E., THIBAUT, P. & ROUX, P. P. 2008. Oncogenic MAPK signaling stimulates mTORC1 activity by promoting RSK-mediated raptor phosphorylation. *Curr Biol*, 18, 1269-77.
- CARVALHO-PEIXOTO, J., ALVES, R. C. & CAMERON, L. C. 2007. Glutamine and carbohydrate supplements reduce ammonemia increase during endurance field exercise. *Appl Physiol Nutr Metab*, 32, 1186-90.
- CASO, G., GARLICK, B. A., CASELLA, G. A., SASVARY, D. & GARLICK, P. J. 2004. Acute metabolic acidosis inhibits muscle protein synthesis in rats. *Am J Physiol Endocrinol Metab*, 287, E90-96.
- CAULI, O., GONZALEZ-USANO, A., AGUSTI, A. & FELIPO, V. 2011. Differential modulation of the glutamate-nitric oxide-cyclic GMP pathway by distinct neurosteroids in cerebellum in vivo. *Neuroscience*, 190, 27-36.
- CAULI, O., LLANSOLA, M., ERCEG, S. & FELIPO, V. 2006. Hypolocomotion in rats with chronic liver failure is due to increased glutamate and activation of metabotropic glutamate receptors in substantia nigra. *Journal of Hepatology*, 45, 654-661.
- CAULI, O., LÓPEZ-LARRUBIA, P., RODRIGUES, T. B., CERDÁN, S. & FELIPO, V. 2007a. Magnetic resonance analysis of the effects of acute ammonia intoxication on rat brain. Role of NMDA receptors. *Journal of Neurochemistry*, 103, 1334-1343.
- CAULI, O., MANSOURI, M. T., AGUSTI, A. & FELIPO, V. 2009a. Hyperammonemia increases GABAergic tone in the cerebellum but decreases it in the rat cortex. *Gastroenterology*, 136, 1359-67, e1-2.
- CAULI, O., MLILI, N., LLANSOLA, M. & FELIPO, V. 2007b. Motor activity is modulated via different neuronal circuits in rats with chronic liver failure than in normal rats. *European Journal of Neuroscience*, 25, 2112-2122.
- CAULI, O., MLILI, N., RODRIGO, R. & FELIPO, V. 2007c. Hyperammonemia alters the mechanisms by which metabotropic glutamate receptors in nucleus accumbens modulate motor function. *Journal of Neurochemistry*, 103, 38-46.
- CAULI, O., RODRIGO, R., LLANSOLA, M., MONTOLIU, C., MONFORT, P., PIEDRAFITA, B., EL MLILI, N., BOIX, J., AGUSTI, A. & FELIPO, V. 2009b. Glutamatergic and gabaergic neurotransmission and neuronal circuits in hepatic encephalopathy. *Metab Brain Dis*, 24, 69-80.
- CAULI, O., RODRIGO, R., LLANSOLA, M., MONTOLIU, C., MONFORT, P., PIEDRAFITA, B., EL MLILI, N., BOIX, J., AGUSTÍ, A. & FELIPO, V. 2009c. Glutamatergic and gabaergic neurotransmission and neuronal circuits in hepatic encephalopathy. *Metabolic Brain Disease*, 24, 69-80.
- CAULI, O., RODRIGO, R., PIEDRAFITA, B., BOIX, J. & FELIPO, V. 2007d. Inflammation and hepatic encephalopathy: ibuprofen restores learning ability in rats with portacaval shunts. *Hepatology*, 46, 514-9.
- CAULI, O., RODRIGO, R., PIEDRAFITA, B., LLANSOLA, M., MANSOURI, M. T. & FELIPO, V. 2009d. Neuroinflammation contributes to hypokinesia in rats with hepatic

- encephalopathy: ibuprofen restores its motor activity. *Journal of Neuroscience Research*, 87, 1369-74.
- CERCIGNANI, M., INGLESE, M., PAGANI, E., COMI, G. & FILIPPI, M. 2001. Mean Diffusivity and Fractional Anisotropy Histograms of Patients with Multiple Sclerosis. *AJNR Am J Neuroradiol*, 22, 952-958.
- CHAN, H. & BUTTERWORTH, R. F. 2006. Glutamatergic synaptic regulation deficit in liver failure: a review of molecular mechanisms. In: HAUSSINGER, D., KIRCHEIS, G. & SCHLIESS, F. (eds.) *Hepatic Encephalopathy and Nitrogen Metabolism*. Dordrecht: Springer.
- CHAN, H., HAZELL, A. S., DESJARDINS, P. & BUTTERWORTH, R. F. 2000. Effects of ammonia on glutamate transporter (GLAST) protein and mRNA in cultured rat cortical astrocytes. *Neurochemistry International*, 37, 243-248.
- CHANEY, A. & MARBACH, E. 1962. Modified Reagents for Determination of Urea and Ammonia. *Clinical Chemistry*, 8, 130-132.
- CHRASTIL, J. 1975. Colorimetric estimation of phenols and tyrosine. *Anal Chem*, 47, 2293-6.
- CHURCHILL, L. & KALIVAS, P. W. 1999. The involvement of the mediodorsal nucleus of the thalamus and the midbrain extrapyramidal area in locomotion elicited from the ventral pallidum. *Behavioural Brain Research*, 104, 63-71.
- CHURCHILL, L., ZAHM, D. S., DUFFY, P. & KALIVAS, P. W. 1996a. The mediodorsal nucleus of the thalamus in rats--II. Behavioral and neurochemical effects of GABA agonists. *Neuroscience*, 70, 103-12.
- CHURCHILL, L., ZAHM, D. S. & KALIVAS, P. W. 1996b. The mediodorsal nucleus of the thalamus in rats--I. Forebrain gabaergic innervation. *Neuroscience*, 70, 93-102.
- CLAUSEN, T. & NIELSEN, O. B. 2007. Potassium, Na⁺,K⁺-pumps and fatigue in rat muscle. *J Physiol*, 584, 295-304.
- CLEMMESSEN, J. O., KONDRUP, J. & OTT, P. 2000. Splanchnic and leg exchange of amino acids and ammonia in acute liver failure. *Gastroenterology*, 118, 1131-1139.
- CLEMMESSEN, J. O., LARSEN, F. S., KONDRUP, J., HANSEN, B. A. & OTT, P. 1999. Cerebral herniation in patients with acute liver failure is correlated with arterial ammonia concentration. *Hepatology*, 29, 648-653.
- COLES, J. A., MARCAGGI, P., VEGA, C. & COTILLON, N. 1996. Effects of photoreceptor metabolism on interstitial and glial cell pH in bee retina: evidence of a role for NH₄⁺. *The Journal of Physiology*, 495, 305-318.
- COLES, J. A., MARTIEL, J.-L. & LASKOWSKA, K. 2008. A glia-neuron alanine/ammonium shuttle is central to energy metabolism in bee retina. *The Journal of Physiology Online*, 586, 2077-2091.
- COLLE, I., GEERTS, A. M., VAN STEENKISTE, C. & VAN VLIERBERGHE, H. 2008. Hemodynamic changes in splanchnic blood vessels in portal hypertension. *Anat Rec (Hoboken)*, 291, 699-713.
- CONWAY E.J & BYRNE A. An absorption apparatus for the micro-determination of certain volatile substances: The micro-determination of ammonia. *Biochem J*. 1933;27(2):419-429.
- COOPER, A., J. L. , MORA, S., N. , CRUZ, N., F. & GELBARD, A., S. 1985. Cerebral Ammonia Metabolism in Hyperammonemic Rats. *Journal of Neurochemistry*, 44, 1716-1723.
- COOPER, A. J. L. 2001. Role of glutamine in cerebral nitrogen metabolism and ammonia neurotoxicity. *Mental Retardation and Developmental Disabilities Research Reviews*, 7, 280-286.
- CORBALÁN, R., CHATAURET, N., BEHREND, S., BUTTERWORTH, R. F. & FELIPO, V. 2002. Region selective alterations of soluble guanylate cyclase content and modulation in brain of cirrhotic patients. *Hepatology*, 36, 1155-1162.
- CORDOBA, J., ALONSO, J., ROVIRA, A., JACAS, C., SANPEDRO, F., CASTELLS, L., VARGAS, V., MARGARIT, C., KULISEWSKY, J., ESTEBAN, R. & GUARDIA, J. 2001. The development of low-grade cerebral edema in cirrhosis is supported by the evolution of (1)H-

- magnetic resonance abnormalities after liver transplantation. *J Hepatol*, 35, 598-604.
- CORDOBA, J., CABRERA, J., LATAIF, L., PENEV, P., ZEE, P. & BLEI, A. T. 1998. High prevalence of sleep disturbance in cirrhosis. *Hepatology*, 27, 339-345.
- COUSINS, J. 1995. Clinical MR spectroscopy: fundamentals, current applications, and future potential. *Am. J. Roentgenol.*, 164, 1337-1347.
- COX, I. J. 1996. Development and applications of in vivo clinical magnetic resonance spectroscopy. *Prog Biophys Mol Biol*, 65, 45-81.
- DALSGAARD, M. K., OTT, P., DELA, F., JUUL, A., PEDERSON, B. K., WARBERG, J., FAHRENKRUG, J. & SECHER, N. H. 2004. The CSF and arterial to jugular venous hormonal differences during exercise in humans. *Experimental Physiology*, 89, 271-277.
- DAS, F., GHOSH-CHOUHDURY, N., KASINATH, B. S. & CHOUHDURY, G. G. 2010. TGFbeta enforces activation of eukaryotic elongation factor-2 (eEF2) via inactivation of eEF2 kinase by p90 ribosomal S6 kinase (p90Rsk) to induce mesangial cell hypertrophy. *FEBS Lett*, 584, 4268-72.
- DASARATHY, S., DODIG, M., MUC, S. M., KALHAN, S. C. & MCCULLOUGH, A. J. 2004. Skeletal muscle atrophy is associated with an increased expression of myostatin and impaired satellite cell function in the portacaval anastomosis rat. *American Journal of Physiology - Gastrointestinal and Liver Physiology*, 287, G1124-G1130.
- DASARATHY, S., MCCULLOUGH, A. J., MUC, S., SCHNEYER, A., BENNETT, C. D., DODIG, M. & KALHAN, S. C. 2011. Sarcopenia associated with portosystemic shunting is reversed by follistatin. *Journal of Hepatology*, 54, 915-921.
- DASARATHY, S., YANG, Y., PRASAD, S. V. N., DODIG, M. & MCCULLOUGH, A. J. 2010. AMMONIA MEDIATES AN INCREASE IN SKELETAL MUSCLE MYOSTATIN THROUGH TRANSCRIPTIONAL REGULATION AND CROSS TALKS WITH MTOR. *Hepatology*, 52, 897A-897A.
- DE ALMEIDA, R. D., PRADO, E. S., LLOSA, C. D., MAGALHAES-NETO, A. & CAMERON, L. C. 2010. Acute supplementation with keto analogues and amino acids in rats during resistance exercise. *Br J Nutr*, 104, 1438-42.
- DE LEEUW, R., STUUDTS, J. L. & CARLSON, C. R. 2005. Fatigue and fatigue-related symptoms in an orofacial pain population. *Oral Surgery, Oral Medicine, Oral Pathology, Oral Radiology, and Endodontology*, 99, 168-174.
- DEDERING, A., NEMETH, G. & HARMS-RINGDAHL, K. 1999. Correlation between electromyographic spectral changes and subjective assessment of lumbar muscle fatigue in subjects without pain from the lower back. *Clin Biomech (Bristol, Avon)*, 14, 103-11.
- DELLA NAVE, R., FORESTI, S., PRATESI, A., GINESTRONI, A., INZITARI, M., SALVADORI, E., GIANNELLI, M., DICIOTTI, S., INZITARI, D. & MASCALCHI, M. 2007. Whole-brain histogram and voxel-based analyses of diffusion tensor imaging in patients with leukoaraiosis: correlation with motor and cognitive impairment. *AJNR Am J Neuroradiol*, 28, 1313-9.
- DENIS, C., DORMOIS, D., LINOSSIER, M. T., EYCHENNE, J. L., HAUSEUX, P. & LACOUR, J. R. 1991. Effect of arginine aspartate on the exercise-induced hyperammoniemia in humans: a two periods cross-over trial. *Arch Int Physiol Biochim Biophys*, 99, 123-7.
- DHIMAN, R. & CHAWLA, Y. 2009. Minimal hepatic encephalopathy. *Indian Journal of Gastroenterology*, 28, 5-16.
- DIENST, S. 1961. An ion exchange method for plasma ammonia concentration. *Journal of Clinical and Laboratory Medicine*, 58, 149-55.
- DONG, M. H. & SAAB, S. 2008. Complications of Cirrhosis. *Disease-a-Month*, 54, 445-456.
- DOUGLASS, A., AL MARDINI, H. & RECORD, C. 2001. Amino acid challenge in patients with cirrhosis: a model for the assessment of treatments for hepatic encephalopathy. *Journal of Hepatology*, 34, 658-664.

- DRAGANSKI, B., ASHBURNER, J., HUTTON, C., KHERIF, F., FRACKOWIAK, R. S., HELMS, G. & WEISKOPF, N. 2011. Regional specificity of MRI contrast parameter changes in normal ageing revealed by voxel-based quantification (VBQ). *NeuroImage*, 55, 1423-34.
- DREYER, H. C., FUJITA, S., CADENAS, J. G., CHINKES, D. L., VOLPI, E. & RASMUSSEN, B. B. 2006. Resistance exercise increases AMPK activity and reduces 4E-BP1 phosphorylation and protein synthesis in human skeletal muscle. *The Journal of Physiology*, 576, 613-624.
- DUBOSE, T. D., JR., GOOD, D. W., HAMM, L. L. & WALL, S. M. 1991. Ammonium transport in the kidney: new physiological concepts and their clinical implications. *J Am Soc Nephrol*, 1, 1193-1203.
- EASTON, N. & MARSDEN, C. A. 2006. Ecstasy: Are animal data consistent between species and can they translate to humans? *Journal of Psychopharmacology*, 20, 194-210.
- EL-MLILI, N., RODRIGO, R., NAGHIZADEH, B., CAULI, O. & FELIPO, V. 2008. Chronic hyperammonemia reduces the activity of neuronal nitric oxide synthase in cerebellum by altering its localization and increasing its phosphorylation by calcium-calmodulin kinase II. *Journal of Neurochemistry*, 106, 1440-1449.
- ERCEG, S., MONFORT, P., HERNANDEZ-VADEL, M., LLANSOLA, M., MONTOLIU, C. & FELIPO, V. 2005a. Restoration of learning ability in hyperammonemic rats by increasing extracellular cGMP in brain. *Brain Research*, 1036, 115-121.
- ERCEG, S., MONFORT, P., HERNANDEZ-VADEL, M., RODRIGO, R., MONTOLIU, C. & FELIPO, V. 2005b. Oral administration of sildenafil restores learning ability in rats with hyperammonemia and with portacaval shunts. *Hepatology*, 41, 299-306.
- ERIKSSON, L. S., BROBERG, S., BJORKMAN, O. & WAHREN, J. 1985. Ammonia metabolism during exercise in man. *Clin Physiol*, 5, 325-36.
- ESBJORNSSON-LILJEDAHL, M. & JANSSON, E. 1999. Sex difference in plasma ammonia but not in muscle inosine monophosphate accumulation following sprint exercise in humans. *European Journal of Applied Physiology*, 79, 404-408.
- ESBJORNSSON, M., BULOW, J., NORMAN, B., SIMONSEN, L., NOWAK, J., ROOYACKERS, O., KAIJSER, L. & JANSSON, E. 2006. Adipose tissue extracts plasma ammonia after sprint exercise in women and men. *Journal of Applied Physiology*, 101, 1576-1580.
- ETO, B., PERES, G. & LE MOEL, G. 1994. Effects of an ingested glutamate arginine salt on ammonemia during and after long lasting cycling. *Arch Int Physiol Biochim Biophys*, 102, 161-2.
- EVANS, K., NASIM, Z., BROWN, J., BUTLER, H., KAUSER, S., VAROQUI, H., ERICKSON, J. D., HERBERT, T. P. & BEVINGTON, A. 2007. Acidosis-sensing glutamine pump SNAT2 determines amino acid levels and mammalian target of rapamycin signalling to protein synthesis in L6 muscle cells. *J Am Soc Nephrol*, 18, 1426-36.
- EVANS, K., NASIM, Z., BROWN, J., CLAPP, E., AMIN, A., YANG, B., HERBERT, T. P. & BEVINGTON, A. 2008. Inhibition of SNAT2 by Metabolic Acidosis Enhances Proteolysis in Skeletal Muscle. *Journal of the American Society of Nephrology*, 19, 2119-2129.
- FAN, P. & SZERB, J. C. 1993. Effects of ammonium ions on synaptic transmission and on responses to quisqualate and N-methyl-d-aspartate in hippocampal CA1 pyramidal neurons in vitro. *Brain Research*, 632, 225-231.
- FATOUROS, P. P., MARMAROU, A., KRAFT, K. A., INAO, S. & SCHWARZ, F. P. 1991. In Vivo Brain Water Determination by T1 Measurements: Effect of Total Water Content, Hydration Fraction, and Field Strength. *Magnetic Resonance in Medicine*, 17, 402-413.
- FEDELE, E. & RAITERI, M. 1999. In vivo studies of the cerebral glutamate receptor/NO/cGMP pathway. *Prog Neurobiol*, 58, 89-120.
- FELIPO, V. & BUTTERWORTH, R. F. 2002. Neurobiology of Ammonia. *Progress in Neurobiology*, 67, 259-279.

- FELIPO, V., URIOS, A., MONTESINOS, E., MOLINA, I., GARCIA-TORRES, M. L., CIVERA, M., DEL OLMO, J. A., ORTEGA, J., MARTINEZ-VALLS, J., SERRA, M. A., CASSINELLO, N., WASSEL, A., JORDA, E. & MONTOLIU, C. 2011. Contribution of hyperammonemia and inflammatory factors to cognitive impairment in minimal hepatic encephalopathy. *Metab Brain Dis*.
- FENTON, T. R. & GOUT, I. T. 2011. Functions and regulation of the 70kDa ribosomal S6 kinases. *Int J Biochem Cell Biol*, 43, 47-59.
- FERNANDEZ, M., MEJIAS, M., ANGERMAYR, B., GARCIA-PAGAN, J. C., RODÉS, J. & BOSCH, J. 2005. Inhibition of VEGF receptor-2 decreases the development of hyperdynamic splanchnic circulation and portal-systemic collateral vessels in portal hypertensive rats. *Journal of Hepatology*, 43, 98-103.
- FERREIRA, L. F. & REID, M. B. 2008. Muscle-derived ROS and thiol regulation in muscle fatigue. *J Appl Physiol*, 104, 853-60.
- FRANCH, H. A. 2000. Modification of the Epidermal Growth Factor Response by Ammonia in Renal Cell Hypertrophy. *J Am Soc Nephrol*, 11, 1631-1638.
- FRANCH, H. A., RAISSI, S., WANG, X., ZHENG, B., BAILEY, J. L. & PRICE, S. R. 2004. Acidosis impairs insulin receptor substrate-1-associated phosphoinositide 3-kinase signaling in muscle cells: consequences on proteolysis. *American Journal of Physiology - Renal Physiology*, 287, F700-F706.
- FRAYN, K. N. & MACDONALD, I. A. 1992. Methodological considerations in arterialization of venous blood. *Clinical Chemistry*, 38, 316-317.
- FURST, P., JOSEPHSON, B., MASCHIO, G. & VINNARS, E. 1969. Nitrogen Balance after Intravenous and Oral Administration of Ammonium Salts to Man. *Journal of Applied Physiology*, 26, 13-22.
- GAM, C. M. B., NIELSEN, H. B., SECHER, N. H., LARSEN, F. S., OTT, P. & QUISTORFF, B. 2011. In cirrhotic patients reduced muscle strength is unrelated to muscle capacity for ATP turnover suggesting a central limitation. *Clinical Physiology and Functional Imaging*, 31, 169-174.
- GANDA, O. P. & RUDERMAN, N. B. 1976. Muscle nitrogen metabolism in chronic hepatic insufficiency. *Metabolism*, 25, 427-435.
- GARAVAN, H., ROSS, T. J. & STEIN, E. A. 1999. Right hemispheric dominance of inhibitory control: an event-related functional MRI study. *Proceedings of the National Academy of Science U S A*, 96, 8301-6.
- GAUTSCH, T. A., ANTHONY, J. C., KIMBALL, S. R., PAUL, G. L., LAYMAN, D. K. & JEFFERSON, L. S. 1998. Availability of eIF4E regulates skeletal muscle protein synthesis during recovery from exercise. *Am J Physiol Cell Physiol*, 274, C406-414.
- GEISSLER, A., LOCK, G., FRUND, R., HELD, P., HOLLERBACH, S., ANDUS, T., SCHOLMERICH, J., FEUERBACH, S. & HOLSTEGE, A. 1997. Cerebral abnormalities in patients with cirrhosis detected by proton magnetic resonance spectroscopy and magnetic resonance imaging. *Hepatology*, 25, 48-54.
- GIACOMINI, P. S., LEVESQUE, I. R., RIBEIRO, L., NARAYANAN, S., FRANCIS, S. J., PIKE, G. B. & ARNOLD, D. L. 2009a. Measuring demyelination and remyelination in acute multiple sclerosis lesion voxels. *Arch Neurol*, 66, 375-81.
- GIACOMINI, P. S., LEVESQUE, I. R., RIBEIRO, L., NARAYANAN, S., FRANCIS, S. J., PIKE, G. B. & ARNOLD, D. L. 2009b. Measuring Demyelination and Remyelination in Acute Multiple Sclerosis Lesion Voxels. *Arch Neurol*, 66, 375-381.
- GOEL, A., YADAV, S., SARASWAT, V., SRIVASTAVA, A., THOMAS, M. A., PANDEY, C. M., RATHORE, R. & GUPTA, R. 2010. Cerebral oedema in minimal hepatic encephalopathy due to extrahepatic portal venous obstruction. *Liver International*, 30, 1143-1151.
- GOLCHINI, K., NORMAN, J., BOHMAN, R. & KURTZ, I. 1989. Induction of hypertrophy in cultured proximal tubule cells by extracellular NH₄Cl. *J Clin Invest*, 84, 1767-79.
- GOLDBECKER, A., BUCHERT, R., BERDING, G., BOKEMEYER, M., LICHTINGHAGEN, R., WILKE, F., AHL, B. & WEISSENBORN, K. 2010. Blood-brain barrier permeability for ammonia

- in patients with different grades of liver fibrosis is not different from healthy controls. *J Cereb Blood Flow Metab*, 30, 1384-93.
- GOMES, M. D., LECKER, S. H., JAGOE, R. T., NAVON, A. & GOLDBERG, A. L. 2001. Atrogin-1, a muscle-specific F-box protein highly expressed during muscle atrophy. *Proceedings of the National Academy of Sciences*, 98, 14440-14445.
- GÖRG, B., QVARTSKHAVA, N., KEITEL, V., BIDMON, H. J., SELBACH, O., SCHLIESS, F. & HÄUSSINGER, D. 2008. Ammonia induces RNA oxidation in cultured astrocytes and brain *in vivo*. *Hepatology*, 48, 567-579.
- GRAHAM, T., BANGSBO, J. & SALTIN, B. 1993. Skeletal muscle ammonia production and repeated, intense exercise in humans. *Can J Physiol Pharmacol*, 71, 484-90.
- GRAHAM, T. E., BANGSBO, J., GOLLNICK, P. D., JUEL, C. & SALTIN, B. 1990. Ammonia metabolism during intense dynamic exercise and recovery in humans. *Am J Physiol*, 259, E170-6.
- GRAHAM, T. E., TURCOTTE, L. P., KIENS, B. & RICHTER, E. A. 1995. Training and muscle ammonia and amino acid metabolism in humans during prolonged exercise. *J Appl Physiol*, 78, 725-35.
- GREENHAFF, P. L., LEIPER, J. B., BALL, D. & MAUGHAN, R. J. 1991. The influence of dietary manipulation on plasma ammonia accumulation during incremental exercise in man. *European Journal of Applied Physiology*, 63, 338-344.
- GROVER, V. B., DRESNER, M. A., FORTON, D. M., COUNSELL, S., LARKMAN, D. J., PATEL, N., THOMAS, H. C. & TAYLOR-ROBINSON, S. D. 2006. Current and future applications of magnetic resonance imaging and spectroscopy of the brain in hepatic encephalopathy. *World Journal of Gastroenterology*, 12, 2969-2978.
- GUEZENNEC, C. Y., ABDELMALKI, A., SERRURIER, B., MERINO, D., BIGARD, X., BERTHELOT, M., PIERARD, C. & PERES, M. 1998. Effects of prolonged exercise on brain ammonia and amino acids. *Int J Sports Med*, 19, 323-7.
- HAGER, K. M. R. 2003. *Reliability of Fatigue Measures in an Overhead Work Task: A Study of Shoulder Muscle Electromyography and Perceived Discomfort*. MSc Masters, Virginia Polytechnic Institute and State University.
- HAMADEH, M. J. & HOFFER, L. J. 1998. Tracer methods underestimate short-term variations in urea production in humans. *Am J Physiol Endocrinol Metab*, 274, E547-553.
- HANDLOGTEN, M. E., HONG, S.-P., ZHANG, L., VANDER, A. W., STEINBAUM, M. L., CAMPBELL-THOMPSON, M. & WEINER, I. D. 2005. Expression of the ammonia transporter proteins Rh B glycoprotein and Rh C glycoprotein in the intestinal tract. *Am J Physiol Gastrointest Liver Physiol*, 288, G1036-1047.
- HAREL, N., UGURBIL, K., ULUDAG, K. & YACOUB, E. 2006. Frontiers of brain mapping using MRI. *J Magn Reson Imaging*, 23, 945-57.
- HASAN, K. M., GUPTA, R. K., SANTOS, R. M., WOLINSKY, J. S. & NARAYANA, P. A. 2005. Diffusion tensor fractional anisotropy of the normal-appearing seven segments of the corpus callosum in healthy adults and relapsing-remitting multiple sclerosis patients. *J Magn Reson Imaging*, 21, 735-43.
- HASKEW-LAYTON, R. E., RUDKOUSKAYA, A., JIN, Y. Q., FEUSTEL, P. J., KIMELBERG, H. K. & MONGIN, A. A. 2008. Two Distinct Modes of Hypoosmotic Medium-Induced Release of Excitatory Amino Acids and Taurine in the Rat Brain *In Vivo*. *Plos One*, 3.
- HAUBER, W. 1998. Involvement of basal ganglia transmitter systems in movement initiation. *Progress in Neurobiology*, 56, 507-540.
- HAUSSINGER, D. 1983. Hepatocyte Heterogeneity in Glutamine and Ammonia Metabolism and the Role of an Intercellular Glutamine Cycle during Ureogenesis in Perfused Rat Liver. *European Journal of Biochemistry*, 133, 269-275.
- HAUSSINGER, D., KIRCHEIS, G., FISCHER, R., SCHLIESS, F. & DAHL, S. V. 2000. Hepatic encephalopathy in chronic liver disease: a clinical manifestation of astrocyte swelling and low-grade cerebral edema? *Journal of Hepatology*, 32, 1035-1038.

- HAUSSINGER, D., LAMERS, W. H. & MOORMAN, A. F. 1992. Hepatocyte heterogeneity in the metabolism of amino acids and ammonia. *Enzyme*, 46, 72-93.
- HAUSSINGER, D., LAUBENBERGER, J., VOM DAHL, S., ERNST, T., BAYER, S., LANGER, M., GEROK, W. & HENNIG, J. 1994. Proton magnetic resonance spectroscopy studies on human brain myo-inositol in hypo-osmolarity and hepatic encephalopathy. *Gastroenterology*, 107, 1475-1480.
- HAUSSINGER, D. & SCHLIESS, F. 2008. Pathogenetic mechanisms of hepatic encephalopathy. *Gut*, 57, 1156-1165.
- HE, Y., HAKVOORT, T. B., KOHLER, S. E., VERMEULEN, J. L., DE WAART, D. R., DE THEIJE, C., TEN HAVE, G. A., VAN EIJK, H. M., KUNNE, C., LABRUYERE, W. T., HOUTEN, S. M., SOKOLOVIC, M., RUIJTER, J. M., DEUTZ, N. E. & LAMERS, W. H. 2010. Glutamine synthetase in muscle is required for glutamine production during fasting and extrahepatic ammonia detoxification. *J Biol Chem*, 285, 9516-24.
- HEALD, D. E. 1975. Influence of ammonium ions on mechanical and electrophysiological responses of skeletal muscle. *Am J Physiol*, 229, 1174-9.
- HEIDELBAUGH, J. J. & BRUDERLY, M. 2006. Cirrhosis and chronic liver failure: part I. Diagnosis and evaluation. *Am Fam Physician*, 74, 756-62.
- HEIERVANG, E., BEHRENS, T. E., MACKAY, C. E., ROBSON, M. D. & JOHANSEN-BERG, H. 2006. Between session reproducibility and between subject variability of diffusion MR and tractography measures. *Neuroimage*, 33, 867-77.
- HELLSTEN, Y., RICHTER, E. A., KIENS, B. & BANGSBO, J. 1999. AMP deamination and purine exchange in human skeletal muscle during and after intense exercise. *Journal of Physiology*, 520, 909-920.
- HENKELMAN, R. M., STANISZ, G. J. & GRAHAM, S. J. 2001. Magnetization transfer in MRI: a review. *NMR Biomed*, 14, 57-64.
- HERMENEGILDO, C., MONFORT, P. & FELIPO, V. 2000. Activation of N-methyl-D-aspartate receptors in rat brain in vivo following acute ammonia intoxication: Characterization by in vivo brain microdialysis. *Hepatology*, 31, 709-715.
- HERMENEGILDO, C., MONTOLIU, C., LLANSOLA, M., MUNOZ, M.-D., GAZTELU, J.-M., MINANA, M.-D. & FELIPO, V. 1998a. Chronic hyperammonemia impairs the glutamate-nitric oxide-cyclic GMP pathway in cerebellar neurons in culture and in the rat in vivo. *European Journal of Neuroscience*, 10, 3201-3209.
- HERMENEGILDO, C., MONTOLIU, C., LLANSOLA, M., MUÑOZ, M. D., GAZTELU, J. M., MIÑANA, M. D. & FELIPO, V. 1998b. Chronic hyperammonemia impairs the glutamate-nitric oxide-cyclic GMP pathway in cerebellar neurons in culture and in the rat in vivo. *European Journal of Neuroscience*, 10, 3201-3209.
- HILGIER, W., ZIELINSKA, M., BORKOWSKA, H. D., GADAMSKI, R., WALSKI, M., OJA, S. S., SARANSAARI, P. & ALBRECHT, J. 1999. Changes in the extracellular profiles of neuroactive amino acids in the rat striatum at the asymptomatic stage of hepatic failure. *J Neurosci Res*, 56, 76-84.
- HISATOME, I., MORISAKI, T., KAMMA, H., SUGAMA, T., MORISAKI, H., OHTAHARA, A. & HOLMES, E. W. 1998. Control of AMP deaminase 1 binding to myosin heavy chain. *Am J Physiol Cell Physiol*, 275, C870-881.
- HOBLER, S. C., WILLIAMS, A. B., FISCHER, J. E. & HASSELGREN, P.-O. 1998. IGF-I stimulates protein synthesis but does not inhibit protein breakdown in muscle from septic rats. *American Journal of Physiology - Regulatory, Integrative and Comparative Physiology*, 274, R571-R576.
- HOLECEK, M. 2002. Relation between glutamine, branched-chain amino acids, and protein metabolism. *Nutrition*, 18, 130-133.
- HOLECEK, M. 2010. Three targets of branched-chain amino acid supplementation in the treatment of liver disease. *Nutrition*, 26, 482-90.
- HOLECEK, M., KANDAR, R., SISPERA, L. & KOVARIK, M. 2011. Acute hyperammonemia activates branched-chain amino acid catabolism and decreases their extracellular

- concentrations: different sensitivity of red and white muscle. *Amino Acids*, 40, 575-84.
- HOLECEK, M., SPRONGL, L. & TICHÝ, M. 2000. Effect of hyperammonemia on leucine and protein metabolism in rats. *Metabolism*, 49, 1330-1334.
- HOPGOOD, M. F., CLARK, M. G. & BALLARD, F. J. 1977. Inhibition of protein degradation in isolated rat hepatocytes. *Biochem J*, 164, 399-407.
- HU, S., SHENG, W. S., EHRLICH, L. C., PETERSON, P. K. & CHAO, C. C. 2000. Cytokine effects on glutamate uptake by human astrocytes. *Neuroimmunomodulation*, 7, 153-9.
- HUDA, A., GUZE, B. H., THOMAS, A., BUGBEE, M., FAIRBANKS, L., STROUSE, T. & FAWZY, F. I. 1998. Clinical correlation of neuropsychological tests with 1H magnetic resonance spectroscopy in hepatic encephalopathy. *Psychosom Med*, 60, 550-556.
- HUIZENGA, J. & GIPS, C. 1983. Determination of blood ammonia using the Ammonia Checker. *Annals of Clinical Biochemistry*, 20, 187-9.
- HUNDAL, H. S. & TAYLOR, P. M. 2009. Amino acid transporters: gate keepers of nutrient exchange and regulators of nutrient signaling. *Am J Physiol Endocrinol Metab*, 296, E603-13.
- IDE, K. & SECHER, N. H. 2000. Cerebral blood flow and metabolism during exercise. *Prog Neurobiol*, 61, 397-414.
- IQBAL, K. & OTTAWAY, J. H. 1970. Glutamine synthetase in muscle and kidney. *Biochem J*, 119, 145-56.
- IWASA, M., KINOSADA, Y., NAKATSUKA, A., WATANABE, S. & ADACHI, Y. 1999. Magnetization Transfer Contrast of Various Regions of the Brain in Liver Cirrhosis. *AJNR Am J Neuroradiol*, 20, 652-654.
- JACOBSEN, E. B., HAMBERG, O., QUISTORFF, B. & OTT, P. 2001. Reduced mitochondrial adenosine triphosphate synthesis in skeletal muscle in patients with child-pugh class B and C cirrhosis. *Hepatology*, 34, 7-12.
- JALAN, R., DAMINK, S. W. M. O., LUI, H. F., GLABUS, M., DEUTZ, N. E. P., HAYES, P. C. & EBMEIER, K. 2003. Oral Amino Acid Load Mimicking Hemoglobin Results in Reduced Regional Cerebral Perfusion and Deterioration in Memory Tests in Patients with Cirrhosis of the Liver. *Metabolic Brain Disease*, 18, 37-49.
- JAMES, L. A., LUNN, P. G. & ELIA, M. 1998. Glutamine metabolism in the gastrointestinal tract of the rat assessed by the relative activities of glutaminase (EC 3.5.1.2) and glutamine synthetase (EC 6.3.1.2). *British Journal of Nutrition*, 79, 365-372.
- JAYAKUMAR, A. R., RAMA RAO, K. V., KALAISELVI, P. & NORENBURG, M. D. 2004a. Combined effects of ammonia and manganese on astrocytes in culture. *Neurochem Res*, 29, 2051-6.
- JAYAKUMAR, A. R., RAMA RAO, K. V., MURTHY, C. R. K. & NORENBURG, M. D. 2006. Glutamine in the mechanism of ammonia-induced astrocyte swelling. *Neurochemistry International*, 48, 623-628.
- JAYAKUMAR, A. R., RAMA RAO, K. V., SCHOUSBOE, A. & NORENBURG, M. D. 2004b. Glutamine-induced free radical production in cultured astrocytes. *Glia*, 46, 296-301.
- JAYAKUMAR, A. R., RAO, K. V. R., TONG, X. Y. & NORENBURG, M. D. 2009. Calcium in the mechanism of ammonia-induced astrocyte swelling. *Journal of Neurochemistry*, 109, 252-257.
- JESSUP, W., SHIRAZI, M. F. & DEAN, R. T. 1983. Inhibition of some spontaneous secretory processes in macrophages and fibroblasts by ammonium chloride. *Biochemical Pharmacology*, 32, 2703-2710.
- JONES, D. L. & MOGENSEN, G. J. 1980. Nucleus accumbens to globus pallidus GABA projection subserving ambulatory activity. *Am J Physiol*, 238, R65-9.
- KALE, R. A., GUPTA, R. K., SARASWAT, V. A., HASAN, K. M., TRIVEDI, R., MISHRA, A. M., RANJAN, P., PANDEY, C. M. & NARAYANA, P. A. 2006. Demonstration of interstitial cerebral edema with diffusion tensor MR imaging in type C hepatic encephalopathy. *Hepatology*, 43, 698-706.

- KANTARCI, K. & JACK, C. R., JR. 2004. Quantitative magnetic resonance techniques as surrogate markers of Alzheimer's disease. *NeuroRx*, 1, 196-205.
- KARL, A., WURM, A., PANNICKE, T., KRUGEL, K., OBARA-MICHLEWSKA, M., WIEDEMANN, P., REICHENBACH, A., ALBRECHT, J. & BRINGMANN, A. 2011. Synergistic Action of Hypoosmolarity and Glutamine in Inducing Acute Swelling of Retinal Glial (Muller) Cells. *Glia*, 59, 256-266.
- KASPEREK, G. J., DOHM, G. L. & SNIDER, R. D. 1985. Activation of branched-chain keto acid dehydrogenase by exercise. *Am J Physiol*, 248, R166-71.
- KATZ, A., SAHLIN, K. & HENRIKSSON, J. 1986. Muscle ammonia metabolism during isometric contraction in humans. *AJP - Cell Physiology*, 250, C834-840.
- KAUL, G., PATTAN, G. & RAFEEQUI, T. 2011. Eukaryotic elongation factor-2 (eEF2): its regulation and peptide chain elongation. *Cell Biochemistry and Function*, 29, 227-234.
- KEIDING, S., SORENSEN, M., BENDER, D., MUNK, O. L., OTT, P. & VILSTRUP, H. 2006a. Correction. *Hepatology*, 44, 1056.
- KEIDING, S., SØRENSEN, M., BENDER, D., MUNK, O. L., OTT, P. & VILSTRUP, H. 2006b. Brain Metabolism of ¹³N-Ammonia During Acute Hepatic Encephalopathy in Cirrhosis Measured by Positron Emission Tomography. *Hepatology*, 43, 42-50.
- KEMEL, M. L., DESBAN, M., GAUCHY, C., GLOWINSKI, J. & BESSON, M. J. 1988. Topographical organization of efferent projections from the cat substantia nigra pars reticulata. *Brain Research*, 455, 307-323.
- KIMBALL, S. R., FABIAN, J. R., PAVITT, G. D., HINNEBUSCH, A. G. & JEFFERSON, L. S. 1998a. Regulation of guanine nucleotide exchange through phosphorylation of eukaryotic initiation factor eIF2alpha. Role of the alpha- and delta-subunits of eIF2b. *J Biol Chem*, 273, 12841-5.
- KIMBALL, S. R., HORETSKY, R. L. & JEFFERSON, L. S. 1998b. Implication of eIF2B rather than eIF4E in the regulation of global protein synthesis by amino acids in L6 myoblasts. *J Biol Chem*, 273, 30945-53.
- KIMELBERG, H. K. 2004. Increased release of excitatory amino acids by the actions of ATP and peroxynitrite on volume-regulated anion channels (VRACs) in astrocytes. *Neurochemistry International*, 45, 511-519.
- KIMELBERG, H. K., GODERIE, S. K., HIGMAN, S., PANG, S. & WANIEWSKI, R. A. 1990. Swelling-induced release of glutamate, aspartate, and taurine from astrocyte cultures. *Journal of Neuroscience*, 10, 1583-1591.
- KNECHT, K., MICHALAK, A., ROSE, C., ROTHSTEIN, J. D. & BUTTERWORTH, R. F. 1997. Decreased glutamate transporter (GLT-1) expression in frontal cortex of rats with acute liver failure. *Neuroscience Letters*, 229, 201-203.
- KOSENKO, E., KAMINSKY, Y., LOPATA, O., MURAVYOV, N. & FELIPO, V. 1999. Blocking NMDA receptors prevents the oxidative stress induced by acute ammonia intoxication. *Free Radical Biology and Medicine*, 26, 1369-1374.
- KOSENKO, E., KAMINSKY, Y., SOLOMADIN, I., MAROV, N., VENEDIKTOVA, N., FELIPO, V. & MONTOLIU, C. 2007. Acute ammonia neurotoxicity in vivo involves increase in cytoplasmic protein P53 without alterations in other markers of apoptosis. *Journal of Neuroscience Research*, 85, 2491-2499.
- KOSENKO, E., VENEDIKTOVA, N., KAMINSKY, Y., MONTOLIU, C. & FELIPO, V. 2003. Sources of oxygen radicals in brain in acute ammonia intoxication in vivo. *Brain Res*, 981, 193-200.
- KREIS, R., FARROW, N. & ROSS, B. D. 1991. LOCALIZED H-1-NMR SPECTROSCOPY IN PATIENTS WITH CHRONIC HEPATIC-ENCEPHALOPATHY - ANALYSIS OF CHANGES IN CEREBRAL GLUTAMINE, CHOLINE AND INOSITOLS. *NMR in Biomedicine*, 4, 109-116.
- KREIS, R., ROSS, B. D., FARROW, N. A. & ACKERMAN, Z. 1992. METABOLIC DISORDERS OF THE BRAIN IN CHRONIC HEPATIC-ENCEPHALOPATHY DETECTED WITH H-1 MR SPECTROSCOPY. *Radiology*, 182, 19-27.

- KUMAR, R., GUPTA, R. K., ELDERKIN-THOMPSON, V., HUDA, A., SAYRE, J., KIRSCH, C., GUZE, B., HAN, S. & THOMAS, M. A. 2008. Voxel-based diffusion tensor magnetic resonance imaging evaluation of low-grade hepatic encephalopathy. *J Magn Reson Imaging*, 27, 1061-8.
- KUMAR V, SELBY A, RANKIN D, PATEL R, ATHERTON P, HILDEBRANDT W, WILLIAMS J, SMITH K, SEYNNES O, HISCOCK N & RENNIE M.J. 2009. Age-related differences in the dose-response relationship of muscle protein synthesis to resistance exercise in young and old men. *The Journal of physiology* 587, 211–217.
- KUN, E. & KEARNEY, E. B. 1974. Ammonia. In: BERGMAYER, H. U. (ed.) *Methods of Enzymatic Analysis*. Second ed. New York: Verlag Chemie Weinheim Academic Press Inc.
- KUNDRA, A., JAIN, A., BANGA, A., BAJAJ, G. & KAR, P. 2005. Evaluation of plasma ammonia levels in patients with acute liver failure and chronic liver disease and its correlation with the severity of hepatic encephalopathy and clinical features of raised intracranial tension. *Clinical Biochemistry*, 38, 696-699.
- KUO, Y.-T., HERLIHY, A. H., SO, P.-W., BHAKOO, K. K. & BELL, J. D. 2005. In vivo measurements of T1 relaxation times in mouse brain associated with different modes of systemic administration of manganese chloride. *Journal of Magnetic Resonance Imaging*, 21, 334-339.
- LAISH, I. & BEN ARI, Z. 2011. Noncirrhotic hyperammonaemic encephalopathy. *Liver International*.
- LAMBERT, C., GREENHAFF, P., BALL, D. & MAUGHAN, R. 1993. Influence of sodium bicarbonate ingestion on plasma ammonia accumulation during incremental exercise in man. *European Journal of Applied Physiology*, 66, 49-54.
- LANG, F., BUSCH, G. L., RITTER, M., VOLKL, H., WALDEGGER, S., GULBINS, E. & HAUSSINGER, D. 1998. Functional Significance of Cell Volume Regulatory Mechanisms. *Physiological Reviews*, 78, 247-306.
- LANSBERG, M. G., THUIS, V. N., O'BRIEN, M. W., ALI, J. O., DE CRESPIGNY, A. J., TONG, D. C., MOSELEY, M. E. & ALBERS, G. W. 2001. Evolution of Apparent Diffusion Coefficient, Diffusion-weighted, and T2-weighted Signal Intensity of Acute Stroke. *AJNR Am J Neuroradiol*, 22, 637-644.
- LAPLANTE, M. & SABATINI, D. M. 2009. mTOR signaling at a glance. *Journal of Cell Science*, 122, 3589-3594.
- LARSON, A. M. 2008. Acute Liver Failure. *Disease-a-Month*, 54, 457-485.
- LE BIHAN, D. 2003. Looking into the functional architecture of the brain with diffusion MRI. *Nat Rev Neurosci*, 4, 469-80.
- LE BIHAN, D., MANGIN, J. F., POUPON, C., CLARK, C. A., PAPPATA, S., MOLKO, N. & CHABRIAT, H. 2001. Diffusion tensor imaging: concepts and applications. *J Magn Reson Imaging*, 13, 534-46.
- LEE, J. H., SEO, D. W., LEE, Y.-S., KIM, S.-T., MUN, C.-W., LIM, T.-H., MIN, Y. I. & SUH, D.-J. 1999. Proton magnetic resonance spectroscopy (1H-MRS) findings for the brain in patients with liver cirrhosis reflect the hepatic functional reserve. *Am J Gastroenterol*, 94, 2206-2213.
- LEUNG, L. H. T., OOI, G.-C., KWONG, D. L. W., CHAN, G. C. F., CAO, G. & KHONG, P.-L. 2004. White-matter diffusion anisotropy after chemo-irradiation: a statistical parametric mapping study and histogram analysis. *Neuroimage*, 21, 261-268.
- LI, W., HONG, L., HU, L. & MAGIN, R. L. 2010. Magnetization transfer imaging provides a quantitative measure of chondrogenic differentiation and tissue development. *Tissue Eng Part C Methods*, 16, 1407-15.
- LISTROM, C. D., MORIZONO, H., RAJAGOPAL, B. S., MCCANN, M. T., TUCHMAN, M. & ALLEWELL, N. M. 1997. Expression, purification, and characterization of recombinant human glutamine synthetase. *Biochem J*, 328 (Pt 1), 159-63.
- LOCKWOOD, A. H. 2007. Controversies in ammonia metabolism: implications for hepatic encephalopathy. *Metab Brain Dis*, 22, 285-9.

- LOCKWOOD, A. H., MCDONALD, J. M., REIMAN, R. E., GELBARD, A. S., LAUGHLIN, J. S., DUFFY, T. E. & PLUM, F. 1979. The dynamics of ammonia metabolism in man. Effects of liver disease and hyperammonemia. *J. Clin. Invest.*, 63, 449-460
- LOCKWOOD, A. H., WEISENBORN, K., BOKEMEYER, M., TIETGE, U. & BURCHERT, W. 2002. Correlations Between Cerebral Glucose Metabolism and Neuropsychological Test Performance in Nonalcoholic Cirrhotics. *Metabolic Brain Disease*, 17, 29-40.
- LOCKWOOD, A. H., YAP, E. W. H. & WONG, W. H. 1991. Cerebral Ammonia Metabolism in Patients with Severe Liver-Disease and Minimal Hepatic-Encephalopathy. *Journal of Cerebral Blood Flow and Metabolism*, 11, 337-341.
- LODI, R., TONON, C., STRACCIARI, A., WEIGER, M., CAMAGGI, V., IOTTI, S., DONATI, G., GUARINO, M., BOLONDI, L. & BARBIROLI, B. 2004. Diffusion MRI shows increased water apparent diffusion coefficient in the brains of cirrhotics. *Neurology*, 62, 762-766.
- LOWENSTEIN, J. M. 1990. The purine nucleotide cycle revisited [corrected]. *Int J Sports Med*, 11 Suppl 2, S37-46.
- LU, M. T., PRESTON, J. B. & STRICK, P. L. 1994. Interconnections between the prefrontal cortex and the premotor areas in the frontal lobe. *J Comp Neurol*, 341, 375-92.
- LUND, P. 1970. A radiochemical assay for glutamine synthetase, and activity of the enzyme in rat tissues. *Biochem J*, 118, 35-9.
- LYNCH, M. A. 2004. Long-Term Potentiation and Memory. *Physiological Reviews*, 84, 87-136.
- MADDOCK, R. J., CASAZZA, G. A., BUONOCORE, M. H. & TANASE, C. 2011. Vigorous exercise increases brain lactate and Glx (glutamate + glutamine): A dynamic 1H-MRS study. *Neuroimage*, 57, 1324-1330.
- MADHUSOODANAN, K. S. & MURAD, F. 2007. NO-cGMP signaling and regenerative medicine involving stem cells. *Neurochem Res*, 32, 681-94.
- MAKEIG, S. & JOLLEY, M. 1996. COMPTRACK: a compensatory tracking task for monitoring alertness. *Technical Document 96-3C Naval Health Research Centre, San Diego*.
- MALAGUARNERA, M., BELLA, R., VACANTE, M., GIORDANO, M., MALAGUARNERA, G., GARGANTE, M. P., MOTTA, M., MISTRETTA, A., RAMPELLO, L. & PENNISI, G. 2011a. Acetyl-L-carnitine reduces depression and improves quality of life in patients with minimal hepatic encephalopathy. *Scandinavian Journal of Gastroenterology*, 46, 750-759.
- MALAGUARNERA, M., VACANTE, M., GIORDANO, M., PENNISI, G., BELLA, R., RAMPELLO, L., VOLTI, G. L. & GALVANO, F. 2011b. Oral acetyl-L-carnitine therapy reduces fatigue in overt hepatic encephalopathy: a randomized, double-blind, placebo-controlled study. *American Journal of Clinical Nutrition*, 93, 799-808.
- MARCAGGI, P. & COLES, J. A. 2001. Ammonium in nervous tissue: transport across cell membranes, fluxes from neurons to glial cells, and role in signalling. *Progress in Neurobiology*, 64, 157-183.
- MARDINI, H., SAXBY, B. K. & RECORD, C. O. 2008. Computerized psychometric testing in minimal encephalopathy and modulation by nitrogen challenge and liver transplant. *Gastroenterology*, 135, 1582-90.
- MARDINI, H., SMITH, F. E., RECORD, C. O. & BLAMIRE, A. M. 2011. Magnetic resonance quantification of water and metabolites in the brain of cirrhotics following induced hyperammonaemia. *J Hepatol*.
- MARINI, J. C. & BROUSSARD, S. R. 2006. Hyperammonemia increases sensitivity to LPS. *Molecular Genetics and Metabolism*, 88, 131-137.
- MASINI, A., EFRATI, C., MERLI, M., NICOLAO, F., AMODIO, P., DEL PICCOLO, F. & RIGGIO, O. 2003. Effect of blood ammonia elevation following oral glutamine load on the psychometric performance of cirrhotic patients. *Metab Brain Dis*, 18, 27-35.
- MASTER, S., GOTTSTEIN, J. & BLEI, A., T. 1999. Cerebral blood flow and the development of ammonia-induced brain edema in rats after portacaval anastomosis. *Hepatology*, 30, 876-880.

- MAWHINNEY, T. P., ROBINETT, R. S., ATALAY, A. & MADSON, M. A. 1986. Analysis of amino acids as their tert.-butyldimethylsilyl derivatives by gas-liquid chromatography and mass spectrometry. *J Chromatogr*, 358, 231-42.
- MAY, R. C., KELLY, R. A. & MITCH, W. E. 1986. Metabolic acidosis stimulates protein degradation in rat muscle by a glucocorticoid-dependent mechanism. *J Clin Invest*, 77, 614-21.
- MCCULLOUGH, A. J., MULLEN, K. D. & KALHAN, S. C. 1998. Defective nonoxidative leucine degradation and endogenous leucine flux in cirrhosis during an amino acid infusion. *Hepatology*, 28, 1357-1364.
- MCDERMOTT JR., W. V. & ADAMS, R. D. 1954. Episodic stupor associated with an Eck fistula in the human with particular reference to the metabolism of ammonia. *J Clin Invest*, 33, 1-9.
- MCKINNEY, A. M., LOHMAN, B. D., SARIKAYA, B., UHLMANN, E., SPANBAUER, J., SINGEWALD, T. & BRACE, J. R. 2010. Acute Hepatic Encephalopathy: Diffusion-Weighted and Fluid-Attenuated Inversion Recovery Findings, and Correlation with Plasma Ammonia Level and Clinical Outcome. *AJNR Am J Neuroradiol*, 31, 1471-1479.
- MEEKER, D., KIM, J.-H. & VEZINA, P. 1998. Depletion of dopamine in the nucleus accumbens prevents the generation of locomotion by metabotropic glutamate receptor activation. *Brain Research*, 812, 260-264.
- MEIER-AUGENSTEIN, W. 1999. Use of gas chromatography-combustion-isotope ratio mass spectrometry in nutrition and metabolic research. *Current opinion in clinical nutrition and metabolic care* 2, 465-470.
- MENDEZ, M., MENDEZ-LOPEZ, M., LOPEZ, L., ALLER, M. A., ARIAS, J. & ARIAS, J. L. 2009. Associative learning deficit in two experimental models of hepatic encephalopathy. *Behavioural Brain Research*, 198, 346-51.
- MÉNDEZ, M., MÉNDEZ-LÓPEZ, M., LÓPEZ, L., ALLER, M. A., ARIAS, J. & ARIAS, J. L. 2011. Portosystemic hepatic encephalopathy model shows reversal learning impairment and dysfunction of neural activity in the prefrontal cortex and regions involved in motivated behavior. *Journal of Clinical Neuroscience*, 18, 690-694.
- MEYER, R. A. & TERJUNG, R. L. 1979. Differences in ammonia and adenylate metabolism in contracting fast and slow muscle. *American Journal of Physiology*, 237, C111-118.
- MICHALAK, A., ROSE, C., BUTTERWORTH, J. & BUTTERWORTH, R. F. 1996. Neuroactive amino acids and glutamate (NMDA) receptors in frontal cortex of rats with experimental acute liver failure. *Hepatology*, 24, 908-913.
- MIESE, F., KIRCHEIS, G., WITTSACK, H. J., WENSERSKI, F., HEMKER, J., MODDER, U., HAUSSINGER, D. & COHNEN, M. 2006. 1H-MR Spectroscopy, Magnetization Transfer, and Diffusion-Weighted Imaging in Alcoholic and Nonalcoholic Patients with Cirrhosis with Hepatic Encephalopathy. *American Journal of Neuroradiology*, 27, 1019-1026.
- MIESE, F. R., WITTSACK, H. J., KIRCHEIS, G., HOLSTEIN, A., MATHYS, C., MODDER, U. & COHNEN, M. 2009. Voxel-based analyses of magnetization transfer imaging of the brain in hepatic encephalopathy. *World J Gastroenterol*, 15, 5157-64.
- MÍNGUEZ, B., GARCÍA-PAGÁN, J. C., BOSCH, J., TURNES, J., ALONSO, J., ROVIRA, A. & CÓRDOBA, J. 2006. Noncirrhotic portal vein thrombosis exhibits neuropsychological and MR changes consistent with minimal hepatic encephalopathy. *Hepatology*, 43, 707-714.
- MITCH, W. E., MEDINA, R., GRIEBER, S., MAY, R. C., ENGLAND, B. K., PRICE, S. R., BAILEY, J. L. & GOLDBERG, A. L. 1994. Metabolic acidosis stimulates muscle protein degradation by activating the adenosine triphosphate-dependent pathway involving ubiquitin and proteasomes. *J Clin Invest*, 93, 2127-33.

- MIYAMOTO, Y. & JINNAI, K. 1994. The inhibitory input from the substantia nigra to the mediodorsal nucleus neurons projecting to the prefrontal cortex in the cat. *Brain Research*, 649, 313-318.
- MOATS, R. A., LIEN, Y. H., FILIPPI, D. & ROSS, B. D. 1993. Decrease in cerebral inositols in rats and humans. *Biochem. J.*, 295, 15-18.
- MOGENSON, G. J., SWANSON, L. W. & WU, M. 1983. Neural projections from nucleus accumbens to globus pallidus, substantia innominata, and lateral preoptic-lateral hypothalamic area: an anatomical and electrophysiological investigation in the rat. *J Neurosci*, 3, 189-202.
- MOHR, M., RASMUSSEN, P., DRUST, B., NIELSEN, B. & NYBO, L. 2006. Environmental heat stress, hyperammonemia and nucleotide metabolism during intermittent exercise. *European Journal of Applied Physiology*, 97, 89-95.
- MONFORT, P., CAULI, O., MONTOLIU, C., RODRIGO, R., LLANSOLA, M., PIEDRAFITA, B., EL MLILI, N., BOIX, J., AGUSTÍ, A. & FELIPO, V. 2009. Mechanisms of cognitive alterations in hyperammonemia and hepatic encephalopathy: Therapeutical implications. *Neurochemistry International*, 55, 106-112.
- MONFORT, P., CORBALÁN, R., MARTINEZ, L., LÓPEZ-TALAVERA, J. C., CÓRDOBA, J. & FELIPO, V. 2001. Altered content and modulation of soluble guanylate cyclase in the cerebellum of rats with portacaval anastomosis. *Neuroscience*, 104, 1119-1125.
- MONFORT, P., ERCEG, S., PIEDRAFITA, B., LLANSOLA, M. & FELIPO, V. 2007. Chronic liver failure in rats impairs glutamatergic synaptic transmission and long-term potentiation in hippocampus and learning ability. *European Journal of Neuroscience*, 25, 2103-2111.
- MONFORT, P., MUÑOZ, M.-D. & FELIPO, V. 2004. Hyperammonemia impairs long-term potentiation in hippocampus by altering the modulation of cGMP-degrading phosphodiesterase by protein kinase G. *Neurobiology of Disease*, 15, 1-10.
- MONFORT, P., MUÑOZ, M.-D. & FELIPO, V. 2005a. Chronic hyperammonemia *in vivo* impairs long-term potentiation in hippocampus by altering activation of cyclic GMP-dependent-protein kinase and of phosphodiesterase 5. *Journal of Neurochemistry*, 94, 934-942.
- MONFORT, P., MUÑOZ, M.-D. & FELIPO, V. 2005b. Molecular Mechanisms of the Alterations in NMDA Receptor-Dependent Long-Term Potentiation in Hyperammonemia. *Metabolic Brain Disease*, 20, 265-274.
- MONFORT, P., MUNOZ, M.-D., KOSENKO, E. & FELIPO, V. 2002. Long-Term Potentiation in Hippocampus Involves Sequential Activation of Soluble Guanylate Cyclase, cGMP-Dependent Protein Kinase, and cGMP-Degrading Phosphodiesterase. *J. Neurosci.*, 22, 10116-10122.
- MONGIN, A. A. & KIMELBERG, H. K. 2002. ATP potently modulates anion channel-mediated excitatory amino acid release from cultured astrocytes. *AJP - Cell Physiology*, 283, C569-578.
- MONTARON, M. F., DENIAU, J. M., MENETREY, A., GLOWINSKI, J. & THIERRY, A. M. 1996. Prefrontal cortex inputs of the nucleus accumbens-nigro-thalamic circuit. *Neuroscience*, 71, 371-382.
- MONTOLIU, C., RODRIGO, R., MONFORT, P., LLANSOLA, M., CAULI, O., BOIX, J., ELMLILI, N., AGUSTI, A. & FELIPO, V. 2010. Cyclic GMP pathways in hepatic encephalopathy. Neurological and therapeutic implications. *Metab Brain Dis*, 25, 39-48.
- MORI, S. & ZHANG, J. 2006. Principles of diffusion tensor imaging and its applications to basic neuroscience research. *Neuron*, 51, 527-39.
- MORRIS, R. G. 1989. Synaptic plasticity and learning: selective impairment of learning rats and blockade of long-term potentiation *in vivo* by the N-methyl-D- aspartate receptor antagonist AP5. *J. Neurosci.*, 9, 3040-3057.
- MUÑOZ, M.-D., MONFORT, P., GAZTELU, J.-M. & FELIPO, V. 2000. Hyperammonemia Impairs NMDA Receptor-Dependent Long-Term Potentiation in the CA1 of Rat Hippocampus *In Vitro*. *Neurochemical Research*, 25, 437-441.

- MUTCH, B. J. C. & BANISTER, E. W. 1983. Ammonia metabolism in exercise and fatigue: a review. *Medicine and Science in Sports and Exercise*, 15, 41-50.
- NAGARAJA, T. N. & BROOKES, N. 1998. Intracellular acidification induced by passive and active transport of ammonium ions in astrocytes. *Am J Physiol Cell Physiol*, 274, C883-891.
- NAIRN, A. C. & PALFREY, H. C. 1987. Identification of the major Mr 100,000 substrate for calmodulin-dependent protein kinase III in mammalian cells as elongation factor-2. *Journal of Biological Chemistry*, 262, 17299-17303.
- NATH, K., SARASWAT, V. A., KRISHNA, Y. R., THOMAS, M. A., RATHORE, R. K. S., PANDEY, C. M. & GUPTA, R. K. 2008. Quantification of cerebral edema on diffusion tensor imaging in acute-on-chronic liver failure. *NMR in Biomedicine*, 21, 713-722.
- NEEB, H., ZILLES, K. & SHAH, N. J. 2006. A new method for fast quantitative mapping of absolute water content in vivo. *NeuroImage*, 31, 1156-1168.
- NORDGREN, A., KARLSSON, T. & WIKLUND, L. 2006. Ammonium chloride and alpha-ketoglutaric acid increase glutamine availability in the early phase of induced acute metabolic acidosis. *Acta Anaesthesiologica Scandinavica*, 50, 840-847.
- NORENBERG, M. D., RAMA RAO, K. V. & JAYAKUMAR, A. R. 2009. Signaling factors in the mechanism of ammonia neurotoxicity. *Metab Brain Dis*, 24, 103-117.
- NUNOMURA, A., HONDA, K., TAKEDA, A., HIRAI, K., ZHU, X., SMITH, M. A. & PERRY, G. 2006. Oxidative damage to RNA in neurodegenerative diseases. *J Biomed Biotechnol*, 2006, 82323.
- NYBO, L., DALSGAARD, M. K., STEENBERG, A., MOLLER, K. & SECHER, N. H. 2005. Cerebral ammonia uptake and accumulation during prolonged exercise in humans *Journal of Physiology*, 563, 285-290.
- OBARA-MICHLEWSKA, M., PANNICKE, T., KARL, A., BRINGMANN, A., REICHENBACH, A., SZELIGA, M., HILGIER, W., WRZOSEK, A., SZEWCZYK, A. & ALBRECHT, J. 2011. Down-regulation of Kir4.1 in the cerebral cortex of rats with liver failure and in cultured astrocytes treated with glutamine: Implications for astrocytic dysfunction in hepatic encephalopathy. *Journal of Neuroscience Research*, n/a-n/a.
- ODEH, M., SABO, E., SRUGO, I. & OLIVEN, A. 2005. Relationship between tumor necrosis factor-alpha and ammonia in patients with hepatic encephalopathy due to chronic liver failure. *Annals of medicine*, 37, 603-12.
- OLDE DAMINK, S. W., JALAN, R. & DEJONG, C. H. 2009. Interorgan ammonia trafficking in liver disease. *Metab Brain Dis*, 24, 169-81.
- OLDE DAMINK, S. W. M., DEUTZ, N. E. P., DEJONG, C. H. C., SOETERS, P. B. & JALAN, R. 2002a. Interorgan ammonia metabolism in liver failure. *Neurochemistry International*, 41, 177-188.
- OLDE DAMINK, S. W. M., JALAN, R., DEUTZ, N. E. P., REDHEAD, D. N., DEJONG, C. H. C., HYND, P., JALAN, R. A., HAYES, P. C. & SOETERS, P. B. 2003. The kidney plays a major role in the hyperammonemia seen after simulated or actual GI bleeding in patients with cirrhosis. *Hepatology*, 37, 1277-1285.
- OLDE DAMINK, S. W. M., JALAN, R., REDHEAD, D. N., HAYES, P. C., DEUTZ, N. E. P. & SOETERS, P. B. 2002b. Interorgan ammonia and amino acid metabolism in metabolically stable patients with cirrhosis and a TIPSS. *Hepatology*, 36, 1163-1171.
- ONG, J. P., AGGARWAL, A., KRIEGER, D., EASLEY, K. A., KARAFI, M. T., VAN LENTE, F., ARROLIGA, A. C. & MULLEN, K. D. 2003. Correlation between ammonia levels and the severity of hepatic encephalopathy. *The American Journal of Medicine*, 114, 188-193.
- OPPONG, K. N., AL-MARDINI, H., THICK, M. & RECORD, C. O. 1997. Oral glutamine challenge in cirrhotics pre- and post-liver transplantation: A psychometric and analyzed EEG study. *Hepatology*, 26, 870-876.
- ORTIZ, M., CORDOBA, J., JACAS, C., FLAVIÀ, M., ESTEBAN, R. & GUARDIA, J. 2006. Neuropsychological abnormalities in cirrhosis include learning impairment. *Journal of Hepatology*, 44, 104-110.

- ORTIZ, M., JACAS, C. & CORDOBA, J. 2005. Minimal hepatic encephalopathy: diagnosis, clinical significance and recommendations. *Journal of Hepatology*, 42, S45-S53.
- OTT, P. & LARSEN, F. S. 2004. Blood-brain barrier permeability to ammonia in liver failure: a critical reappraisal. *Neurochemistry International*, 44, 185-198.
- PAGANI, E., BAMMER, R., HORSFIELD, M. A., ROVARIS, M., GASS, A., CICCARELLI, O. & FILIPPI, M. 2007. Diffusion MR imaging in multiple sclerosis: technical aspects and challenges. *AJNR Am J Neuroradiol*, 28, 411-20.
- PAIN, V. M. 1996. Initiation of protein synthesis in eukaryotic cells. *Eur J Biochem*, 236, 747-71.
- PANNICKE, T., IANDIEV, I., UCKERMANN, O., BIEDERMANN, B., KUTZERA, F., WIEDEMANN, P., WOLBURG, H., REICHENBACH, A. & BRINGMANN, A. 2004. A potassium channel-linked mechanism of glial cell swelling in the postischemic retina. *Molecular and Cellular Neuroscience*, 26, 493-502.
- PARNAS, J. K. 1929. Ammonia Formation in Muscle and its Source. . *American Journal of Physiology*, 90, 467.
- PARNAS, J. K. & MOZOLOWSKI, W. 1927. Über die Ammoniakbildung im Muskel und Ihren Zusammenhang mit Tätigkeit und Zustandsänderung. *Journal of Molecular Medicine*, 6, 998-999.
- PATTERSON, B. W., CARRARO, F., KLEIN, S. & WOLFE, R. R. 1995. Quantification of incorporation of [15N]ammonia into plasma amino acids and urea. *Am J Physiol*, 269, E508-15.
- PAYNE, J. A., XU, J.-C., HAAS, M., LYTLE, C. Y., WARD, D. & FORBUSH, B., III 1995. Primary Structure, Functional Expression, and Chromosomal Localization of the Bumetanide-sensitive Na-K-Cl Cotransporter in Human Colon. *J. Biol. Chem.*, 270, 17977-17985.
- PEDERSEN, H. R., RING-LARSEN, H., OLSEN, N. V. & LARSEN, F. S. 2007. Hyperammonemia acts synergistically with lipopolysaccharide in inducing changes in cerebral hemodynamics in rats anaesthetised with pentobarbital. *Journal of Hepatology*, 47, 245-252.
- PEPICELLI, O., RAITERI, M. & FEDELE, E. 2004. The NOS/sGC pathway in the rat central nervous system: a microdialysis overview. *Neurochem Int*, 45, 787-97.
- PFEFFERBAUM, A. & SULLIVAN, E. V. 2005. Disruption of brain white matter microstructure by excessive intracellular and extracellular fluid in alcoholism: evidence from diffusion tensor imaging. *Neuropsychopharmacology*, 30, 423-32.
- PHONGSAMRAN, P. V., KIM, J. W., CUPO ABBOTT, J. & ROSENBLATT, A. 2010. Pharmacotherapy for hepatic encephalopathy. *Drugs*, 70, 1131-48.
- PICHILI, V. B., RAO, K. V., JAYAKUMAR, A. R. & NORENBURG, M. D. 2007. Inhibition of glutamine transport into mitochondria protects astrocytes from ammonia toxicity. *Glia*, 55, 801-9.
- PIROT, S., GLOWINSKI, J. & THIERRY, A.-M. 1995. Excitatory responses evoked in prefrontal cortex by mediodorsal thalamic nucleus stimulation: influence of anaesthesia. *European Journal of Pharmacology*, 285, 45-54.
- PITTS, R. F., PILKINGTON, L. A., MACLEOD, M. B. & LEAL-PINTO, E. 1972. Metabolism of glutamine by the intact functioning kidney of the dog. Studies in metabolic acidosis and alkalosis. *J Clin Invest*, 51, 557-65.
- POVEDA, M.-J., BERNABEU, Á., CONCEPCIÓN, L., ROA, E., DE MADARIA, E., ZAPATER, P., PÉREZ-MATEO, M. & JOVER, R. 2010. Brain edema dynamics in patients with overt hepatic encephalopathy: A magnetic resonance imaging study. *NeuroImage*, 52, 481-487.
- PRADO, E. S., DE REZENDE NETO, J. M., DE ALMEIDA, R. D., DÓRIA DE MELO, M. G. & CAMERON, L.-C. 2011a. Keto analogue and amino acid supplementation affects the ammoniaemia response during exercise under ketogenic conditions. *British Journal of Nutrition*, 105, 1729-1733.

- PRADO, E. S., DE REZENDE NETO, J. M., DE ALMEIDA, R. D., DORIA DE MELO, M. G. & CAMERON, L. C. 2011b. Keto analogue and amino acid supplementation affects the ammoniaemia response during exercise under ketogenic conditions. *Br J Nutr*, 1-5.
- PROUD, C. G. 2007. Signalling to translation: how signal transduction pathways control the protein synthetic machinery. *Biochem J*, 403, 217-234.
- RAMA RAO, K. V., JAYAKUMAR, A. R. & NOREMBERG, M. D. 2003. Induction of the mitochondrial permeability transition in cultured astrocytes by glutamine. *Neurochem Int*, 43, 517-23.
- RAMA RAO, K. V., REDDY, P. V. B., HAZELL, A. S. & NOREMBERG, M. D. 2007. Manganese induces cell swelling in cultured astrocytes. *NeuroToxicology*, 28, 807-812.
- RANJAN, P., MISHRA, A. M., KALE, R., SARASWAT, V. A. & GUPTA, R. K. 2005. Cytotoxic edema is responsible for raised intracranial pressure in fulminant hepatic failure: In vivo demonstration using diffusion-weighted MRI in human subjects. *Metabolic Brain Disease*, 20, 181-192.
- RASHID, W., HADJIPROCOPIIS, A., GRIFFIN, C. M., CHARD, D. T., DAVIES, G. R., BARKER, G. J., TOFTS, P. S., THOMPSON, A. J. & MILLER, D. H. 2004. Diffusion tensor imaging of early relapsing-remitting multiple sclerosis with histogram analysis using automated segmentation and brain volume correction. *Multiple Sclerosis*, 10, 9-15.
- REACH, D., CHANNON, S. M., SCRIMGEOUR, C. M. & GOODSHIP, T. H. J. 1992. Ammonium chloride-induced acidosis increases protein breakdown and amino-acid oxidation in humans. *American Journal of Physiology*, 263, E735-E739.
- REED, S. A., SANDESARA, P. B., SENF, S. M. & JUDGE, A. R. 2011. Inhibition of FoxO transcriptional activity prevents muscle fiber atrophy during cachexia and induces hypertrophy. *Faseb J*.
- REES, C. J., OPPONG, K., AL MARDINI, H., HUDSON, M. & RECORD, C. O. 2000. Effect of L-ornithine-L-aspartate on patients with and without TIPS undergoing glutamine challenge: a double blind, placebo controlled trial. *Gut*, 47, 571-574.
- REINEHR, R., GORG, B., BECKER, S., QVARTSKHAVA, N., BIDMON, H. J., SELBACH, O., HAAS, H. L., SCHLISS, F. & HAUSSINGER, D. 2007. Hypoosmotic swelling and ammonia increase oxidative stress by NADPH oxidase in cultured astrocytes and vital brain slices. *Glia*, 55, 758-71.
- RENNIE, M. J., SELBY, A., ATHERTON, P., SMITH, K., KUMAR, V., GLOVER, E. L. & PHILIPS, S. M. 2010. Facts, noise and wishful thinking: muscle protein turnover in aging and human disuse atrophy. *Scand J Med Sci Sports*, 20, 5-9.
- RODRIGO, R., CAULI, O., BOIX, J., ELMILILI, N., AGUSTI, A. & FELIPO, V. 2009. Role of NMDA receptors in acute liver failure and ammonia toxicity: Therapeutical implications. *Neurochemistry International*, 55, 113-118.
- RODRIGO, R., CAULI, O., GOMEZ-PINEDO, U., AGUSTI, A., HERNANDEZ-RABAZA, V., GARCIA-VERDUGO, J. M. & FELIPO, V. 2010. Hyperammonemia Induces Neuroinflammation That Contributes to Cognitive Impairment in Rats With Hepatic Encephalopathy. *Gastroenterology*, 139, 675-684.
- RODRIGO, R., ERCEG, S. & FELIPO, V. 2005. Neurons exposed to ammonia reproduce the differential alteration in nitric oxide modulation of guanylate cyclase in the cerebellum and cortex of patients with liver cirrhosis. *Neurobiology of Disease*, 19, 150-161.
- ROMERO-GOMEZ, M., BOZA, F., GARCIA-VALDECASAS, M. S., GARCIA, E. & AGUILAR-REINA, J. 2001. Subclinical hepatic encephalopathy predicts the development of overt hepatic encephalopathy. *Am J Gastroenterol*, 96, 2718-23.
- ROMERO-GÓMEZ, M., JOVER, M., GALAN, J. J. & RUIZ, A. 2009. Gut Ammonia Production and its modulation. *Metabolic Brain Disease*, 24, 147-157.
- ROMMEL, C., BODINE, S. C., CLARKE, B. A., ROSSMAN, R., NUNEZ, L., STITT, T. N., YANCOPOULOS, G. D. & GLASS, D. J. 2001. Mediation of IGF-1-induced skeletal myotube hypertrophy by PI(3)K/Akt/mTOR and PI(3)K/Akt/GSK3 pathways. *Nature Cell Biology*, 3, 1009-1009-1013.

- ROSE, A. J., ALSTED, T. J., JENSEN, T. E., KOBBERÄ, J. B., MAARBJERG, S. J., JENSEN, J. R. & RICHTER, E. A. 2009. A Ca²⁺-calmodulin-eEF2K-eEF2 signalling cascade, but not AMPK, contributes to the suppression of skeletal muscle protein synthesis during contractions. *The Journal of Physiology*, 587, 1547-1563.
- ROSE, A. J., BROHOLM, C., KIILLERICH, K., FINN, S. G., PROUD, C. G., RIDER, M. H., RICHTER, E. A. & KIENS, B. 2005a. Exercise rapidly increases eukaryotic elongation factor 2 phosphorylation in skeletal muscle of men. *The Journal of Physiology*, 569, 223-228.
- ROSE, A. J. & RICHTER, E. A. 2009. Regulatory mechanisms of skeletal muscle protein turnover during exercise. *J Appl Physiol*, 106, 1702-1711.
- ROSE, C. 2006. Effect of ammonia on astrocytic glutamate uptake/release mechanisms. *Journal of Neurochemistry*, 97, 11-15.
- ROSE, C., KRESSE, W. & KETTENMANN, H. 2005b. Acute Insult of Ammonia Leads to Calcium-dependent Glutamate Release from Cultured Astrocytes, an Effect of pH. *Journal of Biological Chemistry*, 280, 20937-20944.
- ROSS, B. D., JACOBSON, S., VILLAMIL, F., KORULA, J., KREIS, R., ERNST, T., SHONK, T. & MOATS, R. A. 1994. SUBCLINICAL HEPATIC-ENCEPHALOPATHY - PROTON MR SPECTROSCOPIC ABNORMALITIES. *Radiology*, 193, 457-463.
- ROUX, P. P., BALLIF, B. A., ANJUM, R., GYGI, S. P. & BLENIS, J. 2004. Tumor-promoting phorbol esters and activated Ras inactivate the tuberous sclerosis tumor suppressor complex via p90 ribosomal S6 kinase. *Proceedings of the National Academy of Science U S A*, 101, 13489-13494.
- ROVIRA, A., ALONSO, J. & CORDOBA, J. 2008. MR Imaging Findings in Hepatic Encephalopathy. *American Journal of Neuroradiology*, ajnr.A1139.
- ROVIRA, A., ALONSO, J., CUCURELLA, G., NOS, C., TINTORE, M., PEDRAZA, S., RIO, J. & MONTALBAN, X. 1999. Evolution of multiple sclerosis lesions on serial contrast-enhanced T1-weighted and magnetization-transfer MR images. *AJNR Am J Neuroradiol*, 20, 1939-45.
- ROVIRA, A., GRIVE, E., PEDRAZA, S., ROVIRA, A. & ALONSO, J. 2001. Magnetization Transfer Ratio Values and Proton MR Spectroscopy of Normal-appearing Cerebral White Matter in Patients with Liver Cirrhosis. *American Journal of Neuroradiology*, 22, 1137-1142.
- RUDMAN, D., DIFULCO, T. J., GALAMBOS, J. T., SMITH, R. B., 3RD, SALAM, A. A. & WARREN, W. D. 1973. Maximal rates of excretion and synthesis of urea in normal and cirrhotic subjects. *J Clin Invest*, 52, 2241-9.
- RUNDELL, K. W., TULLSON, P. C. & TERJUNG, R. L. 1992. AMP deaminase binding in contracting rat skeletal muscle. *AJP - Cell Physiology*, 263, C287-293.
- RUSH, J. W., MACLEAN, D. A., HULTMAN, E. & GRAHAM, T. E. 1995. Exercise causes branched-chain oxoacid dehydrogenase dephosphorylation but not AMP deaminase binding. *J Appl Physiol*, 78, 2193-200.
- RYAZANOV, A. G. & DAVYDOVA, E. K. 1989. Mechanism of elongation factor 2 (EF-2) inactivation upon phosphorylation Phosphorylated EF-2 is unable to catalyze translocation. *FEBS Letters*, 251, 187-190.
- SAFRÁNEK, R., HOLECEK, M., KADLČIKOVÁ, J., SPRONGL, L., MISLANOVÁ, C., KUKAN, M. & CHLÁDEK, J. 2003. Effect of acute acidosis on protein and amino acid metabolism in rats. *Clinical Nutrition*, 22, 437-443.
- SANDRI, M., SANDRI, C., GILBERT, A., SKURK, C., CALABRIA, E., PICARD, A., WALSH, K., SCHIAFFINO, S., LECKER, S. H. & GOLDBERG, A. L. 2004. Foxo Transcription Factors Induce the Atrophy-Related Ubiquitin Ligase Atrogin-1 and Cause Skeletal Muscle Atrophy. *Cell*, 117, 399-412.
- SAWARA, K., KATO, A., YOSHIOKA, Y. & SUZUKI, K. 2004. Brain glutamine and glutamate levels in patients with liver cirrhosis: assessed by 3.0-T MRS. *Hepatology Research*, 30, 18-23.
- SCHIFF, S., VALLESI, A., MAPELLI, D., ORSATO, R., PELLEGRINI, A., UMILTÀ, C., GATTA, A. & AMODIO, P. 2005. Impairment of Response Inhibition Precedes Motor Alteration in

- the Early Stage of Liver Cirrhosis: A Behavioral and Electrophysiological Study. *Metabolic Brain Disease*, 20, 381-392.
- SCHLISS, F., FOSTER, N., GORG, B., REINEHR, R. & HAUSSINGER, D. 2004. Hypoosmotic swelling increases protein tyrosine nitration in cultured rat astrocytes. *Glia*, 47, 21-9.
- SCHLISS, F., GORG, B., REINEHR, R., BIDMON, H. J. & HAUSSINGER, D. 2006. Osmotic and oxidative stress in hepatic encephalopathy. In: HAUSSINGER, D., KIRCHEIS, G. & SCHLISS, F. (eds.) *Hepatic Encephalopathy and Nitrogen Metabolism*. Dordrecht: Springer.
- SCHMIDT, G. 1928. Über fermentative desaminierung in muskel. *Ztscher. f. Physiol. Chem.*, 179, 243-282.
- SCHMITT, E., NAVEAU, M. & MECHULAM, Y. 2010. Eukaryotic and archaeal translation initiation factor 2: a heterotrimeric tRNA carrier. *FEBS Lett*, 584, 405-12.
- SCHOTT, K., POETTER, U. & NEUHOFF, V. 1984. Ammonia inhibits protein synthesis in slices from young rat brain. *J Neurochem*, 42, 644-6.
- SCHUPPAN, D. & AFDHAL, N. H. 2008. Liver cirrhosis. *The Lancet*, 371, 838-851.
- SECHER, N. H., SEIFERT, T. & VAN LIESHOUT, J. J. 2008. Cerebral blood flow and metabolism during exercise: implications for fatigue. *J Appl Physiol*, 104, 306-314.
- SEGLIN, P. O. 1975. Protein degradation in isolated rat hepatocytes is inhibited by ammonia. *Biochemical and Biophysical Research Communications*, 66, 44-52.
- SEGLIN, P. O. 1978. Effects of amino acids, ammonia and leupeptin on protein synthesis and degradation in isolated rat hepatocytes. *Biochem J*, 174, 469-74.
- SEGLIN, P. O. & REITH, A. 1976. Ammonia inhibition of protein degradation in isolated rat hepatocytes : Quantitative ultrastructural alterations in the lysosomal system. *Experimental Cell Research*, 100, 276-280.
- SEVICK, R. J., KANDA, F., MINTOROVITCH, J., ARIEFF, A. I., KUCHARCZYK, J., TSURUDA, J. S., NORMAN, D. & MOSELEY, M. E. 1992. Cytotoxic brain edema: assessment with diffusion-weighted MR imaging. *Radiology*, 185, 687-690.
- SHAH, N. J., NEEB, H., KIRCHEIS, G., ENGELS, P., HAUSSINGER, D. & ZILLES, K. 2008. Quantitative cerebral water content mapping in hepatic encephalopathy. *Neuroimage*, 41, 706-17.
- SHAHBAZIAN, D., ROUX, P. P., MIEULET, V., COHEN, M. S., RAUGHT, B., TAUNTON, J., HERSHEY, J. W. B., BLENIS, J., PENDE, M. & SONENBERG, N. 2006. The mTOR/PI3K and MAPK pathways converge on eIF4B to control its phosphorylation and activity. *EMBO J*, 25, 2781-2791.
- SHANELY, R. A. & COAST, J. R. 2002. Effect of ammonia on in vitro diaphragmatic contractility, fatigue and recovery. *Respiration*, 69, 534-41.
- SHANGRAW, R. E. & JAHOR, F. 1999. Effect of liver disease and transplantation on urea synthesis in humans: relationship to acid-base status. *AJP - Gastrointestinal and Liver Physiology*, 276, G1145-1152.
- SHARMA, P. 1996. Effect of ascorbic acid on hyperoxic rat astrocytes. *Neuroscience*, 72, 391-397.
- SHAWCROSS, D. L., SHABBIR, S., S., TAYLOR, N., J. & HUGHES, R., D. 2010. Ammonia and the neutrophil in the pathogenesis of hepatic encephalopathy in cirrhosis. *Hepatology*, 51, 1062-1069.
- SHAWCROSS, D. L., BALATA, S., OLDE DAMINK, S. W. M., HAYES, P. C., WARDLAW, J., MARSHALL, I., DEUTZ, N. E. P., WILLIAMS, R. & JALAN, R. 2004a. Low myo-inositol and high glutamine levels in brain are associated with neuropsychological deterioration after induced hyperammonemia. *AJP - Gastrointestinal and Liver Physiology*, 287, G503-509.
- SHAWCROSS, D. L., DAVIES, N. A., WILLIAMS, R. & JALAN, R. 2004b. Systemic inflammatory response exacerbates the neuropsychological effects of induced hyperammonemia in cirrhosis. *Journal of Hepatology*, 40, 247-254.

- SHAWCROSS, D. L., SHARIFI, Y., CANAVAN, J. B., YEOMAN, A. D., ABELES, R. D., TAYLOR, N. J., AUZINGER, G., BERNAL, W. & WENDON, J. A. 2011. Infection and systemic inflammation, not ammonia, are associated with Grade 3/4 hepatic encephalopathy, but not mortality in cirrhosis. *Journal of Hepatology*, 54, 640-649.
- SHAWCROSS, D. L., WRIGHT, G. A., STADLBAUER, V., HODGES, S. J., DAVIES, N. A., WHEELER-JONES, C., PITSILLIDES, A. A. & JALAN, R. 2008. Ammonia impairs neutrophil phagocytic function in liver disease. *Hepatology*, 48, 1202-12.
- SHIMOMURA, Y., HONDA, T., SHIRAKI, M., MURAKAMI, T., SATO, J., KOBAYASHI, H., MAWATARI, K., OBAYASHI, M. & HARRIS, R. A. 2006. Branched-Chain Amino Acid Catabolism in Exercise and Liver Disease. *Journal of Nutrition*, 136, 250S-253.
- SHIMOMURA, Y., MURAKAMI, T., NAKAI, N., NAGASAKI, M. & HARRIS, R. A. 2004. Exercise Promotes BCAA Catabolism: Effects of BCAA Supplementation on Skeletal Muscle during Exercise. *Journal of Nutrition*, 134, 1583S-1587.
- SIMPSON, D. P. & ADAM, W. 1975. Glutamine transport and metabolism by mitochondria from dog renal cortex. General properties and response to acidosis and alkalosis. *J. Biol. Chem.*, 250, 8148-8158.
- SINGH, A. K. & BANISTER, E. W. 1981. Relative effects of hyperbaric oxygen on cations and catecholamine metabolism in rats: Protection by lithium against seizures. *Toxicology*, 22, 133-147.
- SINGHAL, A., NAGARAJAN, R., KUMAR, R., HUDA, A., GUPTA, R. K. & THOMAS, M. A. 2009. Magnetic Resonance T-2-Relaxometry and 2D L-Correlated Spectroscopy in Patients with Minimal Hepatic Encephalopathy. *Journal of Magnetic Resonance Imaging*, 30, 1034-1041.
- SNOW, R. J., CAREY, M. F., STATHIS, C. G., FEBBRAIO, M. A. & HARGREAVES, M. 2000. Effect of carbohydrate ingestion on ammonia metabolism during exercise in humans. *Journal of Applied Physiology*, 88, 1576-1580.
- SORENSEN, M. & KEIDING, S. 2007. New findings on cerebral ammonia uptake in HE using functional ¹³N-ammonia PET. *Metab Brain Dis*, 22, 277-84.
- SOTAK, C. H. 2004. Nuclear magnetic resonance (NMR) measurement of the apparent diffusion coefficient (ADC) of tissue water and its relationship to cell volume changes in pathological states. *Neurochem Int*, 45, 569-82.
- SPODARYK, K., SZMATLAN, U. & BERGER, L. 1990. The relationship of plasma ammonia and lactate concentrations to perceived exertion in trained and untrained women. *Eur J Appl Physiol Occup Physiol*, 61, 309-12.
- STANTON, B. A. & KOEPPEN, B. M. 1998. The Kidney. In: BERNE, R. M., LEVY, M. N., KOEPPEN, B. M. & STANTON, B. A. (eds.) *Physiology*. 4th ed. St Louis: Mosby Inc.
- STEIN, K. D., JACOBSEN, P. B., BLANCHARD, C. M. & THORS, C. 2004. Further validation of the multidimensional fatigue symptom inventory-short form. *Journal of Pain and Symptom Management*, 27, 14-23.
- STEIN, K. D., MARTIN, S. C., HANN, D. M. & JACOBSEN, P. B. 1998. A multidimensional measure of fatigue for use with cancer patients. *Cancer Pract*, 6, 143-52.
- STEPHENSON, G. M. M. & STEPHENSON, D. G. 1996. Effects of ammonium ions on the depolarization-induced and direct activation of the contractile apparatus in mechanically skinned fast-twitch skeletal muscle fibres of the rat. *Journal of Muscle Research and Cell Motility*, 17, 611-616.
- STEWART, V. C., SHARPE, M. A., CLARK, J. B. & HEALES, S. J. R. 2000. Astrocyte-Derived Nitric Oxide Causes Both Reversible and Irreversible Damage to the Neuronal Mitochondrial Respiratory Chain. *Journal of Neurochemistry*, 75, 694-700.
- STRANGE, K. 1992. Regulation of solute and water balance and cell volume in the central nervous system. *J Am Soc Nephrol*, 3, 12-27.
- STRANGE, K. 2004. Cellular volume homeostasis. *Advances in Physiology Education*, 28, 155-159.
- SUGIMOTO, R., IWASA, M., MAEDA, M., URAWA, N., TANAKA, H., FUJITA, N., KOBAYASHI, Y., TAKEDA, K., KAITO, M. & TAKEI, Y. 2008. Value of the Apparent Diffusion

- Coefficient for Quantification of Low-Grade Hepatic Encephalopathy. *Am J Gastroenterol*, 103, 1413-1420.
- SUMMERSKILL, W. H. J. & WOLPERT, E. 1970. Ammonia Metabolism in the Gut. *Am J Clin Nutr*, 23, 633-639.
- SVEGLIATI-BARONI, G., DE MINICIS, S. & MARZIONI, M. 2008. Hepatic fibrogenesis in response to chronic liver injury: novel insights on the role of cell-to-cell interaction and transition. *Liver Int*, 28, 1052-64.
- SVENSSON, G. & ANFALT, T. (1982). Rapid determination of ammonia in whole blood and plasma using flow injection analysis. *Clinica Chimica Acta* 119, 7-14.
- TANIGAMI, H., REBEL, A., MARTIN, L. J., CHEN, T. Y., BRUSILOW, S. W., TRAYSTMAN, R. J. & KOEHLER, R. C. 2005. Effect of glutamine synthetase inhibition on astrocyte swelling and altered astroglial protein expression during hyperammonemia in rats. *Neuroscience*, 131, 437-49.
- TARASOW, E., PANASIUK, A., SIERGIEJCZYK, L., ORZECZOWSKA-BOBKIEWICZ, A., LEWSZUK, A., WALECKI, J. & PROKOPOWICZ, D. 2003. MR and 1H MR spectroscopy of the brain in patients with liver cirrhosis and early stages of hepatic encephalopathy. *Hepato-Gastroenterology*, 50, 2149-2153.
- TAYLOR-ROBINSON, S. D. 2001. Applications of magnetic resonance spectroscopy to chronic liver disease. *Clin Med*, 1, 54-60.
- TAYLOR, W. E., BHASIN, S., ARTAZA, J., BYHOWER, F., AZAM, M., WILLARD, D. H., JR., KULL, F. C., JR. & GONZALEZ-CADAVID, N. 2001. Myostatin inhibits cell proliferation and protein synthesis in C2C12 muscle cells. *Am J Physiol Endocrinol Metab*, 280, E221-8.
- THOMAS, R. C. 1984. Experimental displacement of intracellular pH and the mechanism of its subsequent recovery. *J Physiol*, 354, 3P-22P.
- THORBURN, M. S., VISTISEN, B., THORP, R. M., ROCKELL, M. J., JEUKENDRUP, A. E., XU, X. & ROWLANDS, D. S. 2006. Attenuated gastric distress but no benefit to performance with adaptation to octanoate-rich esterified oils in well-trained male cyclists. *J Appl Physiol*, 101, 1733-43.
- TIMMERMAN, L., GROSS, J., BUTZ, M., KIRCHEIS, G., HAUSSINGER, D. & SCHNITZLER, A. 2003. Mini-asterix in hepatic encephalopathy induced by pathologic thalamo-motor-cortical coupling. *Neurology*, 61, 689-692.
- TIMMERMAN, W. & WESTERINK, B. H. C. 1997. Electrical stimulation of the substantia nigra reticulata: Detection of neuronal extracellular GABA in the ventromedial thalamus and its regulatory mechanism using microdialysis in awake rats. *Synapse*, 26, 62-71.
- TIMMERMANN, L., BUTZ, M., GROSS, J., PLONER, M., SÜDMEYER, M., KIRCHEIS, G., HÄUSSINGER, D. & SCHNITZLER, A. 2008. Impaired cerebral oscillatory processing in hepatic encephalopathy. *Clinical Neurophysiology*, 119, 265-272.
- TKAC, I., ANDERSEN, P., ADRIANY, G., MERKLE, H., UGURBIL, K. & GRUETTER, R. 2001. In vivo 1H NMR spectroscopy of the human brain at 7 T. *Magn Reson Med*, 46, 451-6.
- TOFTENG, F., HAUERBERG, J., HANSEN, B. A., PEDERSEN, C. B., JORGENSEN, L. & LARSEN, F. S. 2005. Persistent arterial hyperammonemia increases the concentration of glutamine and alanine in the brain and correlates with intracranial pressure in patients with fulminant hepatic failure. *J Cereb Blood Flow Metab*, 26, 21-27.
- TOFTENG, F., JORGENSEN, L., HANSEN, B. A., OTT, P., KONDRUP, J. & LARSEN, F. S. 2002. Cerebral microdialysis in patients with fulminant hepatic failure. *Hepatology*, 36, 1333-1340.
- TOFTS, P., STEENS, S. & VAN BUCHEM, M. 2003. MT: Magnetization Transfer. In: TOFTS, P. (ed.) *Quantitative MRI of the Brain: Measuring Changes Caused by Disease*. Chichester: Wiley.
- TOFTS, P. & WALDMAN, A. D. 2003. Spectroscopy: ¹H Metabolite Concentrations. In: TOFTS, P. (ed.) *Quantitative MRI of the Brain: Measuring Changes Caused by Disease*. Chichester: Wiley.

- TSACOPOULOS, M., POITRY-YAMATE, C. L. & POITRY, S. 1997. Ammonium and Glutamate Released by Neurons Are Signals Regulating the Nutritive Function of a Glial Cell. *J. Neurosci.*, 17, 2383-2390.
- TULLSON, P. C. & TERJUNG, R. L. 1990. Adenine Nucleotide Degradation in Striated Muscle. *International Journal of Sports Medicine*, 11, S47-S55.
- TYOR, M. P. & WILSON, W. P. 1958. Peripheral biochemical changes associated with the intravenous administration of ammonium salts in normal subjects. *Journal of Laboratory and Clinical Medicine*, 51, 592-9.
- VAN BUCHEM, M. A., MCGOWAN, J. C., KOLSON, D. L., POLANSKY, M. & GROSSMAN, R. I. 1996. Quantitative volumetric magnetization transfer analysis in multiple sclerosis: estimation of macroscopic and microscopic disease burden. *Magn Reson Med*, 36, 632-6.
- VAN DE POLL, M. C. G., SOETERS, P. B., DEUTZ, N. E. P., FEARON, K. C. H. & DEJONG, C. H. C. 2004. Renal metabolism of amino acids: its role in interorgan amino acid exchange. *Am J Clin Nutr*, 79, 185-197.
- VAN DE VEN, M. J. T., COLIER, W., OESEBURG, B. & FOLGERING, H. T. M. 1999. Induction of acute metabolic acid/base changes in humans. *Clinical Physiology*, 19, 290-293.
- VAN DER TOORN, A., SYKOVÁ, E., DIJKHUIZEN, R. M., VOŘIŠEK, I., VARGOVÁ, L., ŠKOBISOVÁ, E., VAN LOOKEREN CAMPAGNE, M., REESE, T. & NICOLAY, K. 1996. Dynamic changes in water ADC, energy metabolism, extracellular space volume, and tortuosity in neonatal rat brain during global ischemia. *Magnetic Resonance in Medicine*, 36, 52-60.
- VAVASOUR, I. M., LAULE, C., LI, D. K., TRABOULSEE, A. L. & MACKAY, A. L. 2011. Is the magnetization transfer ratio a marker for myelin in multiple sclerosis? *J Magn Reson Imaging*, 33, 713-8.
- WAGENMAKERS, A. J. 1998. Muscle amino acid metabolism at rest and during exercise: role in human physiology and metabolism. *Exerc Sport Sci Rev*, 26, 287-314.
- WAGENMAKERS, A. J., BROOKES, J. H., COAKLEY, J. H., REILLY, T. & EDWARDS, R. H. 1989. Exercise-induced activation of the branched-chain 2-oxo acid dehydrogenase in human muscle. *Eur J Appl Physiol Occup Physiol*, 59, 159-67.
- WAGENMAKERS, A. J., COAKLEY, J. H. & EDWARDS, R. H. 1990. Metabolism of branched-chain amino acids and ammonia during exercise: clues from McArdle's disease. *Int J Sports Med*, 11 Suppl 2, S101-13.
- WANG, D. D. & BORDEY, A. 2008. The astrocyte odyssey. *Progress in Neurobiology*, 86, 342-367.
- WANG, L. & PROUD, C. G. 2002. Regulation of the phosphorylation of elongation factor 2 by MEK-dependent signalling in adult rat cardiomyocytes. *FEBS Lett*, 531, 285-9.
- WANG, X., LI, W., WILLIAMS, M., TERADA, N., ALESSI, D. R. & PROUD, C. G. 2001. Regulation of elongation factor 2 kinase by p90RSK1 and p70 S6 kinase. *EMBO J*, 20, 4370-4379.
- WEBSTER, L. T., JR. & GABUZDA, G. J. 1958. Ammonium uptake by the extremities and brain in hepatic coma. *J Clin Invest*, 37, 414-24.
- WEISSENBORN, K. 2008. PHES: One label, different goods?! *Journal of Hepatology*, 49, 308-312.
- WEISSENBORN, K., AHL, B., FISCHER-WASELS, D., VAN DEN HOFF, J., HECKER, H., BURCHERT, W. & KOSTLER, H. 2007. Correlations between magnetic resonance spectroscopy alterations and cerebral ammonia and glucose metabolism in cirrhotic patients with and without hepatic encephalopathy. *Gut*, 56, 1736-1742.
- WEISSENBORN, K., ENNEN, J. C., SCHOMERUS, H., RUCKERT, N. & HECKER, H. 2001. Neuropsychological characterization of hepatic encephalopathy. *Journal of Hepatology*, 34, 768-773.
- WEISSENBORN, K., GIEWEKEMEYER, K., HEIDENREICH, S., BOKEMEYER, M., BERDING, G. & AHL, B. 2005. Attention, Memory, and Cognitive Function in Hepatic Encephalopathy. *Metabolic Brain Disease*, 20, 359-367.

- WEISSENBORN, K., RUCKERT, N., HECKER, H. & MANNS, M. P. 1998. The number connection tests A and B: interindividual variability and use for the assessment of early hepatic encephalopathy. *Journal of Hepatology*, 28, 646-653.
- WHEELER-KINGSHOTT, C. A. M., BARKER, G. J., STEENS, S. C. A. & VAN BUCHEM, M. A. 2003. D: the Diffusion of Water. In: TOFTS, P. (ed.) *Quantitative MRI of the Brain: Measuring Changes Caused by Disease*. Chichester: Wiley.
- WILKINSON, D. J., SMEETON, N. J. & WATT, P. W. 2010. Ammonia metabolism, the brain and fatigue; revisiting the link. *Progress in Neurobiology*, 91, 200-219.
- WILLARD-MACK, C. L., KOEHLER, R. C., HIRATA, T., CORK, L. C., TAKAHASHI, H., TRAYSTMAN, R. J. & BRUSILOW, S. W. 1996. Inhibition of glutamine synthetase reduces ammonia-induced astrocyte swelling in rat. *Neuroscience*, 71, 589-99.
- WILLIAMS, H. R. T., COX, I. J. & TAYLOR-ROBINSON, S. D. 2008. Metabonomics in hepatic encephalopathy: lucidity emerging from confusion. *Liver International*, 28, 1050-1051.
- WOLFF, S. D. & BALABAN, R. S. 1994. Magnetization transfer imaging: practical aspects and clinical applications. *Radiology*, 192, 593-9.
- WRIGHT, G. & JALAN, R. 2007. Management of hepatic encephalopathy in patients with cirrhosis. *Best Practice & Research Clinical Gastroenterology*, 21, 95-110.
- WRIGHT, G., NOIRET, L., DAMINK, S. W. & JALAN, R. 2011a. Interorgan ammonia metabolism in liver failure: the basis of current and future therapies. *Liver Int*, 31, 163-75.
- WRIGHT, G., VAIRAPPAN, B., STADLBAUER, V., MOOKERJEE, R. P., DAVIES, N. A. & JALAN, R. 2011b. Reduction in hyperammonaemia by ornithine phenylacetate prevents lipopolysaccharide-induced brain edema and coma in cirrhotic rats. *Liver International*, n/a-n/a.
- YAMADA, K., HIRAMATSU, M., NODA, Y., MAMIYA, T., MURAI, M., KAMEYAMA, T., KOMORI, Y., NIKAI, T., SUGIHARA, H. & NABESHIMA, T. 1996. Role of nitric oxide and cyclic GMP in the dizocilpine-induced impairment of spontaneous alternation behavior in mice. *Neuroscience*, 74, 365-374.
- YANG, D., HAZEY, J., FRANCE, D., SINGH, J., RIVCHUM, R., STREEM, J., HALPERIN, M. L. & BRUNENGRABER, H. 2000. Integrative physiology of splanchnic glutamine and ammonium metabolism. *American Journal of Physiology. Endocrinology and Metabolism*, 278, E469-E476.
- YANG, S. S., WU, C. H., CHIANG, T. R. & CHEN, D. S. 1998. Somatosensory evoked potentials in subclinical portosystemic encephalopathy: a comparison with psychometric tests. *Hepatology*, 27, 357-61.
- YANG, Y., AN, J., WANG, Y., LUO, W., WANG, W., MEI, X., WU, S. & CHEN, J. 2011. Intrastratial manganese chloride exposure causes acute locomotor impairment as well as partial activation of substantia nigra GABAergic neurons. *Environmental Toxicology and Pharmacology*, 31, 171-178.
- YUE, H. J., BARDWELL, W., ANCOLI-ISRAEL, S., LOREDO, J. S. & DIMSDALE, J. E. 2009. Arousal frequency is associated with increased fatigue in obstructive sleep apnea. *Sleep and Breathing*, 13, 331-339.
- ZHAO, F. Y., KUROIWA, T., MIYASAKAI, N., TANABE, F., NAGAOKA, T., AKIMOTO, H., OHNO, K. & TAMURA, A. 2006. Diffusion tensor feature in vasogenic brain edema in cats. *Acta Neurochir Suppl*, 96, 168-70.
- ZHAO, J., BRAULT, J. J., SCHILD, A., CAO, P., SANDRI, M., SCHIAFFINO, S., LECKER, S. H. & GOLDBERG, A. L. 2007. FoxO3 Coordinately Activates Protein Degradation by the Autophagic/Lysosomal and Proteasomal Pathways in Atrophying Muscle Cells. *Cell metabolism*, 6, 472-483.
- ZHAO, S., SNOW, R. J., STATHIS, C. G., FEBBRAIO, M. A. & CAREY, M. F. 2000. Muscle adenine nucleotide metabolism during and in recovery from maximal exercise in humans. *J Appl Physiol*, 88, 1513-9.

- ZHENG, P. 2009. Neuroactive steroid regulation of neurotransmitter release in the CNS: Action, mechanism and possible significance. *Progress in Neurobiology*, 89, 134-152.
- ZHOU, B.-G. & NOREMBERG, M. D. 1999. Ammonia downregulates GLAST mRNA glutamate transporter in rat astrocyte cultures. *Neuroscience Letters*, 276, 145-148.
- ZIELINSKA, M., RUSZKIEWICZ, J., HILGIER, W., FRESKO, I. & ALBRECHT, J. 2011. Hyperammonemia increases the expression and activity of the glutamine/arginine transporter $\gamma(+)$ LAT2 in rat cerebral cortex: Implications for the nitric oxide/cGMP pathway. *Neurochemistry International*, 58, 190-195.
- ZWINGMANN, C., BRAND, A., RICHTER-LANDSBERG, C. & LEIBFRITZ, D. 1998. Multinuclear NMR spectroscopy studies on NH₄Cl-induced metabolic alterations and detoxification processes in primary astrocytes and glioma cells. *Dev Neurosci*, 20, 417-26.

9. APPENDICES

Appendix 1: Copy of MRI Safety Questionnaire

Clinical Imaging Sciences Centre

MRI SAFETY QUESTIONNAIRE FOR PARTICIPANTS

The MRI Scanner uses a powerful magnetic field so we need to make sure that you are safe to enter the scanning room. Please remove all loose metal objects before your scan eg: keys, coins, credit cards, mobile phones or pagers, watches, hairclips, metallic body piercings.

SURNAME	FIRST NAME	TITLE	DATE OF BIRTH	WEIGHT (approx)	PHONE NUMBER	CISC No:
ADDRESS / POSTCODE				NAME / ADDRESS / POSTCODE OF GP		

Please answer the following questions accurately by ticking the appropriate box. The Radiographer will answer any queries.		Yes	No
Do you have a cardiac (heart) pacemaker?	<input type="checkbox"/>	<input type="checkbox"/>	<input type="checkbox"/>
Have you ever had surgery to your heart? Eg: artificial heart valve	<input type="checkbox"/>	<input type="checkbox"/>	<input type="checkbox"/>
Have you ever had surgery to your head, spine, eyes or ears?	<input type="checkbox"/>	<input type="checkbox"/>	<input type="checkbox"/>
Have you had a cataract operation or intraocular lens surgery?	<input type="checkbox"/>	<input type="checkbox"/>	<input type="checkbox"/>
Do you have a hydrocephalus shunt?	<input type="checkbox"/>	<input type="checkbox"/>	<input type="checkbox"/>
If yes, is it programmable?	<input type="checkbox"/>	<input type="checkbox"/>	<input type="checkbox"/>
Have you had ANY surgery?	<input type="checkbox"/>	<input type="checkbox"/>	<input type="checkbox"/>
Have you ever had any metal implants?	<input type="checkbox"/>	<input type="checkbox"/>	<input type="checkbox"/>
Have you ever had any metal fragments go into your eyes?	<input type="checkbox"/>	<input type="checkbox"/>	<input type="checkbox"/>
Women of child bearing age: Are you breast feeding?	<input type="checkbox"/>	<input type="checkbox"/>	<input type="checkbox"/>
Is there any possibility you may be pregnant?	<input type="checkbox"/>	<input type="checkbox"/>	<input type="checkbox"/>
Do you have any of the following:	<input type="checkbox"/>	<input type="checkbox"/>	<input type="checkbox"/>
Epilepsy	<input type="checkbox"/>	<input type="checkbox"/>	<input type="checkbox"/>
Joint Replacement	<input type="checkbox"/>	<input type="checkbox"/>	<input type="checkbox"/>
False limbs, callipers	<input type="checkbox"/>	<input type="checkbox"/>	<input type="checkbox"/>
Metal Dentures	<input type="checkbox"/>	<input type="checkbox"/>	<input type="checkbox"/>
Neurological stimulators	<input type="checkbox"/>	<input type="checkbox"/>	<input type="checkbox"/>
Skin patches (HRT, Nicotine), tattoos, metallic eye makeup, contact lens	<input type="checkbox"/>	<input type="checkbox"/>	<input type="checkbox"/>
Have you previously had an MRI scan at this centre?	<input type="checkbox"/>	<input type="checkbox"/>	<input type="checkbox"/>
Contrast only: Have you ever had any kidney/bladder related medical problems including dialysis treatment, transplant, kidney surgery etc?	<input type="checkbox"/>	<input type="checkbox"/>	<input type="checkbox"/>

CHECKLIST:	
Scanning	<input type="checkbox"/>
Ear plugs refused?	<input type="checkbox"/>
Radiographer	<input type="checkbox"/>

	R'GIST	R'PHER	Product	Dose	Batch N ^o	Expiry
IV GAD						
Oral contrast						
Other contrast						

	R'GIST	REPORT
Renal function tests		Results within safe limit for administration of IV Contrast.
Orbit X-rays		No evidence of radio-opaque foreign body

I confirm that I have answered the above questions and the information is correct to the best of my knowledge.

PARTICIPANT'S SIGNATURE (PARENT/GUARDIAN – IF UNDER 16)	DATE	SIGNATURE (RADIOGRAPHER)	DATE
---	------	--------------------------	------

Appendix 2: Health and Medical Questionnaire/Consent Form

UNIVERSITY OF BRIGHTON
CHELSEA SCHOOL
WELKIN LABORATORIES

PHYSIOLOGY INFORMED CONSENT & MEDICAL QUESTIONNAIRE

Name: D.O.B.:
.....

Address:
.....

..... E-mail:
.....

Home tel.: Mobile tel.
no.:

Emergency contact name: Tel. no.:
.....

Height (cm)..... Body Mass (kg)

MEDICAL HISTORY (please circle)

Are you in good health? Yes No
If NO, please explain:

How often do you regularly participate in vigorous physical activity?
(e.g. prolonged running, cycling or high intensity team sports).

- < once a month
- Once a month
- Once a week
- 2-3 times a week
- 4-5 times a week
- >5 times a week

Have you suffered from a serious illness or accident? Yes No
If YES, please explain:

Do you suffer, or have you ever suffered from (please give particulars where appropriate):

Respiratory problems (e.g. asthma, bronchitis, COPD)?.....Yes No

High or low blood pressure?.....Yes No

Fainting, light-headedness or dizziness?.....Yes No

Heart problems (e.g. abnormal ECG, angina, atherosclerosis)?.....Yes No

Diabetes?.....Yes No

Epilepsy?.....Yes No

Any Liver or Kidney Problems Yes No

Any injuries or muscle, joint or bone problems? Yes No

Do you have any family history of the following conditions:

- Renal Failure/Kidney Disease Yes No
- Heart Conditions Yes No
- Diabetes Yes No
- High/Low BP Yes No

In the last 3 months, have you consulted your GP for any condition? Yes No

If YES, please give particulars:

Are you currently taking medication or dietary supplements? Yes No

(this includes any over the counter pain killers or NSAIDs)

If YES, please give particulars:

Have you eaten in the last 12 hours (only applicable to infusion trials)? Yes No

Have you consumed alcohol or caffeine in the last 24 hours? Yes No

Are you currently taking part (or recently taken part) in any other laboratory experiment? Yes No

Do you have any other medical conditions or problems not previously mentioned? Yes No

Is there anything to your knowledge that may prevent you from successfully completing the tests that have been outlined to you? Yes No

PERSONS WILL BE CONSIDERED UNFIT TO PARTAKE IN THIS INVESTIGATION IF THEY:

Have a fever; suffer from fainting spells or dizziness

Have a known history of medical disorders (ie high blood pressure, diabetes, heart, lung, liver or kidney problems)

Study Title:

The effects of hyperammonaemia on cognition and motor function

DECLARATION

I (participant name) hereby volunteer to be a subject in the experiment/investigation titled above.

My replies to the above questions are correct to the best of my belief and I understand that they will be treated with the strictest confidence. The experimenter has provided me with full written information of, and I have understood the purposes of the experiment and possible risks involved.

I understand that I may withdraw from the experiment at any time and that I am under no obligation to give reasons for withdrawal or to attend again for experimentation.

I undertake to obey the laboratory/study regulations and the instructions of the experimenter regarding safety, subject only to my right to withdraw declared above.

Visit 1(Familiarisation)	Signature of Participant..... Date:..... Time:.....
Visit 2(Constant Infusion 1)	Signature of Participant..... Date:..... Time:.....
Visit 3(Constant Infusion 2)	Signature of Participant..... Date:..... Time:.....

I (the experimenter) have reviewed the above information given by the subject and consider that he/she is suitable to take part in this experiment/investigation.

Signature of Experimenter:.....
Date:.....

Appendix 3: Example MFSI-SF Data Sheet

Participant:

Date:

Trial no.:

Pre/+2hrs/+4hrs

The Multidimensional Fatigue Symptom Inventory-Short Form (MFSI-SF)

Below is a list of statements that describe how people sometimes feel.
Please read each item carefully,
then circle the one number next to each item which best describes **how true each statement is at this moment**

		Not at all	A little	Moderately	Quite a bit	Extremely
1	I have trouble remembering things	0	1	2	3	4
2	My muscles ache	0	1	2	3	4
3	I feel upset	0	1	2	3	4
4	My legs feel weak	0	1	2	3	4
5	I feel cheerful	0	1	2	3	4
6	My head feels heavy	0	1	2	3	4
7	I feel lively	0	1	2	3	4
8	I feel nervous	0	1	2	3	4
9	I feel relaxed	0	1	2	3	4
10	I feel pooped	0	1	2	3	4
11	I am confused	0	1	2	3	4
12	I am worn out	0	1	2	3	4
13	I feel sad	0	1	2	3	4
14	I feel fatigued	0	1	2	3	4
15	I have trouble paying attention	0	1	2	3	4
16	My arms feel weak	0	1	2	3	4
17	I feel sluggish	0	1	2	3	4
18	I feel run down	0	1	2	3	4
19	I ache all over	0	1	2	3	4
20	I am unable to concentrate	0	1	2	3	4
21	I feel depressed	0	1	2	3	4
22	I feel refreshed	0	1	2	3	4
23	I feel tense	0	1	2	3	4
24	I feel energetic	0	1	2	3	4
25	I make more mistakes than usual	0	1	2	3	4
26	My body feels heavy all over	0	1	2	3	4
27	I am forgetful	0	1	2	3	4
28	I feel tired	0	1	2	3	4
29	I feel calm	0	1	2	3	4
30	I am distressed	0	1	2	3	4

Appendix 4: Example AVL Task Word Lists

<u>Word List A₁</u>	<u>Word List A₂</u> <u>(Testing trial 2)</u>	<u>Word List B₁</u>	<u>Word List B₂</u> <u>(Testing trial 2)</u>
DRUM	DOLL	DESK	DISH
CURTAIN	MIRROR	RANGER	JESTER
BELL	NAIL	BIRD	HILL
COFFEE	SAILOR	SHOE	COAT
SCHOOL	HEART	STOVE	TOOL
PARENT	DESERT	MOUNTAIN	FOREST
MOON	FACE	GLASSES	WATER
GARDEN	LETTER	TOWEL	LADDER
HAT	BED	CLOUD	GIRL
FARMER	MACHINE	BOAT	FOOT
NOSE	MILK	LAMB	SHEILD
TURKEY	HELMET	GUN	PIE
COLOUR	MUSIC	PENCIL	INSECT
HOUSE	HORSE	CHURCH	BALL
RIVER	ROAD	FISH	CAR

Appendix 5: Exercise Peak Plasma Ammonia Concentration Meta-analysis

No.	Ref	n	Art/Ven/Art-Ven	Type of Ex./Duration	Intensity	Basal Concentration (µmol/l)	Peak Concentration (µmol/l)
1	<i>Ebsjornsson et al. (2006)</i>	6	Art	3 x 30s Max Sprint Cycles	Max.	25	220
2	<i>Yellsten et al. (1999)</i>	7	Art	4 mins of Knee extension to exhaustion		40	105
3	<i>Mohr et al (2006)</i>	8	Ven	40 min (Int. 15s:15s cycling) followed by 15mins int maximal sprints	65% to max	30	115
5	<i>Sahlin et al. (1999)</i>	10	Ven	To fatigue (44 - 116mins)	75%max	50	194
8	<i>Snow et al (2000)</i>	8	Ven	2 hours	65%max	20	75.5
9	<i>Mourtzakis and Graham (2002)</i>	7	Art	15mins (cycling)	85%max	40	90
10	<i>Nybo et al. (2005)</i>	24	Art	2 hours (cycling)	60%max		190
11	<i>Dalsgaard et al. (2004)</i>	9	Art	12mins	incremental	23	67
12	<i>Graham et al. (1990)</i>	8	Art	3.2mins (Single knee ext)	140%VO ₂ max	40	110
13	<i>Graham et al. (1990)</i>	8	Ven	3.2mins (Single knee ext)	140%VO ₂ max	40	175
14	<i>Bangsbo et al. (1996)</i>	6	Art	Incremental Arm and Leg exercise	Increasing	79.6	235
15	<i>Katz et al. (1986)</i>	8	Art	5.2mins	100%max	95	210
16	<i>Dudley et al. (1983)</i>	5	Ven	3mins	110%max	71	140.8
17	<i>Dudley et al. (1983)</i>	6	Ven	3mins	110%max	71	224.6
18	<i>Tong et al. (2003)</i>	7	Ven	7mins(12s rep. sprints to exhaustion)	160%max	24.1	140
19	<i>Morris et al. (1998)</i>	12	Ven	90mins (Intermittent sprint protocol)		32.3	121.8
20	<i>Snow et al. (1998)</i>	8	Ven	20s (max cycle sprint)	Max	15	125
21	van Hall et al. (1995)	10	Ven	125mins	70-75%max	49	105
22	Graham et al. (1987)	9	Ven	40 mins (cycling)	70%VO ₂ max	85	158
23	Schaefer et al., (2002)	8	Ven	Incremental cycling	Incremental	25	75
24	Calvert et al. (2008)	13	Art-Ven	Incremental ex to exhaustion (cycling)	Incremental	63.7	106.2

Appendix 6: Publications arising from thesis

Wilkinson, DJ., Smeeton, NJ. and Watt PW. (2010). Ammonia Metabolism, Fatigue and the Brain; Revisiting the Link. *Progress in Neurobiology*. 91 200-219.

Wilkinson DJ., Smeeton NJ., Castle PC., and Watt PW. (2011). Absence of Neuropsychological Impairment in Hyperammonaemia in Healthy Young Adults; Possible Synergism in Development of Hepatic Encephalopathy (HE) Symptoms? *Metabolic Brain Disease*. 26:203-212